

WPO 44158

411582

SANDIA NATIONAL LABORATORIES  
WASTE ISOLATION PILOT PLANT

EXPEDITED CCA ACTIVITY

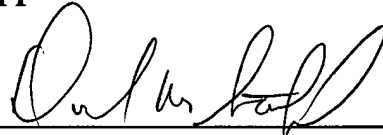
WPO #44158  
Revision 1.0

**TITLE: Supplementary Analyses of the Effect of Salt Water Disposal and Waterflooding on the WIPP**

Authors:

Daniel M. Stoelzel, Org. 6848

Print



Signature

6/13/97

Date

Peter N. Swift, Org. 6801

Print



Signature

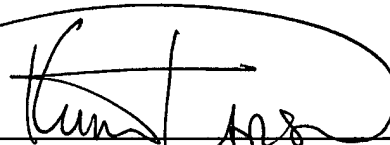
6/13/97

Date

Technical  
Review:

Kurt W. Larson, Org. 6821

Print



Signature

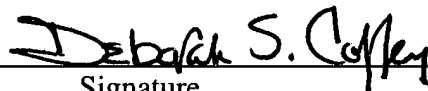
6/16/97

Date

QA Review:

Deborah S. Coffey, Org. 6811

Print



Signature

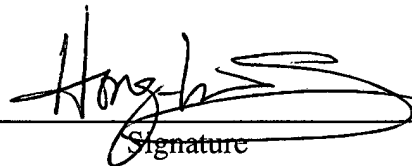
6/13/97

Date

Managerial  
Review:

Hong-Nian Jow, Org. 6848

Print



Signature


6/16/97

Date

Project Office  
Review:

Margaret S.Y. Chu, Org. 6801

Print



Signature

6/16/97

Date

SNL WIPP QAP 9-6

SWCF-A:1.2.01.5.3.1:CO/CCA:QA:Salt Water Disposal and Waterflooding

Information Only

# Supplementary Analyses of the Effects of Salt Water Disposal and Waterflooding on the WIPP

## Contents

<b>1.0 INTRODUCTION .....</b>	<b>5</b>
<b>2.0 CONCEPTUAL MODEL FOR LEAKS FROM INJECTION WELLS.....</b>	<b>7</b>
2.1 CURRENT INJECTION PRACTICE.....	7
2.1.1 Injection for Salt Water Disposal.....	7
2.1.2 Injection for Enhanced Oil Recovery.....	8
2.2 HOW AN INJECTION WELL MIGHT LEAK.....	9
2.2.1 Injection Well Construction.....	9
2.2.2 Injection Well Testing and Maintenance.....	12
2.2.3 Possible Pathways for Leaks from Injection Wells.....	12
2.2.3.1 Leaks in the Cement Sheath.....	13
2.2.3.2 Casing Leaks with Tubing or Packer Leaks.....	14
2.3 TOTAL DURATION OF LEAKS FROM FLUID INJECTION NEAR THE WIPP.....	15
<b>3.0 COMPUTATIONAL MODELING.....</b>	<b>15</b>
3.1 GENERAL MODELING ASSUMPTIONS.....	16
3.1.1 Stratigraphy.....	16
3.1.2 Boreholes.....	18
3.1.2.1 Permeability of a Leaky Cement Sheath During Injection.....	19
3.1.2.2 Permeability of a Tubing/Packer and Casing Leak During Injection.....	19
3.1.2.3 Permeability of the Borehole Above the Salado During Injection.....	19
3.1.2.4 Permeability of the Borehole After Plugging and Abandonment.....	20
3.1.3 The Repository.....	20
3.2 THE RADIAL MODEL.....	21
3.3 THE CROSS-SECTIONAL MODEL.....	25
<b>4.0 MODEL RESULTS .....</b>	<b>29</b>
4.1 CASES MODELED.....	29
4.1.1 The Radial Model Cases.....	29
4.1.1.1 Radial Cases R1 through R3.....	29
4.1.1.2 Radial Cases R4 through R7.....	30
4.1.1.3 Radial Cases R8 through R10.....	30
4.1.2 The Cross-Sectional Model Case.....	31
4.2 RADIAL MODEL RESULTS.....	33
4.2.1 Volume of Brine Injected (Radial Models).....	33
4.2.2 Volume of Brine Leaking above the Bell Canyon Formation (Radial Models).....	34
4.2.3 Volume of Brine Entering Anhydrite Layers (Radial Models).....	36
4.2.4 Pressure in the Injection Wellbore at MB 139 (Radial Models).....	40
4.2.5 Distance of Fracture Propagation in Anhydrite Layers (Radial Models).....	43
4.3 CROSS-SECTIONAL MODEL RESULTS.....	45
4.3.1 Volume of Brine Injected (Cross-Sectional Model).....	46
4.3.2 Volume of Brine Leaking Above the Bell Canyon Formation (Cross-Sectional Model).....	47
4.3.3 Volume of Brine Entering Anhydrite Layers (Cross-Sectional Model).....	48
4.3.4 Pressure in the Injection Wellbore at MB139 (Cross-Sectional Model).....	49
4.3.5 Distance of Fracture Propagation in Anhydrite Layers (Cross-Sectional Model).....	50
4.3.6 Long-term Effects on the Repository (Cross-Sectional Model).....	51

4.3.6.1 *Brine Flow into Repository (Cross-Sectional Model)*.....51  
4.3.6.2 *Pressures and Saturations in the Repository (Cross-Sectional Model)*.....52  
5.0 CONCLUSIONS .....54  
REFERENCES.....57  
APPENDIX A: GRID-BLOCK DIMENSIONS AND LAYERING INFORMATION FOR THE RADIAL  
AND CROSS-SECTIONAL MODELS.....59  
APPENDIX B: LOCATIONS AND NAMES OF COMPUTER CODES AND INPUT/OUTPUT FILES USED  
IN THIS STUDY .....62  
APPENDIX C: COMPLETE LISTING OF PARAMETERS USED FOR THE RADIAL MODELS .....70  
APPENDIX D: COMPLETE LISTING OF PARAMETERS USED FOR THE CROSS-SECTIONAL  
MODEL .....89

**ATTACHMENTS:**

- **Attachment 1: Injection Methods: Current Practices and Failure Rates in the Delaware Basin**
- **Attachment 2: Technical Review by Swift et al. of *The HARTMAN Scenario: Implications for WIPP*, by John Bredehoeft**
- **Attachment 3: Derivation of Fracture Parameters Used in Brine Injection Modeling**

## List of Figures

FIGURE 1: WIPP AREA GEOLOGY TYPICAL DISPOSAL WELL COMPLETION AND HYPOTHETICAL LEAKY PATHWAYS	11
FIGURE 2: SINGLE WELL RADIAL MODEL CONCEPTUALIZATION	22
FIGURE 3: ILLUSTRATION OF 2D SINGLE WELL FINITE-DIFFERENCE GRID WITH RADIAL FLARING IN "THICKNESS" DIRECTION	24
FIGURE 4: CROSS-SECTIONAL MODEL DIMENSIONS AND LAYERING	27
FIGURE 5: CROSS-SECTIONAL MODEL WITH RADIAL FLARING ILLUSTRATED	28
FIGURE 6: CUMULATIVE BRINE INJECTED INTO ALL FORMATIONS: RADIAL MODELS	34
FIGURE 7: CUMULATIVE BRINE LEAKING UP WELLBORE AT BELL CANYON / CASTILE INTERFACE: RADIAL MODELS	36
FIGURE 8: CUMULATIVE FLOW INTO MARKER BED 139: RADIAL MODELS	38
FIGURE 9: CUMULATIVE FLOW INTO MARKER BED 138: RADIAL MODELS	38
FIGURE 10: CUMULATIVE FLOW INTO CASTILE ANHYDRITE: RADIAL MODELS	39
FIGURE 11: CUMULATIVE FLOW INTO UPPER ANHYDRITE COMPOSITE: RADIAL MODELS	39
FIGURE 12: PRESSURE IN WELLBORE AT MARKER BED 139: RADIAL MODELS	41
FIGURE 13: PRESSURE RESPONSE IN WELLBORE AT VARIOUS TIMES FOR RADIAL CASE R7	42
FIGURE 14: MAXIMUM DISTANCE OF $10^{-12}$ m <sup>2</sup> FRACTURE AT VARIOUS CEMENT LEAK PERMEABILITIES: RADIAL MODELS	44
FIGURE 15: MAXIMUM DISTANCE OF $10^{-12}$ m <sup>2</sup> FRACTURE DUE TO HYPOTHETICAL WATERFLOOD INJECTION INTO DEEPER FORMATIONS: RADIAL MODELS	44
FIGURE 16: MAXIMUM DISTANCE OF $10^{-12}$ m <sup>2</sup> FRACTURE: EFFECTS OF UPPER BELL CANYON PERMEABILITY (RADIAL MODELS)	45
FIGURE 17: TOTAL FLUID INJECTED INTO ALL FORMATIONS: CROSS-SECTIONAL MODEL	46
FIGURE 18: CUMULATIVE BRINE FLOWS IN WELLBORES UPWARDS PAST BELL CANYON / CASTILE INTERFACE: CROSS-SECTIONAL MODEL	47
FIGURE 19: CUMULATIVE FLOWS INTO MARKER BEDS 139 & 138: CROSS-SECTIONAL MODEL	48
FIGURE 20: CUMULATIVE FLOWS INTO CASTILE AND UPPER COMPOSITE ANHYDRITE LAYERS: CROSS-SECTIONAL MODEL	49
FIGURE 21: PRESSURE IN SOUTH WELLBORE AT MARKER BED 139 HORIZON: CROSS-SECTIONAL MODEL	50
FIGURE 22: MAXIMUM DISTANCE FROM SOUTH WELLBORE REACHED BY $10^{-12}$ m <sup>2</sup> FRACTURES IN THE ANHYDRITES: CROSS-SECTIONAL MODEL	51
FIGURE 23: BRINE FLOW INTO REPOSITORY FROM ANHYDRITES: CROSS-SECTIONAL MODEL	52
FIGURE 24: AVERAGE PRESSURE IN WASTE REGION: CROSS-SECTIONAL MODEL	53
FIGURE 25: AVERAGE BRINE SATURATION IN WASTE REGION: CROSS-SECTIONAL MODEL	53

## List of Tables

TABLE 1: SUMMARY OF THE SPECIFICATION OF RADIAL CASES R1 THROUGH R3	29
TABLE 2: SUMMARY OF THE SPECIFICATION OF THE RADIAL MODEL CASES R4 THROUGH R7	30
TABLE 3: SUMMARY OF THE SPECIFICATION OF RADIAL CASES R8 THROUGH R10	31
TABLE 4: SUMMARY OF THE SPECIFICATION OF THE CROSS-SECTIONAL MODEL CASE	32
TABLE 5: X-DIRECTION GRID-BLOCKS FOR RADIAL MODELS	59
TABLE 6: X-DIRECTION GRID-BLOCKS FOR CROSS-SECTIONAL MODEL	60
TABLE 7: Y-DIRECTION GRID-BLOCKS FOR RADIAL AND CROSS-SECTIONAL MODELS	61



## 1.0 Introduction

This report documents analyses of the effects on the Waste Isolation Pilot Plant (WIPP) of the subsurface injection of brine outside the WIPP Land Withdrawal Area. Brine is presently injected under pressure into stratigraphic units deeper than the Salado Formation both to dispose of salt water produced as a byproduct of oil and gas production, and to enhance oil recovery by maintaining pressure and waterflooding oil reservoirs. Brine injection activities may continue in the region as long as oil and gas resources continue to be produced.

Stoelzel and O'Brien (1996) examined whether leakage from a poorly maintained injection well could enter anhydrite interbeds above or below the WIPP (Marker Beds 138 and 139), with sufficient pressure to fracture the anhydrite layers and result in brine flow into the repository. Based on a computational model that they argued was conservative, Stoelzel and O'Brien concluded that, if oil and gas operators allowed injection wells to leak for up to 50 years, some flow into the marker beds was possible. However, significant flow to the WIPP was unlikely. The worst combination of conditions they considered resulted in approximately 1000 m<sup>3</sup> of brine flowing into the WIPP in 10,000 yr, which they noted was "significantly less than the mean from the three replicates for the undisturbed CCA [Compliance Certification Application] calculations" (Stoelzel and O'Brien, 1996, page 40). Based on this analysis, the Department of Energy (DOE) concluded that brine injection could be screened out of the full performance assessment calculations for the CCA (DOE, 1996, section SCR.3.3.1.3).

Some reviewers of the CCA have questioned whether Stoelzel and O'Brien's (1996) analysis forms a sufficient basis for the DOE's decision to screen brine injection out of the performance assessment (e.g., Neill, 1997), based in part on an independent analysis of the phenomenon prepared for the New Mexico Attorney General (Bredehoeft, 1997). In a letter dated March 19, 1997 (Trovato, 1997), the Environmental Protection Agency (EPA) has formally requested the collection of additional information about current injection practice in the region and additional modeling studies related to fluid injection. The required additional studies and modeling changes are outlined below (from Trovato, 1997, Enclosure 1, page 8):

*"DOE needs to :*

- (a) Use a 150-year period as the period of simulation.*
- (b) Identify the extent to which the initial conditions (i.e., conditions before an intrusion event) of the repository could change with the longer period of fluid injection.*
- (c) Analyze the effects of a human intrusion event subsequent to fluid reaching the repository via a fluid injection event.*
- (d) Increase the transmissivity of Bell Canyon to allow higher volumes of brine to be injected.*
- (e) Reduce, by one-half, the DRZ volume.*

Information Only

- (f) Estimate the frequency of fluid injection wells that have failed or appear to have failed.*
- (g) Substantiate why a two-dimensional cross-sectional modeling approach is appropriate for this analysis."*

This report documents the supplementary analyses of brine injection requested by the EPA. These analyses incorporate additional information the DOE Carlsbad Area Office (CAO) has compiled about current injection practice in the region (DOE, 1997 [See Attachment 1]), and address specific directives from the EPA stated in the March 19, 1997 letter (Trovalo, 1997). These analyses in general do not specifically address modeling issues raised by Bredehoeft (1997), with the exception of his concern that the cross-sectional geometry used by Stoelzel and O'Brien (1996) underestimates brine flow in the anhydrite layers. As discussed in a detailed review of Bredehoeft's work by Swift et al. (1997 [See Attachment 2]), we do not believe that Bredehoeft's (1997) model represents a credible analysis of the phenomena associated with brine injection, and we do not attempt here to evaluate his model results or compare them in detail to ours.

Our approach in preparing this analysis has been to examine current injection practice in the region (DOE, 1997) to verify the adequacy of Stoelzel and O'Brien's (1996) conceptual model for leakage from injection wells. We have expanded on their work by adding additional geologic realism, and by including injection into deeper stratigraphic horizons at higher pressures. We have examined the appropriateness of the cross-sectional geometry used in their analysis (EPA comment g above) by developing two alternative models, one using a modification of the cross-sectional geometry that allows brine flow toward the WIPP from a 180-degree arc at the borehole, and one using an axisymmetric radial geometry that captures flow behavior in the full 360-degrees around an isolated borehole. We also began development of a third alternative as part of this study, using a two-dimensional areal model to simulate flow and fracturing in Marker Bed 139 (MB139) of the Salado Formation. The areal model was not completed and used in this analysis, however, because results of the radial model calculations did not indicate sufficient flow in MB139 to warrant further development of the areal approach.

Because of the large uncertainty about future human actions, we have taken what we believe is a conservative approach to estimating the frequency and duration of injection well failure in the future, the pressures at which these wells may inject, and the effectiveness of plugs emplaced when these wells are abandoned. In general, however, we have focused on what we believe are reasonable and realistic conditions. Modeling assumptions and parameter values are consistent with those used in the CCA performance assessment, except where noted otherwise. Parameters that were sampled in the CCA have been set to their median values.

Results of this study are intended to supplement Stoelzel and O'Brien's (1996) analysis, rather than to replace it. Overall, these analyses confirm the decision to screen out brine injection from the CCA performance assessment.

Information Only

## 2.0 Conceptual Model for Leaks from Injection Wells

The conceptual model used here is like that described by Stoelzel and O'Brien (1996, section A2), although the cases considered for computational modeling have been expanded to include injection at higher pressures and into deeper units, and, for the cross-sectional model only, brine removal to simulate offset oil production during waterflood operations. Current practice in the region and reasonable speculation about future practice form the basis for the assignment of the injection intervals and pressures. Possible leak pathways are considered outside casing through a faulty cement sheath, and inside casing through faulty tubing or packers and then through failed casing directly into the Salado Formation. Assumptions about the duration of leaks are based on records of past and current injection wells in the region (DOE, 1997).

### 2.1 *Current Injection Practice*

#### 2.1.1 Injection for Salt Water Disposal

Salt water (brine) is routinely brought to the surface as a byproduct of oil and gas production, and oil and gas operators dispose of this brine by injecting it back into the subsurface. Injection occurs into relatively deep strata to protect shallow groundwater resources. In most cases, disposal wells are converted dry holes or production wells that are no longer profitable. Injection pressures for disposal must be above the hydrostatic pressure of the injection interval for brine to flow down the hole: for the New Mexico portion of the Delaware Basin, disposal injection pressure gradients are generally 0.2 psi/ft (4,524 Pa/m) or less above the hydrostatic gradient (DOE, 1997, Section 2.0). The pressure gradient and the depth of the injection interval together define the downhole pressure (the hydrostatic pressure of the column of brine in the borehole) and the surface pressure the operator must maintain by pumping ( $0.2 \text{ psi/ft} \times \text{the depth}$ ). For the purposes of this analysis, we have conservatively neglected pressure loss in the hole due to friction during flow through tubing. This assumption results in calculated downhole pressures that are somewhat higher than those that are observed in practice.

In the nine-township region (324 square miles) including and surrounding the WIPP, there are currently 21 salt water disposal wells in operation (DOE, 1997, Attachment 1). (Note that this number changes as additional wells are brought into service or unneeded wells are shut in.) All of these wells currently inject into the Bell Canyon Formation or deeper formations, at depths that range from 3,820 ft (1,000 m) to 8,710 ft (2,655 m). Injection pressure gradients are 0.725 psi/ft (16,400 Pa/m) or less (0.2 psi/ft above a brine-hydrostatic gradient of 0.525 psi/ft) in 20 of the 21 salt water disposal wells. One disposal well, the Cal-Mon # 5 in section 35, Township 23 S, Range 31 E, has been permitted by the New Mexico Oil Conservation Division (NMOCD) following testing to inject at a depth of 4,931 ft with a surface pressure of 998 psi (6.9 MPa), corresponding to a gradient of 0.727 psi/ft (DOE, 1997, Section 5.1.2).

Disposal wells inject intermittently, as brine is delivered for disposal, rather than continuously. Disposal rates vary considerably in the region. The most prolific disposal well in the region, the David Ross AIT Federal # 1, injected between 1991 and 1997 at an average rate of approximately 137,000 m<sup>3</sup>/yr. Other disposal wells in the region operate at lower rates, ranging from approximately 108,000 m<sup>3</sup>/yr to less than 2,000 m<sup>3</sup>/yr. (DOE, 1997, Attachment 1).

### 2.1.2 Injection for Enhanced Oil Recovery

Pore pressure in subsurface reservoirs declines as oil is produced, reducing the efficiency of production operations. Oil producers may choose, therefore, to maintain high pressure in the production interval by injecting brine to replace the produced oil. Waterflooding techniques, in which brine injection is used to drive oil toward production wells, are commonly used in mature fields where a sufficiently large fraction of the oil originally present has been extracted such that the primary production is no longer profitable.

Three brine injection wells are currently in use for enhanced oil and gas recovery in the nine-township area including and surrounding the WIPP (DOE, 1997, Attachment 1). All three wells inject into oil-producing horizons in the Cherry Canyon and Brushy Canyon Formations, at depths between 4,802 and 7,408 feet (1,464 and 2,258 m). Each of these three wells injects at pressures at or below a gradient of 0.725 psi/ft. The Neff Federal # 3 well, located about 1.8 km east of the WIPP Land Withdrawal Area in Section 25 of Township 22 S, Range 31 E, injects at 1,410 psi (9.7 MPa), which is the highest surface pressure of any injection well (disposal or enhanced recovery) in the nine-township area. This surface pressure corresponds to 5,111 psi (35. MPa) at the injection depth of 7,050 ft (2,149 m), assuming a brine hydrostatic gradient of 0.525 psi/ft and no friction effects in the tubing.

Injection rates for enhanced recovery operations are available for two of the three active wells (DOE, 1997, Attachment 1). The James A # 3 and the James A # 12 wells, in the Cabin Lake Field northwest of the WIPP Land Withdrawal Area, have averaged approximately 92,000 m<sup>3</sup>/yr and 116,000 m<sup>3</sup>/yr, respectively, over the last 3 to 4 years. Injection rates for the Neff Federal # 3 well are not currently available.

Most of the oil fields in the WIPP vicinity are relatively young (developed in the 1990s), and brine injection for enhanced recovery may increase as the fields mature. Analyses of future production trends are speculative, and we have not attempted to predict the details of future injection. However, we believe it is possible that injection pressures may increase above the present 0.725 psi/ft gradient, because past practice in the oil industry demonstrates that productivity in older fields can be increased by higher waterflood injection pressures. As described by DOE (1997, Section 4.1), the NMOCD grants exceptions to the 0.2 psi/ft above brine hydrostatic limit if operators demonstrate, by field testing, that the proposed injection pressures are below the pressure at which the rock of the injection interval fractures. The pressure at which rocks will fracture varies with depth and lithology, and ranges from only

slightly above hydrostatic pressure to approximately lithostatic pressure (Craft et al., 1962, p. 488). We therefore use 1.0 psi/ft (22,621 Pa/m), corresponding to a typical lithostatic gradient for sedimentary basins (Levorsen, 1967, p. 402) as a reasonable and very likely conservative upper bound for the future injection pressure gradient in the WIPP vicinity.

The future depth of injection in the WIPP vicinity is also uncertain. Current injection for enhanced recovery occurs in the Cherry Canyon and Brushy Canyon Formations. However, oil is also produced from some wells from the deeper Bone Spring Formation (NMBMMR, 1995), and it is possible that brine injection for enhanced recovery may occur in this unit in the future. Our analyses therefore consider the consequences of leaky injection wells operating at a 1.0 psi/ft gradient in the Bone Spring Formation. Formations deeper than the Bone Spring are not realistic targets for brine injection in the WIPP area because known hydrocarbon resources below the Bone Spring are gas (NMBMMR, 1995), rather than oil, and injection techniques are not used for gas recovery in the region.

## ***2.2 How an Injection Well Might Leak***

The types of leaks that might occur from injection wells and the length of time that they might persist without being repaired depend on well construction practices and the frequency of well testing and maintenance. See DOE (1997, Sections 2.0-4.0) for detailed information on these topics.

### **2.2.1 Injection Well Construction**

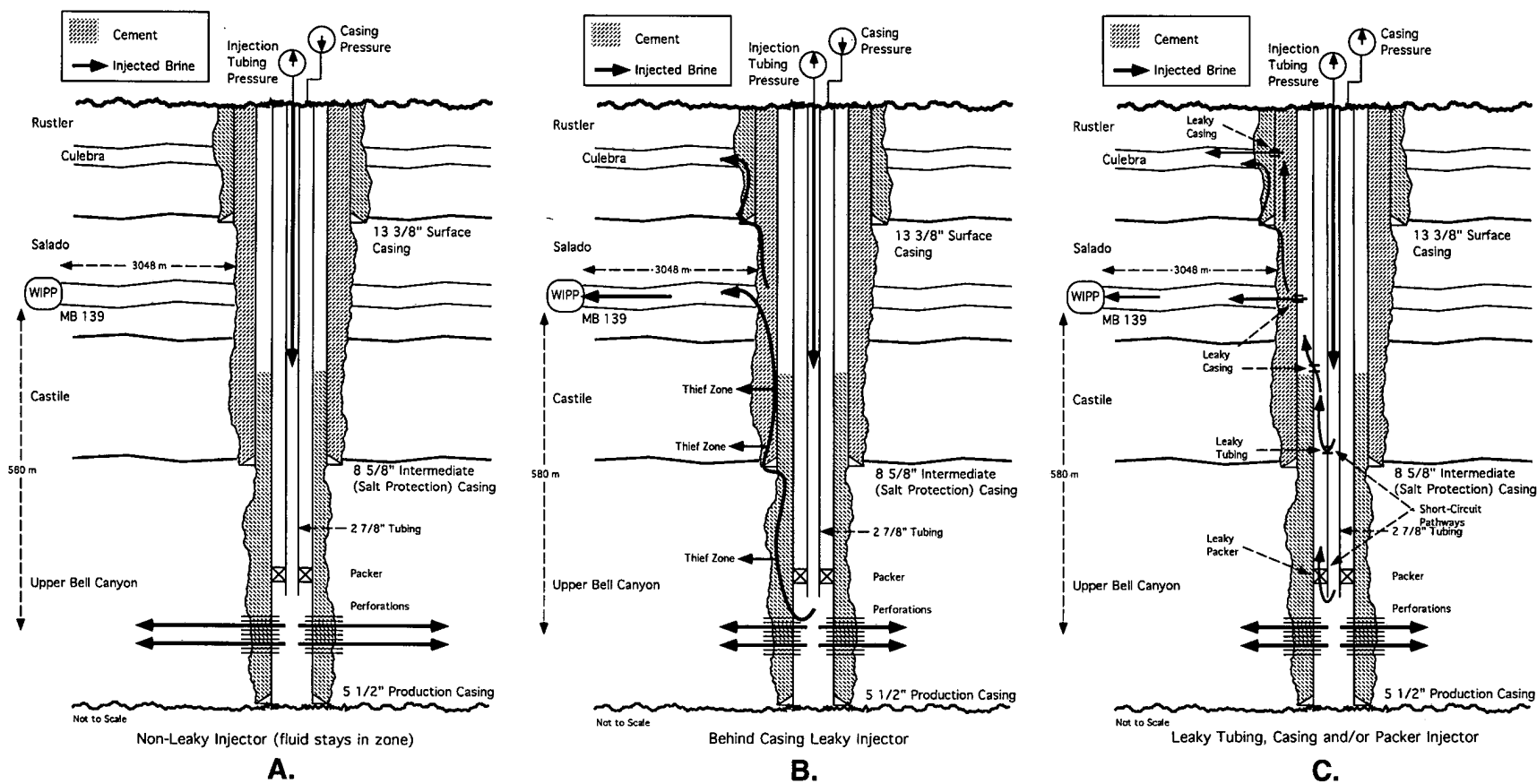
Figure 1A (reproduced from Figure 1 of Stoelzel and O'Brien, 1996) illustrates the construction of a typical injection well. See DOE (1997, Attachment 2) for illustrations of the construction of all active injection wells in the nine-township area surrounding the WIPP. From the outside in, most injection wells have a cement sheath filling the outermost annulus between the casing and the rock, then one or more "strings" of steel casing, with annuli between casing strings often cemented, and then an inner "tubing" string through which fluid is pumped down the hole. At the top of the injection interval the tubing passes through a "packer," which separates the annulus between the tubing and the casing from the injection interval. Deeper formations penetrated by the borehole, if any, are typically plugged off with cement. In a properly functioning injection well, high pressures are confined to the tubing and the injection interval, and all injection occurs into the target horizon. The annulus between the tubing and the casing, and any other uncemented annuli, are filled with water with corrosion-inhibiting additives, to maintain a hydrostatic pressure gradient on the casing, tubing, and packer.

The number of casing strings and length of the cement sheaths varies with the total depth of the hole, the time at which the well was completed, and other factors. At a minimum, all injection wells have a "surface" casing string that protects near-surface groundwater (emplaced to the top of the Salado in the WIPP vicinity) and a "production casing," emplaced either through or to the



top of the production or injection interval. Like the example shown in Figure 1, most wells in the WIPP region also have an "intermediate casing," emplaced through the evaporite section. Surface casing is cemented throughout its entire length, and intermediate casing is cemented throughout the salt section in all but three of the active injectors in the nine-township region. Nine of the 24 active injection wells in the nine-township area, including the Neff Federal # 3 that operates with the highest surface pressure, have two cement sheaths through the salt section, one outside the intermediate casing and one within the annulus between the intermediate and production casings. In the three active injection wells that have only a single string of production casing without cement through the salt section, the injection interval is isolated from the overlying formations by a minimum of 629 feet of cement sheath (in the James Federal # 1, section 29, Township 23 S, Range 32 E) (DOE, 1997, Attachment 2).

Information Only



**Figure 1: WIPP area geology typical Disposal Well Completion and Hypothetical Leaky Pathways**



## **2.2.2 Injection Well Testing and Maintenance**

The NMOCD requires periodic scheduled testing of injection wells (DOE, 1997, Section 2.0). Results of "Bradenhead" tests, in which pressures at the land surface are recorded in each open annulus in the well, are reported annually to the NMOCD, and mechanical integrity tests (MITs) are required prior to commencement of injection and then every five years following or whenever the tubing and packers are replaced.

Because of the design of injection wells, Bradenhead tests will detect all tubing and packer leaks, and some casing leaks. In a properly functioning injection well, only the tubing pressure should be elevated at the surface. All other annular pressures should be atmospheric. Even a small leak in the tubing or packer will result in overpressurization of the annulus between the tubing and casing, and the operator will observe casing pressures above atmospheric (zero gage pressure). Casing leaks, if they occur independently of tubing and packer leaks, will cause pressure in the casing annuli to rise or fall to the highest pressure of the formation(s) in which the leak occurs, less hydrostatic pressure to that depth.

Mechanical integrity tests directly evaluate the integrity of the casing by pressurizing the casing/tubing annulus to a minimum surface pressure of 300 psi. Annular pressure is recorded for 30 minutes, and any anomalous loss of pressure indicates a leak in the casing.

Detailed test records are available for all injection wells within the nine-township region surrounding the WIPP documenting mechanical integrity tests and Bradenhead tests since 1982 (DOE, 1997). Leaks have been reported in three injection wells (all salt water disposal wells) in the region. Two were repaired and returned to service the same day, and the third was repaired and returned to service after nine days (DOE, 1997, Section 5.1).

## **2.2.3 Possible Pathways for Leaks from Injection Wells**

Five basic types of failures are possible in injection wells (DOE, 1997, Section 4.1). 1) The tubing may fail, allowing flow from the tubing into the casing/tubing annulus. 2) The packer may fail, allowing flow from the tubing into the casing/tubing annulus. 3) The casing may fail, allowing flow between the casing/tubing annulus and the surrounding formation. 4) The cement sheath may fail, allowing flow upward from the injection horizon outside the casing. 5) Leaks may occur out of the injection interval through fractures or other pathways in the rock, away from the injection borehole. The first three types of failure are readily detected by routine testing at the surface, as described in the previous section, and are repaired rapidly. Cement leaks, however, are difficult to detect because they may not significantly affect pressures within the well. Radioactive tracer tests can identify cement leaks but these tests are not performed routinely, and cement leaks may persist for relatively long times, particularly in salt water disposal operations where pressure in the injection interval is not being monitored in surrounding production wells. Leaks through the formation away from the borehole are unlikely to be

detected unless the operator of the well notes pressure drops in nearby production wells or anomalously high injection rates.

The first two types of failure are the most common (DOE, 1997, Section 9.0), but, as long as they do not coincide with a casing failure, they do not create a flow path between the well and the surrounding formations. Tubing and packer leaks pose a problem for the well operator and must be repaired, but they do not result in flow away from the well. Casing leaks do create a pathway for flow from the borehole to the surrounding formation, but unless they coincide with a tubing or packer leak, the pressure gradient for flow is relatively small and the volume of liquid available is limited to that contained in the annulus. As discussed by DOE (1997, Section 4.1) large leaks through hydraulic fractures in the target horizon away from the borehole are highly unlikely because of relatively poor fracturing properties of salt water, and we assume that small leaks from the injection horizon will be indistinguishable from leaks through the cement sheath. We have therefore limited our modeling to two types of leaks that we believe have a potential to create significant flow into formations other than the target horizon: simultaneous tubing (or packer) and casing leaks, and leaks in the cement sheath.

We have not modeled the circumstance in which an injection well functions properly, but brine flows out of the injection horizon through leaks in a nearby production well open to the injection horizon. We believe that flow along this pathway is bounded by the cases we have considered because possible leak paths within the production well will be analogous to those described for the injection well.

### **2.2.3.1 Leaks in the Cement Sheath**

Figure 1B (reproduced from Figure 1 of Stoelzel and O'Brien, 1996) illustrates the hypothetical flow path from the injection interval to the WIPP for a leak through the cement sheath of an injection well. In this analysis, the degraded cement sheath is characterized as a porous medium, and the rate of flow is controlled by the pressure gradients, the length of the flow path, the permeabilities of other units intersected by the flow path, and the permeability assigned to the degraded cement. Cement permeability is discussed in Section 3.1, along with other modeling assumptions and parameter values. Model geometry is described in Sections 3.2 and 3.3.

As noted in the previous section, flow along a cement leak pathway will be difficult to detect, particularly if it is slow. For modeling purposes, cement leaks are assumed to persist for the lifetime of a typical oil field, assumed to be 50 years. Individual injection wells in the region are unlikely to remain in operation that long (the oldest injector still active in the nine-township region, the Todd 26 Federal # 3, began disposal operations in 1971), but enhanced recovery operations could perhaps persist that long. For example, Neill (1997) reports that a proposed waterflood operation at the Avalon Field north of the city of Carlsbad will have a 40-year life expectancy.

### 2.2.3.2 Casing Leaks with Tubing or Packer Leaks

Figure 1C (reproduced from Figure 1 of Stoelzel and O'Brien, 1996) illustrates the hypothetical flow path from the injection interval to the WIPP for a leak through a failed tubing or packer and casing. As is the case for the cement leak, Darcy flow is assumed to occur along the leak pathway. For the portion of the flow that occurs within the casing, this assumption may not be rigorously correct, but the permeability of the pathway is assigned a high enough value ( $10^{-5} \text{ m}^2$ , as discussed in Section 3.2) that there is very little resistance to flow. Pressure gradients, the length of the flow path, and the permeabilities of other units intersected by the flow path remain important factors in determining the rate of flow up the leak.

As noted in Section 2.2.2, leaks that involve tubing or packer failures will be detected by annual tests. Records indicate that once leaks are detected, wells are shut in immediately and repaired promptly (DOE, 1997, Section 5.1). Therefore, the maximum duration of a tubing or packer and casing failure in any single well can be assumed to be one year, and most will be detected sooner. One year is not, however, the maximum duration for the sum of all leaks that may occur during the life of an oil field. Our estimate for the total duration of leaks in a field is necessarily imprecise and speculative, and therefore we have used what we believe is a conservative approach.

Based on records from all injection wells in that portion of the Delaware Basin that is within the State of New Mexico (and therefore subject to New Mexico regulatory requirements and practices) DOE (1997, Section 8) has identified a total of 8 casing failures in 772 well-years of injection since 1982. This yields a rate for individual injection wells of 0.0104 casing failures per year. Records do not indicate how many of these casing failures also involved tubing or packer failures, but we have conservatively assumed that all may have.

Our estimate of the total duration of such leaks in a single oil field is based on a scale-up of this rate to a representative field. Neill (1997) reports that the proposed waterflood at the Avalon field north of the city of Carlsbad will use 19 injectors for 40 years, and that the Rhodes-Yates field east of Jal, New Mexico has used 18 injectors during 26 years. Thus, we believe that assuming fields in the WIPP region may have as many as 20 injectors operating for 50 years is reasonably conservative. This estimate corresponds to 1,000 well-years of injection per field, which, when combined with the casing failure rate derived from historical data, yields a total of ten casing leaks during the operation of the field. We conservatively assumed that each of these casing leaks coincides with a packer or tubing failure and persists for the maximum duration of one year, yielding a total of ten years of casing and tubing or packer leaks during the operation of the field.

There is no simple way of estimating when or where these leaks will occur within a field. We assume that they occur continuously for 10 years at a single location, maximizing the time for which a single portion of the Salado Formation is exposed to high pressure brine. We believe that this assumption is conservative compared to actual practice, in which injection wells within a field are likely to be spread out over many square kilometers and separated by a minimum of

several hundred meters. We assume that the 10-year period comes at the end of the life of the field (from 40 to 50 years), consistent with our belief that injection pressures are likely to be highest late in a field's development and that older casing and tubing will be more likely to fail.

### ***2.3 Total Duration of Leaks from Fluid Injection Near the WIPP***

As described in the previous section, we believe that 50 years is a reasonable limit for the life of enhanced recovery operations from a single field. Stoelzel and O'Brien (1996) chose 50 years as the total duration of injection in their simulations based on the requirement in 40 CFR § 194.32(c) that performance assessments must consider "... any existing boreholes and the development of any existing leases that can be reasonably expected to be developed in the near future, including boreholes and leases that may be used for fluid injection activities" (US EPA, 1996).

In its March 19, 1997 letter to the DOE (Trovato, 1997 - see section 1), the EPA stated, among other things, that "DOE needs to ... use a 150-year period as the period of simulation" for fluid injection modeling. Our modeling analyses therefore consider the possibility that new fields may be developed at different locations in different stratigraphic horizons during the next 150 years. Brine injection for waterflooding may occur for up to 50 years at a time in any of the units known to have oil reserves (the Cherry Canyon, the Brushy Canyon, and the Bone Spring Formations), and brine disposal may occur into the Bell Canyon Formation at various locations throughout the 150 period. The specific combinations of waterflooding and disposal operations that we have modeled are described in Section 4.1.

## **3.0 Computational Modeling**

All modeling reported for this analysis was performed using the BRAGFLO code, version 4.10 (BRAGFLO, 1996). The source code and executable are stored in the WIPP PA Configuration Management System (see Appendix B). Support codes used for analysis and plotting are outlined below:

The following software was run on the DEC ALPHA platform under the OPEN VMS AXP ver 6.1 operating system:

- ALGEBRACDB: version 2.35
- SUMMARIZE: version 2.10
- PREBRAG: version 6.00
- POSTBRAG: version 4.00
- GENMESH: version 6.08
- MATSET: version 9.00 (accessed view CCA6 of the INGRESS6.4 database)
- ICSET: version 2.22
- BLOTADB: version 1.37

The following software was run on the Gateway 2000 P5-90 desk top PC platform under the Microsoft Windows 95 (ver 4.00) operating system:

- CANVAS: version 5.02: serial number w121-058519011 Deneba software 7400 SW 87th Ave., Miami, Florida 33173. (Used to down-load and convert BLOTADB Adobe Illustrator formatted files, and create graphics for this report).
- EXCEL: version 5.0c, Microsoft Corporation, Product ID OEM43-F11-2200217
- WORD: version 6.0c, Microsoft Corporation, Product ID OEM43-F11-2200217
- FTP: File transfer utility by Microsoft Corporation. Executed as DOS shell in Windows 95.

General modeling assumptions and values for key input parameters are described in Section 3.1. Complete listings of parameter values are provided in Appendices C and D. The geometry of the meshes and the initial and boundary conditions used in this analysis are described below in Sections 3.2 and 3.3.

### ***3.1 General Modeling Assumptions***

Unless stated otherwise, all modeling assumptions are similar to analogous assumptions used in BRAGFLO modeling for the CCA. For example, BRAGFLO is used in the cross-sectional model, which contains a representation of the repository, to model gas generation and two-phase flow. In the radial model, which does not contain a representation of the repository, BRAGFLO models single-phase flow only. In both the cross-sectional and radial models, BRAGFLO simulates fracturing of anhydrite interbeds using the same equations relating pressure, permeability, and porosity that were used in the CCA calculations. Values of parameters that were sampled in the CCA were set to their median values, unless stated otherwise. Fixed value parameters were unchanged from the CCA.

Important differences in modeling assumptions and parameters between the CCA and this analysis are discussed in the following sections. Many of these differences are similar to differences between Stoelzel and O'Brien's (1996) model and the CCA model. Major differences between Stoelzel and O'Brien's (1996) model and this work are also noted in the following sections.

#### **3.1.1 Stratigraphy**

The model representation of stratigraphy has been modified from that of the CCA to include additional layers that have the potential to affect disposal system performance in the presence of brine injection and to exclude layers that have little role. Specific details of the stratigraphy are illustrated in Section 3.3, which describes the mesh used in the cross-sectional model.



As in Stoelzel and O'Brien's (1996) work, anhydrites a and b have been lumped with Marker Bed 138 above the repository, and the Castile Brine Reservoir and units above the Culebra have been omitted for modeling efficiency. Additional layers have been added below the Castile Formation to allow simulation of deeper hydrocarbon reservoirs and the less permeable layers separating them. Parameter values for the permeability and porosity of these stratigraphic units are taken from Stoelzel and O'Brien (1996), except for model cases in which the permeability of the Bell Canyon Formation was increased one order of magnitude in response to a comment in the EPA's March 19, 1997 letter (Trovato, 1997). These cases are discussed in Section 4.1.2.3

Anhydrite layers that were not present in either the CCA or in Stoelzel and O'Brien's (1996) model have been included to allow additional realism in modeling the response of the evaporite sequence to the high brine injection pressures. Anhydrite units above MB138 with thicknesses greater than 2 m were combined into single, composite layer assigned a thickness-weighted elevation. (Where halite layers were reported within anhydrite beds, their thicknesses were deducted from the total.) As a result, a 15.85 m-thick anhydrite layer has been added above the repository at an elevation of 552 m above mean sea level to represent a composite of MB109, the Union anhydrite, MB123, MB124, and MB136. The elevation and thickness of this anhydrite layer was established by examination of the core log from the ERDA-9 borehole (Sandia National Laboratories and United States Geological Survey, 1983). Similarly, a 9.45 m-thick anhydrite layer was added below the repository at an elevation of 296 m above mean sea level to represent a composite of MB140 and the Cowden anhydrite. Anhydrite layers in the Salado Formation with thicknesses less than 2 m (except for MB 138 and MB 139 near the repository horizon) were lumped with the halite layers of the model, limiting brine flow to the thicker interbeds and the marker beds immediately above and below the repository. Based on data from the DOE-1 borehole (Freeland, 1982), a 243-m thick anhydrite layer was added within the Castile Formation at an elevation of 12.4 m below mean sea level, representing the composite thicknesses of the A1, A2, and A3 anhydrite layers.

In the absence of experimental data for Salado anhydrites other than those near the repository, initial properties (e.g., permeability and porosity) of each of these layers were assumed to be the same as those assigned to MB138 and MB139 in the CCA. Fracturing in all anhydrite layers in response to elevated pressures was approximated using the same approach used in the CCA for MB138, anhydrites a and b, and MB139, which differs slightly from the approach used by Stoelzel and O'Brien (1996). Porosity and permeability increased as a function of pressure as pressure approached and exceeded lithostatic. Because the fracture model parameters developed for the CCA are specific to the thicknesses and depths of the individual layers, fracture parameter values were developed for this study for each of the new anhydrite layers. Derivation of these values is shown in Attachment 3.

Inclusion of additional anhydrite layers required an adjustment to the vertical pressure gradient assumed within the evaporite sequence in the CCA. For the CCA BRAGFLO calculations, the initial pressure gradient in the Salado was assumed to be hydrostatic, adjusted vertically from a sampled value assigned to MB139 at its intersection with the shafts. For the CCA, this assumption had essentially no effect on flow in the Salado above MB138 or below MB139

because of the very low permeability of the halite. However, assuming a hydrostatic gradient in this analysis would have resulted in an unrealistic relationship between initial pore pressure and lithostatic pressure in the upper and lower anhydrite layers. Therefore, the initial pressure gradient within the entire evaporite sequence was assumed to be 0.84 psi/ft (intermediate between hydrostatic and lithostatic) for this analysis, referenced to the median CCA value (12.47 MPa) for initial pressure in MB139 at the shaft elevation. This gradient resulted in a consistent relationship between initial pore pressure and the fracture initiation pressure (0.2 MPa above initial pressure) in each of the anhydrite layers. The change in initial gradient has essentially no effect on flow in the halite portions of the evaporite sequences, or across the upper and lower boundaries of the evaporites, because of the extremely low permeability of the halite.

Unlike Stoelzel and O'Brien's (1996) modeling and the CCA, all stratigraphic units are assumed to be horizontal. The regional one-degree dip included in previous work has been omitted for simplicity because results of Stoelzel and O'Brien's (1996, page A15) show very little difference in anhydrite fracturing in the updip and downdip directions away from injection boreholes. Modeling results from the CCA (Helton, 1996, Table 2.5.5) indicate that fractures initiated by high gas pressure in the repository appear to be somewhat more likely to propagate updip (north in the CCA model) rather than downdip, but the influence of dip on repository-induced fracturing is not strong enough to suggest that it needs to be incorporated in the design of the injection models.

### **3.1.2 Boreholes**

The models used in this analysis and Stoelzel and O'Brien's (1996) study contain boreholes for brine injection and oil production that are not present in the CCA models. These boreholes are located 2.4 km from the waste disposal panels in the cross-sectional model, corresponding to the shortest distance from the waste to the Land Withdrawal Boundary. This is a conservative assumption, because it underestimates the true distance from essentially all reasonable injection or production well locations to the waste. For example, the Neff Federal # 3 injector is approximately 4.85 km from the waste panels. The radial model contains a single borehole, conceptually located at the center of the model domain.

Brine injection within a borehole is simulated by defining a pressure source term at the elevation chosen for injection. The rate at which brine is injected, and the volumes of brine injected, are therefore calculated model results dependent on the assumed injection pressure and the properties of the units through which the brine flows. Injection rates are not prescribed based on current practice. Oil production is simulated the same way, using a pressure sink below the hydrostatic value for the elevation. (Note, however, that the "oil" in these simulations is modeled as brine. The only purpose of including production in the analysis is to produce pressure gradients in reservoirs analogous to those observed in the field. We have not attempted a realistic two-phase simulation of oil and water flow.) Normal downward or upward flow of fluid from the surface is not simulated in this approach, and borehole regions within the model are used only to simulate the leak pathway in a failed or abandoned well. The permeability of the borehole region



above (and below) the injection or production interval is set at various values representing different degrees of cement degradation or casing and tubing leaks.

### **3.1.2.1 Permeability of a Leaky Cement Sheath During Injection**

The values used to characterize the cement sheath are based on values used in the CCA. Intact (nondegraded) cement is assumed to have a permeability of  $5 \times 10^{-17} \text{ m}^2$ , consistent with the value used in the CCA to describe borehole plugs during the first 200 years after their emplacement. Conceptually, this is the value we would have used for the permeability of the borehole above and below the injection horizon if we had simulated a properly functioning injection well. We did not simulate this case, although we believe it is the most likely condition in injection wells. Based on results described in Section 4.2 for higher permeability cases, we are confident that simulations using  $5 \times 10^{-17} \text{ m}^2$  for the borehole permeability would have shown no brine flowing out of the injection zone.

We used a value of  $10^{-11} \text{ m}^2$  to characterize the permeability of a fully degraded cement sheath. This is the upper end of the range of values used in the CCA to characterize the permeability of an abandoned borehole after plugs and casings have fully degraded and material has sloughed into the hole from the borehole walls. The value is in the middle of the range of permeabilities described by Freeze and Cherry (1979, p. 29) for clean sand and in the upper portion of the overlapping range described for silty sand.

We used two intermediate permeability values to characterize lesser degrees of degradation of the cement sheath:  $10^{-13.65} \text{ m}^2$  and  $10^{-12.5} \text{ m}^2$ . The first value was chosen as the median of a loguniform distribution between the values for intact cement and fully degraded cement. The second value was chosen as the median of the CCA distribution characterizing the permeability of an abandoned borehole.

### **3.1.2.2 Permeability of a Tubing/Packer and Casing Leak During Injection**

We used a single value,  $10^{-5} \text{ m}^2$ , to characterize the permeability of the borehole in cases that simulate tubing or packer and casing leaks. This value is not intended to represent an actual porous medium present along the flow path: realistically, for much of the length of the path flow will occur within an open pipe. Instead, we chose an extremely high value that allows essentially unrestricted flow through the borehole. Examination of the results shown in Section 4.0 indicates that the chosen value is high enough to prevent significant pressure drops due to flow through the borehole.

### **3.1.2.3 Permeability of the Borehole Above the Salado During Injection**

We assume that the borehole does not fail above the Salado during the period of active injection, and we therefore assign the portion of the borehole above the Salado Formation the permeability of cement during the period of active injection. In practice, some wells do leak in the near-surface section, but we believe it is conservative for the purpose of this analysis to neglect near-surface leaks because they will tend to reduce pressure and brine flow in the Salado.

#### **3.1.2.4 Permeability of the Borehole After Plugging and Abandonment**

Plugging and abandonment of the injection boreholes is assumed to be similar to conditions used for intrusion boreholes in the CCA. When the injection well is abandoned (either 50 or 150 years after injection begins, depending on the case being simulated) concrete plugs are assumed to be emplaced above the Salado Formation and directly below the Castile. (The continuous concrete plug and the three-plug configuration considered in the CCA are omitted here for simplicity. Inclusion of these plugging patterns would lessen the impact of injection on the Salado Formation.) Unlike the assumption made in the CCA, both plugs are assumed to fail 200 years after abandonment, allowing communication between the deeper units and the evaporites. The assumption that the lower plug will fail at 200 years is unrealistic because chemical conditions at that depth will greatly slow concrete degradation (see Appendix MASS, Section MASS16.3 and Attachment MASS 16-3 of the CCA), and is inconsistent with the assumption in the CCA that this plug will remain intact for at least 10,000 years. Assuming the lower plug will fail prematurely is a conservative assumption for the purposes of this analysis, however, because it increases the possibility that injected brine will continue to flow upward from deeper units after the borehole is abandoned. Plugs are also assumed to be emplaced deeper in the hole isolating each injection interval. As is the case for the plug at the base of the Castile Formation, these deeper plugs are unrealistically and conservatively assumed to fail after 200 years.

Two hundred years after abandonment, at the time the plugs are assumed to fail, the permeability of the injection boreholes is assigned the median value ( $10^{-12.5} \text{ m}^2$ ) from the range of values used in the CCA to characterize the material filling degraded boreholes. This value is reduced one order of magnitude (to  $10^{-13.5} \text{ m}^2$ ) through the lower salt section from MB139 to the Castile, 1,000 years after plug failure (1,200 years after abandonment) to remain consistent with the CCA. The rest of the borehole's permeability is unchanged during abandonment. Flow in the borehole at the Culebra is possible during this period, and pressure at the top of the borehole is held constant at a pressure corresponding to a water table elevation of 980 meters above mean sea level.

#### **3.1.3 The Repository**

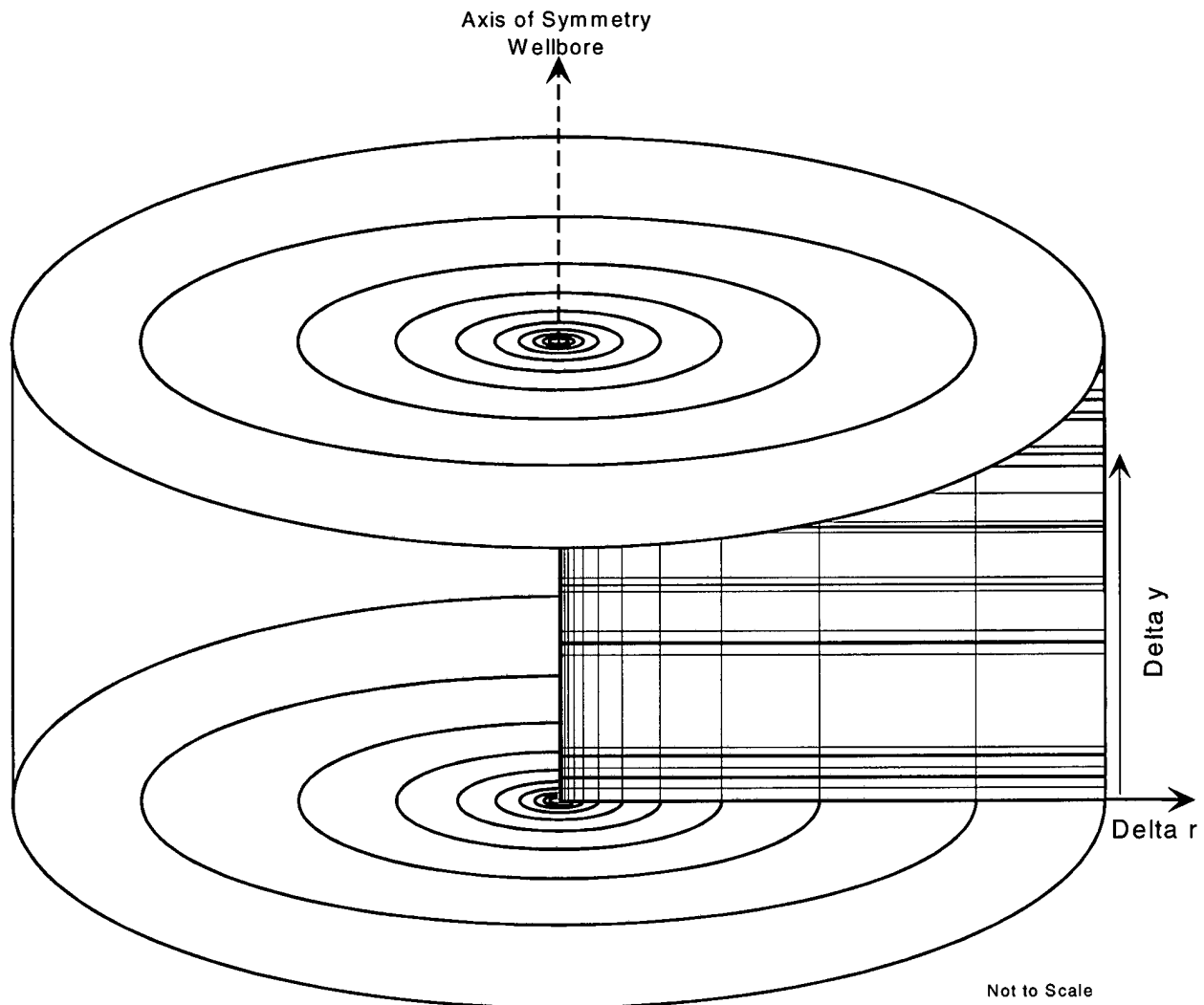
The representation of the repository used in the cross-sectional model is a simplification of those used in the CCA and by Stoelzel and O'Brien (1996). The shaft system has been omitted for computational efficiency because it has little or no effect on fluid flow with or without injection. The volume of the disturbed rock zone (DRZ) was reduced by approximately one half of what it

was in the Stoelzel and O'Brien (1996) model by changing the height from 5.118 meters to 2.23 meters. An additional borehole region was included in the mesh at the middle of the waste region to simulate the effects of future intrusions. However, this region was never "activated," or assigned borehole properties, because the injection well(s) did not significantly influence the pressure or saturation profiles in the waste region. These changes were incorporated as per EPA's written request (see Section 1.0).

### ***3.2 The Radial Model***

Figure 2 shows the conceptualization of the single-well radial model. This model is based on the assumption that flow is radially away from or toward the wellbore, and that other sources and sinks in the region, including the repository, are sufficiently far from the injection well to have a negligible effect on flow into and out of the well. We chose this geometry in part to address the EPA's concern *g* (see Section 1.0), because the radial geometry simulates flow into the full 360-degree cylinder around the borehole. Our intent in developing this model was to calculate total flow into the anhydrite layers closest to WIPP (MB138 and MB139). If flow volumes were large, we planned to use the radial model to calculate a source term to be used in a two-dimensional areal model simulating flow and fracturing in MB139 between one or more injection wells and the WIPP. Based on model results described in Section 4.2.1, however, we concluded that it was not necessary to proceed with the development of the areal model.

The wellbore in the radial model is meshed discretely in the first vertical row of grid-blocks, and acts as the axis of symmetry surrounded by successively larger "cylinders". To accommodate BRAGFLO's 2D finite difference mesh requirements, each 360 degree cylinder is translated to an equivalent volume rectangular grid-block, where  $\Delta x$  is equal to  $\Delta r$ , and the cylindrical volume is made up, or flared, via the "thickness" dimension (Figure 3).



**Figure 2: Single Well Radial Model Conceptualization**

Figure 3 illustrates the single-well radial flaring as implemented in BRAGFLO. The thinner layers represent the various injection intervals and anhydrite interbeds. Actual delta x (delta r), delta y, and thickness dimensions are tabulated in Appendix A. The layers are horizontal (i.e., no formation dip). Unlike the CCA BRAGFLO mesh, the layering does not extend to the surface to include the Dewey Lake, Santa Rosa, and other formations. Instead, the layering stops at the Culebra. Note that the layering differs from that of the CCA and Stoelzel and O'Brien's (1996) model by the addition of three more anhydrite layers in the Salado and Castile (see section 3.1.1).

*Initial and Boundary Conditions:*

- Initial brine saturations are set at 100% throughout the mesh. Initial brine pressures are equivalent to the hydrostatic gradient (measured from the surface) for the Bell Canyon layer and deeper, and calculated at a 0.84 psi/ft (18,947 Pa/m) gradient at the MB 139 elevation for the Salado and Castile layers.
- Dirichlet boundary conditions (constant pressure) equivalent to the initial pressures are assigned to the outermost column of grid-blocks, representing the farthest most region in each layer out from the wellbore.
- As in the CCA calculations, there is a five-year time period (from -5 to 0 years) to allow the mesh to equilibrate before the well boundary conditions are “turned on”.

*Representation of the injection wellbore:*

The first vertical column of grid-blocks (at  $I = 1$ ) is meshed such that the delta x times thickness area (vertical grid-block interface) is equivalent to that of a 12.25 inch diameter bit (0.1556 m radius), consistent with the bit diameter used in the CCA. Initially, the wellbore column is assigned properties equivalent to the layers it intersects, but is re-assigned either cement leak or casing leak properties over various intervals during the time period over which the leak occurs. After the period(s) of active injection, the borehole sections of interest are re-assigned plugged, or open, and later abandoned, borehole properties for the duration of the 10,000-year simulation period. This is similar to the treatment of intrusion boreholes in the CCA. During this time a constant-pressure boundary condition is assigned to the wellbore grid-block at the top layer (Culebra) equivalent to the water table pressure at that depth. Brine injection is simulated by assigning specific constant injection pressures in the wellbore regions at the grid-blocks adjacent to the injection layers of interest for that time period. The leaky wellbore permeabilities and injection pressures used for each radial case are explained further in sections 3.1.2 and 4.1.1.

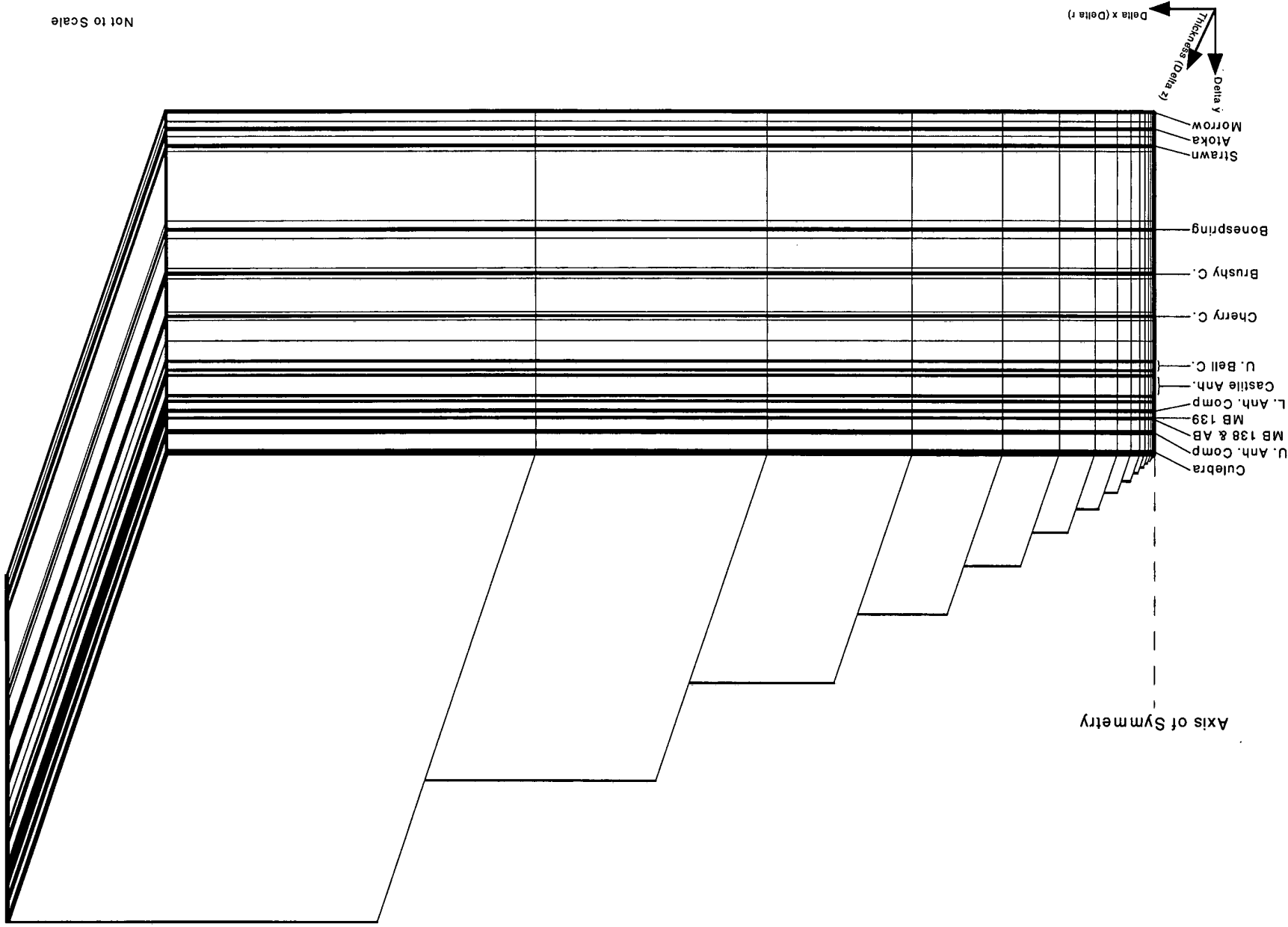


Figure 3: Illustration of 2D Single Well Finite-Difference Grid with Radial Flaring in "Thickness" Direction

Information Only

### 3.3 The Cross-Sectional Model

Figure 4 shows the mesh used for the cross-sectional model on a unit scale. The layering is identical to that used in the radial model, and the grid-block dimensions are also tabulated in Appendix A. The model differs from the radial model in the following ways:

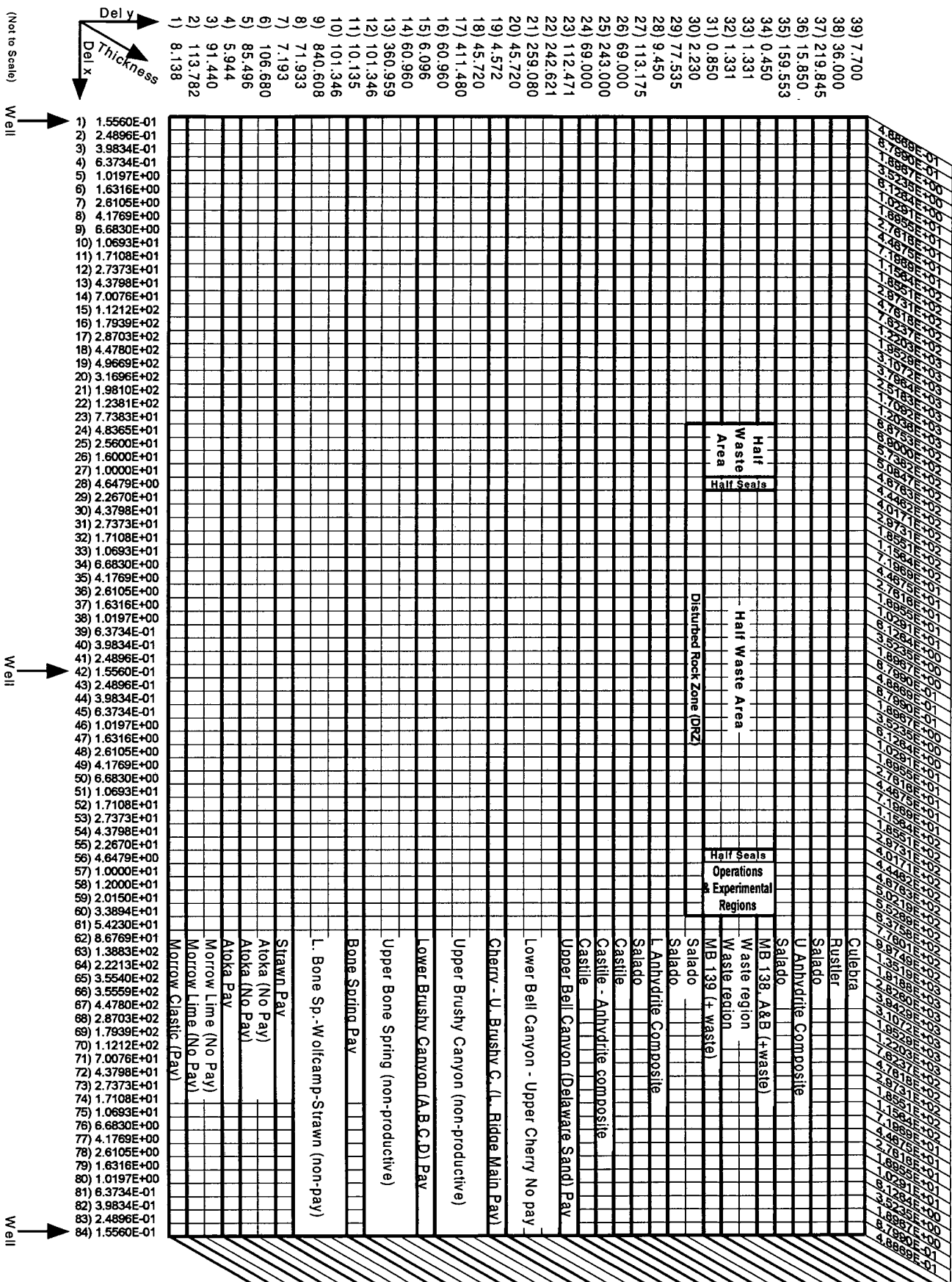
- The mesh contains a waste region, which behaves similarly to the way the waste region is modeled in the CCA. This includes gas generation via the corrosion model, creep closure of the salt, panel seal regions, and grid-blocks representing the experimental and operations regions.
- As in Stoelzel and O'Brien's (1996) model, the disturbed rock zone (DRZ) exists below the waste, not above and below the waste as it is modeled in the CCA. The height of the DRZ has been reduced as per EPA request (see item *(e)* in section 1.0), effectively reducing its pore volume by one half.
- The mesh contains three discrete wellbore regions, each gridded the same way as in the radial model. The "South" well is at the edge of the mesh at  $I=1$ , the "North" well is at the opposite edge at  $I=84$ , and the third well runs through the middle of the waste area at  $I=42$ . The third well was meant to act as a later "intrusion" well (see item *(c)* in section 1.0), but was never "activated" (or re-assigned wellbore properties from its initial layer properties), since little or no injected brine from the edge wells ever reaches the waste area (see section 4.3.6). The radial flaring outward from the wellbore regions is meant to simulate 180 degrees of effective flow inward from the edge wellbores and 180 degrees in each outward direction (or 360 degrees total) for the middle wellbore. The flaring in the thickness direction increases in volume up to the midway point between each edge wellbore and the middle wellbore (about 1,000 meters from the waste region in each direction). The flaring is illustrated in Figure 5. This differs from the flaring geometry used by Stoelzel and O'Brien (1996), as they flared outward from the wellbores in a 90 degree arc to a constant thickness of one quarter mile for most of the mesh. The geometry used in this study partially addresses EPA's concern *(g)* (section 1.0), by allowing potentially higher volumes of brine to flow into the waste region, relatively unrestricted by the geometry of the cross-sectional mesh.
- Treatment of injection and leaks is the same as in the single-well radial model (see section 4.1.2). The "production" of the waterflood layers (Bone Spring, Brushy Canyon, and Cherry Canyon) in the North well is simulated by creating a constant-pressure "sink" in the North wellbore grid-blocks adjacent to the layer being waterflooded from the South well during the same time period.



Initial conditions are the same as in the radial model, except in the waste region, which is treated the same as in the CCA calculations (i.e., set to atmospheric pressure and low initial brine saturation at time zero).

Constant-pressure sources and sinks simulate injection and production in the wellbores and the water-table pressure in the Culebra during the abandoned phase of the wells. As in the CCA models, the corrosion submodel provides a source of gas, as well as a brine sink, in the waste region. All of the "sides" of the cross-sectional model are no-flow boundaries; i.e., at the bottom layer, top layer (except at the wellbore grid blocks in the upper corners where the Culebra water-table pressure is held constant during the abandoned phase of the wells), and edge (wellbore region) layers, except during the active injection/production times detailed in Section 4.1.2.

The cross-sectional mesh was designed to represent radially divergent flow out of the wellbores and radially convergent flow into the repository in a two-dimensional geometry. Flow away from (and towards) the wellbores is approximately radial (as described for the radial model in Section 3.2) for approximately half the distance between the wellbores and the repository. Closer to the repository, flow is approximately radial toward (or away from) the repository. Thus, all brine flowing away from the wellbores within the 180-degree arcs facing the repository has the potential to flow to the repository. Brine flowing away from (or toward) the wellbores in the 180-degree arcs facing away from the repository is not modeled, and is assumed to have no effect on repository conditions. We believe that the geometry is conservative with respect to flow toward the repository from the inward-facing 180-degree arcs, because no-flow boundaries prevent fluid from leaving the model in the third (thickness) dimension. We believe it is reasonable to assume that the repository is sufficiently distant from the wellbores that flow occurring out of the wellbores away from the repository can be neglected. As discussed in Section 3.2, we initially planned to develop a two-dimensional areal model of flow and fracturing in MB139 should flows into the anhydrite layers be large enough to bring the adequacy of this assumption into question. Model results described in Section 4.2 show very low total brine flows into the anhydrite layers, thus we did not continue with development of the areal model.



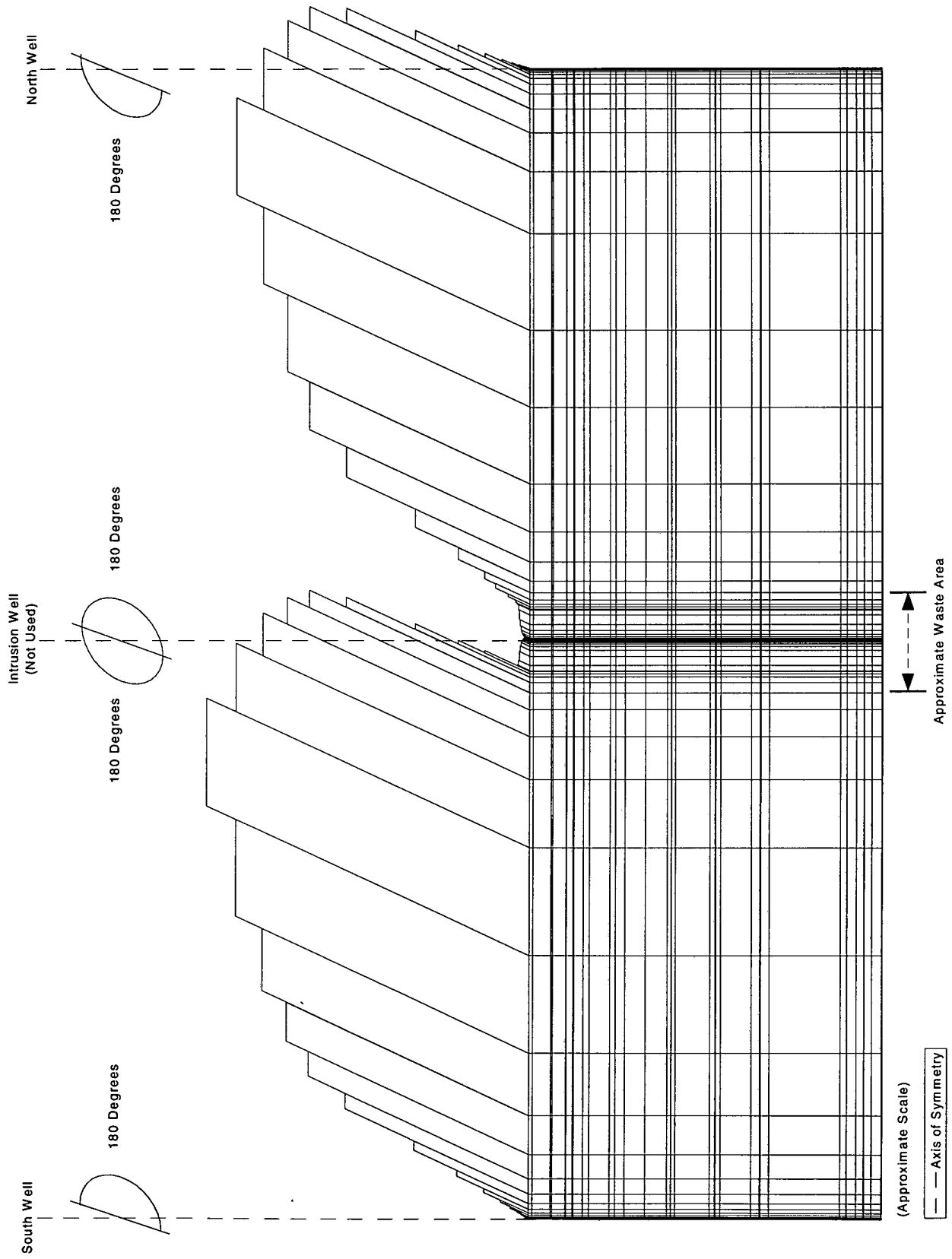


Figure 5: Cross-Sectional Model with Radial Flaring Illustrated

## 4.0 Model Results

This chapter describes results of 10 runs using the radial model and 1 model run using the cross-sectional model. All cases simulated a total of 10,000 years, including an initial period of either 50 or 150 years of fluid injection, a 200-year period when the borehole was assumed to be plugged, and a remaining period in which the plugs were assumed to have degraded. See Section 3.1.2.4 for a discussion of the assumptions about properties of the borehole during the period of plugging and abandonment.

### 4.1 Cases Modeled

#### 4.1.1 The Radial Model Cases

Details of the design of the 10 radial model cases are summarized in Tables 1 through 3. These cases fall into three groups, each of which has a different purpose.

##### 4.1.1.1 Radial Cases R1 through R3

As summarized in Table 1, cases R1 through R3 simulate leaks through degraded cement sheaths during 150 years of continuous injection at a single location. Salt water disposal is simulated in the Bell Canyon from 0 to 50 years and again from 100 to 150 years, using an injection gradient of 0.725 psi/ft. Waterflood injection is simulated in the Cherry Canyon from 50 to 100 years, using a 0.725 psi/ft gradient in R1 and a 1.0 psi/ft injection gradient in R2 and R3. As noted in the previous section, the higher value exceeds pressure gradients used in current practice, but is a reasonable upper bound for possible future injection pressure gradients. The three cases also differ in the permeability assigned to the borehole during the period of active injection: case R1 uses a permeability of  $10^{-13.65} \text{ m}^2$ , case R2 uses  $10^{-12.5} \text{ m}^2$ , and case R3 uses  $10^{-11} \text{ m}^2$ . All other properties of these cases are identical.

**Table 1: Summary of the Specification of Radial Cases R1 through R3**

Case Number	Leaky BH Permeability $\log(\text{m}^2)$	U Bell Canyon Permeability $\text{m}^2$	Bell Canyon SWD		Cherry Can WF		Brushy Can WF		Bonespring WF	
			Interval Inj gradient (psi/ft)	Injection Time (years)	Interval Inj gradient (psi/ft)	Injection Time (years)	Interval Inj grad (psi/ft)	Injection Time (years)	Interval Inj grad (psi/ft)	Injection Time (years)
R1	-13.65	1.27E-13	0.725	0 TO 50, 100 TO 150	0.725	0 TO 50	0.725	50 TO 100	0.725	100 TO 150
R2	-12.50	1.27E-13	1.000	0 TO 50, 100 TO 150	1.000	0 TO 50	1.000	50 TO 100	1.000	100 TO 150
R3	-11.00	1.27E-13	1.000	0 TO 50, 100 TO 150	1.000	0 TO 50	1.000	50 TO 100	1.000	100 TO 150

### 4.1.1.2 Radial Cases R4 through R7

Cases R4 through R7 examine 50 years of brine injection with both tubing/casing leaks and a partially degraded cement sheath (Table 2). The total duration of injection for these cases was limited to 50 years because the cases are intended to simulate the behavior of a leaks resulting from a single oil field. More than a one such oil field with leaky injection wells could exist near the WIPP in the next 150 years, but they are unlikely to occur in the same location. Thus, the 50-year time intervals simulated in cases R4 through R7 can be thought of conceptually as occurring anywhere outside the Land Withdrawal Boundary at any time during the next 150 years.

**Table 2: Summary of the Specification of the Radial Model Cases R4 through R7**

Case Number	Bell Canyon SWD				Cherry Can WF				Brushy Can WF				Bonespring WF			
	Interval Inj grad (psi/ft)	Injection Time (years)	Borehole Perm from Bell Canyon to Rustler During Inj. Log m <sup>2</sup>		Interval Inj grad (psi/ft)	Injection Time (years)	Borehole Perm from Cherry C. to Rustler During Inj. Log m <sup>2</sup>		Interval Inj grad (psi/ft)	Injection Time (years)	Borehole Perm from Brushy C. to Rustler During Inj. Log m <sup>2</sup>		Interval Inj grad (psi/ft)	Injection Time (years)	Borehole Perm from Bonesprg to Rustler During Inj. Log m <sup>2</sup>	
R4	0.725	0 TO 50	-13.65 (0 to 30 yrs), -5.00 (30 to 50 yrs)	X	X	X		X	X	X		X	X	X		
R5	0.725	0 TO 50	-13.65 (0 to 30 yrs), -5.00 (30 to 50 yrs)	1.000	0 TO 50	-13.65 (0 to 40 yrs), -5.00 (40 to 50 yrs)		X	X	X		X	X	X		
R6	0.725	0 TO 50	-13.65 (0 to 30 yrs), -5.00 (30 to 50 yrs)	X	X	X		1.000	0 TO 50	-13.65 (0 to 40 yrs), -5.00 (40 to 50 yrs)		X	X	X		
R7	0.725	0 TO 50	-13.65 (0 to 30 yrs), -5.00 (30 to 50 yrs)	X	X	X		X	X	X		1.000	0 TO 50	-13.65 (0 to 40 yrs), -5.00 (40 to 50 yrs)		

Note: Permeability of U Bell Canyon is 1.2E-13 m<sup>2</sup> for Case Numbers R4 through R7

Cases R4 through R7 each assume that salt water disposal occurs into the Bell Canyon Formation from 0 to 50 years. The cases differ in the assumption of the depth of the waterflood operation. Waterflood injection does not occur in case R4, and occurs from 0 to 50 years into the Cherry Canyon in case R5, the Brushy Canyon in case R6, and the Bone Spring in R7. All borehole permeabilities during the period of active injection were set at 10<sup>-13.65</sup> m<sup>2</sup> except when tubing/casing leaks occurred. Tubing/casing leaks were assumed to occur with a frequency of 0.01 leaks per well per year of injection, as described in Section 2.2.3.2. Also as described in Section 2.2.3.2, we assumed that this would result in an aggregate of 10 years of tubing/casing leaks per field. Inconsistent with this premise, we conservatively assumed that tubing and casing leaks occurred in disposal operations for 20 years following 30 years of operations. Thus, permeability in the borehole from the Bell Canyon upward was 10<sup>-5</sup> m<sup>2</sup> from 30 to 50 years. Tubing/casing leaks were assumed to occur in waterflood operations for 10 years following 40 years of operation. Thus, permeability was increased to 10<sup>-5</sup> m<sup>2</sup> from the waterflood horizons upward for the final 10 years of injection.

### 4.1.1.3 Radial Cases R8 through R10

The final three radial cases, R8, R9, and R10, are special cases designed to examine model sensitivity to two input assumptions: the pressure gradient used for waterflood operations, and the permeability assigned to the Bell Canyon Formation. These cases do not simulate realistic conditions: to achieve relatively larger flows into the Salado Formation anhydrite layers and

therefore allow a clearer display of model sensitivity, we assumed 50 years of continuous tubing/casing leaks. Table 3 summarizes the specification of these cases.

**Table 3: Summary of the Specification of Radial Cases R8 through R10**

Case Number	Leaky BH Permeability log(m <sup>2</sup> )	U Bell Canyon Permeability m <sup>2</sup>	Bell Canyon SWD		Cherry Can WF		Brushy Can WF		Bonespring WF	
			Interval Inj gradient (psi/ft)	Injection Time (years)	Interval Inj gradient (psi/ft)	Injection Time (years)	Interval Inj grad (psi/ft)	Injection Time (years)	Interval Inj grad (psi/ft)	Injection Time (years)
R8	-5.00	1.27E-13	0.725	0 TO 50	1.000	0 TO 50	X	X	X	X
R9	-5.00	1.27E-12	0.725	0 TO 50	1.000	0 TO 50	X	X	X	X
R10	-5.00	1.27E-12	0.725	0 TO 50	0.725	0 TO 50	X	X	X	X

Case R8 simulates 50 years of simultaneous salt water disposal into the Bell Canyon and waterflooding into the Cherry Canyon, assuming a continuous tubing/casing leak with the borehole permeability set at  $10^{-5} \text{ m}^2$ . Except for the unrealistic assumption of the continuous tubing/casing leak, other assumptions are similar to those used in Cases R1 through R7. Case R8 serves as a base case for comparison with cases R9 and R10. Case R9 examines model sensitivity to the assumed value of permeability in the Bell Canyon,  $10^{-13} \text{ m}^2$ . In direct response to a request from the EPA to “increase the transmissivity of the Bell Canyon to allow higher volumes of brine to be injected” (Trovato, 1997), we raised the permeability of the Bell Canyon one order of magnitude, to  $10^{-12} \text{ m}^2$  for this simulation. Case R10 is a modification of case R9 in which we examine the sensitivity of the model to the assumption that future waterflood operations will inject at higher pressures than those currently used. Injection into the Cherry Canyon is assumed to occur at a gradient of 0.725 psi/ft, consistent with current practice. Case R10 is otherwise like Case R9.

#### 4.1.2 The Cross-Sectional Model Case

Details of the design of the single cross-sectional case are summarized in Table 4. This case simulated 150 years of total injection. Salt water disposal occurred into the Bell Canyon Formation in the south well from 0 to 50 years and again from 100 to 150 years, and in the north well from 50 to 100 years. Waterflood injection occurred continuously in the south well, beginning in the Cherry Canyon Formation from 0 to 50 years, shifting to the Brushy Canyon Formation from 50 to 100 years, and finally injecting into the deeper Bone Spring Formation between 100 and 150 years. Oil production was assumed to occur from the north well simultaneously with injection in the same horizon in the south well.



**Table 4: Summary of the Specification of the Cross-Sectional Model Case**

Bell Canyon SWD			Cherry Canyon WF		
Interval Inj gradient (psi/ft)	Injection Time (years)	Borehole Permeability from Bell Canyon to Rustler Log m <sup>2</sup>	Interval Inj/prod gradient (psi/ft)	Injection/prod Time (years)	Borehole Permeability from Cherry C. to Bell C. Log m <sup>2</sup>
0.725 (both South and North Wells)	0 TO 50, 100 to 150 (South Well), 50 to 100 (North Well)	South: -13.65 (0 to 30, 50 to 90, 100 to 130 yrs), -5 (30 to 50, 90 to 100, 130 to 150 yrs) North: -13.65 (0 to 80, 100 to 150 yrs), -5 (80 to 100 yrs)	South: 1.0 (Injection), North: 0.512 (production)	0 TO 50 for both South and North	South: -13.65 (0 to 40, 50 to 90, 100 to 140 yrs), -5 (40 to 50, 90 to 100, 140 to 150 yrs) North: -13.65 (0 to 150 yrs)

Brushy Canyon WF			Bonespring WF		
Interval Inj/prod gradient (psi/ft)	Injection/prod Time (years)	Borehole Permeability from Brushy C. to Cherry C. Log m <sup>2</sup>	Interval Inj/prod gradient (psi/ft)	Injection/prod Time (years)	Borehole Permeability from Bonesprg to Brushy C. Log m <sup>2</sup>
South: 1.0 (Injection), North: 0.512 (production)	50 to 100 for both South and North	South: -13.65 (50 to 90, 100 to 140 yrs), -5 (90 to 100, 140 to 150 yrs) North: -13.65 (0 to 150 yrs)	South: 1.0 (Injection), North: 0.512 (production)	100 to 150 for both South and North	South: -13.65 (100 to 140 yrs), -5 (140 to 150 yrs) North: -13.65 (0 to 150 yrs)

Injection pressure for salt water disposal was set in the Bell Canyon to be consistent with a 0.725 psi/ft gradient, which is the highest gradient used in the region today for disposal injection, and is the highest gradient reasonably foreseeable in the future. Injection pressures for waterflooding were set in each of the deeper units to be consistent with a 1.0 psi/ft gradient, which exceeds the highest gradient used in the region today (see Section 2.1.2), but which is a reasonable upper bound for gradients that might be used in the future as oil fields mature. Production pressures in the north well were set consistent with a 0.512 psi/ft gradient (0.013 psi/ft below a brine hydrostatic gradient of 0.525 psi/ft), similar to pumping gradients used in oil production operations.

This case was designed to simulate the behavior of the WIPP disposal system in the presence of poorly maintained injection operations directly adjacent to the Land Withdrawal Boundary. Thus, leaks were assumed to occur through both partially degraded cement sheaths and combination tubing/casing leaks. Both boreholes were assigned a permeability of  $10^{-13.65} \text{ m}^2$  at all times during active injection except when tubing/casing leaks occurred. Tubing/casing leaks were assumed to occur with a frequency of 0.01 leaks per well per year of injection, as described in Section 2.2.3.2. Also as described in Section 2.2.3.2, we assumed that this would result in an aggregate of 10 years of tubing/casing leaks per field. Inconsistent with this premise, we conservatively assumed that tubing and casing leaks occurred in disposal operations for 20 years following 30 years of operations: thus, permeability in both boreholes from the Bell Canyon up was increased to  $10^{-5} \text{ m}^2$  from 30 to 50 years and from 130 to 150 years. Tubing/casing leaks were assumed to occur in waterflood injectors for 10 years following 40 years of operation: thus, permeability in the south borehole was increased to  $10^{-5} \text{ m}^2$  from the Cherry Canyon up from 40 to 50 years, from the Brushy Canyon up from 90 to 100 years, and from the Bone Spring up from 140 to 150 years.



## 4.2 Radial Model Results

Performance measures described in the following sections for each of the 10 radial model cases include the total amount of brine injected into the borehole, the total amount of brine leaking above the Bell Canyon Formation, brine flow into MB139 and other anhydrite layers, pressure in the wellbore at MB139, and the distance fractures propagate from the wellbore in each anhydrite layer.

### 4.2.1 Volume of Brine Injected (Radial Models)

Figure 6 shows the cumulative amount of brine injected from the wellbore into all formations, for each of the 10 radial cases. Cases R1, R2, and R3 show injection continuing for 150 years, consistent with the design of the cases. All other cases show injection ceasing at 50 years.

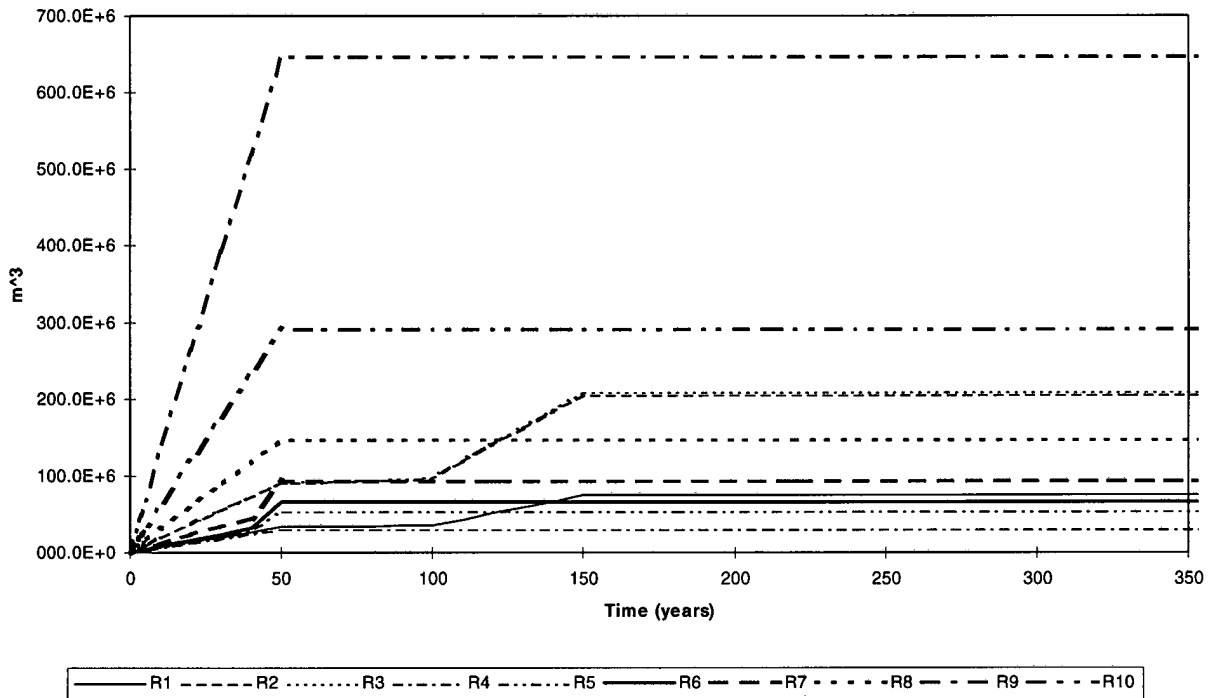
Total injected volumes range from  $30.8 \times 10^6 \text{ m}^3$  for case R4 to  $647.4 \times 10^6 \text{ m}^3$  for R9. As expected given the intent to simulate the behavior of multiple injection wells rather than a single well, these numbers are much larger than the volumes of brine that can be expected to be injected by any single well in the region. The larger volumes also unrealistically overestimate the total volume of brine that might reasonably be injected into a representative oil field during its operational lifetime. For example, Neill (1997) reports that the proposed waterflood operation at the Avalon field north of Carlsbad is designed to inject  $22.4 \times 10^6 \text{ m}^3$  (141 million barrels) of brine during 40 years. We believe that the smaller injection volumes calculated by our model are plausible, consistent with the conservative assumptions of the analysis about the duration of leaks. We do not believe that our larger calculated volumes could occur: oil-field operators would not continue injection with rates an order of magnitude or more above the expected injection rates. However, we believe that the overestimation of total injection volumes is conservative with respect to the performance of the WIPP, in that it increases the volume of brine available to leak into the Salado Formation anhydrites.

Several factors contribute to the overestimation of the total volume of brine injected. All cases considered here assume some degree of leakage from the injection well, increasing the rate at which injection can occur. All cases assume disposal injection wells operate continuously at a constant pressure, whereas actual disposal wells operate intermittently at the lowest pressure necessary for efficient disposal. All cases except R4 (the lowest volume case) assume that disposal injection and waterflood injection occur simultaneously into multiple horizons.

Comparison of the brine volume injected for case R1 with cases R2 and R3 shows that increasing the permeability of the degraded cement sheath from  $10^{-13.65} \text{ m}^2$  to  $10^{-12.5} \text{ m}^2$  more than doubles the total volume brine injected during the life of the well. This suggests that, although cement leaks will not be detected in the field by monitoring pressure in the injection well, they might be detected by monitoring the total volume of brine injected, particularly in a waterflood operation where the operator tracks production and injection volumes closely to maximize profitability.

Comparison of cases R4 through R7 shows that as the depth of injection increases, the volume of brine injected also increases. This is due to the increase in pressure associated with the greater injection depth, which results in greater flow up the leaky borehole into other units.

Comparison of cases R8, R9, and R10 shows that increasing the permeability of the Bell Canyon Formation, as requested by the EPA (Trovato, 1997), more than triples the total brine injection (cases R8 and R9). We do not believe the larger injection volume associated with the higher permeability value is realistic, however. Case R10, which combines the higher Bell Canyon permeability with an injection gradient consistent with current practice, shows a total injection volume intermediate between R8 and R9, and demonstrates that the total injection volume is sensitive to the assumed injection pressure.



**Figure 6: Cumulative Brine Injected Into All Formations: Radial Models**

#### 4.2.2 Volume of Brine Leaking above the Bell Canyon Formation (Radial Models)

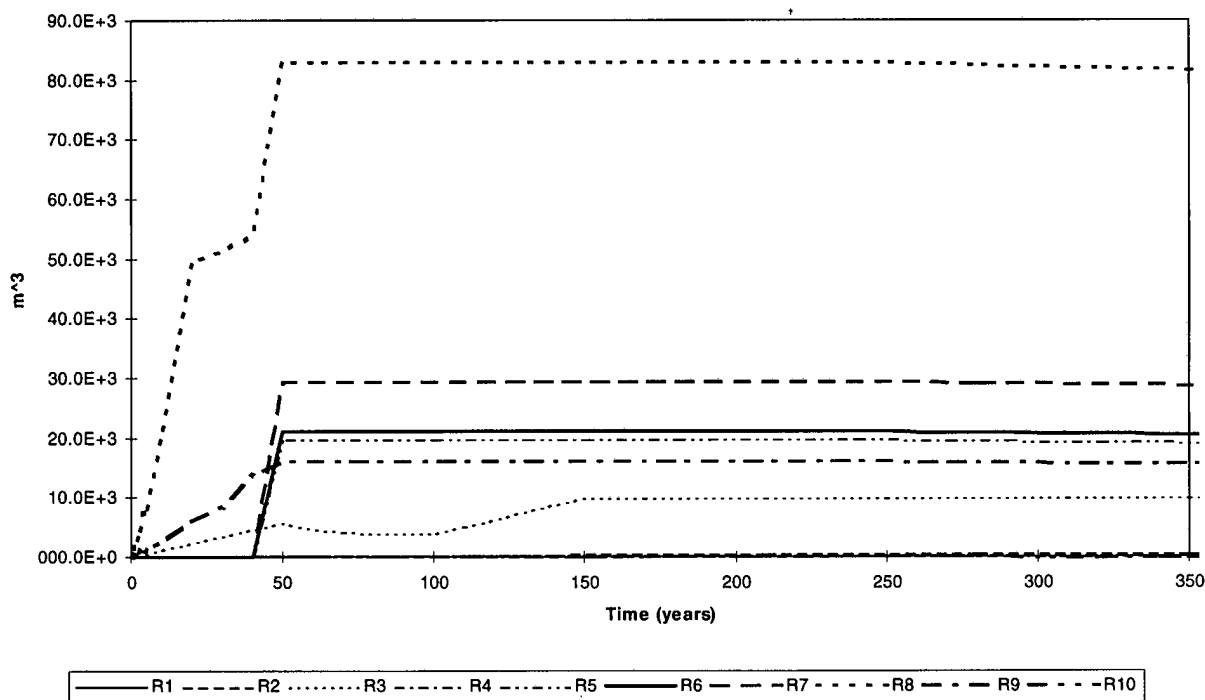
Figure 7 shows the cumulative volume of brine flowing up the borehole at the top of the Bell Canyon Formation. In comparing Figures 6 and 7, note the change in scale: volumes of brine flowing above the Bell Canyon are approximately 3 orders of magnitude less than the total volume injected. This smaller volume of brine represents the portion of leakage from the wellbore that enters the evaporite sequence. Additional leakage occurs into lower units in the model, but it does not contribute to flow in the anhydrites.

Cases R1, R2, R4, and R10 show essentially no flow above the Bell Canyon. We conclude from cases R1 and R2 that, conditional on the assumptions of the model, cement leaks alone do not result in significant flow into the anhydrite layers if cement permeability remains  $10^{-12.5} \text{ m}^2$  or lower, even if they persist for 150 years with injection occurring at pressure gradients up to 1.0 psi/ft. We conclude from case R4 that 20 years of continuous casing and tubing leak during salt water disposal into the Bell Canyon does not result in significant flow into the anhydrite layers. We conclude from Case R10 that even 50 years of continuous casing and tubing leak from waterflood injection into the Cherry Canyon does not result in significant flow into the anhydrite layers.

Case R3 shows that some brine does flow above the Bell Canyon with a borehole permeability of  $10^{-11} \text{ m}^2$ . This case also shows a period of downward flow at the top of the Bell Canyon, from 50 to 100 years. Downward flow occurs during the time when waterflood injection occurs into the Brushy Canyon without simultaneous disposal injection in the Bell Canyon. Without the additional injection provided by the disposal operation, all flow leaking upward from the deeper waterflood enters the Bell Canyon, and some of the brine forced upward during the previous 50 years flows downward and also enters the Bell Canyon. We believe this result is physically reasonable, and demonstrates the importance of the role of the more permeable units in determining flow from the borehole.

Comparison of cases R4 (no upward flow) and cases R5, R6, and R7 shows that upward leakage increases with the depth of injection and therefore with injection pressure. This is a reasonable and expected result. Higher injection pressures cause more leakage.

Examination of the leakage above the Bell Canyon for cases R8 and R9 shows a reversal from their relative positions on Figure 6. Increasing the Bell Canyon permeability one order of magnitude (R9) greatly increases the total volume of brine injected (Figure 6), but decreases the amount leaking upward into the evaporites. The lower value of permeability allows less of the brine leaking upward from the deeper waterflood injection to enter the Bell Canyon, increasing the total upward leakage. We conclude from this result that increasing the permeability of the Bell Canyon causes smaller volumes of brine to reach the Salado anhydrite layers.



**Figure 7: Cumulative Brine Leaking Up Wellbore at Bell Canyon / Castile Interface: Radial Models**

#### 4.2.3 Volume of Brine Entering Anhydrite Layers (Radial Models)

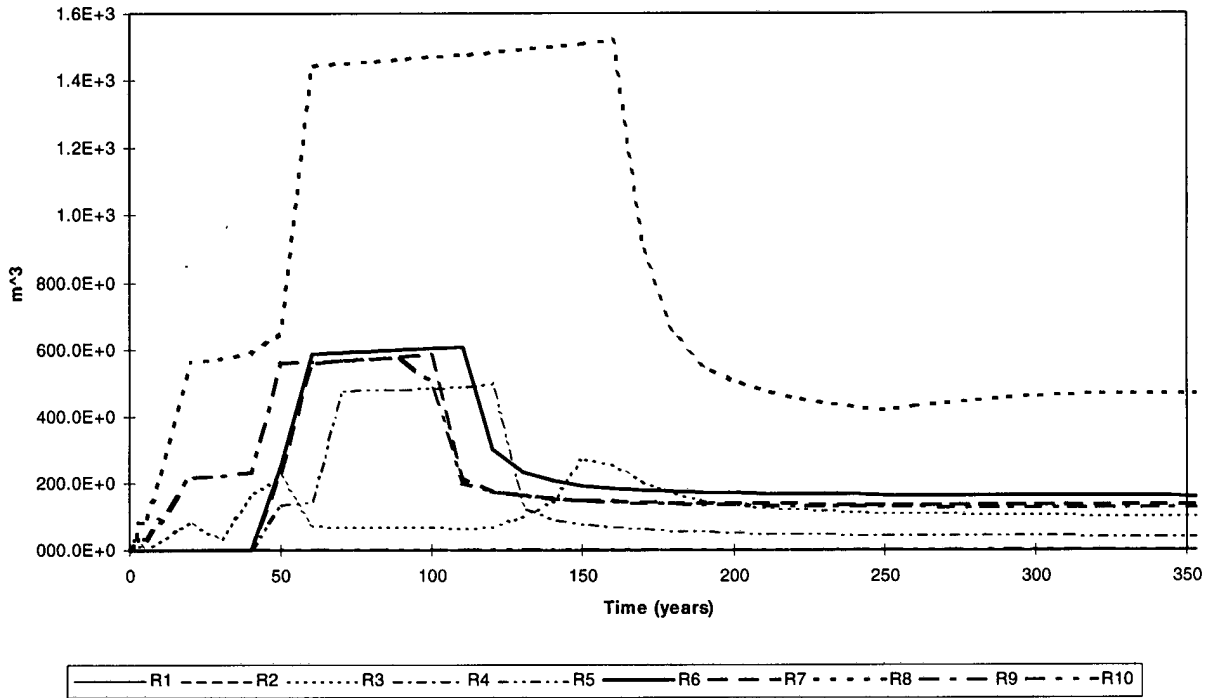
Figures 8 through 11 show the cumulative volume of brine entering the upper composite anhydrite layer in the Salado Formation, MB138, MB139, and the Castile Formation anhydrite for the first 350 years of the simulations. Results for the lower composite anhydrite layer in the Salado Formation are similar to those shown for the upper composite layer.

Interpretation of these figures shows that none of the realizations result in brine flows larger than approximately 1500 m<sup>3</sup> entering MB139 or MB138. This result alone is sufficient to confirm Stoelzel and O'Brien's (1996) conclusion that the volume of brine reaching the repository from injection operations would be comparable to or less than the amount expected from normal brine inflow under undisturbed conditions. These results also support Stoelzel and O'Brien's (1996) conclusion that their model presented a conservative analysis. Cases R1, R2, R4, and R10 result in no flow into MB 139 or MB138, consistent with the observation discussed in Section 4.3.2 that these resulted in essentially no flow above the Bell Canyon. Cases R5, R6, and R7 show as much as 600 m<sup>3</sup> of brine entering MB139. The largest brine flow results from Case 9, in which the casing and tubing leak was unrealistically assumed to persist for 50 years.

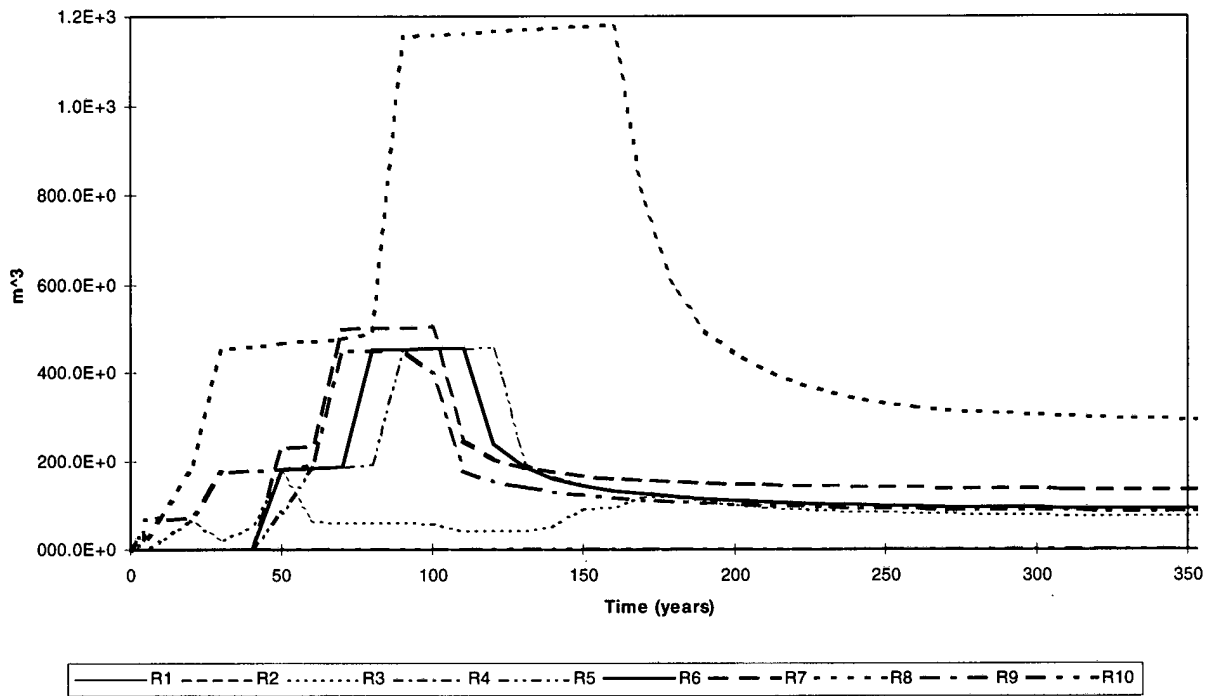
Larger volumes of brine (up to approximately 65,000 m<sup>3</sup>) enter the Castile anhydrite, and intermediate volumes enter the composite layers in the Salado. In all anhydrite layers, the unrealistic assumptions made in the design of case R8 result in the largest brine flows.

Figures 8 through 11 show that cross-flow up and down the borehole between anhydrite layers plays an important role in the simulations. For example, for cases R4 through R9 much of the brine flow into the upper composite anhydrite layer, MB138, and MB139 occurs after injection has ceased at 50 years. Cumulative flow into the Castile anhydrite, however, reaches a maximum at 50 years for these cases, and then declines as brine drains back into the borehole and flows upward into the overlying units. Similarly, flow into MB139 in case R8 reaches a maximum of 1,517 m<sup>3</sup> at approximately 160 to 170 years, and then declines as brine drains back into the hole and flows into the upper composite layer. These changes in flow direction are a physically reasonable response of the system as it adjusts to the initial high pressure pulse imposed by injection. The magnitude of cross-flow is greatly increased, however, by the assumptions made about the plugging and abandonment of the well (Section 3.1.2.4). During the first 200 years following the end of injection, the borehole is assumed to be open throughout the Castile and Salado, and isolated from the deeper horizons. No additional brine enters the evaporites during this period (see Figure 7), and no external pressure sources or sinks act on the system. Cross-flow occurs as calculated, dependent on pressure gradients and the initial and calculated permeabilities of each layer.

Following the time at which borehole plugs are assumed to degrade (350 years for cases R1 through R3 and 250 years for cases R4 through R10), flow occurs into the wellbore from all anhydrite layers because the far-field pressure in the evaporite section (see Section 3.1) exceeds the hydrostatic pressure in the wellbore. This slow draining of the anhydrite layers continues throughout the remainder of the 10,000 years.

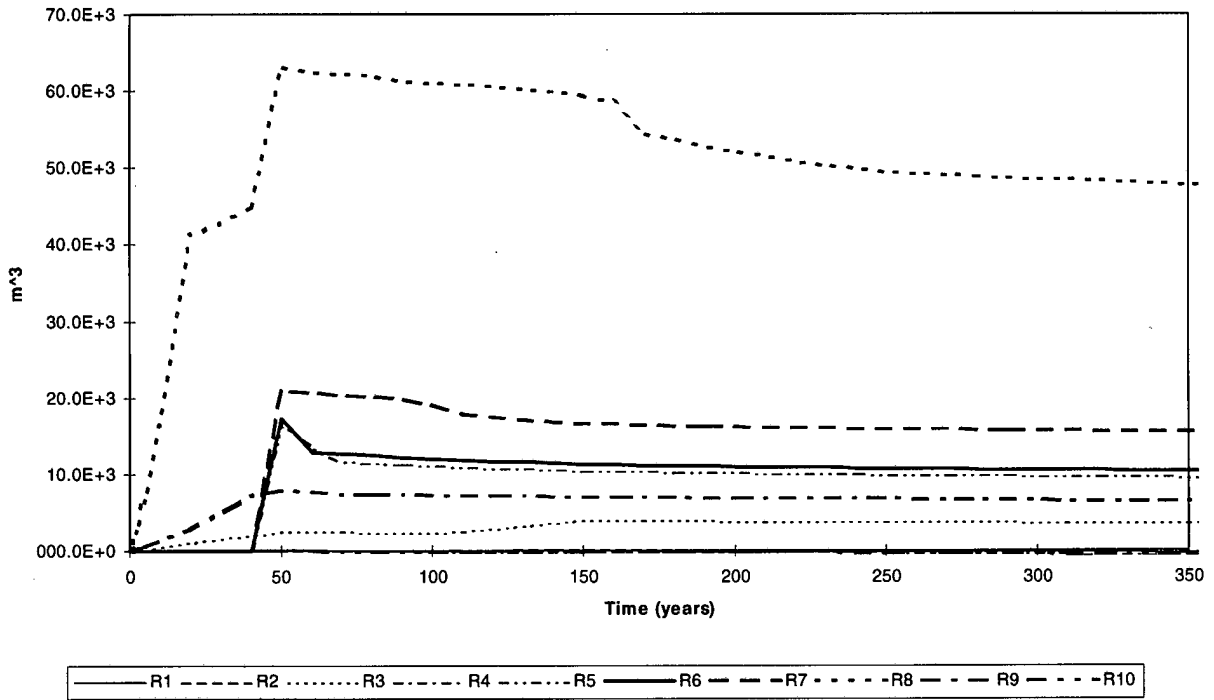


**Figure 8: Cumulative Flow into Marker Bed 139: Radial Models**

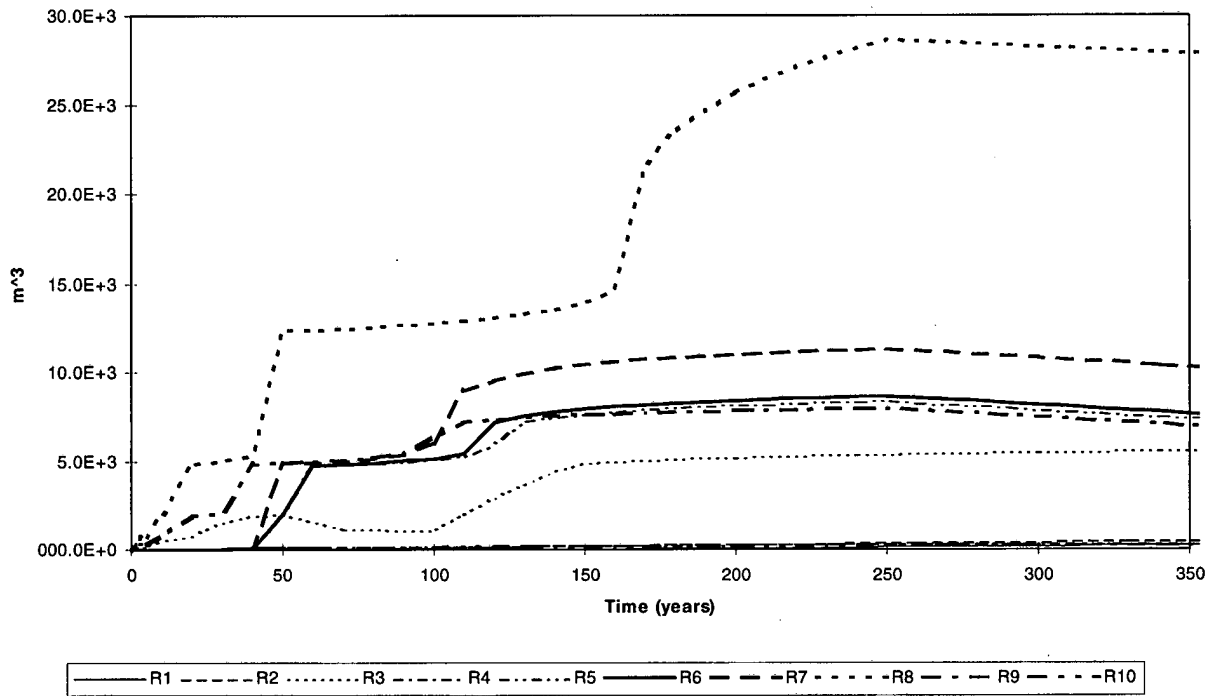


**Figure 9: Cumulative Flow into Marker Bed 138: Radial Models**





**Figure 10: Cumulative Flow into Castile Anhydrite: Radial Models**



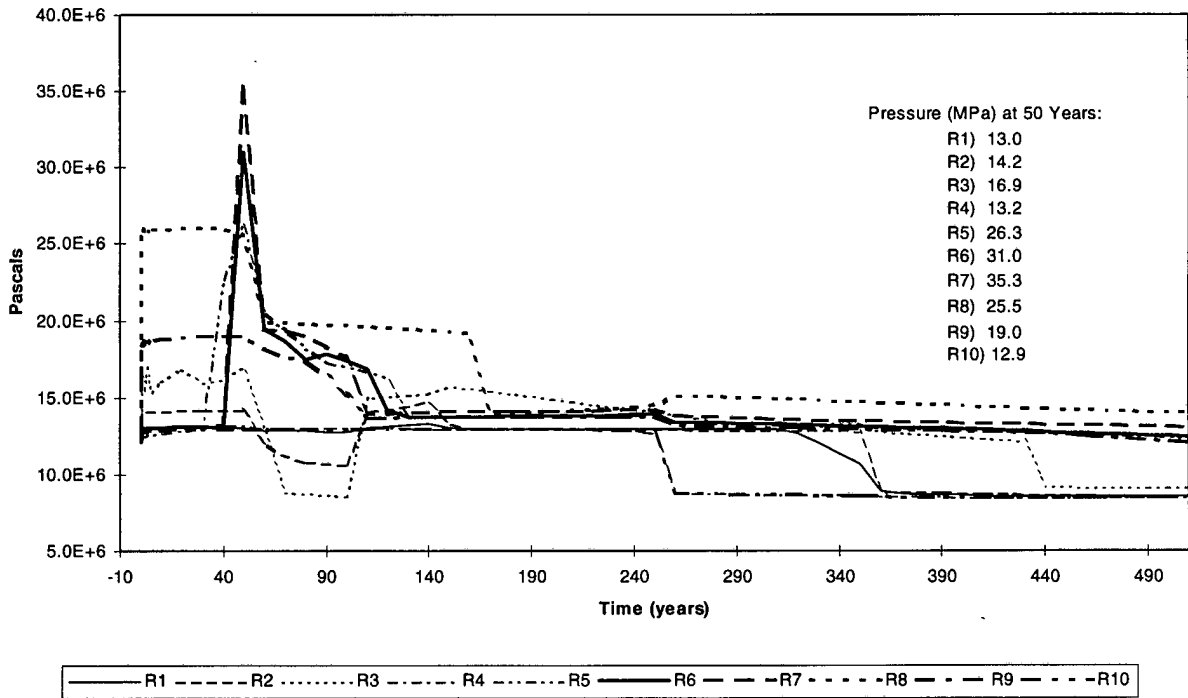
**Figure 11: Cumulative Flow into Upper Anhydrite Composite: Radial Models**

Information Only

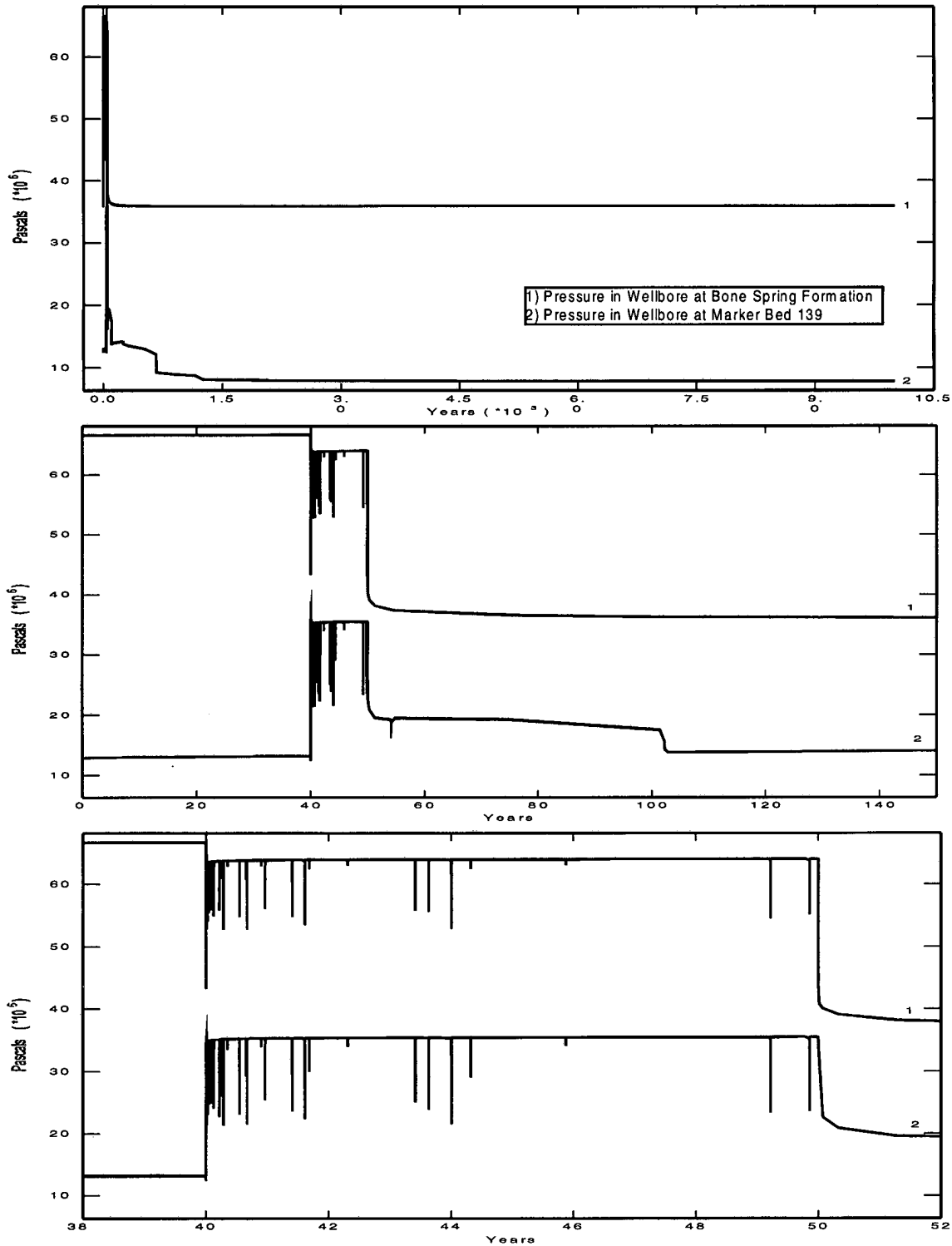
#### 4.2.4 Pressure in the Injection Wellbore at MB 139 (Radial Models)

Figure 12 shows 500-yr time histories of the pressure in the wellbore at the elevation of MB139. Pressure histories show the effects of leakage from injection in deeper units and cross-flow between anhydrite layers, as discussed in Section 4.2.3. Pressure in the wellbore at this elevation is generally above the initial pressure at MB139 (12.47 MPa) during times of active injection. Pressure in the wellbore falls below the initial pressure during times of cross-flow from MB139 upwards to the upper composite anhydrite.

All cases that result in brine flow into MB139 show pressures in the wellbore above lithostatic (14.7 MPa) for that depth. Peak pressures at MB139 during tubing and casing leaks (cases R4-R10) rise rapidly to levels that are up to approximately 90% of the total injection pressure, corrected for the 0.525 psi/ft hydrostatic gradient. For example, the peak pressure at MB139 calculated for case R7, 35.3 MPa, corresponds to an injection pressure in the Bone Spring of 66.9 MPa at a depth of 2959 m. If there were no pressure loss at all along the leak pathway other than the hydrostatic drop, the full injection pressure would correspond to 39.6 MPa at the 658 m depth of MB139. The pressure differentials for Case R7 are illustrated in Figure 13, which shows the wellbore pressures at the Bone Spring and MB139 at different scales for 10,000 years, the first 150 years, and from 40 to 50 years, which is the period of the high permeability tubing/casing leak. The fluctuations in pressure illustrate the transient nature of the fracturing model, which is responding to the dynamic permeability alterations of the anhydrite layers as well as cross-flows between them. The high injection pressures at MB139 and rapid pressure responses confirm the assumption that  $10^{-5} \text{ m}^2$  is a sufficiently high permeability to characterize flow during casing and tubing leaks, as described in Section 3.1.2.2. The small pressure drop that occurs in cases with tubing and casing leaks (e.g., the drop from 39.6 MPa to 35.3 MPa in case R7 discussed above) is due primarily to flow into other, deeper units that reduces the volume of brine reaching MB139. This pressure drop would be larger if the assumption of a pressure-limited, rather than rate-limited, source term had not resulted in an essentially unlimited supply of injection brine.



**Figure 12: Pressure in Wellbore at Marker Bed 139: Radial Models**



**Figure 13: Pressure Response in Wellbore at Various Times for Radial Case R7**

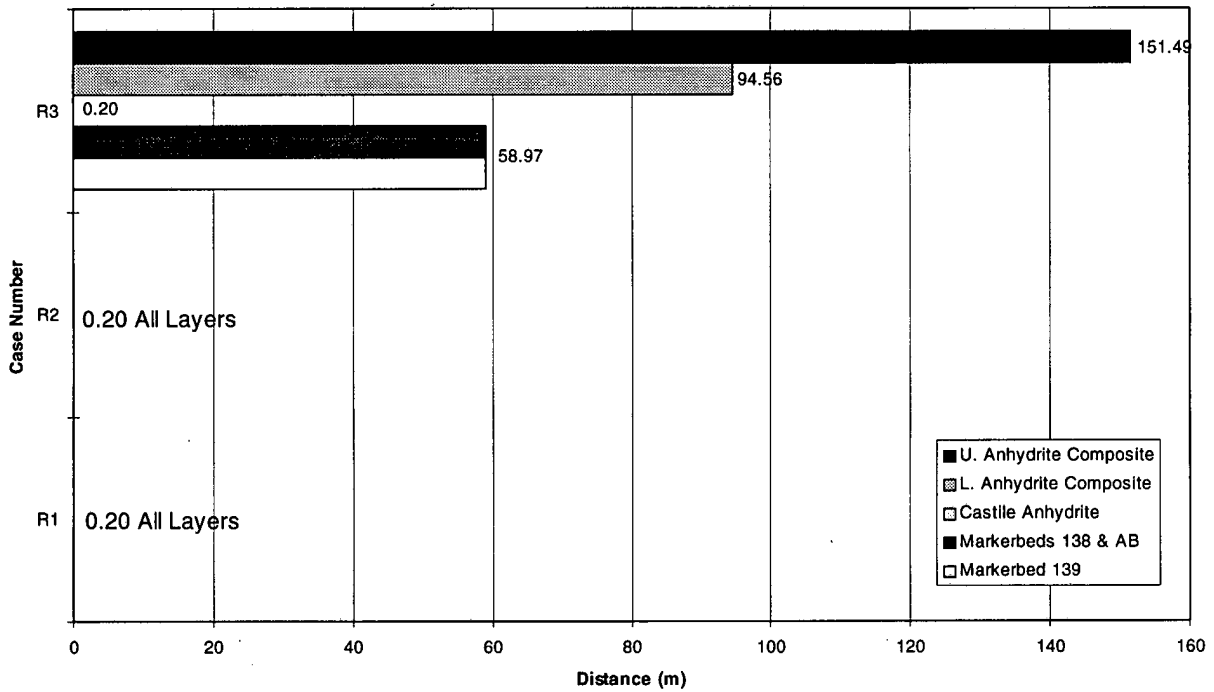
#### 4.2.5 Distance of Fracture Propagation in Anhydrite Layers (Radial Models)

Figures 14, 15, and 16 show the maximum distance that permeabilities of  $10^{-12} \text{ m}^2$  or greater were calculated for each of the anhydrite layers. We interpret this region to correspond to the region in which fracturing of the anhydrite is essentially complete. Because the fracture model allows a continuous increase in anhydrite permeability above its initial value, this distance does not represent the maximum extent of any change in anhydrite permeability. Lower permeability "fractures" extend somewhat further in some cases. The precision in the reported values reflects cell dimensions (see Section 3.2), and our interpretation therefore emphasizes the general trends and relative distances.

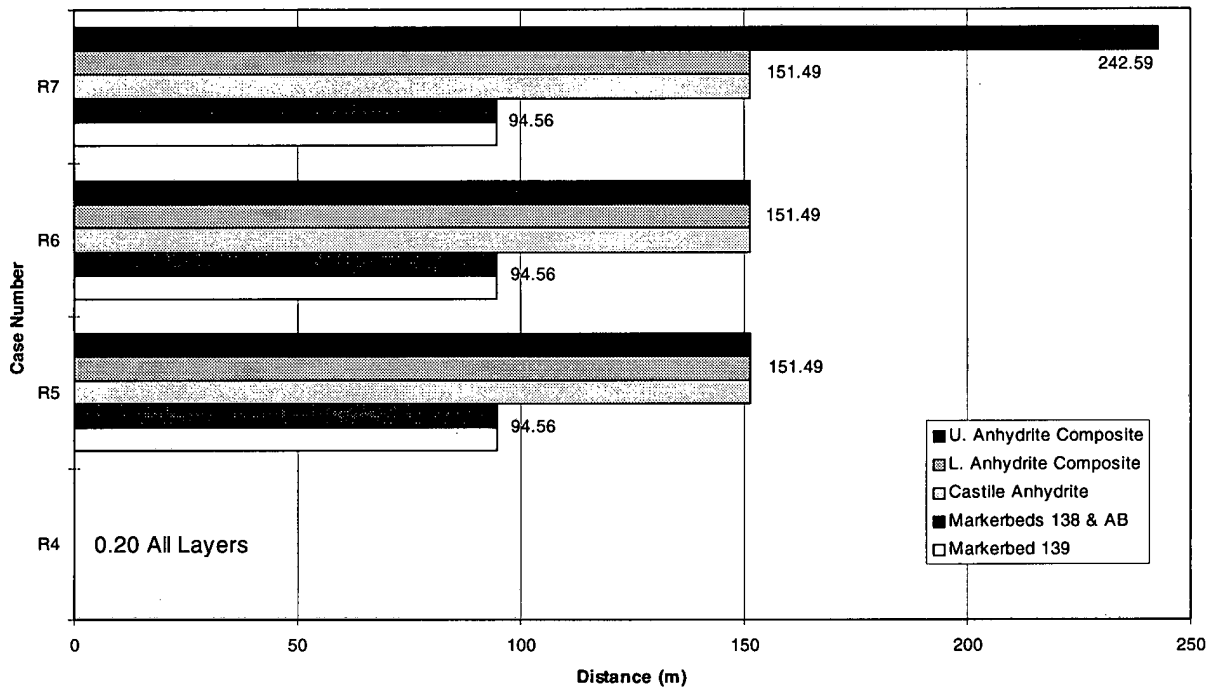
Figure 14 shows that, for the cement leaks considered in cases R1 through R3, fracturing is limited to the immediate vicinity of the wellbore if the cement permeability remains at or above  $10^{-12.5} \text{ m}^2$ . Case R3, with the borehole permeability set at  $10^{-11} \text{ m}^2$ , shows the  $10^{-12} \text{ m}^2$  fracture extending 59 m in MB138 and MB139. Fracturing extends further in the upper and lower composite anhydrite layers, because of their greater thickness and, for the upper layer, its higher elevation that results in a lower fracture initiation pressure. Fracturing does not occur in case R3 in the Castile anhydrite, because of its greater depth and relatively higher fracture initiation pressure, and because flow into the overlying anhydrites can accommodate the relatively slow rate of leakage up the borehole.

Figure 15 shows that 20-year tubing and casing leaks in the Bell Canyon alone are not sufficient to fracture the anhydrite layers away from the wellbore (case R4). Ten-year tubing and casing leaks from waterflood operations into deeper formations result in approximately 95 m fractures with a permeability of  $10^{-12} \text{ m}^2$  in MB138 and MB139. Fractures in other anhydrite layers, including the Castile, extend greater distances. None, however, extend far enough from the wellbore to affect the performance of the WIPP.

Comparison of cases R8, R9, and R10, shown in Figure 16, shows that an unrealistic assumption of 50 years of continuous tubing and casing leak from waterflood injection in the Cherry Canyon (case R8) results in propagation of an approximately 151 m fracture with a permeability of  $10^{-12} \text{ m}^2$  in MB138 and MB139, and longer fractures in other units. Increasing the permeability of the Bell Canyon (case R9) decreases the extent of fracturing in the anhydrite layers. This result is consistent with the result described in sections 4.3.2 and 4.3.3 that case R9 shows a decrease in brine flow above the Bell Canyon and a decrease in flow into each anhydrite layer. Reducing the injection pressure to a gradient of 0.725 psi/ft, consistent with current practice, eliminates fracturing of all anhydrite layers away from the wellbore (case R10).



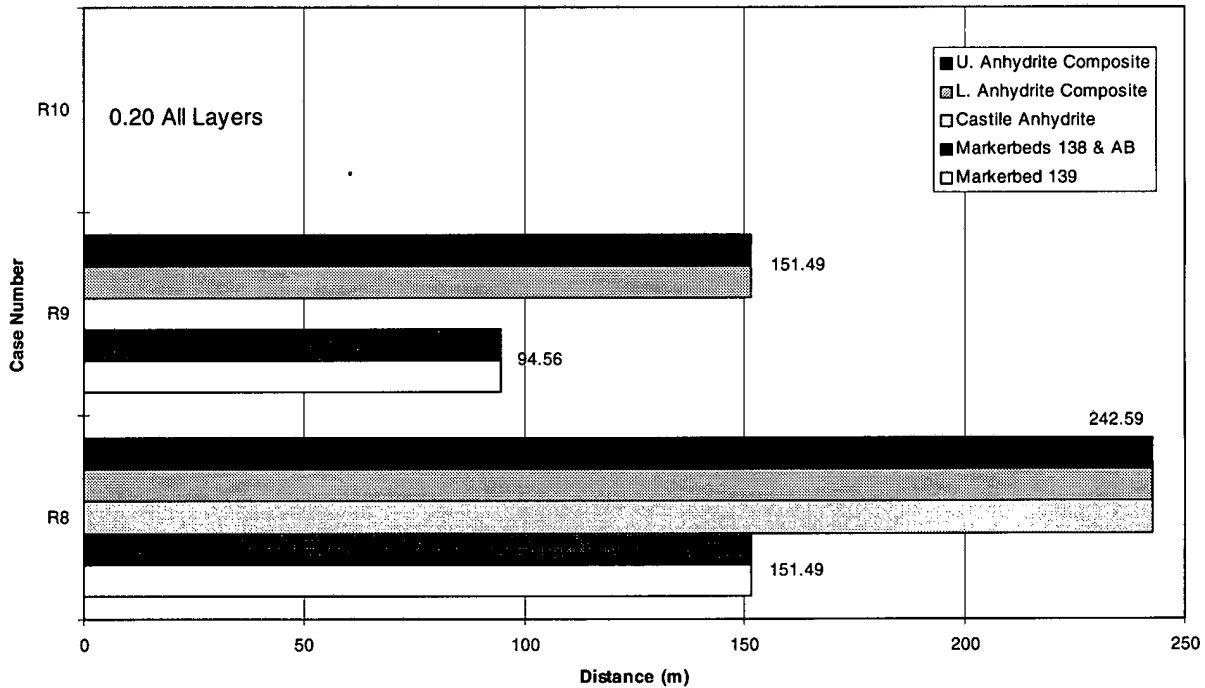
**Figure 14: Maximum Distance of  $10^{-12} \text{ m}^2$  Fracture at Various Cement Leak Permeabilities: Radial Models**



**Figure 15: Maximum Distance of  $10^{-12} \text{ m}^2$  Fracture Due to Hypothetical Waterflood Injection Into Deeper Formations: Radial Models**

Information Only





**Figure 16: Maximum Distance of  $10^{-12} \text{ m}^2$  Fracture: Effects of Upper Bell Canyon Permeability (Radial Models)**

### 4.3 Cross-Sectional Model Results

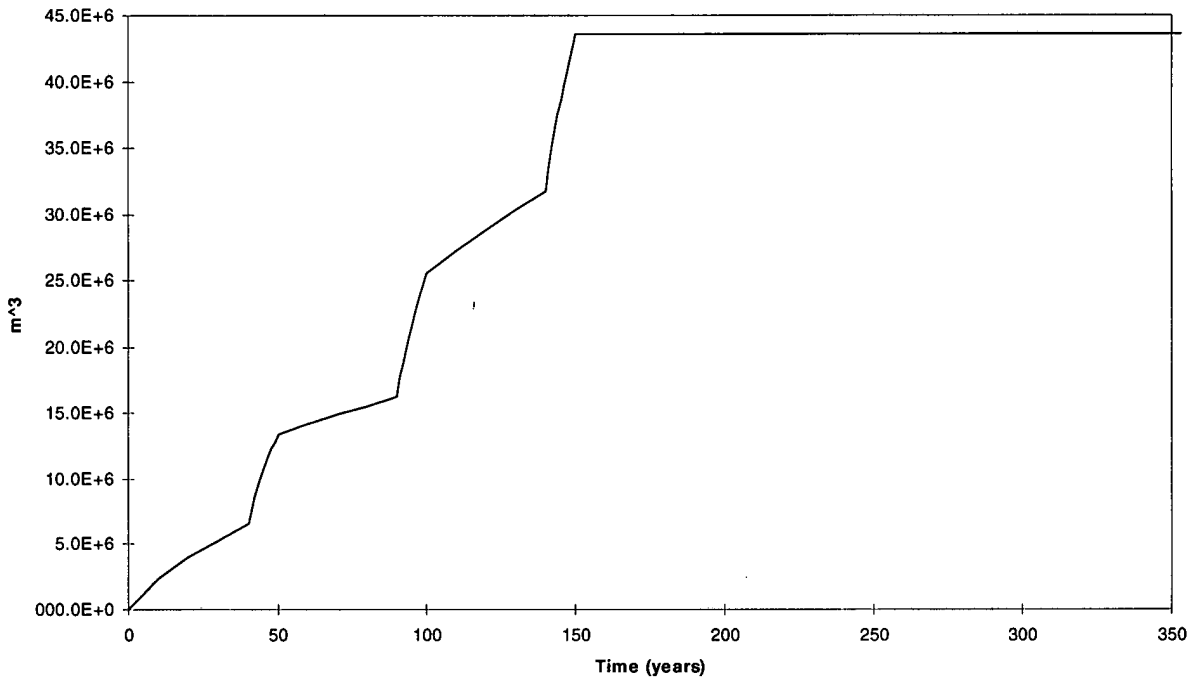
Performance measures described in the following sections for the single cross-sectional model case parallel those described for the radial model cases, and include the total amount of brine injected into the two boreholes, the total amount of brine leaking above the Bell Canyon Formation, brine flow into MB139 and other anhydrite layers, pressure at MB139 in the south well (the well in which the deep waterflood injection occurs), and the distance fractures propagate from the south wellbore in each anhydrite layer. In addition, because the cross-sectional model includes a representation of the repository, we report cumulative brine inflow to the repository.

Results of the cross-sectional model are, in general, not quantitatively comparable to the results of the radial model because of different assumptions about the time of injection and leakage, and because of the role of the north well. Qualitative comparisons are most useful between the cross-sectional case and radial cases R5, R6, and R7, which simulate 50-year waterflood operations in the Cherry Canyon, Brushy Canyon, and Bone Spring, respectively, because the cross-sectional case combines key aspects of these cases by simulating waterfloods consecutively in each layer. Comparisons with these cases are discussed in the following sections where appropriate.

### 4.3.1 Volume of Brine Injected (Cross-Sectional Model)

Figure 17 shows the cumulative volume of brine injected from both wellbores into all formations. The different episodes of injection and leakage assumed for the cross-sectional case can be seen clearly in the cumulative injection profile, with injection rates being most rapid during the ten-year periods of tubing and casing leaks from the deep waterflood operations.

The total volume of brine injected, approximately  $43.6 \times 10^6 \text{ m}^3$ , is less than that injected in radial cases R5, R6, and R7 combined ( $211 \times 10^6 \text{ m}^3$ ). This is reasonable given that the cross-sectional model only captures 180 degrees of injection laterally from each well (rather than 360 degrees), and is areally confined by the grid geometry. Waterflood injection occurs only into the south well in the cross-sectional case, and the volume of brine injected during waterflooding should therefore be less than that injected into a comparable radial model. The effect of modeling 150 years of consecutive waterflooding, rather than three independent 50-year waterfloods, also reduces the total volume of brine injected in 150 years, because early waterfloods pressurize injection horizons and reduce leakage from later injection episodes.

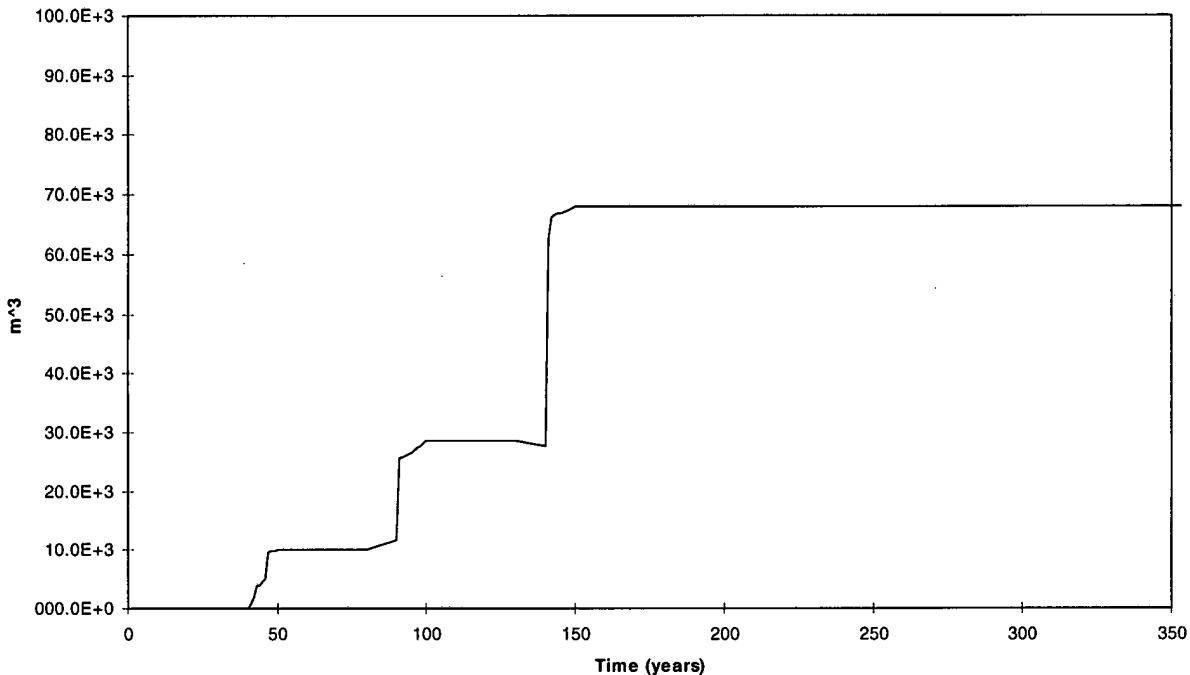


**Figure 17: Total Fluid Injected into All Formations: Cross-Sectional Model**

### 4.3.2 Volume of Brine Leaking Above the Bell Canyon Formation (Cross-Sectional Model)

Figure 18 shows the cumulative volume of brine flowing up the borehole at the top of the Bell Canyon Formation. As is the case for the total volume of brine injected (Figure 17), the different episodes of injection and leakage can be clearly seen in the cumulative profile of leakage, with the largest upward flow occurring during the periods of casing and tubing leaks from the deep waterflood injection. Additional complexity in the cumulative profile relative to those observed for the radial cases (Section 4.2.1) results from the assumptions made in the cross-sectional case about the time and depth of injection. For example, the brief period of downward flow between 130 and 140 years occurs when a casing and tubing leak connects the Bell Canyon and the Castile during a disposal operation. Pressure in the Castile is elevated above that in the Bell Canyon because of previous leaks from waterflooding in deeper units, and a small downward flow occurs until the pressure gradient is reversed by upward flow from the tubing and casing leak in the Bone Spring.

The total volume of upward leakage in the cross-sectional wellbores ( $67.9 \times 10^3 \text{ m}^3$ ) is comparable to that observed in radial cases R5, R6, and R7, combined ( $69.9 \times 10^3$ ). This suggests that vertical flow (leakage) through the borehole is controlled more by the pressure gradients and flow area in the borehole rather than the lateral geometry of the vertical layers through which it intersects.

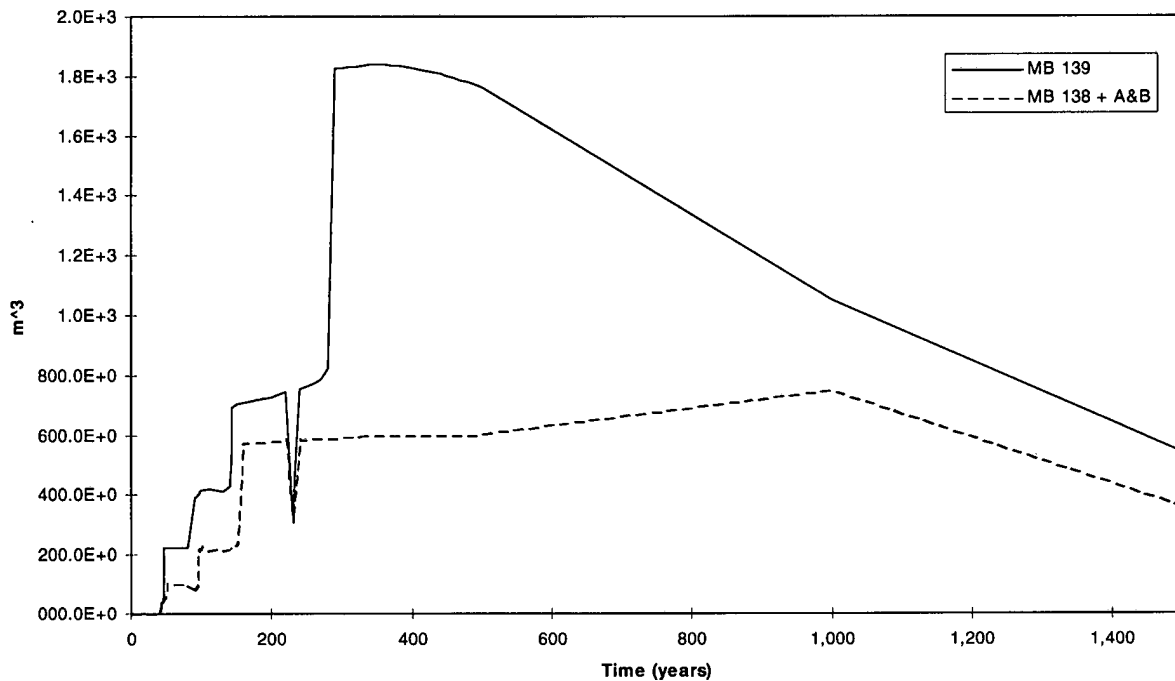


**Figure 18: Cumulative Brine Flows in Wellbores Upwards Past Bell Canyon / Castile Interface: Cross-Sectional Model**

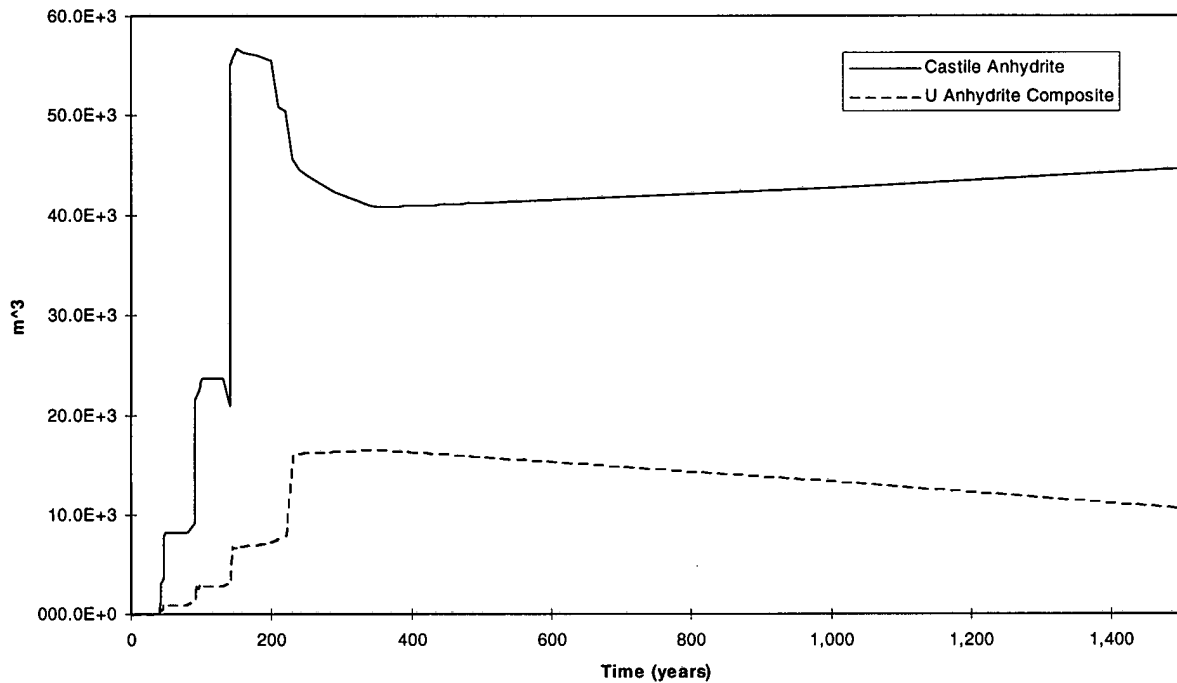
### 4.3.3 Volume of Brine Entering Anhydrite Layers (Cross-Sectional Model)

Figure 19 shows the cumulative volume of brine entering MB138 and MB139. Figure 20 shows brine flows into the upper composite anhydrite layer of the Salado Formation and the Castile Formation anhydrite. Results are similar to those observed for the radial cases. Comparison of the flows into each layer shows a complex pattern of cross-flow between anhydrite layers, both during the period of active injection and during the 200 years after abandonment in which the plugs are effective. Total flow into MB139 (1,842 m<sup>3</sup>) is comparable to the sum of the highest flows into MB139 observed in Radial cases R5, R6, and R7 (1,688 m<sup>3</sup>).

As noted in the discussion of brine flow into the anhydrite layers for the radial model, this volume of brine is sufficiently small that even if it all reached the repository it would not have a significant effect on the undisturbed performance of the repository. As discussed in Section 4.3.6, the cross-sectional model allows direct calculation of brine inflow to the repository.



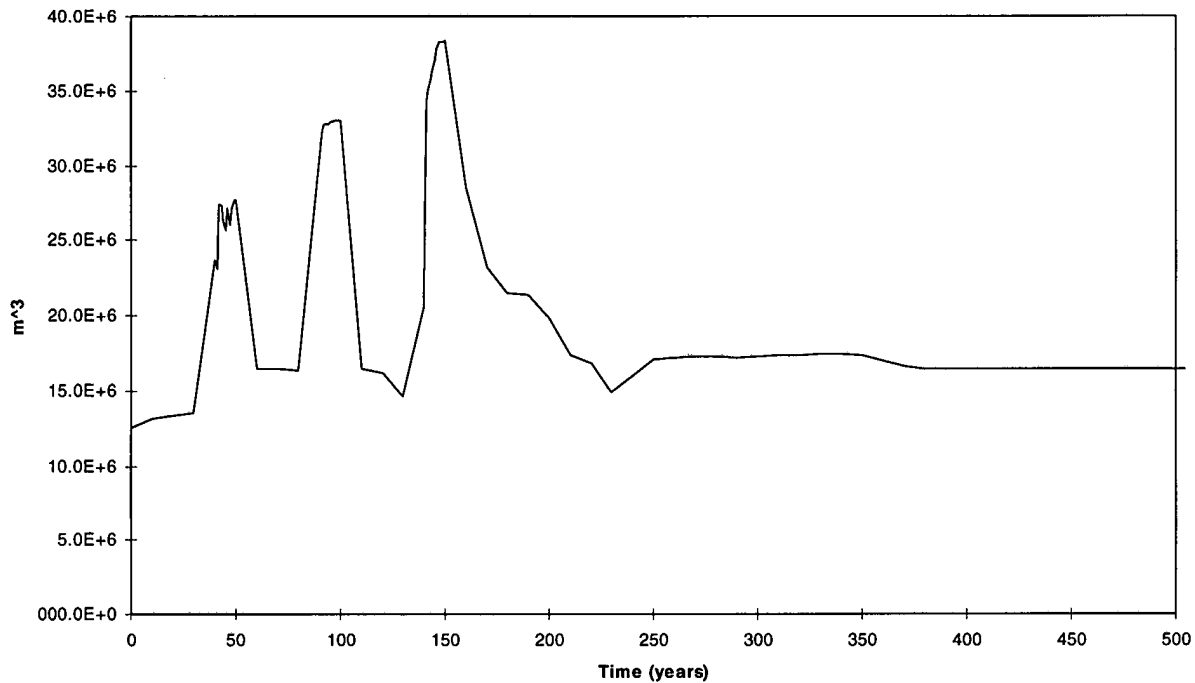
**Figure 19: Cumulative Flows into Marker Beds 139 & 138: Cross-Sectional Model**



**Figure 20: Cumulative Flows into Castile and Upper Composite Anhydrite Layers: Cross-Sectional Model**

#### 4.3.4 Pressure in the Injection Wellbore at MB139 (Cross-Sectional Model)

Figure 21 shows pressure in the wellbore at the elevation of MB139 during the first 500 years of the cross-sectional simulation. Major pressure peaks coincide with casing and tubing leaks from the waterflood operations. Minor fluctuations in pressure reflect cross-flow between anhydrite layers and, before the well is plugged and abandoned at 150 years, the Bell Canyon. The peak pressure reached at MB139, approximately 38.3 MPa, coincides with the tubing and casing leak in the Bone Spring, and is slightly higher than the comparable peak observed in radial case R7. This increase in pressure occurs because deeper units into which flow away from the borehole might occur have been pressurized by leakage during earlier tubing and casing leaks.



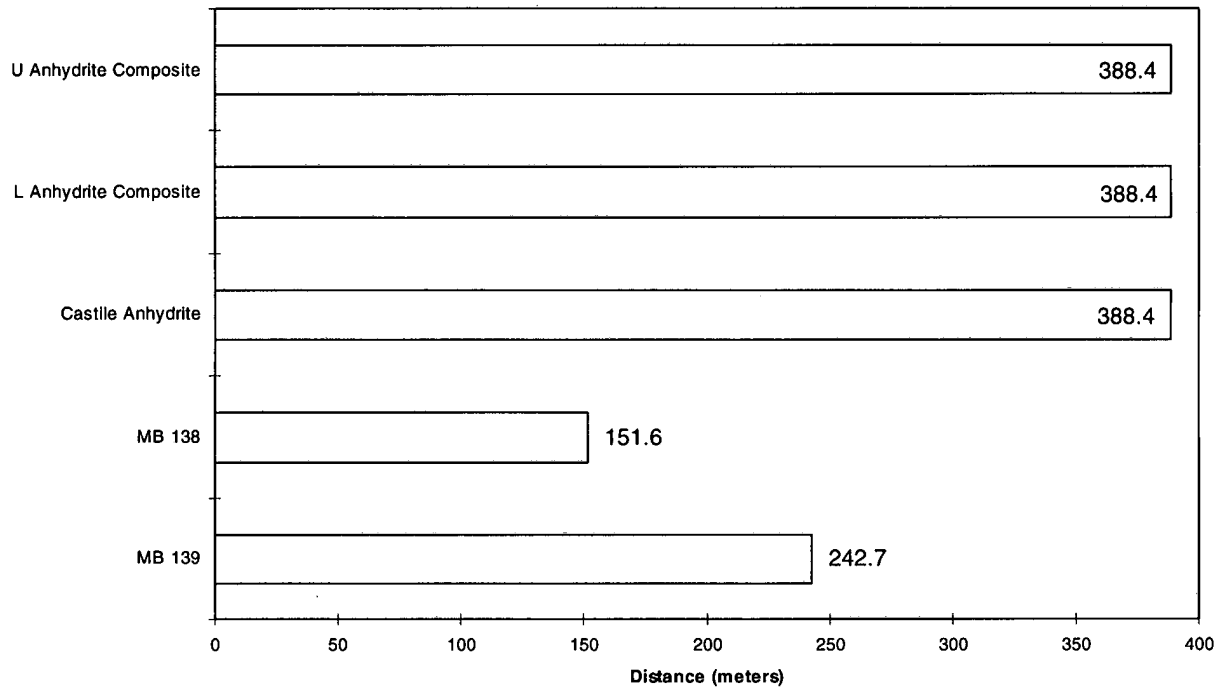
**Figure 21: Pressure In South Wellbore at Marker Bed 139 Horizon: Cross-Sectional Model**

#### 4.3.5 Distance of Fracture Propagation in Anhydrite Layers (Cross-Sectional Model)

Figure 22 shows the maximum distance that permeabilities of  $10^{-12} \text{ m}^2$  or greater were calculated for each of the anhydrite layers. We interpret this region to correspond to the region in which fracturing of the anhydrite is essentially complete. As discussed in Section 4.2.5, lower permeability regions extend somewhat farther from the wellbore.

The maximum distance of fracturing predicted by the cross-sectional model is somewhat longer than that predicted by the radial cases. We believe this is reasonable, given the longer period of simulation and the multiple episodes of tubing and casing leaks. High permeability fractures remain relatively close to the borehole even after 150 years of continuous injection, and extend less than 250 m in MB139.





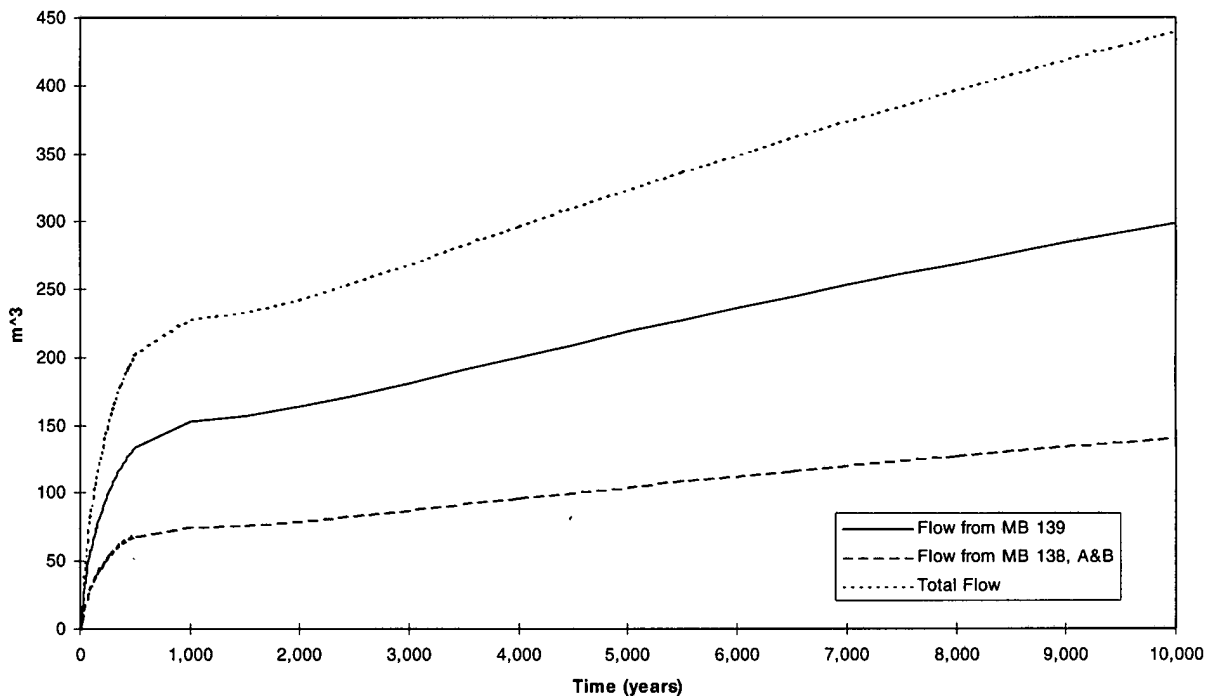
**Figure 22: Maximum Distance from South Wellbore Reached by  $10^{-12} \text{ m}^2$  Fractures in the Anhydrites: Cross-Sectional Model**

#### 4.3.6 Long-term Effects on the Repository (Cross-Sectional Model)

##### 4.3.6.1 Brine Flow into Repository (Cross-Sectional Model)

Figure 23 shows cumulative total brine inflow into the repository from MB138 and MB139 for the entire 10,000 years of the simulation. This volume includes brine inflow from the Salado Formation that would occur during undisturbed performance as well as any additional contribution resulting from the leaky injection boreholes. Most brine inflow occurs in MB139, with a lesser contribution from MB138. As is observed in the undisturbed calculations for the CCA, brine inflow is most rapid in the first several hundred years, when pressure is low in the repository. Brine inflow continues throughout the remainder of the simulation at a reduced rate.

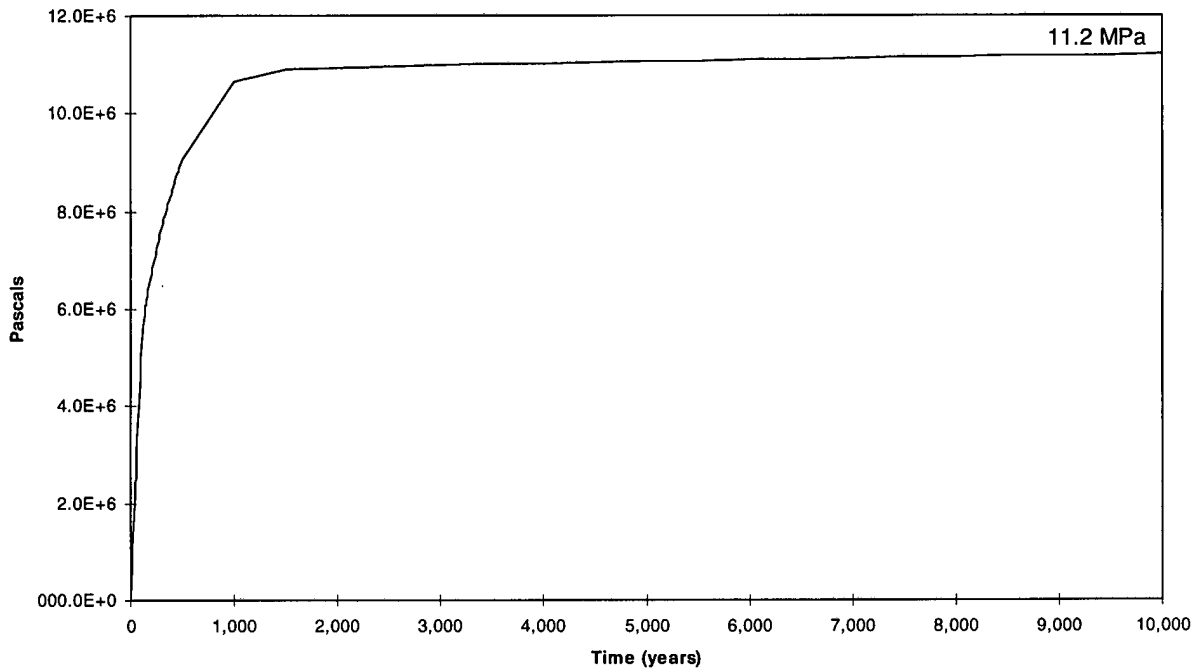
The total amount of brine inflow,  $440 \text{ m}^3$  during 10,000 years, is less than the approximately  $1000 \text{ m}^3$  inflow reported by Stoelzel and O'Brien (1996) and used as the basis of their screening decision, and is comparable to the smaller brine inflows reported in the probabilistic analysis of undisturbed performance included in the CCA (Helton, 1996, Figure 2.1.1).



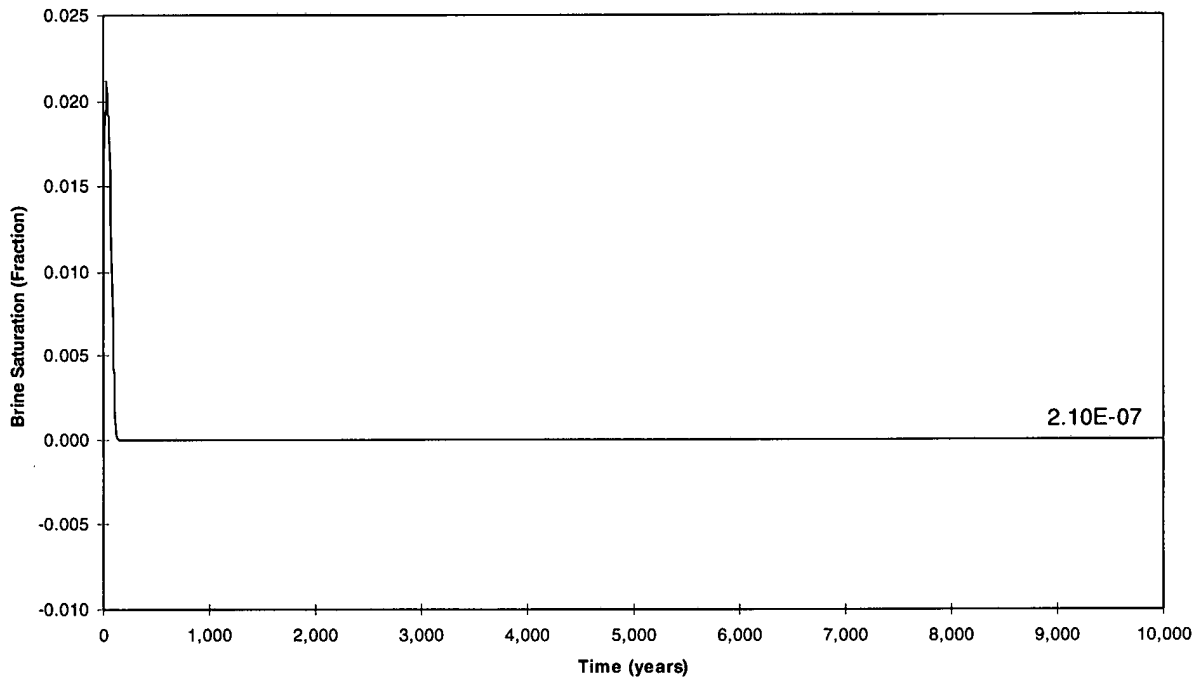
**Figure 23: Brine Flow into Repository from Anhydrites: Cross-Sectional Model**

#### 4.3.6.2 Pressures and Saturations in the Repository (Cross-Sectional Model)

Figures 24 and 25 show the grid-block averaged pressures and brine saturations in the waste region of the repository over 10,000 years. These compare favorably to the waste region pressures and saturations observed in the majority of the undisturbed calculations of the CCA, as well as the "Baseline" case for the WIPP geology fluid injection models presented by Stoelzel and O'Brien (See Figures 9 and 11, pages 35 and 36, of Stoelzel and O'Brien, 1996). This shows that fluid migration resulting from leaky injection wells 2 km from the WIPP will have little or no effect on the repository conditions, and will therefore not influence radionuclide releases from the site.



**Figure 24: Average Pressure in Waste Region: Cross-Sectional Model**



**Figure 25: Average Brine Saturation in Waste Region: Cross-Sectional Model**

Information Only

## 5.0 Conclusions

Results of this study confirm the conclusion of Stoelzel and O'Brien (1996) that leakage from poorly maintained brine injection wells near the WIPP will not have a negative effect on the performance of the repository. Stoelzel and O'Brien (1996) concluded that for the worst combination of conditions they considered, some brine could reach the waste-disposal region as a result of faulty injection, but that the total amount of brine inflow to the waste region (approximately 1000 m<sup>3</sup>) would not affect performance.

This study expands on Stoelzel and O'Brien's (1996) work by considering injection for a longer period of time (up to 150 years) and into deeper horizons at higher pressures. We have developed two computational models (a modified cross-sectional model and a radial model) that are alternatives to the cross-sectional model used by Stoelzel and O'Brien (1996), and we address topics raised by the EPA in their March 19, 1997 (Trovato, 1997) letter to the DOE, and quoted in Section 1.0 of this report. These comments are repeated here, with a summary of how we have addressed them.

*The DOE needs to:*

*(a) Use a 150-year period as the period of simulation.*

Analyses described in this report simulate 10,000-year flow resulting from both 50- and 150-year periods of fluid injection.

*(b) Identify the extent to which the initial conditions (i.e., conditions before an intrusion event) of the repository could change with the longer period of fluid injection.*

Analyses described in this report show that conditions in the undisturbed repository are not affected by the longer period of fluid injection.

*(c) Analyze the effects of a human intrusion event subsequent to fluid reaching the repository via a fluid injection event.*

Analyses described in this report show that, because conditions in the undisturbed repository are not affected by the longer period of fluid injection, the consequences of human intrusion into the repository will be the same with and without fluid injection.

*(d) Increase the transmissivity of Bell Canyon to allow higher volumes of brine to be injected.*

We report results from the radial model cases (R9 and R10) in which the permeability of the Bell Canyon Formation was increased by one order of magnitude. This resulted in

less leakage from the injection well reaching the Salado Formation, and we therefore choose to base our conclusions on analyses using the same value of permeability used by Stoelzel and O'Brien (1996).

*(e) Reduce, by one-half, the DRZ volume.*

The cross-sectional model used in this report has a DRZ with approximately one-half the volume of the DRZ included in the Stoelzel and O'Brien (1996) model.

*(f) Estimate the frequency of fluid injection wells that have failed or appear to have failed.*

We have not addressed this point directly. However, the report by DOE (1997, main body included as Attachment 1) on current fluid injection practice documents the frequency of injection well failure in the New Mexico portion of the Delaware Basin over the past 15 years.

*(g) Substantiate why a two-dimensional cross-sectional modeling approach is appropriate for this analysis.*

We have used both a cross-sectional model and an axisymmetric radial borehole model in these analyses. Leakage up the injection borehole and brine flow away from the borehole in the Salado anhydrites is similar for both models.

Because of the large uncertainty associated with future human actions, we have taken what we believe is a conservative approach to estimating the frequency and duration of injection well failure in the future, pressures at which these wells may inject, and the effectiveness of plugs emplaced when these wells are abandoned. In general, however, we have not attempted to repeat the conservative and bounding approach used by Stoelzel and O'Brien (1996). Rather, we have focused on what we believe are reasonable and realistic conditions for most aspects of the modeling. Modeling assumptions and parameter values are consistent with those used in the CCA wherever possible. Parameters which were sampled in the CCA have been set at their median values.

Model results indicate that, for the cases considered, the largest volume of brine entering MB139 (the primary pathway to the WIPP) from the borehole is approximately 1,500 m<sup>3</sup>, which is a small enough volume that it would not affect Stoelzel and O'Brien's (1996) conclusion even if it somehow all reached the WIPP. Other cases showed from zero to 600 m<sup>3</sup> of brine entering MB139 from the injection well. In all cases, high permeability fractures in the anhydrite layers were restricted to less than 400 meters from the wellbore, and did not extend more than 250 meters in MB138 and MB139. These small brine volumes and relatively short fracture distances provide support for the assumption that flow away from the borehole in the radial model is unaffected by sinks and sources in the far field, and also indicate that it is unnecessary to develop

an areal model of two-dimensional flow and fracturing between one or more injection boreholes and the WIPP.

Analysis of model results confirms the importance of a realistic treatment of borehole properties and site geology in evaluating the possible effects of brine injection on the WIPP. Even the limited amount of flow and fracturing observed in the anhydrite layers required a combination of unfavorable circumstances. No flow entered MB139, nor was there fracturing of the unit away from the borehole, in cases in which leaks in the cement sheath had permeabilities of  $10^{-12.5} \text{ m}^2$  (corresponding to the median value used to characterize fully degraded boreholes in the CCA) or lower. Similarly, there was no flow into MB139 in the case in which a tubing and casing leak occurred with injection pressures equivalent to those used in current practice. The cases we modeled in which flow entered MB139 from the borehole and in which fracturing occurred away from the borehole required injection pressures conservatively higher than any currently in use near the WIPP and either 150 years of leakage through a fully degraded cement sheath or 10 years of simultaneous tubing and casing leaks from a waterflood operation. We do not believe that these conditions are likely to occur in the future. If leaks like these do occur from brine injection near the WIPP, however, results of this modeling study indicate that they will not affect the performance of the repository.

Information Only



## References

- BRAGFLO, Version 4.00. January 31, 1996: *WIPP PA Users Manual for BRAGFLO, Version 4.00: Document Version 1.01*, Sandia National Laboratories WIPP Central Files, WPO #30703
- Bredehoeft, J. 1997. *The HARTMAN Scenario: Implications for WIPP*. Report prepared for the New Mexico Attorney General by the Hydrodynamics Group, La Honda, CA. WPO # 45839.
- Craft, B.C., W.R. Holden, and E.D. Graves. 1962. *Well Design: Drilling and Production*. Prentice-Hall, Inc. Englewood Cliffs, NJ.
- DOE. 1996. *Title 40 CFR Part 191 Compliance Certification Application for the Waste Isolation Pilot Plant*. DOE/CAO-1996-2184. United States Department of Energy Carlsbad Area Office. Carlsbad, NM.
- DOE, 1997. "Injection Methods: Current Practices and Failure Rates in the Delaware Basin". DOE/WIPP97-2240, United States Department of Energy, Carlsbad Area Office, Carlsbad, NM. (Main text included as Attachment 1).
- Freeland, M.H. 1982. *Basic Data Report for Borehole DOE-1, Waste Isolation Pilot Plant (WIPP) Project, Southeastern New Mexico*. TME 3159. United States Department of Energy, Albuquerque, NM. WPO # 42668.
- Freeze, R.A., and J.A. Cherry. 1979. *Groundwater*. Prentice-Hall, Inc. Englewood Cliffs, NJ. CCA Reference # 257.
- Helton, J.C. 1996. *Memo: Preliminary Summary of Uncertainty and Sensitivity Analysis Results Obtained in Support of the 1996 Compliance Certification Application for the Waste Isolation Pilot Plant*. Sandia National Laboratories, Albuquerque, NM. WPO# 42912.
- Levorsen, A.I. 1967. *Geology of Petroleum, Second Edition*. W.H. Freeman and Co., San Francisco.
- Neill, R.H. 1997. Letter to Frank Marcinowski, United States Environmental Protection Agency, dated February 7, 1997, containing comments from the Environmental Evaluation Group on the WIPP Compliance Certification Application. WPO #45836
- NMBMMR. 1995. *Final Report: Evaluation of Mineral Resources at the Waste Isolation Pilot Plant (WIPP) Site, Vol. 1-4, March 31, 1995*. New Mexico Bureau of Mines and Mineral Resources (NMBMMR), Socorro, New Mexico. CCA Reference Number 460.

Stoelzel, D.M., and D.G. O'Brien. 1996. "The Effects of Salt Water Disposal and Waterflooding on WIPP," Summary Memo of Record for FEP NS-7a. Sandia National Laboratories, Albuquerque, NM. WPO 40837. CCA Reference # 611.

Sandia National Laboratories and United States Geological Survey. 1983. *Basic Data Report for Drillhole ERDA-9 (Waste Isolation Pilot Plant-WIPP)*. SAND79-0270. Sandia National Laboratories, Albuquerque, NM. WPO # 28173.

Swift, P.N., D.M. Stoelzel, R.L. Beauheim, P. Vaughn, and K.W. Larson. 1997. "Technical Review of *The HARTMAN Scenario: Implications for WIPP* prepared for the New Mexico Attorney General, March 1997, by John Bredehoeft," memorandum to Margaret S.Y. Chu, dated June 13, 1997. Sandia National Laboratories, Albuquerque, NM. WPO # 45839. (Copy included as Attachment 2).

Trovato, E.R. 1997. Letter to Alvin Alm, United States Department of Energy, dated March 19, 1997, containing a list of issues identified by the United States Environmental Protection Agency that need to be addressed by DOE in order for EPA to render a compliance certification decision. WPO #45835

US EPA. 1996. *40 CFR Part 194. Criteria for the Certification and Re-Certification of the Waste Isolation Pilot Plant's Compliance with the 40 CFR Part 191 Disposal Regulations; Final Rule*. Federal Register v. 61, p. 5224-5245.

## Appendix A: Grid-Block Dimensions and Layering Information for the Radial and Cross-Sectional Models

**Table 5: X-Direction Grid-blocks for Radial Models**

Description	X direction Number	Delta X (delta r) meters	Cumulative Delta X meters	delta z thickness meters	Area Del z * Del x m <sup>2</sup>	Cumulative Area m <sup>2</sup>
South Wellbore	1	7.7780E-02	7.7780E-02	9.7763E-01	7.60E-02	7.6040E-02
V	2	2.4896E-01	3.2674E-01	1.7598E+00	4.38E-01	
V	3	3.9834E-01	7.2508E-01	3.7933E+00	1.51E+00	
V	4	6.3734E-01	1.3624E+00	7.0470E+00	4.49E+00	
V	5	1.0197E+00	2.3822E+00	1.2253E+01	1.25E+01	
V	6	1.6316E+00	4.0137E+00	2.0582E+01	3.36E+01	
V	7	2.6105E+00	6.6243E+00	3.3909E+01	8.85E+01	
V	8	4.1769E+00	1.0801E+01	5.5232E+01	2.31E+02	
V	9	6.6830E+00	1.7484E+01	8.9350E+01	5.97E+02	
V	10	1.0693E+01	2.8177E+01	1.4394E+02	1.54E+03	
V	11	1.7108E+01	4.5285E+01	2.3128E+02	3.96E+03	
V	12	2.7373E+01	7.2659E+01	3.7102E+02	1.02E+04	
V	13	4.3798E+01	1.1646E+02	5.9461E+02	2.60E+04	
V	14	7.0076E+01	1.8653E+02	9.5236E+02	6.67E+04	
V	15	1.1212E+02	2.9865E+02	1.5247E+03	1.71E+05	
V	16	1.7939E+02	4.7805E+02	2.4406E+03	4.38E+05	
V	17	2.8703E+02	7.6508E+02	3.9059E+03	1.12E+06	
V	18	4.4780E+02	1.2129E+03	6.2144E+03	2.78E+06	
V	19	7.1647E+02	1.9293E+03	9.8721E+03	7.07E+06	
V	20	1.1464E+03	3.0757E+03	1.5724E+04	1.80E+07	
V	21	1.8342E+03	4.9099E+03	2.5088E+04	4.60E+07	
V	22	2.9347E+03	7.8445E+03	4.0070E+04	1.18E+08	
V	23	4.6955E+03	1.2540E+04	6.4040E+04	3.01E+08	
V	24	7.5128E+03	2.0053E+04	1.0239E+05	7.69E+08	
V	25	1.2020E+04	3.2073E+04	1.6376E+05	1.97E+09	
V	26	1.9233E+04	5.1306E+04	2.6194E+05	5.04E+09	
V	27	3.0772E+04	8.2078E+04	4.1904E+05	1.29E+10	2.1164E+10

**Table 6: X-Direction Grid-blocks for Cross-Sectional Model**

Description	X direction Number	Delta X (delta r) meters	Cumulative Delta X meters	delta z thickness meters	Area Del z * Del x m <sup>2</sup>	Cumulative Area m <sup>2</sup>
South Wellbore	1	1.5560E-01	1.5560E-01	4.8869E-01	7.60E-02	7.6040E-02
V	2	2.4896E-01	4.0456E-01	8.7990E-01	2.19E-01	
V	3	3.9834E-01	8.0290E-01	1.8967E+00	7.56E-01	
V	4	6.3734E-01	1.4402E+00	3.5235E+00	2.25E+00	
V	5	1.0197E+00	2.4600E+00	6.1264E+00	6.25E+00	
V	6	1.6316E+00	4.0916E+00	1.0291E+01	1.68E+01	
V	7	2.6105E+00	6.7021E+00	1.6955E+01	4.43E+01	
V	8	4.1769E+00	1.0879E+01	2.7616E+01	1.15E+02	
V	9	6.6830E+00	1.7562E+01	4.4675E+01	2.99E+02	
V	10	1.0693E+01	2.8255E+01	7.1969E+01	7.70E+02	
V	11	1.7108E+01	4.5363E+01	1.1564E+02	1.98E+03	
V	12	2.7373E+01	7.2737E+01	1.8551E+02	5.08E+03	5.5511E+06
V	13	4.3798E+01	1.1653E+02	2.9731E+02	1.30E+04	
V	14	7.0076E+01	1.8661E+02	4.7618E+02	3.34E+04	
V	15	1.1212E+02	2.9873E+02	7.6237E+02	8.55E+04	
V	16	1.7939E+02	4.7813E+02	1.2203E+03	2.19E+05	
V	17	2.8703E+02	7.6516E+02	1.9529E+03	5.61E+05	
V	18	4.4780E+02	1.2130E+03	3.1072E+03	1.39E+06	
Λ	19	4.9669E+02	1.7096E+03	3.7964E+03	1.89E+06	
Λ	20	3.1696E+02	2.0266E+03	2.5183E+03	7.98E+05	
Λ	21	1.9810E+02	2.2247E+03	1.7092E+03	3.39E+05	
Λ	22	1.2381E+02	2.3485E+03	1.2036E+03	1.49E+05	
Λ	23	7.7383E+01	2.4259E+03	8.8753E+02	6.87E+04	
South Half of Waste	24	4.8365E+01	2.4743E+03	6.9000E+02	3.34E+04	
South Half of Waste	25	2.5600E+01	2.4999E+03	5.7382E+02	1.47E+04	
South Half of Waste	26	1.6000E+01	2.5159E+03	5.0847E+02	8.14E+03	6.0873E+04
South Half of Waste	27	1.0000E+01	2.5259E+03	4.6763E+02	4.68E+03	
Half Seal Area	28	4.6479E+00	2.5305E+03	4.4462E+02	2.07E+03	2.0666E+03
North Quarter of Waste	29	2.2670E+01	2.5532E+03	4.0171E+02	9.11E+03	
North Quarter of Waste	30	4.3798E+01	2.5970E+03	2.9731E+02	1.30E+04	
North Quarter of Waste	31	2.7373E+01	2.6243E+03	1.8551E+02	5.08E+03	
North Quarter of Waste	32	1.7108E+01	2.6415E+03	1.1564E+02	1.98E+03	
North Quarter of Waste	33	1.0693E+01	2.6522E+03	7.1969E+01	7.70E+02	
North Quarter of Waste	34	6.6830E+00	2.6588E+03	4.4675E+01	2.99E+02	
North Quarter of Waste	35	4.1769E+00	2.6630E+03	2.7616E+01	1.15E+02	3.0438E+04
North Quarter of Waste	36	2.6105E+00	2.6656E+03	1.6955E+01	4.43E+01	
North Quarter of Waste	37	1.6316E+00	2.6673E+03	1.0291E+01	1.68E+01	
North Quarter of Waste	38	1.0197E+00	2.6683E+03	6.1264E+00	6.25E+00	
North Quarter of Waste	39	6.3734E-01	2.6689E+03	3.5235E+00	2.25E+00	
North Quarter of Waste	40	3.9834E-01	2.6693E+03	1.8967E+00	7.56E-01	
North Quarter of Waste	41	2.4896E-01	2.6696E+03	8.7990E-01	2.19E-01	
Intrusion well	42	1.5560E-01	2.6697E+03	4.8869E-01	7.60E-02	7.6040E-02
North Quarter of Waste	43	2.4896E-01	2.6700E+03	8.7990E-01	2.19E-01	
North Quarter of Waste	44	3.9834E-01	2.6704E+03	1.8967E+00	7.56E-01	
North Quarter of Waste	45	6.3734E-01	2.6710E+03	3.5235E+00	2.25E+00	
North Quarter of Waste	46	1.0197E+00	2.6720E+03	6.1264E+00	6.25E+00	
North Quarter of Waste	47	1.6316E+00	2.6736E+03	1.0291E+01	1.68E+01	
North Quarter of Waste	48	2.6105E+00	2.6763E+03	1.6955E+01	4.43E+01	
North Quarter of Waste	49	4.1769E+00	2.6804E+03	2.7616E+01	1.15E+02	3.0438E+04
North Quarter of Waste	50	6.6830E+00	2.6871E+03	4.4675E+01	2.99E+02	
North Quarter of Waste	51	1.0693E+01	2.6978E+03	7.1969E+01	7.70E+02	
North Quarter of Waste	52	1.7108E+01	2.7149E+03	1.1564E+02	1.98E+03	
North Quarter of Waste	53	2.7373E+01	2.7423E+03	1.8551E+02	5.08E+03	
North Quarter of Waste	54	4.3798E+01	2.7861E+03	2.9731E+02	1.30E+04	
North Quarter of Waste	55	2.2670E+01	2.8088E+03	4.0171E+02	9.11E+03	
Half Seal Area	56	4.6479E+00	2.8134E+03	4.4462E+02	2.07E+03	2.0666E+03
Operations (backfilled)	57	1.0000E+01	2.8234E+03	4.6763E+02	4.68E+03	
Operations (backfilled)	58	1.2000E+01	2.8354E+03	5.0219E+02	6.03E+03	2.1839E+04
Operations (backfilled)	59	2.0150E+01	2.8556E+03	5.5269E+02	1.11E+04	
Experimental	60	3.3894E+01	2.8895E+03	6.3758E+02	2.16E+04	2.1610E+04
V	61	5.4230E+01	2.9437E+03	7.7601E+02	4.21E+04	
V	62	8.6769E+01	3.0305E+03	9.9749E+02	8.66E+04	
V	63	1.3883E+02	3.1693E+03	1.3519E+03	1.88E+05	
V	64	2.2213E+02	3.3914E+03	1.9188E+03	4.26E+05	
V	65	3.5540E+02	3.7468E+03	2.8260E+03	1.00E+06	
V	66	3.5559E+02	4.1024E+03	3.9429E+03	1.40E+06	
Λ	67	4.4780E+02	4.5502E+03	3.1072E+03	1.39E+06	
Λ	68	2.8703E+02	4.8372E+03	1.9529E+03	5.61E+05	
Λ	69	1.7939E+02	5.0166E+03	1.2203E+03	2.19E+05	
Λ	70	1.1212E+02	5.1287E+03	7.6237E+02	8.55E+04	
Λ	71	7.0076E+01	5.1988E+03	4.7618E+02	3.34E+04	
Λ	72	4.3798E+01	5.2426E+03	2.9731E+02	1.30E+04	5.4600E+06
Λ	73	2.7373E+01	5.2700E+03	1.8551E+02	5.08E+03	
Λ	74	1.7108E+01	5.2871E+03	1.1564E+02	1.98E+03	
Λ	75	1.0693E+01	5.2978E+03	7.1969E+01	7.70E+02	
Λ	76	6.6830E+00	5.3045E+03	4.4675E+01	2.99E+02	
Λ	77	4.1769E+00	5.3086E+03	2.7616E+01	1.15E+02	
Λ	78	2.6105E+00	5.3113E+03	1.6955E+01	4.43E+01	
Λ	79	1.6316E+00	5.3129E+03	1.0291E+01	1.68E+01	
Λ	80	1.0197E+00	5.3139E+03	6.1264E+00	6.25E+00	
Λ	81	6.3734E-01	5.3145E+03	3.5235E+00	2.25E+00	
Λ	82	3.9834E-01	5.3149E+03	1.8967E+00	7.56E-01	
Λ	83	2.4896E-01	5.3152E+03	8.7990E-01	2.19E-01	
North Wellbore	84	1.5560E-01	5.3154E+03	4.8869E-01	7.60E-02	7.6040E-02

Information Only

**Table 7: Y-Direction Grid-blocks for Radial and Cross-Sectional Models**

Y Direction Number	Y direction Increments		Bottom Grid-block <MSL Elevations>		Mid Grid-block	Depth from Surface	Depth from Surface	Formation	
	Delta Y (ft)	Delta Y (m)	(feet)	(meters)	(feet)	(feet)	(meters)		
39	25.262	7.700	2,676.181	815.700	2,688.812	819.550	720.177	219.510	Culebra
38	118.110	36.000	2,558.071	779.700	2,617.126	797.700	791.864	241.360	Rustler
37	721.276	219.845	1,836.795	559.855	2,197.433	669.778	1,211.557	369.283	Salado
36	52.001	15.850	1,784.793	544.005	1,810.794	551.930	1,598.196	487.130	U Anhydrite Composite
35	523.468	159.553	1,261.325	384.452	1,523.059	464.229	1,885.930	574.832	Salado
34	1.476	0.450	1,259.849	384.002	1,260.587	384.227	2,148.402	654.833	MB 138, A&B
33	4.367	1.331	1,255.482	382.671	1,257.666	383.337	2,151.324	655.724	Salado
32	4.367	1.331	1,251.115	381.340	1,253.299	382.006	2,155.691	657.055	Salado
31	2.789	0.850	1,248.327	380.490	1,249.721	380.915	2,159.268	658.145	MB 139
30	7.316	2.230	1,241.010	378.260	1,244.669	379.375	2,164.321	659.685	Salado
29	254.380	77.535	986.631	300.725	1,113.821	339.493	2,295.169	699.568	Salado
28	31.004	9.450	955.627	291.275	971.129	296.000	2,437.861	743.060	L Anhydrite Composite
27	371.309	113.175	584.318	178.100	769.972	234.688	2,639.017	804.373	Salado
26	226.378	69.000	357.940	109.100	471.129	143.600	2,937.861	895.460	Castile
25	797.244	243.000	-439.304	-133.900	-40.682	-12.400	3,449.672	1,051.460	Castile - Anhydrite composite
24	226.378	69.000	-665.682	-202.900	-552.493	-168.400	3,961.483	1,207.460	Castile
23	369.000	112.471	-1,034.682	-315.371	-850.182	-259.136	4,259.172	1,298.196	Upper Bell Canyon (Delaware Sand) Pay
22	796.000	242.621	-1,830.682	-557.992	-1,432.682	-436.682	4,841.672	1,475.742	Lower Bell Canyon - Upper Cherry No pay
21	850.000	259.080	-2,680.682	-817.072	-2,255.682	-687.532	5,664.672	1,726.592	Lower Bell Canyon - Upper Cherry No pay
20	150.000	45.720	-2,830.682	-862.792	-2,755.682	-839.932	6,164.672	1,878.992	Lower Bell Canyon - Upper Cherry No pay
19	15.000	4.572	-2,845.682	-867.364	-2,838.182	-865.078	6,247.172	1,904.138	Cherry - U. Brushy C. (L. Ridge Main Pay)
18	150.000	45.720	-2,995.682	-913.084	-2,920.682	-890.224	6,329.672	1,929.284	Upper Brushy Canyon (non-productive)
17	1,350.000	411.480	-4,345.682	-1,324.564	-3,670.682	-1,118.824	7,079.672	2,157.884	Upper Brushy Canyon (non-productive)
16	200.000	60.960	-4,545.682	-1,385.524	-4,445.682	-1,355.044	7,854.672	2,394.104	Upper Brushy Canyon (non-productive)
15	20.000	6.096	-4,565.682	-1,391.620	-4,555.682	-1,388.572	7,964.672	2,427.632	Lower Brushy Canyon (A,B,C,D) Pay
14	200.000	60.960	-4,765.682	-1,452.580	-4,665.682	-1,422.100	8,074.672	2,461.160	Upper Bone Spring (non-productive)
13	1,184.250	360.959	-5,949.932	-1,813.539	-5,357.807	-1,633.060	8,766.797	2,672.120	Upper Bone Spring (non-productive)
12	332.500	101.346	-6,282.432	-1,914.885	-6,116.182	-1,864.212	9,525.172	2,903.272	Upper Bone Spring (non-productive)
11	33.250	10.135	-6,315.682	-1,925.020	-6,299.057	-1,919.953	9,708.047	2,959.013	Bone Spring Pay
10	332.500	101.346	-6,648.182	-2,026.366	-6,481.932	-1,975.693	9,890.922	3,014.753	L. Bone Sp.-Wolfcamp-Strawn (non-productive)
9	2,757.900	840.608	-9,406.082	-2,866.974	-8,027.132	-2,446.670	11,436.122	3,485.730	L. Bone Sp.-Wolfcamp-Strawn (non-productive)
8	236.000	71.933	-9,642.082	-2,938.907	-9,524.082	-2,902.940	12,933.072	3,942.000	L. Bone Sp.-Wolfcamp-Strawn (non-productive)
7	23.600	7.193	-9,665.682	-2,946.100	-9,653.882	-2,942.503	13,062.872	3,981.563	Strawn Pay
6	350.000	106.680	-10,015.682	-3,052.780	-9,840.682	-2,999.440	13,249.672	4,038.500	Atoka (No Pay)
5	280.500	85.496	-10,296.182	-3,138.276	-10,155.932	-3,095.528	13,564.922	4,134.588	Atoka (No Pay)
4	19.500	5.944	-10,315.682	-3,144.220	-10,305.932	-3,141.248	13,714.922	4,180.308	Atoka Pay
3	300.000	91.440	-10,615.682	-3,235.660	-10,465.682	-3,189.940	13,874.672	4,229.000	Morrow Lime (No Pay)
2	373.300	113.782	-10,988.982	-3,349.442	-10,802.332	-3,292.551	14,211.322	4,331.611	Morrow Lime (No Pay)
1	26.700	8.138	-11,015.682	-3,357.580	-11,002.332	-3,353.511	14,411.322	4,392.571	Morrow Clastic (Pay)

## **Appendix B: Locations and Names of Computer Codes and Input/Output Files Used in this Study**

The following table contains a complete listing of the files used in this analysis. This includes all inputs, outputs, and executables (other than those already under QA) needed for reproducibility. Many of the intermediate files (such as debug files, ASCII output files, etc.), have been deleted to save disk space.

All files in this table have been stored under the Configuration Management System (CMS). In addition, all the directories and sub-directories in which the files were originally created are included for the reader to trace the flow of the calculations.

**Information Only**

CMS directory for all files:			
DISKSDOLLY_CCA1:[NON_HSM.CMS.BF_WF_EXP1]	Date	Time	
VMS File names	Created	Created	Brief Description
F1:[NOBACK2.DMS_WATERFLOOD.EPA]			Root Directory
ALGEBRA.DIR;1	4-Jun-97	3:29:10 PM	Sub - Directories
BRAGFLO.DIR;1	4-Jun-97	3:29:44 PM	
BRAGFLO_RADIAL.DIR;1	4-Jun-97	3:37:58 PM	
GENMESH.DIR;1	4-Jun-97	4:03:07 PM	
ICSET.DIR;1	4-Jun-97	4:03:15 PM	
MATSET.DIR;1	4-Jun-97	4:03:44 PM	
POST_CROSS.DIR;1	10-Jun-97	6:50:27 AM	
POST_RADIAL.DIR;1	4-Jun-97	4:04:37 PM	
PREBRAG.DIR;1	4-Jun-97	4:05:21 PM	
REPORT.DIR;1	4-Jun-97	4:05:33 PM	
F1:[NOBACK2.DMS_WATERFLOOD.EPA.ALGEBRA]			Algebra Sub - Directory: Step performed between ICSET and PREBRAG
ALGEBRA_EPA_WF_DUMBELL_R001.CDB;2	21-May-97	9:13:08 AM	Cross-Sectional Model Algebra output CDB
ALGEBRA_EPA_WF_RADIAL_R015.CDB;1	24-Apr-97	5:20:36 PM	Radial Model Case R9 Algebra output CDB
ALGEBRA_EPA_WF_RADIAL_R028.CDB;1	2-May-97	2:23:48 PM	Radial Model Case R8 Algebra output CDB
ALGEBRA_EPA_WF_RADIAL_R029.CDB;1	2-May-97	2:23:54 PM	Radial Model Case R10 Algebra output CDB
ALGEBRA_EPA_WF_RADIAL_R031.CDB;1	28-May-97	10:10:26 AM	Radial Model Case R4 Algebra output CDB
ALGEBRA_EPA_WF_RADIAL_R033.CDB;1	28-May-97	10:11:14 AM	Radial Model Case R5 Algebra output CDB
ALGEBRA_EPA_WF_RADIAL_R034.CDB;1	28-May-97	10:11:38 AM	Radial Model Case R6 Algebra output CDB
ALGEBRA_EPA_WF_RADIAL_R035.CDB;1	28-May-97	10:11:48 AM	Radial Model Case R7 Algebra output CDB
ALGEBRA_EPA_WF_RADIAL_R039.CDB;1	3-Jun-97	2:37:24 PM	Radial Model Case R1 Algebra output CDB
ALGEBRA_EPA_WF_RADIAL_R040.CDB;1	3-Jun-97	2:37:28 PM	Radial Model Case R2 Algebra output CDB
ALGEBRA_EPA_WF_RADIAL_R041.CDB;1	3-Jun-97	2:37:32 PM	Radial Model Case R3 Algebra output CDB
ALG_DUMBELL_EPA.INP;34	17-Apr-97	3:58:35 PM	Early version of Cross-sectional model Algebra input file
ALG_DUMBELL_EPA2.INP;3	21-May-97	9:12:58 AM	Cross-sectional model Algebra input file used for This study
ALG_DUMBELL_EPA_CCA_APRIL8.INP;1	8-Apr-97	3:21:13 PM	Early version of Radial model Algebra input file
ALG_RADIAL.COM;1	18-Apr-97	5:15:41 PM	VMS command file to execute Algebra: Radial model(s)
ALG_RADIAL_EPA.INP;3	20-Apr-97	10:17:05 PM	Radial model Algebra input file used for some of the cases
ALG_RADIAL_EPA2.INP;1	28-May-97	10:06:38 AM	Radial model Algebra input file used for the rest of the cases
ALG_RAD_ALL.COM;3	3-Jun-97	2:37:11 PM	VMS command file to execute Algebra: Radial model(s)
ALG_RAD_ALL2.COM;2	29-Apr-97	3:55:03 PM	VMS command file to execute Algebra: Radial model(s)
ALG_RAD_ALL3.COM;4	28-May-97	10:09:59 AM	VMS command file to execute Algebra: Radial model(s)
ALG_RAD_R011.COM;1	24-Apr-97	7:23:17 AM	VMS command file to execute earlier versions of Algebra: Radial model(s)
ALG_RAD_R030.COM;1	6-May-97	12:12:59 PM	VMS command file to execute Algebra: Radial model(s)
DMS_ALG.COM;1	7-Apr-97	3:29:43 PM	VMS command file to execute earlier versions of Algebra: Radial model(s)
DMS_CCA.COM;1	8-Apr-97	3:23:19 PM	VMS command file to execute earlier versions of Algebra: Radial model(s)
DUMB_ALG.COM;1	21-May-97	12:12:25 PM	VMS command file to execute Algebra: Cross-sectional model
R011.COM;3	6-May-97	7:29:05 AM	VMS command file to execute earlier versions of Algebra: Radial model(s)
RAD_DIRI.TXT;1	20-Apr-97	9:29:20 PM	Text file containing Radial model(s) Dirichlet boundary conditions
F1:[NOBACK2.DMS_WATERFLOOD.EPA.BRAGFLO]			BRAGFLO sub-directory for Cross-sectional model (step between Pre- & Post-BRAGFLO)

Information Only



CMS directory for all files: DISK\$DOLLY_CCA1:[NON_HSM.CMS.BF_WF_EXP1]			
VMS File names	Date Created	Time Created	Brief Description
BF2_BRAGFLO.COM;25 (renamed BF2_BRAGFLO_CROSS.COM for CMS to resolve file conflicts)	21-Jan-96	3:04:49 PM	VMS command file to build BRAGFLO cross-sectional model executable
BF2_BRAGFLO.EXE;1 (renamed BF2_BRAGFLO_CROSS.EXE for CMS to resolve file conflicts)	17-Apr-97	6:30:11 PM	BRAGFLO Cross-sectional model executable
BF2_BRAGFLO.FOR;8 (renamed BF2_BRAGFLO_CROSS.FOR for CMS to resolve file conflicts)	29-Jan-97	3:57:17 PM	BRAGFLO source listing (FORTRAN) used for cross-sectional model
BF2_BRAGFLO.MAP;2 (renamed BF2_BRAGFLO_CROSS.MAP for CMS to resolve file conflicts)	21-Apr-97	11:28:39 AM	FORTRAN compiler intermediate file
BF2_BRAGFLO.OBJ;2 (renamed BF2_BRAGFLO_CROSS.OBJ for CMS to resolve file conflicts)	21-Apr-97	11:27:35 AM	FORTRAN compiler intermediate file
BF2_PARAMS.INC;5 (renamed BF2_PARAMS_CROSS.INC for CMS to resolve file conflicts)	17-Apr-97	6:27:40 PM	BRAGFLO include file that defines Cross-sectional problem to dimension arrays
BRAGFLO_EPA_WF_DUMBELL_R001.BIN;1	21-May-97	11:54:15 AM	BRAGFLO cross-sectional model binary output
BRAGFLO_EPA_WF_DUMBELL_R001.CDB;1	2-Jun-97	7:57:10 AM	POST-BRAG_PA96 cross-sectional model binary output (Camdat database)
BRAGFLO_EPA_WF_DUMBELL_R001.INP;1	21-May-97	11:40:42 AM	BRAGFLO cross-sectional model ascii input file from PREBRAG
D_R001.COM;1	21-May-97	11:49:31 AM	VMS command file to run cross-sectional model in batch mode
POST_BRAG_CROSS.COM;1	2-Jun-97	1:30:48 PM	VMS command file to run post-brag in batch mode
F1:[NOBACK2.DMS_WATERFLOOD.EPA.BRAGFLO_ RADIAL]			BRAGFLO sub-directory for Radial models (step between Pre- & Post-BRAGFLO)
BF2_BRAGFLO.COM;25 (renamed BF2_BRAGFLO_RADIAL.COM for CMS to resolve file conflicts)	21-Jan-96	3:04:49 PM	VMS command file to build BRAGFLO Radial model executable
BF2_BRAGFLO.EXE;1 (renamed BF2_BRAGFLO_RADIAL.EXE for CMS to resolve file conflicts)	21-Apr-97	9:57:35 AM	BRAGFLO Radial model executable
BF2_BRAGFLO.FOR;8 (renamed BF2_BRAGFLO_RADIAL.FOR for CMS to resolve file conflicts)	29-Jan-97	3:57:17 PM	BRAGFLO source listing (FORTRAN) used for Radial model
BF2_BRAGFLO.MAP;3 (renamed BF2_BRAGFLO_RADIAL.MAP for CMS to resolve file conflicts)	21-Apr-97	11:34:00 AM	FORTRAN compiler intermediate file
BF2_BRAGFLO.OBJ;4 (renamed BF2_BRAGFLO_RADIAL.OBJ for CMS to resolve file conflicts)	21-Apr-97	11:42:41 AM	FORTRAN compiler intermediate file
BF2_PARAMS.INC;6 (renamed BF2_PARAMS_RADIAL.INC for CMS to resolve file conflicts)	21-Apr-97	9:55:29 AM	BRAGFLO include file that defines Radial problem to dimension arrays
BRAGFLO_EPA_WF_RADIAL_R015.BIN;2	28-Apr-97	3:01:40 PM	Radial Model Case R9 BRAGFLO output binary

Information Only

CMS directory for all files:			
DISKSDOLLY_CCA1:[NON_HSM.CMS.BF_WF_EXP1]	Date	Time	
VMS File names	Created	Created	Brief Description
BRAGFLO_EPA_WF_RADIAL_R015.CDB;2	29-Apr-97	7:10:13 AM	Radial Model Case R9 POST-BRAG output binary (Camdat database)
BRAGFLO_EPA_WF_RADIAL_R015.INP;2	28-Apr-97	11:44:34 AM	Radial Model Case R9 BRAGFLO ascii input file (from Prebrag)
BRAGFLO_EPA_WF_RADIAL_R028.BIN;1	2-May-97	2:51:39 PM	Radial Model Case R8 BRAGFLO output binary
BRAGFLO_EPA_WF_RADIAL_R028.CDB;1	5-May-97	9:03:40 AM	Radial Model Case R8 POST-BRAG output binary (Camdat database)
BRAGFLO_EPA_WF_RADIAL_R028.INP;1	2-May-97	2:33:36 PM	Radial Model Case R8 BRAGFLO ascii input file (from Prebrag)
BRAGFLO_EPA_WF_RADIAL_R029.BIN;1	2-May-97	2:51:53 PM	Radial Model Case R10 BRAGFLO output binary
BRAGFLO_EPA_WF_RADIAL_R029.CDB;1	5-May-97	9:18:36 AM	Radial Model Case R10 POST-BRAG output binary (Camdat database)
BRAGFLO_EPA_WF_RADIAL_R029.INP;1	2-May-97	2:33:48 PM	Radial Model Case R10 BRAGFLO ascii input file (from Prebrag)
BRAGFLO_EPA_WF_RADIAL_R031.BIN;1	28-May-97	2:07:19 PM	Radial Model Case R4 BRAGFLO output binary
BRAGFLO_EPA_WF_RADIAL_R031.CDB;1	30-May-97	3:13:17 PM	Radial Model Case R4 POST-BRAG output binary (Camdat database)
BRAGFLO_EPA_WF_RADIAL_R031.INP;1	28-May-97	1:01:15 PM	Radial Model Case R4 BRAGFLO ascii input file (from Prebrag)
BRAGFLO_EPA_WF_RADIAL_R033.BIN;1	28-May-97	5:16:01 PM	Radial Model Case R5 BRAGFLO output binary
BRAGFLO_EPA_WF_RADIAL_R033.CDB;1	30-May-97	3:14:19 PM	Radial Model Case R5 POST-BRAG output binary (Camdat database)
BRAGFLO_EPA_WF_RADIAL_R033.INP;1	28-May-97	1:55:31 PM	Radial Model Case R5 BRAGFLO ascii input file (from Prebrag)
BRAGFLO_EPA_WF_RADIAL_R034.BIN;1	29-May-97	5:25:33 AM	Radial Model Case R6 BRAGFLO output binary
BRAGFLO_EPA_WF_RADIAL_R034.CDB;1	30-May-97	3:16:55 PM	Radial Model Case R6 POST-BRAG output binary (Camdat database)
BRAGFLO_EPA_WF_RADIAL_R034.INP;1	28-May-97	1:55:47 PM	Radial Model Case R6 BRAGFLO ascii input file (from Prebrag)
BRAGFLO_EPA_WF_RADIAL_R035.BIN;1	29-May-97	8:05:39 PM	Radial Model Case R7 BRAGFLO output binary
BRAGFLO_EPA_WF_RADIAL_R035.CDB;1	30-May-97	3:20:10 PM	Radial Model Case R7 POST-BRAG output binary (Camdat database)
BRAGFLO_EPA_WF_RADIAL_R035.INP;1	28-May-97	1:56:02 PM	Radial Model Case R7 BRAGFLO ascii input file (from Prebrag)
BRAGFLO_EPA_WF_RADIAL_R039.BIN;1	3-Jun-97	5:00:41 PM	Radial Model Case R1 BRAGFLO output binary
BRAGFLO_EPA_WF_RADIAL_R039.CDB;1	4-Jun-97	7:21:56 AM	Radial Model Case R1 POST-BRAG output binary (Camdat database)
BRAGFLO_EPA_WF_RADIAL_R039.INP;1	3-Jun-97	2:40:14 PM	Radial Model Case R1 BRAGFLO ascii input file (from Prebrag)
BRAGFLO_EPA_WF_RADIAL_R040.BIN;1	3-Jun-97	7:13:42 PM	Radial Model Case R2 BRAGFLO output binary
BRAGFLO_EPA_WF_RADIAL_R040.CDB;1	4-Jun-97	7:22:38 AM	Radial Model Case R2 POST-BRAG output binary (Camdat database)
BRAGFLO_EPA_WF_RADIAL_R040.INP;1	3-Jun-97	2:40:27 PM	Radial Model Case R2 BRAGFLO ascii input file (from Prebrag)
BRAGFLO_EPA_WF_RADIAL_R041.BIN;1	3-Jun-97	9:54:42 PM	Radial Model Case R3 BRAGFLO output binary
BRAGFLO_EPA_WF_RADIAL_R041.CDB;1	4-Jun-97	7:23:27 AM	Radial Model Case R3 POST-BRAG output binary (Camdat database)
BRAGFLO_EPA_WF_RADIAL_R041.INP;1	3-Jun-97	2:40:40 PM	Radial Model Case R3 BRAGFLO ascii input file (from Prebrag)
POST.COM;3	7-May-97	7:22:59 AM	VMS command file to run POSTBRAG for radial models
POST_ALL.COM;2	29-Apr-97	7:08:16 AM	VMS command file to run POSTBRAG for radial models
POST_ALL2.COM;5	4-Jun-97	7:21:49 AM	VMS command file to run POSTBRAG for radial models
RAD1.COM;1	28-May-97	2:05:08 PM	VMS command file to run BRAGFLO for radial models
RAD2.COM;1	28-May-97	2:06:07 PM	VMS command file to run BRAGFLO for radial models
RAD_ALL.COM;2	3-Jun-97	2:43:26 PM	VMS command file to run BRAGFLO for radial models
RAD_ALL2.COM;2	28-Apr-97	11:52:10 AM	VMS command file to run BRAGFLO for radial models
F1:[NOBACK2.DMS_WATERFLOOD.EPA.GENMESH]			GENMESH sub-directory: build meshes for cross-sectional and radial models
GENMESH_EPA.INP;1	14-Apr-97	4:03:47 PM	Cross-sectional model GENMESH input file
GENMESH_EPA_APRIL3.INP;1	3-Apr-97	7:40:31 AM	Cross-sectional model GENMESH input file (early version)
GENMESH_EPA_RADIAL.INP;2	18-Apr-97	2:46:51 PM	Radial models GENMESH input file
PRECAMDAT_EPA.CDB;4	14-Apr-97	4:07:15 PM	Cross-sectional model GENMESH output file (Camdat database)
PRECAMDAT_EPA_RADIAL.CDB;1	18-Apr-97	2:49:09 PM	Radial models GENMESH output file (Camdat database)

Information Only

CMS directory for all files: DISKSDOLLY_CCA1:[NON_HSM.CMS.BF_WF_EXP1]			
VMS File names	Date Created	Time Created	Brief Description
F1:[NOBACK2.DMS_WATERFLOOD.EPA.ICSET]			ICSET sub-directory: assign temporary initial conditions to all elements (later changed in ALGEBRA): step between MATSET and ALGEBRA
DUMB_ICSET.COM;1	21-May-97	12:11:42 PM	VMS command file to run Cross-sectional model for ICSET
ICSET.COM;1	3-Apr-97	3:28:43 PM	VMS command file to run Cross-sectional model for ICSET (early version)
ICSET_EPA.INP;2	3-Apr-97	2:07:43 PM	ICSET input file for cross-sectional model
ICSET_EPA_RADIAL.INP;2	21-Apr-97	12:02:13 PM	ICSET input file for radial models
ICSET_EPA_WF_DUMBELL_R001.CDB;1	20-May-97	3:26:26 PM	ICSET output binary file for Cross-sectional model (camdat database)
ICSET_EPA_WF_RADIAL_R015.CDB;1	24-Apr-97	5:18:11 PM	Radial Model Case R9 ICSET output CDB
ICSET_EPA_WF_RADIAL_R028.CDB;1	2-May-97	2:21:27 PM	Radial Model Case R8 ICSET output CDB
ICSET_EPA_WF_RADIAL_R029.CDB;1	2-May-97	2:21:30 PM	Radial Model Case R10 ICSET output CDB
ICSET_EPA_WF_RADIAL_R031.CDB;1	28-May-97	9:54:09 AM	Radial Model Case R4 ICSET output CDB
ICSET_EPA_WF_RADIAL_R033.CDB;1	28-May-97	9:54:32 AM	Radial Model Case R5 ICSET output CDB
ICSET_EPA_WF_RADIAL_R034.CDB;1	28-May-97	9:54:53 AM	Radial Model Case R6 ICSET output CDB
ICSET_EPA_WF_RADIAL_R035.CDB;1	28-May-97	9:55:07 AM	Radial Model Case R7 ICSET output CDB
ICSET_EPA_WF_RADIAL_R039.CDB;1	3-Jun-97	2:33:50 PM	Radial Model Case R1 ICSET output CDB
ICSET_EPA_WF_RADIAL_R040.CDB;1	3-Jun-97	2:33:53 PM	Radial Model Case R2 ICSET output CDB
ICSET_EPA_WF_RADIAL_R041.CDB;1	3-Jun-97	2:33:56 PM	Radial Model Case R3 ICSET output CDB
IC_RADIAL.COM;1	18-Apr-97	4:10:48 PM	VMS command file to run Radial models for ICSET
IC_RAD_ALL.COM;2	21-Apr-97	5:35:48 PM	VMS command file to run Radial models for ICSET
IC_RAD_ALL2.COM;2	29-Apr-97	3:52:28 PM	VMS command file to run Radial models for ICSET
IC_RAD_ALL3.COM;5	3-Jun-97	2:33:36 PM	VMS command file to run Radial models for ICSET
IC_RAD_R011.COM;1	24-Apr-97	7:21:48 AM	VMS command file to run Radial models for ICSET
F1:[NOBACK2.DMS_WATERFLOOD.EPA.MATSET]			MATSET sub-directory: assign parameter values from database view CCA6, some are assigned by analyst, some are changed in ALGEBRA later
CAMDAT_EPA_WF_DUMBELL_R001.CDB;1	20-May-97	3:06:21 PM	MATSET output binary file for Cross-sectional model (camdat database)
CAMDAT_EPA_WF_RADIAL_R015.CDB;1	24-Apr-97	5:14:13 PM	Radial Model Case R9 MATSET output CDB
CAMDAT_EPA_WF_RADIAL_R028.CDB;1	2-May-97	2:13:53 PM	Radial Model Case R8 MATSET output CDB
CAMDAT_EPA_WF_RADIAL_R029.CDB;1	2-May-97	2:14:25 PM	Radial Model Case R10 MATSET output CDB
CAMDAT_EPA_WF_RADIAL_R031.CDB;2	28-May-97	8:32:21 AM	Radial Model Case R4 MATSET output CDB
CAMDAT_EPA_WF_RADIAL_R033.CDB;1	28-May-97	9:46:05 AM	Radial Model Case R5 MATSET output CDB
CAMDAT_EPA_WF_RADIAL_R034.CDB;1	28-May-97	9:46:52 AM	Radial Model Case R6 MATSET output CDB
CAMDAT_EPA_WF_RADIAL_R035.CDB;1	28-May-97	9:47:38 AM	Radial Model Case R7 MATSET output CDB
CAMDAT_EPA_WF_RADIAL_R039.CDB;1	3-Jun-97	2:30:56 PM	Radial Model Case R1 MATSET output CDB
CAMDAT_EPA_WF_RADIAL_R040.CDB;1	3-Jun-97	2:31:28 PM	Radial Model Case R2 MATSET output CDB
CAMDAT_EPA_WF_RADIAL_R041.CDB;1	3-Jun-97	2:31:59 PM	Radial Model Case R3 MATSET output CDB
DMS.COM;13	3-Apr-97	11:31:29 AM	VMS command file: early version
DUMB_MAT.COM;1	21-May-97	12:05:31 PM	VMS command file to run cross-sectional model: early version
DUMB_R001.COM;2	20-May-97	3:05:36 PM	VMS command file to run cross-sectional model case
MATSET_DUMBELL_R001.INP;1	20-May-97	3:02:09 PM	MATSET input file for cross sectional model
MATSET_EPA.INP;32	18-Apr-97	3:55:58 PM	MATSET input file: early version
MATSET_EPA_APRIL10.INP;1	10-Apr-97	1:44:46 PM	MATSET input file: early version
MATSET_EPA_RADIAL.INP;2	18-Apr-97	3:55:04 PM	MATSET input file for radial models: early version
MATSET_EPA_RADIAL_R015.INP;1	24-Apr-97	5:08:16 PM	Radial Model Case R9 MATSET input file

Information Only

CMS directory for all files:			
DISKSDOLLY_CCA1:[NON_HSM.CMS.BF_WF_EXP1]	Date	Time	
VMS File names	Created	Created	Brief Description
MATSET_EPA_RADIAL_R028.INP;1	2-May-97	2:10:14 PM	Radial Model Case R8 MATSET input file
MATSET_EPA_RADIAL_R029.INP;1	2-May-97	2:05:48 PM	Radial Model Case R10 MATSET input file
MATSET_EPA_RADIAL_R031.INP;2	28-May-97	8:31:44 AM	Radial Model Case R4 MATSET input file
MATSET_EPA_RADIAL_R033.INP;1	28-May-97	9:36:04 AM	Radial Model Case R5 MATSET input file
MATSET_EPA_RADIAL_R034.INP;1	28-May-97	9:36:15 AM	Radial Model Case R6 MATSET input file
MATSET_EPA_RADIAL_R035.INP;1	28-May-97	9:36:23 AM	Radial Model Case R7 MATSET input file
MATSET_EPA_RADIAL_R039.INP;1	3-Jun-97	2:26:23 PM	Radial Model Case R1 MATSET input file
MATSET_EPA_RADIAL_R040.INP;1	3-Jun-97	2:27:36 PM	Radial Model Case R2 MATSET input file
MATSET_EPA_RADIAL_R041.INP;1	3-Jun-97	2:28:15 PM	Radial Model Case R3 MATSET input file
MAT_RADIAL.COM;1	18-Apr-97	3:56:56 PM	VMS command file to run some of the radial MATSET cases
MAT_RAD_ALL.COM;2	21-Apr-97	5:27:50 PM	VMS command file to run some of the radial MATSET cases
MAT_RAD_ALL2.COM;2	29-Apr-97	3:07:38 PM	VMS command file to run some of the radial MATSET cases
MAT_RAD_ALL3.COM;6	3-Jun-97	2:30:14 PM	VMS command file to run some of the radial MATSET cases
RAD_MAT.COM;1	28-May-97	7:27:38 AM	VMS command file to run some of the radial MATSET cases
F1:[NOBACK2.DMS_WATERFLOOD.EPA.POST_CROSS]			Post-processing sub-directory for Cross-sectional model
POSTALG_CROSS.INP;5	10-Jun-97	12:52:01 PM	ALGEBRA input file for processing output CDB from BRAGFLO
POSTALG_EPA_WF_DUMBELL_R001.CDB;3	10-Jun-97	12:53:23 PM	Output binary from ALGEBRA (camdat database)
R001.COM;3	10-Jun-97	9:58:47 AM	VMS command file to run ALGEBRA
F1:[NOBACK2.DMS_WATERFLOOD.EPA.POST_RADIAL]			Post-processing sub-directory for Radial model(s)
ALL.COM;3	4-Jun-97	7:28:58 AM	VMS command file to run ALGEBRA
ALL2.COM;3	12-May-97	2:52:29 PM	VMS command file to run ALGEBRA
POSTALG_EPA_WF_RADIAL_R015.CDB;1	2-May-97	10:16:17 AM	Radial Model Case R9 ALGEBRA output binary file (Camdat database)
POSTALG_EPA_WF_RADIAL_R028.CDB;1	5-May-97	9:58:40 AM	Radial Model Case R8 ALGEBRA output binary file (Camdat database)
POSTALG_EPA_WF_RADIAL_R029.CDB;1	5-May-97	10:04:38 AM	Radial Model Case R10 ALGEBRA output binary file (Camdat database)
POSTALG_EPA_WF_RADIAL_R031.CDB;1	30-May-97	3:39:32 PM	Radial Model Case R4 ALGEBRA output binary file (Camdat database)
POSTALG_EPA_WF_RADIAL_R033.CDB;1	30-May-97	3:40:28 PM	Radial Model Case R5 ALGEBRA output binary file (Camdat database)
POSTALG_EPA_WF_RADIAL_R034.CDB;1	30-May-97	3:42:14 PM	Radial Model Case R6 ALGEBRA output binary file (Camdat database)
POSTALG_EPA_WF_RADIAL_R035.CDB;1	30-May-97	3:44:12 PM	Radial Model Case R7 ALGEBRA output binary file (Camdat database)
POSTALG_EPA_WF_RADIAL_R039.CDB;1	4-Jun-97	7:29:12 AM	Radial Model Case R1 ALGEBRA output binary file (Camdat database)
POSTALG_EPA_WF_RADIAL_R040.CDB;1	4-Jun-97	7:29:36 AM	Radial Model Case R2 ALGEBRA output binary file (Camdat database)
POSTALG_EPA_WF_RADIAL_R041.CDB;1	4-Jun-97	7:30:06 AM	Radial Model Case R3 ALGEBRA output binary file (Camdat database)
POSTALG_RAD.INP;12	2-May-97	9:40:24 AM	ALGEBRA input file to post-process radial model BRAGFLO .cdb's
F1:[NOBACK2.DMS_WATERFLOOD.EPA.PREBRAG]			PREBRAG sub-directory: step between ALGEBRA and BRAGFLO
DUMB.COM;2	21-May-97	12:13:22 PM	VMS command file to run PREBRAG cross-sectional model
PREB.COM;3	1-May-97	10:46:04 AM	VMS command file: early version
PREBRAG_EPA.INP;7	5-May-97	8:50:24 AM	PREBRAG input file for cross-sectional model: early version
PREBRAG_EPA2.INP;2	21-May-97	11:38:57 AM	PREBRAG input file for cross-sectional model
PREBRAG_EPA_RADIAL.INP;3	21-Apr-97	10:15:57 AM	PREBRAG input file for some radial cases

Information Only



CMS directory for all files:			
DISK\$DOLLY_CCA1:[NON_HSM.CMS.BF_WF_EXP1]	Date	Time	
VMS File names	Created	Created	Brief Description
PREBRAG_EPA_RADIAL_50YR.INP;2	28-Apr-97	11:42:52 AM	PREBRAG input file for some radial cases
PREBRAG_EPA_RADIAL_R012.INP;1	24-Apr-97	5:24:13 PM	PREBRAG input file for some radial cases
PREBRAG_EPA_RADIAL_R018.INP;1	28-Apr-97	11:06:20 AM	PREBRAG input file for some radial cases
PREBRAG_EPA_RADIAL_R031.INP;1	28-May-97	11:22:33 AM	PREBRAG input file for some radial cases
PREBRAG_EPA_RADIAL_R033.INP;2	28-May-97	1:49:57 PM	PREBRAG input file for some radial cases
PREBRAG_EPA_RADIAL_R034.INP;3	28-May-97	1:25:25 PM	PREBRAG input file for some radial cases
PREBRAG_EPA_RADIAL_R035.INP;1	28-May-97	1:28:30 PM	PREBRAG input file for some radial cases
PREB_RAD.COM;1	21-Apr-97	8:36:48 AM	VMS command file to run PREBRAG radial cases
PREB_RAD_50YR.COM;3	2-May-97	2:32:51 PM	VMS command file to run PREBRAG radial cases
PREB_RAD_ALL.COM;2	3-Jun-97	2:39:53 PM	VMS command file to run PREBRAG radial cases
RAD.COM;2	28-May-97	1:57:09 PM	VMS command file to run PREBRAG radial cases
TEST.COM;4	28-May-97	1:06:49 PM	VMS command file to run PREBRAG radial cases
F1:[NOBACK2.DMS_WATERFLOOD.EPA.REPORT]			SUMMARIZE sub-directory to organize output from POSTALG .cdb's to port to the PC (via FTP) for plotting and further analysis
CROSS_01.INP;1	10-Jun-97	2:14:47 PM	SUMMARIZE input file for cross-sectional model
CROSS_01.TBL;1	10-Jun-97	2:15:33 PM	SUMMARIZE output text file for cross-sectional model
FRACTURE.INP;3	4-Jun-97	10:42:34 AM	SUMMARIZE input file for radial models: obtain fracture lengths
FRACTURE.TBL;1	4-Jun-97	10:43:08 AM	SUMMARIZE output text file for radial models fracture lengths
FRAC_CRO.INP;1	10-Jun-97	1:55:03 PM	SUMMARIZE input file for cross-sectional model: obtain fracture lengths
FRAC_CRO.TBL;1	10-Jun-97	1:55:34 PM	SUMMARIZE output text file for cross-sectional model fracture lengths
POSTALG_EPA_WF_RADIAL_CASE01.CDB;1	4-Jun-97	10:07:43 AM	Copied from POSTALG_EPA_WF_RADIAL_R039.CDB;1 (accessed by SUMMARIZE)
POSTALG_EPA_WF_RADIAL_CASE02.CDB;1	4-Jun-97	10:08:12 AM	Copied from POSTALG_EPA_WF_RADIAL_R040.CDB;1 (accessed by SUMMARIZE)
POSTALG_EPA_WF_RADIAL_CASE03.CDB;1	4-Jun-97	10:08:36 AM	Copied from POSTALG_EPA_WF_RADIAL_R041.CDB;1 (accessed by SUMMARIZE)
POSTALG_EPA_WF_RADIAL_CASE04.CDB;1	4-Jun-97	10:08:55 AM	Copied from POSTALG_EPA_WF_RADIAL_R031.CDB;1 (accessed by SUMMARIZE)
POSTALG_EPA_WF_RADIAL_CASE05.CDB;1	4-Jun-97	10:09:14 AM	Copied from POSTALG_EPA_WF_RADIAL_R033.CDB;1 (accessed by SUMMARIZE)
POSTALG_EPA_WF_RADIAL_CASE06.CDB;1	4-Jun-97	10:09:40 AM	Copied from POSTALG_EPA_WF_RADIAL_R034.CDB;1 (accessed by SUMMARIZE)
POSTALG_EPA_WF_RADIAL_CASE07.CDB;1	4-Jun-97	10:10:00 AM	Copied from POSTALG_EPA_WF_RADIAL_R035.CDB;1 (accessed by SUMMARIZE)
POSTALG_EPA_WF_RADIAL_CASE08.CDB;1	4-Jun-97	10:10:26 AM	Copied from POSTALG_EPA_WF_RADIAL_R028.CDB;1 (accessed by SUMMARIZE)
POSTALG_EPA_WF_RADIAL_CASE09.CDB;1	4-Jun-97	10:10:48 AM	Copied from POSTALG_EPA_WF_RADIAL_R015.CDB;1 (accessed by SUMMARIZE)
POSTALG_EPA_WF_RADIAL_CASE10.CDB;1	4-Jun-97	10:11:10 AM	Copied from POSTALG_EPA_WF_RADIAL_R029.CDB;1 (accessed by SUMMARIZE)
SUMM_RAD.INP;7	4-Jun-97	10:27:15 AM	SUMMARIZE input file for radial models (output files for each variable fr radial models follow)
VAR_01.TBL;1	4-Jun-97	10:28:28 AM	Time-history output fr SUMMARIZE for variable: RAT_TOT (total inj rate m <sup>3</sup> /s)
VAR_02.TBL;1	4-Jun-97	10:28:28 AM	Time-history output fr SUMMARIZE for variable: MON_TOT (monthly inj bbl/mo)
VAR_03.TBL;1	4-Jun-97	10:28:29 AM	Time-history output fr SUMMARIZE for variable: INJ_BONE (tot inj at Bone-Spring m <sup>3</sup> )
VAR_04.TBL;1	4-Jun-97	10:28:29 AM	Time-history output fr SUMMARIZE for variable: INJ_BRSH (tot inj at Brushy C m <sup>3</sup> )
VAR_05.TBL;1	4-Jun-97	10:28:29 AM	Time-history output fr SUMMARIZE for variable: INJ_CHER (tot inj at Cherry C m <sup>3</sup> )
VAR_06.TBL;1	4-Jun-97	10:28:30 AM	Time-history output fr SUMMARIZE for variable: INJ_UBEL (tot inj at U Bell C m <sup>3</sup> )
VAR_07.TBL;1	4-Jun-97	10:28:30 AM	Time-history output fr SUMMARIZE for variable: TOT_INJ (tot inj at all formation m <sup>3</sup> )
VAR_08.TBL;1	4-Jun-97	10:28:31 AM	Time-history output fr SUMMARIZE for variable: CUM_M139 (cum flow into MB139 m <sup>3</sup> )
VAR_09.TBL;1	4-Jun-97	10:28:31 AM	Time-history output fr SUMMARIZE for variable: CUM_M138 (cum flow into MB138, AB m <sup>3</sup> )
VAR_10.TBL;1	4-Jun-97	10:28:31 AM	Time-history output fr SUMMARIZE for variable: CUM_CASA (cum flow into Castile Anh m <sup>3</sup> )
VAR_11.TBL;1	4-Jun-97	10:28:32 AM	Time-history output fr SUMMARIZE for variable: CUM_LCOM (cum flow into L Anh Com m <sup>3</sup> )
VAR_12.TBL;1	4-Jun-97	10:28:32 AM	Time-history output fr SUMMARIZE for variable: CUM_UCOM (cum flow into U Anh Com m <sup>3</sup> )
VAR_13.TBL;1	4-Jun-97	10:28:32 AM	Time-history output fr SUMMARIZE for variable: CUM_LEAK (cum leak up well into Salt m <sup>3</sup> )

Information Only

CMS directory for all files: DISKSDOLLY_CCA1:[NON_HSM.CMS.BF_WF_EXP1]			
VMS File names	Date Created	Time Created	Brief Description
VAR_14.TBL;1	4-Jun-97	10:28:33 AM	Time-history output fr SUMMARIZE for variable: FLO_BONE (tot flow into Bone-Spring m <sup>3</sup> )
VAR_15.TBL;1	4-Jun-97	10:28:33 AM	Time-history output fr SUMMARIZE for variable: FLO_BRSH (tot flow into Brushy C m <sup>3</sup> )
VAR_16.TBL;1	4-Jun-97	10:28:34 AM	Time-history output fr SUMMARIZE for variable: FLO_CHER (tot flow into Cherry C m <sup>3</sup> )
VAR_17.TBL;1	4-Jun-97	10:28:34 AM	Time-history output fr SUMMARIZE for variable: FLO_UBEL (tot flow into U Bell C m <sup>3</sup> )
VAR_18.TBL;1	4-Jun-97	10:28:34 AM	Time-history output fr SUMMARIZE for variable: TOT_FLO (tot flow into all formation m <sup>3</sup> )
VAR_19.TBL;1	4-Jun-97	10:28:35 AM	Time-history output fr SUMMARIZE for variable: CUM_SALT (leak-off into Halite from well m <sup>3</sup> )
VAR_20.TBL;1	4-Jun-97	10:28:35 AM	Time-history output fr SUMMARIZE for variable: WELL_TOP (flow up well at Culebra m <sup>3</sup> )
VAR_21.TBL;1	4-Jun-97	10:28:36 AM	Time-history output fr SUMMARIZE for variable: CUM_LOFF (total of cum_salt+well_top m <sup>3</sup> )
VAR_22.TBL;1	4-Jun-97	10:28:36 AM	Time-history output fr SUMMARIZE for variable: OUT_ZONE (flow into deeper non_pay m <sup>3</sup> )
VAR_23.TBL;1	4-Jun-97	10:28:36 AM	Time-history output fr SUMMARIZE for variable: WB_BONES (pressure in well at BoneSp, Pa)
VAR_24.TBL;1	4-Jun-97	10:28:37 AM	Time-history output fr SUMMARIZE for variable: WB_BRUSH (pressure in well at Brushy C, Pa)
VAR_25.TBL;1	4-Jun-97	10:28:37 AM	Time-history output fr SUMMARIZE for variable: WB_CHERR (pressure in well at Cherry C, Pa)
VAR_26.TBL;1	4-Jun-97	10:28:37 AM	Time-history output fr SUMMARIZE for variable: WB_UBELL (pressure in well at U Bell C, Pa)
VAR_27.TBL;1	4-Jun-97	10:28:38 AM	Time-history output fr SUMMARIZE for variable: WB_CANHY (pressure in well at Castile, Pa)
VAR_28.TBL;1	4-Jun-97	10:28:38 AM	Time-history output fr SUMMARIZE for variable: WB_LCOMP (pressure in well at L Anhyd, Pa)
VAR_29.TBL;1	4-Jun-97	10:28:38 AM	Time-history output fr SUMMARIZE for variable: WB_MB139 (pressure in well at MB 139, Pa)
VAR_30.TBL;1	4-Jun-97	10:28:38 AM	Time-history output fr SUMMARIZE for variable: WB_MB138 (pressure in well at MB 138, Pa)
VAR_31.TBL;1	4-Jun-97	10:28:39 AM	Time-history output fr SUMMARIZE for variable: WB_UCOMP (pressure in well at U Anhyd, Pa)
VAR_32.TBL;1	4-Jun-97	10:28:39 AM	Time-history output fr SUMMARIZE for variable: PR_UBELL (avg pressure at 3km, U Bell C, Pa)
VAR_33.TBL;1	4-Jun-97	10:28:39 AM	Time-history output fr SUMMARIZE for variable: PR_MB139 (avg pressure at 3km, MB 139, Pa)
VAR_34.TBL;1	4-Jun-97	10:28:39 AM	Time-history output fr SUMMARIZE for variable: PR_MB138 (avg pressure at 3km, MB 138, Pa)
VAR_35.TBL;1	4-Jun-97	10:28:39 AM	Time-history output fr SUMMARIZE for variable: M139_2KM (cum flow at 2km, MB139 m <sup>3</sup> )
VAR_36.TBL;1	4-Jun-97	10:28:40 AM	Time-history output fr SUMMARIZE for variable: M138_2KM (cum flow at 2km, MB138 m <sup>3</sup> )

Information Only

## **Appendix C: Complete Listing of Parameters Used for the Radial Models**

The following table lists all parameters used for the radial model cases, except where noted in Tables One through Three, section 4.1.

**Information Only**



Database		Database Source: F1:[NOBACK2.DMS_WATERFLOOD.EPA.ALGEBRA]ALGEBRA_EPA_WF_RADIAL_R033.CDB;1 (Radial Case R5)						
ID Number	Material	Property	Value	Material Description	Property Value Description	Usage	Source	
1	N/A	MORRO_PI	CAP_MOD	2.000E+00	Morrow Formation, Pay 1	Capillary Pressure Model Number (same as Culebra)	Required for BRAGFLO	Analyst: DM Stoelzel
2	N/A	MORRO_PI	COMP_RCK	3.015E-10	Morrow Formation, Pay 1	Rock compressibility (also pore compress) from Petroleum literature	Not used	Analyst: DM Stoelzel
3	N/A	MORRO_PI	PC_MAX	1.000E+08	Morrow Formation, Pay 1	Max capillary pressure (same as Culebra)	Required for BRAGFLO	Analyst: DM Stoelzel
4	N/A	MORRO_PI	PCT_A	2.600E-01	Morrow Formation, Pay 1	Capillary pressure multiplier (same as Culebra)	Required for BRAGFLO	Analyst: DM Stoelzel
5	N/A	MORRO_PI	PCT_EXP	-3.480E-01	Morrow Formation, Pay 1	Capillary pressure exponent (same as Culebra)	Required for BRAGFLO	Analyst: DM Stoelzel
6	N/A	MORRO_PI	KPT	0.000E+00	Morrow Formation, Pay 1	Not used - placeholder	Not used	Analyst: DM Stoelzel
7	N/A	MORRO_PI	PO_MIN	1.013E+05	Morrow Formation, Pay 1	Minimum Brine pressure (same for all materials)	Required for BRAGFLO	Analyst: DM Stoelzel
8	N/A	MORRO_PI	PORE_DIS	7.000E-01	Morrow Formation, Pay 1	Pore distribution (fraction)	Required for BRAGFLO	Analyst: DM Stoelzel
9	N/A	MORRO_PI	POROSITY	1.100E-01	Morrow Formation, Pay 1	Porosity (fraction)	Required for BRAGFLO	Analyst: DM Stoelzel
10	N/A	MORRO_PI	PRESSURE	5.292E+07	Morrow Formation, Pay 1	Hydrostatic initial pressure (Pa)	Not used	Analyst: DM Stoelzel
11	N/A	MORRO_PI	PRMX_LOG	-1.369E+01	Morrow Formation, Pay 1	Log x-direction permeability (from NM Bureau of Mines)	Intermediate value	Analyst: DM Stoelzel
12	N/A	MORRO_PI	PRMY_LOG	-1.369E+01	Morrow Formation, Pay 1	Log y-direction permeability	Intermediate value	Analyst: DM Stoelzel
13	N/A	MORRO_PI	PRMZ_LOG	-1.369E+01	Morrow Formation, Pay 1	Log z-direction permeability (BRAGFLO required input)	Not used - 2D model	Analyst: DM Stoelzel
14	N/A	MORRO_PI	RELP_MOD	4.000E+00	Morrow Formation, Pay 1	Relative permeability model number	Required for BRAGFLO	Analyst: DM Stoelzel
15	N/A	MORRO_PI	SAT_RBRN	2.000E-01	Morrow Formation, Pay 1	Residual Brine saturation	Required for BRAGFLO	Analyst: DM Stoelzel
16	N/A	MORRO_PI	SAT_RGAS	1.000E-02	Morrow Formation, Pay 1	Residual Gas saturation	Required for BRAGFLO	Analyst: DM Stoelzel
17	N/A	MORRO_PI	PERM_X	2.061E-14	Morrow Formation, Pay 1	X-direction permeability (m <sup>2</sup> ) from Log value (NM B of Mines)	Required for BRAGFLO	Analyst: DM Stoelzel
18	N/A	MORRO_PI	PERM_Y	2.061E-14	Morrow Formation, Pay 1	Y-direction permeability (m <sup>2</sup> ) from Log value	Required for BRAGFLO	Analyst: DM Stoelzel
19	N/A	MORRO_PI	PERM_Z	2.061E-14	Morrow Formation, Pay 1	Z-direction permeability (m <sup>2</sup> ) Not used in 2D	Required for BRAGFLO	Analyst: DM Stoelzel
20	N/A	MORRO_PI	SB_MIN	2.100E-01	Morrow Formation, Pay 1	Minimum saturation (SAT_RBRN * 1.05)	Required for BRAGFLO	Analyst: DM Stoelzel
21	N/A	MORRO_PI	POR_COMP	3.015E-10	Morrow Formation, Pay 1	Pore compress from petroleum literature as function of depth (1/Pa)	Required for BRAGFLO	Analyst: DM Stoelzel
22	N/A	MORRO_NP	CAP_MOD	2.000E+00	Morrow Formation, No pay	Capillary Pressure Model Number (same as Culebra)	Required for BRAGFLO	Analyst: DM Stoelzel
23	N/A	MORRO_NP	COMP_RCK	3.081E-10	Morrow Formation, No pay	Rock compressibility (also pore compress) from Petroleum literature	Not used	Analyst: DM Stoelzel
24	N/A	MORRO_NP	PC_MAX	1.000E+08	Morrow Formation, No pay	Max capillary pressure (same as Culebra)	Required for BRAGFLO	Analyst: DM Stoelzel
25	N/A	MORRO_NP	PCT_A	2.600E-01	Morrow Formation, No pay	Capillary pressure multiplier (same as Culebra)	Required for BRAGFLO	Analyst: DM Stoelzel
26	N/A	MORRO_NP	PCT_EXP	-3.480E-01	Morrow Formation, No pay	Capillary pressure exponent (same as Culebra)	Required for BRAGFLO	Analyst: DM Stoelzel
27	N/A	MORRO_NP	KPT	0.000E+00	Morrow Formation, No pay	Not used - placeholder	Not used	Analyst: DM Stoelzel
28	N/A	MORRO_NP	PO_MIN	1.013E+05	Morrow Formation, No pay	Minimum Brine pressure (same for all materials)	Required for BRAGFLO	Analyst: DM Stoelzel
29	N/A	MORRO_NP	PORE_DIS	7.000E-01	Morrow Formation, No pay	Pore distribution (fraction)	Required for BRAGFLO	Analyst: DM Stoelzel
30	N/A	MORRO_NP	POROSITY	4.000E-02	Morrow Formation, No pay	Porosity (fraction)	Required for BRAGFLO	Analyst: DM Stoelzel
31	N/A	MORRO_NP	PRESSURE	5.163E+07	Morrow Formation, No pay	Hydrostatic initial pressure (Pa)	Not used	Analyst: DM Stoelzel
32	N/A	MORRO_NP	PRMX_LOG	-1.575E+01	Morrow Formation, No pay	Log x-direction permeability (from NM Bureau of Mines)	Intermediate value	Analyst: DM Stoelzel
33	N/A	MORRO_NP	PRMY_LOG	-1.575E+01	Morrow Formation, No pay	Log y-direction permeability	Intermediate value	Analyst: DM Stoelzel
34	N/A	MORRO_NP	PRMZ_LOG	-1.575E+01	Morrow Formation, No pay	Log z-direction permeability (BRAGFLO required input)	Not used - 2D model	Analyst: DM Stoelzel
35	N/A	MORRO_NP	RELP_MOD	4.000E+00	Morrow Formation, No pay	Relative permeability model number	Required for BRAGFLO	Analyst: DM Stoelzel
36	N/A	MORRO_NP	SAT_RBRN	2.000E-01	Morrow Formation, No pay	Residual Brine saturation	Required for BRAGFLO	Analyst: DM Stoelzel
37	N/A	MORRO_NP	SAT_RGAS	1.000E-02	Morrow Formation, No pay	Residual Gas saturation	Required for BRAGFLO	Analyst: DM Stoelzel
38	N/A	MORRO_NP	PERM_X	1.778E-16	Morrow Formation, No pay	X-direction permeability (m <sup>2</sup> ) from Log value (NM B of Mines)	Required for BRAGFLO	Analyst: DM Stoelzel
39	N/A	MORRO_NP	PERM_Y	1.778E-16	Morrow Formation, No pay	Y-direction permeability (m <sup>2</sup> ) from Log value	Required for BRAGFLO	Analyst: DM Stoelzel
40	N/A	MORRO_NP	PERM_Z	1.778E-16	Morrow Formation, No pay	Z-direction permeability (m <sup>2</sup> ) Not used in 2D	Required for BRAGFLO	Analyst: DM Stoelzel
41	N/A	MORRO_NP	SB_MIN	2.100E-01	Morrow Formation, No pay	Minimum saturation (SAT_RBRN * 1.05)	Required for BRAGFLO	Analyst: DM Stoelzel
42	N/A	MORRO_NP	POR_COMP	3.081E-10	Morrow Formation, No pay	Pore compress from petroleum literature as function of depth (1/Pa)	Required for BRAGFLO	Analyst: DM Stoelzel
43	N/A	ATOKA_PI	CAP_MOD	2.000E+00	Atoka Formation, Pay 1	Capillary Pressure Model Number (same as Culebra)	Required for BRAGFLO	Analyst: DM Stoelzel
44	N/A	ATOKA_PI	COMP_RCK	3.149E-10	Atoka Formation, Pay 1	Rock compressibility (also pore compress) from Petroleum literature	Not used	Analyst: DM Stoelzel
45	N/A	ATOKA_PI	PC_MAX	1.000E+08	Atoka Formation, Pay 1	Max capillary pressure (same as Culebra)	Required for BRAGFLO	Analyst: DM Stoelzel
46	N/A	ATOKA_PI	PCT_A	2.600E-01	Atoka Formation, Pay 1	Capillary pressure multiplier (same as Culebra)	Required for BRAGFLO	Analyst: DM Stoelzel

Information Only

Database				Database Source: F1:[NOBACK2.DMS_WATERFLOOD.EPA_ALGEBRA]ALGEBRA_EPA_WF_RADIAL_R033.CDB;1 (Radial Case R5)				
ID Number	Material	Property	Value	Material Description	Property Value Description	Usage	Source	
47	N/A	ATOKA_P1	PCT_EXP	-3.480E-01	Atoka Formation, Pay 1	Capillary pressure exponent (same as Culebra)	Required for BRAGFLO	Analyst: DM Stoelzel
48	N/A	ATOKA_P1	KPT	0.000E+00	Atoka Formation, Pay 1	Not used - placeholder	Not used	Analyst: DM Stoelzel
49	N/A	ATOKA_P1	PO_MIN	1.013E+05	Atoka Formation, Pay 1	Minimum Brine pressure (same for all materials)	Required for BRAGFLO	Analyst: DM Stoelzel
50	N/A	ATOKA_P1	PORE_DIS	7.000E-01	Atoka Formation, Pay 1	Pore distribution (fraction)	Required for BRAGFLO	Analyst: DM Stoelzel
51	N/A	ATOKA_P1	POROSITY	9.000E-02	Atoka Formation, Pay 1	Porosity (fraction)	Required for BRAGFLO	Analyst: DM Stoelzel
52	N/A	ATOKA_P1	PRESSURE	5.036E+07	Atoka Formation, Pay 1	Hydrostatic initial pressure (Pa)	Not used	Analyst: DM Stoelzel
53	N/A	ATOKA_P1	PRMX_LOG	-1.369E+01	Atoka Formation, Pay 1	Log x-direction permeability (from NM Bureau of Mines)	Intermediate value	Analyst: DM Stoelzel
54	N/A	ATOKA_P1	PRMY_LOG	-1.369E+01	Atoka Formation, Pay 1	Log y-direction permeability	Intermediate value	Analyst: DM Stoelzel
55	N/A	ATOKA_P1	PRMZ_LOG	-1.369E+01	Atoka Formation, Pay 1	Log z-direction permeability (BRAGFLO required input)	Not used - 2D model	Analyst: DM Stoelzel
56	N/A	ATOKA_P1	RELP_MOD	4.000E+00	Atoka Formation, Pay 1	Relative permeability model number	Required for BRAGFLO	Analyst: DM Stoelzel
57	N/A	ATOKA_P1	SAT_RBRN	2.000E-01	Atoka Formation, Pay 1	Residual Brine saturation	Required for BRAGFLO	Analyst: DM Stoelzel
58	N/A	ATOKA_P1	SAT_RGAS	1.000E-02	Atoka Formation, Pay 1	Residual Gas saturation	Required for BRAGFLO	Analyst: DM Stoelzel
59	N/A	ATOKA_P1	PERM_X	2.061E-14	Atoka Formation, Pay 1	X-direction permeability (m <sup>2</sup> ) from Log value (NM B of Mines)	Required for BRAGFLO	Analyst: DM Stoelzel
60	N/A	ATOKA_P1	PERM_Y	2.061E-14	Atoka Formation, Pay 1	Y-direction permeability (m <sup>2</sup> ) from Log value	Required for BRAGFLO	Analyst: DM Stoelzel
61	N/A	ATOKA_P1	PERM_Z	2.061E-14	Atoka Formation, Pay 1	Z-direction permeability (m <sup>2</sup> ) Not used in 2D	Required for BRAGFLO	Analyst: DM Stoelzel
62	N/A	ATOKA_P1	SB_MIN	2.100E-01	Atoka Formation, Pay 1	Minimum saturation (SAT_RBRN * 1.05)	Required for BRAGFLO	Analyst: DM Stoelzel
63	N/A	ATOKA_P1	POR_COMP	3.149E-10	Atoka Formation, Pay 1	Pore compress from petroleum literature as function of depth (1/Pa)	Required for BRAGFLO	Analyst: DM Stoelzel
64	N/A	ATOKA_NP	CAP_MOD	2.000E+00	Atoka Formation, No pay	Capillary Pressure Model Number (same as Culebra)	Required for BRAGFLO	Analyst: DM Stoelzel
65	N/A	ATOKA_NP	COMP_RCK	3.216E-10	Atoka Formation, No pay	Rock compressibility (also pore compress) from Petroleum literature	Not used	Analyst: DM Stoelzel
66	N/A	ATOKA_NP	PC_MAX	1.000E+08	Atoka Formation, No pay	Max capillary pressure (same as Culebra)	Required for BRAGFLO	Analyst: DM Stoelzel
67	N/A	ATOKA_NP	PCT_A	2.600E-01	Atoka Formation, No pay	Capillary pressure multiplier (same as Culebra)	Required for BRAGFLO	Analyst: DM Stoelzel
68	N/A	ATOKA_NP	PCT_EXP	-3.480E-01	Atoka Formation, No pay	Capillary pressure exponent (same as Culebra)	Required for BRAGFLO	Analyst: DM Stoelzel
69	N/A	ATOKA_NP	KPT	0.000E+00	Atoka Formation, No pay	Not used - placeholder	Not used	Analyst: DM Stoelzel
70	N/A	ATOKA_NP	PO_MIN	1.013E+05	Atoka Formation, No pay	Minimum Brine pressure (same for all materials)	Required for BRAGFLO	Analyst: DM Stoelzel
71	N/A	ATOKA_NP	PORE_DIS	7.000E-01	Atoka Formation, No pay	Pore distribution (fraction)	Required for BRAGFLO	Analyst: DM Stoelzel
72	N/A	ATOKA_NP	POROSITY	1.000E-02	Atoka Formation, No pay	Porosity (fraction)	Required for BRAGFLO	Analyst: DM Stoelzel
73	N/A	ATOKA_NP	PRESSURE	4.917E+07	Atoka Formation, No pay	Hydrostatic initial pressure (Pa)	Not used	Analyst: DM Stoelzel
74	N/A	ATOKA_NP	PRMX_LOG	-1.575E+01	Atoka Formation, No pay	Log x-direction permeability (from NM Bureau of Mines)	Intermediate value	Analyst: DM Stoelzel
75	N/A	ATOKA_NP	PRMY_LOG	-1.575E+01	Atoka Formation, No pay	Log y-direction permeability	Intermediate value	Analyst: DM Stoelzel
76	N/A	ATOKA_NP	PRMZ_LOG	-1.575E+01	Atoka Formation, No pay	Log z-direction permeability (BRAGFLO required input)	Not used - 2D model	Analyst: DM Stoelzel
77	N/A	ATOKA_NP	RELP_MOD	4.000E+00	Atoka Formation, No pay	Relative permeability model number	Required for BRAGFLO	Analyst: DM Stoelzel
78	N/A	ATOKA_NP	SAT_RBRN	2.000E-01	Atoka Formation, No pay	Residual Brine saturation	Required for BRAGFLO	Analyst: DM Stoelzel
79	N/A	ATOKA_NP	SAT_RGAS	1.000E-02	Atoka Formation, No pay	Residual Gas saturation	Required for BRAGFLO	Analyst: DM Stoelzel
80	N/A	ATOKA_NP	PERM_X	1.778E-16	Atoka Formation, No pay	X-direction permeability (m <sup>2</sup> ) from Log value (NM B of Mines)	Required for BRAGFLO	Analyst: DM Stoelzel
81	N/A	ATOKA_NP	PERM_Y	1.778E-16	Atoka Formation, No pay	Y-direction permeability (m <sup>2</sup> ) from Log value	Required for BRAGFLO	Analyst: DM Stoelzel
82	N/A	ATOKA_NP	PERM_Z	1.778E-16	Atoka Formation, No pay	Z-direction permeability (m <sup>2</sup> ) Not used in 2D	Required for BRAGFLO	Analyst: DM Stoelzel
83	N/A	ATOKA_NP	SB_MIN	2.100E-01	Atoka Formation, No pay	Minimum saturation (SAT_RBRN * 1.05)	Required for BRAGFLO	Analyst: DM Stoelzel
84	N/A	ATOKA_NP	POR_COMP	3.216E-10	Atoka Formation, No pay	Pore compress from petroleum literature as function of depth (1/Pa)	Required for BRAGFLO	Analyst: DM Stoelzel
85	N/A	STRWN_P1	CAP_MOD	2.000E+00	Strawn Formation, Pay 1	Capillary Pressure Model Number (same as Culebra)	Required for BRAGFLO	Analyst: DM Stoelzel
86	N/A	STRWN_P1	COMP_RCK	3.286E-10	Strawn Formation, Pay 1	Rock compressibility (also pore compress) from Petroleum literature	Not used	Analyst: DM Stoelzel
87	N/A	STRWN_P1	PC_MAX	1.000E+08	Strawn Formation, Pay 1	Max capillary pressure (same as Culebra)	Required for BRAGFLO	Analyst: DM Stoelzel
88	N/A	STRWN_P1	PCT_A	2.600E-01	Strawn Formation, Pay 1	Capillary pressure multiplier (same as Culebra)	Required for BRAGFLO	Analyst: DM Stoelzel
89	N/A	STRWN_P1	PCT_EXP	-3.480E-01	Strawn Formation, Pay 1	Capillary pressure exponent (same as Culebra)	Required for BRAGFLO	Analyst: DM Stoelzel
90	N/A	STRWN_P1	KPT	0.000E+00	Strawn Formation, Pay 1	Not used - placeholder	Not used	Analyst: DM Stoelzel
91	N/A	STRWN_P1	PO_MIN	1.013E+05	Strawn Formation, Pay 1	Minimum Brine pressure (same for all materials)	Required for BRAGFLO	Analyst: DM Stoelzel
92	N/A	STRWN_P1	PORE_DIS	7.000E-01	Strawn Formation, Pay 1	Pore distribution (fraction)	Required for BRAGFLO	Analyst: DM Stoelzel

Information Only

				Database Source: F1:[NOBACK2.DMS_WATERFLOOD.EPA_ALGEBRA]ALGEBRA_EPA_WF_RADIAL_R033.CDB;1 (Radial Case R5)					
ID Number	Material	Property	Value	Material Description	Property Value Description	Usage	Source		
93	N/A	STRWN_P1	POROSITY	1.000E-01	Strawn Formation, Pay 1	Porosity (fraction)	Required for BRAGFLO	Analyst: DM Stoezel	
94	N/A	STRWN_P1	PRESSURE	4.797E+07	Strawn Formation, Pay 1	Hydrostatic initial pressure (Pa)	Not used	Analyst: DM Stoezel	
95	N/A	STRWN_P1	PRMX_LOG	-1.369E+01	Strawn Formation, Pay 1	Log x-direction permeability (from NM Bureau of Mines)	Intermediate value	Analyst: DM Stoezel	
96	N/A	STRWN_P1	PRMY_LOG	-1.369E+01	Strawn Formation, Pay 1	Log y-direction permeability	Intermediate value	Analyst: DM Stoezel	
97	N/A	STRWN_P1	PRMZ_LOG	-1.369E+01	Strawn Formation, Pay 1	Log z-direction permeability (BRAGFLO required input)	Not used - 2D model	Analyst: DM Stoezel	
98	N/A	STRWN_P1	RELP_MOD	4.000E+00	Strawn Formation, Pay 1	Relative permeability model number	Required for BRAGFLO	Analyst: DM Stoezel	
99	N/A	STRWN_P1	SAT_RBRN	2.000E-01	Strawn Formation, Pay 1	Residual Brine saturation	Required for BRAGFLO	Analyst: DM Stoezel	
100	N/A	STRWN_P1	SAT_RGAS	1.000E-02	Strawn Formation, Pay 1	Residual Gas saturation	Required for BRAGFLO	Analyst: DM Stoezel	
101	N/A	STRWN_P1	PERM_X	2.061E-14	Strawn Formation, Pay 1	X-direction permeability (m <sup>2</sup> ) from Log value (NM B of Mines)	Required for BRAGFLO	Analyst: DM Stoezel	
102	N/A	STRWN_P1	PERM_Y	2.061E-14	Strawn Formation, Pay 1	Y-direction permeability (m <sup>2</sup> ) from Log value	Required for BRAGFLO	Analyst: DM Stoezel	
103	N/A	STRWN_P1	PERM_Z	2.061E-14	Strawn Formation, Pay 1	Z-direction permeability (m <sup>2</sup> ) Not used in 2D	Required for BRAGFLO	Analyst: DM Stoezel	
104	N/A	STRWN_P1	SB_MIN	2.100E-01	Strawn Formation, Pay 1	Minimum saturation (SAT_RBRN * 1.05)	Required for BRAGFLO	Analyst: DM Stoezel	
105	N/A	STRWN_P1	POR_COMP	3.286E-10	Strawn Formation, Pay 1	Pore compress from petroleum literature as function of depth (1/Pa)	Required for BRAGFLO	Analyst: DM Stoezel	
106	N/A	STRWN_NP	CAP_MOD	2.000E+00	L Bone Sp-Wolfcamp-Strawn NP	Capillary Pressure Model Number (same as Culebra)	Required for BRAGFLO	Analyst: DM Stoezel	
107	N/A	STRWN_NP	COMP_RCK	3.699E-10	L Bone Sp-Wolfcamp-Strawn NP	Rock compressibility (also pore compress) from Petroleum literature	Not used	Analyst: DM Stoezel	
108	N/A	STRWN_NP	PC_MAX	1.000E+08	L Bone Sp-Wolfcamp-Strawn NP	Max capillary pressure (same as Culebra)	Required for BRAGFLO	Analyst: DM Stoezel	
109	N/A	STRWN_NP	PCT_A	2.600E-01	L Bone Sp-Wolfcamp-Strawn NP	Capillary pressure multiplier (same as Culebra)	Required for BRAGFLO	Analyst: DM Stoezel	
110	N/A	STRWN_NP	PCT_EXP	-3.480E-01	L Bone Sp-Wolfcamp-Strawn NP	Capillary pressure exponent (same as Culebra)	Required for BRAGFLO	Analyst: DM Stoezel	
111	N/A	STRWN_NP	KPT	0.000E+00	L Bone Sp-Wolfcamp-Strawn NP	Not used - placeholder	Not used	Analyst: DM Stoezel	
112	N/A	STRWN_NP	PO_MIN	1.013E+05	L Bone Sp-Wolfcamp-Strawn NP	Minimum Brine pressure (same for all materials)	Required for BRAGFLO	Analyst: DM Stoezel	
113	N/A	STRWN_NP	PORE_DIS	7.000E-01	L Bone Sp-Wolfcamp-Strawn NP	Pore distribution (fraction)	Required for BRAGFLO	Analyst: DM Stoezel	
114	N/A	STRWN_NP	POROSITY	2.000E-02	L Bone Sp-Wolfcamp-Strawn NP	Porosity (fraction)	Required for BRAGFLO	Analyst: DM Stoezel	
115	N/A	STRWN_NP	PRESSURE	4.182E+07	L Bone Sp-Wolfcamp-Strawn NP	Hydrostatic initial pressure (Pa)	Not used	Analyst: DM Stoezel	
116	N/A	STRWN_NP	PRMX_LOG	-1.575E+01	L Bone Sp-Wolfcamp-Strawn NP	Log x-direction permeability (from NM Bureau of Mines)	Intermediate value	Analyst: DM Stoezel	
117	N/A	STRWN_NP	PRMY_LOG	-1.575E+01	L Bone Sp-Wolfcamp-Strawn NP	Log y-direction permeability	Intermediate value	Analyst: DM Stoezel	
118	N/A	STRWN_NP	PRMZ_LOG	-1.575E+01	L Bone Sp-Wolfcamp-Strawn NP	Log z-direction permeability (BRAGFLO required input)	Not used - 2D model	Analyst: DM Stoezel	
119	N/A	STRWN_NP	RELP_MOD	4.000E+00	L Bone Sp-Wolfcamp-Strawn NP	Relative permeability model number	Required for BRAGFLO	Analyst: DM Stoezel	
120	N/A	STRWN_NP	SAT_RBRN	2.000E-01	L Bone Sp-Wolfcamp-Strawn NP	Residual Brine saturation	Required for BRAGFLO	Analyst: DM Stoezel	
121	N/A	STRWN_NP	SAT_RGAS	1.000E-02	L Bone Sp-Wolfcamp-Strawn NP	Residual Gas saturation	Required for BRAGFLO	Analyst: DM Stoezel	
122	N/A	STRWN_NP	PERM_X	1.778E-16	L Bone Sp-Wolfcamp-Strawn NP	X-direction permeability (m <sup>2</sup> ) from Log value (NM B of Mines)	Required for BRAGFLO	Analyst: DM Stoezel	
123	N/A	STRWN_NP	PERM_Y	1.778E-16	L Bone Sp-Wolfcamp-Strawn NP	Y-direction permeability (m <sup>2</sup> ) from Log value	Required for BRAGFLO	Analyst: DM Stoezel	
124	N/A	STRWN_NP	PERM_Z	1.778E-16	L Bone Sp-Wolfcamp-Strawn NP	Z-direction permeability (m <sup>2</sup> ) Not used in 2D	Required for BRAGFLO	Analyst: DM Stoezel	
125	N/A	STRWN_NP	SB_MIN	2.100E-01	L Bone Sp-Wolfcamp-Strawn NP	Minimum saturation (SAT_RBRN * 1.05)	Required for BRAGFLO	Analyst: DM Stoezel	
126	N/A	STRWN_NP	POR_COMP	3.699E-10	L Bone Sp-Wolfcamp-Strawn NP	Pore compress from petroleum literature as function of depth (1/Pa)	Required for BRAGFLO	Analyst: DM Stoezel	
127	N/A	BONES_P1	CAP_MOD	2.000E+00	Bone Spring Formation, Pay 1	Capillary Pressure Model Number (same as Culebra)	Required for BRAGFLO	Analyst: DM Stoezel	
128	N/A	BONES_P1	COMP_RCK	4.232E-10	Bone Spring Formation, Pay 1	Rock compressibility (also pore compress) from Petroleum literature	Not used	Analyst: DM Stoezel	
129	N/A	BONES_P1	PC_MAX	1.000E+08	Bone Spring Formation, Pay 1	Max capillary pressure (same as Culebra)	Required for BRAGFLO	Analyst: DM Stoezel	
130	N/A	BONES_P1	PCT_A	2.600E-01	Bone Spring Formation, Pay 1	Capillary pressure multiplier (same as Culebra)	Required for BRAGFLO	Analyst: DM Stoezel	
131	N/A	BONES_P1	PCT_EXP	-3.480E-01	Bone Spring Formation, Pay 1	Capillary pressure exponent (same as Culebra)	Required for BRAGFLO	Analyst: DM Stoezel	
132	N/A	BONES_P1	KPT	0.000E+00	Bone Spring Formation, Pay 1	Not used - placeholder	Not used	Analyst: DM Stoezel	
133	N/A	BONES_P1	PO_MIN	1.013E+05	Bone Spring Formation, Pay 1	Minimum Brine pressure (same for all materials)	Required for BRAGFLO	Analyst: DM Stoezel	
134	N/A	BONES_P1	PORE_DIS	7.000E-01	Bone Spring Formation, Pay 1	Pore distribution (fraction)	Required for BRAGFLO	Analyst: DM Stoezel	
135	N/A	BONES_P1	POROSITY	1.150E-01	Bone Spring Formation, Pay 1	Porosity (fraction)	Required for BRAGFLO	Analyst: DM Stoezel	
136	N/A	BONES_P1	PRESSURE	3.565E+07	Bone Spring Formation, Pay 1	Hydrostatic initial pressure (Pa)	Not used	Analyst: DM Stoezel	
137	N/A	BONES_P1	PRMX_LOG	-1.269E+01	Bone Spring Formation, Pay 1	Log x-direction permeability (from NM Bureau of Mines)	Intermediate value	Analyst: DM Stoezel	
138	N/A	BONES_P1	PRMY_LOG	-1.269E+01	Bone Spring Formation, Pay 1	Log y-direction permeability	Intermediate value	Analyst: DM Stoezel	

Information Only



				Database Source: F1:[NOBACK2.DMS_WATERFLOOD.EPA.ALGEBRA]ALGEBRA_EPA_WF_RADIAL_R033.CDB;1 (Radial Case R5)				
ID Number	Material	Property	Value	Material Description	Property Value Description	Usage	Source	
139	N/A	BONES_P1	PRMZ_LOG	-1.269E+01	Bone Spring Formation, Pay 1	Log z-direction permeability (BRAGFLO required input)	Not used - 2D model	Analyst: DM Stoelzel
140	N/A	BONES_P1	REL_P_MOD	4.000E+00	Bone Spring Formation, Pay 1	Relative permeability model number	Required for BRAGFLO	Analyst: DM Stoelzel
141	N/A	BONES_P1	SAT_RBRN	2.000E-01	Bone Spring Formation, Pay 1	Residual Brine saturation	Required for BRAGFLO	Analyst: DM Stoelzel
142	N/A	BONES_P1	SAT_RGAS	1.000E-02	Bone Spring Formation, Pay 1	Residual Gas saturation	Required for BRAGFLO	Analyst: DM Stoelzel
143	N/A	BONES_P1	PERM_X	2.061E-13	Bone Spring Formation, Pay 1	X-direction permeability (m <sup>2</sup> ) from Log value (NM B of Mines)	Required for BRAGFLO	Analyst: DM Stoelzel
144	N/A	BONES_P1	PERM_Y	2.061E-13	Bone Spring Formation, Pay 1	Y-direction permeability (m <sup>2</sup> ) from Log value	Required for BRAGFLO	Analyst: DM Stoelzel
145	N/A	BONES_P1	PERM_Z	2.061E-13	Bone Spring Formation, Pay 1	Z-direction permeability (m <sup>2</sup> ) Not used in 2D	Required for BRAGFLO	Analyst: DM Stoelzel
146	N/A	BONES_P1	SB_MIN	2.100E-01	Bone Spring Formation, Pay 1	Minimum saturation (SAT_RBRN * 1.05)	Required for BRAGFLO	Analyst: DM Stoelzel
147	N/A	BONES_P1	POR_COMP	4.232E-10	Bone Spring Formation, Pay 1	Pore compress from petroleum literature as function of depth (1/Pa)	Required for BRAGFLO	Analyst: DM Stoelzel
148	N/A	BONES1NP	CAP_MOD	2.000E+00	U. Bone Spring Form. No Pay	Capillary Pressure Model Number (same as Culebra)	Required for BRAGFLO	Analyst: DM Stoelzel
149	N/A	BONES1NP	COMP_RCK	4.576E-10	U. Bone Spring Form. No Pay	Rock compressibility (also pore compress) from Petroleum literature	Not used	Analyst: DM Stoelzel
150	N/A	BONES1NP	PC_MAX	1.000E+08	U. Bone Spring Form. No Pay	Max capillary pressure (same as Culebra)	Required for BRAGFLO	Analyst: DM Stoelzel
151	N/A	BONES1NP	PCT_A	2.600E-01	U. Bone Spring Form. No Pay	Capillary pressure multiplier (same as Culebra)	Required for BRAGFLO	Analyst: DM Stoelzel
152	N/A	BONES1NP	PCT_EXP	-3.480E-01	U. Bone Spring Form. No Pay	Capillary pressure exponent (same as Culebra)	Required for BRAGFLO	Analyst: DM Stoelzel
153	N/A	BONES1NP	KPT	0.000E+00	U. Bone Spring Form. No Pay	Not used - placeholder	Not used	Analyst: DM Stoelzel
154	N/A	BONES1NP	PO_MIN	1.013E+05	U. Bone Spring Form. No Pay	Minimum Brine pressure (same for all materials)	Required for BRAGFLO	Analyst: DM Stoelzel
155	N/A	BONES1NP	PORE_DIS	7.000E-01	U. Bone Spring Form. No Pay	Pore distribution (fraction)	Required for BRAGFLO	Analyst: DM Stoelzel
156	N/A	BONES1NP	POROSITY	1.400E-01	U. Bone Spring Form. No Pay	Porosity (fraction)	Required for BRAGFLO	Analyst: DM Stoelzel
157	N/A	BONES1NP	PRESSURE	3.244E+07	U. Bone Spring Form. No Pay	Hydrostatic initial pressure (Pa)	Not used	Analyst: DM Stoelzel
158	N/A	BONES1NP	PRMX_LOG	-1.575E+01	U. Bone Spring Form. No Pay	Log x-direction permeability (from NM Bureau of Mines)	Intermediate value	Analyst: DM Stoelzel
159	N/A	BONES1NP	PRMY_LOG	-1.575E+01	U. Bone Spring Form. No Pay	Log y-direction permeability	Intermediate value	Analyst: DM Stoelzel
160	N/A	BONES1NP	PRMZ_LOG	-1.575E+01	U. Bone Spring Form. No Pay	Log z-direction permeability (BRAGFLO required input)	Not used - 2D model	Analyst: DM Stoelzel
161	N/A	BONES1NP	REL_P_MOD	4.000E+00	U. Bone Spring Form. No Pay	Relative permeability model number	Required for BRAGFLO	Analyst: DM Stoelzel
162	N/A	BONES1NP	SAT_RBRN	2.000E-01	U. Bone Spring Form. No Pay	Residual Brine saturation	Required for BRAGFLO	Analyst: DM Stoelzel
163	N/A	BONES1NP	SAT_RGAS	1.000E-02	U. Bone Spring Form. No Pay	Residual Gas saturation	Required for BRAGFLO	Analyst: DM Stoelzel
164	N/A	BONES1NP	PERM_X	1.778E-16	U. Bone Spring Form. No Pay	X-direction permeability (m <sup>2</sup> ) from Log value (NM B of Mines)	Required for BRAGFLO	Analyst: DM Stoelzel
165	N/A	BONES1NP	PERM_Y	1.778E-16	U. Bone Spring Form. No Pay	Y-direction permeability (m <sup>2</sup> ) from Log value	Required for BRAGFLO	Analyst: DM Stoelzel
166	N/A	BONES1NP	PERM_Z	1.778E-16	U. Bone Spring Form. No Pay	Z-direction permeability (m <sup>2</sup> ) Not used in 2D	Required for BRAGFLO	Analyst: DM Stoelzel
167	N/A	BONES1NP	SB_MIN	2.100E-01	U. Bone Spring Form. No Pay	Minimum saturation (SAT_RBRN * 1.05)	Required for BRAGFLO	Analyst: DM Stoelzel
168	N/A	BONES1NP	POR_COMP	4.576E-10	U. Bone Spring Form. No Pay	Pore compress from petroleum literature as function of depth (1/Pa)	Required for BRAGFLO	Analyst: DM Stoelzel
169	N/A	LBRSH_P1	CAP_MOD	2.000E+00	L. Brushy Can. (ABCD) Pay 1	Capillary Pressure Model Number (same as Culebra)	Required for BRAGFLO	Analyst: DM Stoelzel
170	N/A	LBRSH_P1	COMP_RCK	4.977E-10	L. Brushy Can. (ABCD) Pay 1	Rock compressibility (also pore compress) from Petroleum literature	Not used	Analyst: DM Stoelzel
171	N/A	LBRSH_P1	PC_MAX	1.000E+08	L. Brushy Can. (ABCD) Pay 1	Max capillary pressure (same as Culebra)	Required for BRAGFLO	Analyst: DM Stoelzel
172	N/A	LBRSH_P1	PCT_A	2.600E-01	L. Brushy Can. (ABCD) Pay 1	Capillary pressure multiplier (same as Culebra)	Required for BRAGFLO	Analyst: DM Stoelzel
173	N/A	LBRSH_P1	PCT_EXP	-3.480E-01	L. Brushy Can. (ABCD) Pay 1	Capillary pressure exponent (same as Culebra)	Required for BRAGFLO	Analyst: DM Stoelzel
174	N/A	LBRSH_P1	KPT	0.000E+00	L. Brushy Can. (ABCD) Pay 1	Not used - placeholder	Not used	Analyst: DM Stoelzel
175	N/A	LBRSH_P1	PO_MIN	1.013E+05	L. Brushy Can. (ABCD) Pay 1	Minimum Brine pressure (same for all materials)	Required for BRAGFLO	Analyst: DM Stoelzel
176	N/A	LBRSH_P1	PORE_DIS	7.000E-01	L. Brushy Can. (ABCD) Pay 1	Pore distribution (fraction)	Required for BRAGFLO	Analyst: DM Stoelzel
177	N/A	LBRSH_P1	POROSITY	2.900E-01	L. Brushy Can. (ABCD) Pay 1	Porosity (fraction)	Required for BRAGFLO	Analyst: DM Stoelzel
178	N/A	LBRSH_P1	PRESSURE	2.925E+07	L. Brushy Can. (ABCD) Pay 1	Hydrostatic initial pressure (Pa)	Not used	Analyst: DM Stoelzel
179	N/A	LBRSH_P1	PRMX_LOG	-1.290E+01	L. Brushy Can. (ABCD) Pay 1	Log x-direction permeability (from NM Bureau of Mines)	Intermediate value	Analyst: DM Stoelzel
180	N/A	LBRSH_P1	PRMY_LOG	-1.290E+01	L. Brushy Can. (ABCD) Pay 1	Log y-direction permeability	Intermediate value	Analyst: DM Stoelzel
181	N/A	LBRSH_P1	PRMZ_LOG	-1.290E+01	L. Brushy Can. (ABCD) Pay 1	Log z-direction permeability (BRAGFLO required input)	Not used - 2D model	Analyst: DM Stoelzel
182	N/A	LBRSH_P1	REL_P_MOD	4.000E+00	L. Brushy Can. (ABCD) Pay 1	Relative permeability model number	Required for BRAGFLO	Analyst: DM Stoelzel
183	N/A	LBRSH_P1	SAT_RBRN	2.000E-01	L. Brushy Can. (ABCD) Pay 1	Residual Brine saturation	Required for BRAGFLO	Analyst: DM Stoelzel
184	N/A	LBRSH_P1	SAT_RGAS	1.000E-02	L. Brushy Can. (ABCD) Pay 1	Residual Gas saturation	Required for BRAGFLO	Analyst: DM Stoelzel

Information Only

Database		Database Source: F1:[NOBACK2.DMS_WATERFLOOD.EPA.ALGEBRA]ALGEBRA_EPA_WF_RADIAL_R033.CDB;1 (Radial Case R5)						
ID Number	Material	Property	Value	Material Description	Property Value Description	Usage	Source	
185	N/A	LBRSH_P1	PERM_X	1.268E-13	L. Brushy Can. (ABCD) Pay 1	X-direction permeability (m <sup>2</sup> ) from Log value (NM B of Mines)	Required for BRAGFLO	Analyst: DM Stoelzel
186	N/A	LBRSH_P1	PERM_Y	1.268E-13	L. Brushy Can. (ABCD) Pay 1	Y-direction permeability (m <sup>2</sup> ) from Log value	Required for BRAGFLO	Analyst: DM Stoelzel
187	N/A	LBRSH_P1	PERM_Z	1.268E-13	L. Brushy Can. (ABCD) Pay 1	Z-direction permeability (m <sup>2</sup> ) Not used in 2D	Required for BRAGFLO	Analyst: DM Stoelzel
188	N/A	LBRSH_P1	SB_MIN	2.100E-01	L. Brushy Can. (ABCD) Pay 1	Minimum saturation (SAT_RBRN * 1.05)	Required for BRAGFLO	Analyst: DM Stoelzel
189	N/A	LBRSH_P1	POR_COMP	4.977E-10	L. Brushy Can. (ABCD) Pay 1	Pore compress from petroleum literature as function of depth (1/Pa)	Required for BRAGFLO	Analyst: DM Stoelzel
190	N/A	UBRSH1NP	CAP_MOD	2.000E+00	U. Brushy Canyon -- No Pay	Capillary Pressure Model Number (same as Culebra)	Required for BRAGFLO	Analyst: DM Stoelzel
191	N/A	UBRSH1NP	COMP_RCK	5.449E-10	U. Brushy Canyon -- No Pay	Rock compressibility (also pore compress) from Petroleum literature	Not used	Analyst: DM Stoelzel
192	N/A	UBRSH1NP	PC_MAX	1.000E+08	U. Brushy Canyon -- No Pay	Max capillary pressure (same as Culebra)	Required for BRAGFLO	Analyst: DM Stoelzel
193	N/A	UBRSH1NP	PCT_A	2.600E-01	U. Brushy Canyon -- No Pay	Capillary pressure multiplier (same as Culebra)	Required for BRAGFLO	Analyst: DM Stoelzel
194	N/A	UBRSH1NP	PCT_EXP	-3.480E-01	U. Brushy Canyon -- No Pay	Capillary pressure exponent (same as Culebra)	Required for BRAGFLO	Analyst: DM Stoelzel
195	N/A	UBRSH1NP	KPT	0.000E+00	U. Brushy Canyon -- No Pay	Not used - placeholder	Not used	Analyst: DM Stoelzel
196	N/A	UBRSH1NP	PO_MIN	1.013E+05	U. Brushy Canyon -- No Pay	Minimum Brine pressure (same for all materials)	Required for BRAGFLO	Analyst: DM Stoelzel
197	N/A	UBRSH1NP	PORE_DIS	7.000E-01	U. Brushy Canyon -- No Pay	Pore distribution (fraction)	Required for BRAGFLO	Analyst: DM Stoelzel
198	N/A	UBRSH1NP	POROSITY	1.400E-01	U. Brushy Canyon -- No Pay	Porosity (fraction)	Required for BRAGFLO	Analyst: DM Stoelzel
199	N/A	UBRSH1NP	PRESSURE	2.609E+07	U. Brushy Canyon -- No Pay	Hydrostatic initial pressure (Pa)	Not used	Analyst: DM Stoelzel
200	N/A	UBRSH1NP	PRMX_LOG	-1.601E+01	U. Brushy Canyon -- No Pay	Log x-direction permeability (from NM Bureau of Mines)	Intermediate value	Analyst: DM Stoelzel
201	N/A	UBRSH1NP	PRMY_LOG	-1.601E+01	U. Brushy Canyon -- No Pay	Log y-direction permeability	Intermediate value	Analyst: DM Stoelzel
202	N/A	UBRSH1NP	PRMZ_LOG	-1.601E+01	U. Brushy Canyon -- No Pay	Log z-direction permeability (BRAGFLO required input)	Not used - 2D model	Analyst: DM Stoelzel
203	N/A	UBRSH1NP	RELP_MOD	4.000E+00	U. Brushy Canyon -- No Pay	Relative permeability model number	Required for BRAGFLO	Analyst: DM Stoelzel
204	N/A	UBRSH1NP	SAT_RBRN	2.000E-01	U. Brushy Canyon -- No Pay	Residual Brine saturation	Required for BRAGFLO	Analyst: DM Stoelzel
205	N/A	UBRSH1NP	SAT_RGAS	1.000E-02	U. Brushy Canyon -- No Pay	Residual Gas saturation	Required for BRAGFLO	Analyst: DM Stoelzel
206	N/A	UBRSH1NP	PERM_X	9.863E-17	U. Brushy Canyon -- No Pay	X-direction permeability (m <sup>2</sup> ) from Log value (NM B of Mines)	Required for BRAGFLO	Analyst: DM Stoelzel
207	N/A	UBRSH1NP	PERM_Y	9.863E-17	U. Brushy Canyon -- No Pay	Y-direction permeability (m <sup>2</sup> ) from Log value	Required for BRAGFLO	Analyst: DM Stoelzel
208	N/A	UBRSH1NP	PERM_Z	9.863E-17	U. Brushy Canyon -- No Pay	Z-direction permeability (m <sup>2</sup> ) Not used in 2D	Required for BRAGFLO	Analyst: DM Stoelzel
209	N/A	UBRSH1NP	SB_MIN	2.100E-01	U. Brushy Canyon -- No Pay	Minimum saturation (SAT_RBRN * 1.05)	Required for BRAGFLO	Analyst: DM Stoelzel
210	N/A	UBRSH1NP	POR_COMP	5.449E-10	U. Brushy Canyon -- No Pay	Pore compress from petroleum literature as function of depth (1/Pa)	Required for BRAGFLO	Analyst: DM Stoelzel
211	N/A	UBRSH_P1	CAP_MOD	2.000E+00	U. Brushy Can - Cherry C, Pay 1	Capillary Pressure Model Number (same as Culebra)	Required for BRAGFLO	Analyst: DM Stoelzel
212	N/A	UBRSH_P1	COMP_RCK	6.020E-10	U. Brushy Can - Cherry C, Pay 1	Rock compressibility (also pore compress) from Petroleum literature	Not used	Analyst: DM Stoelzel
213	N/A	UBRSH_P1	PC_MAX	1.000E+08	U. Brushy Can - Cherry C, Pay 1	Max capillary pressure (same as Culebra)	Required for BRAGFLO	Analyst: DM Stoelzel
214	N/A	UBRSH_P1	PCT_A	2.600E-01	U. Brushy Can - Cherry C, Pay 1	Capillary pressure multiplier (same as Culebra)	Required for BRAGFLO	Analyst: DM Stoelzel
215	N/A	UBRSH_P1	PCT_EXP	-3.480E-01	U. Brushy Can - Cherry C, Pay 1	Capillary pressure exponent (same as Culebra)	Required for BRAGFLO	Analyst: DM Stoelzel
216	N/A	UBRSH_P1	KPT	0.000E+00	U. Brushy Can - Cherry C, Pay 1	Not used - placeholder	Not used	Analyst: DM Stoelzel
217	N/A	UBRSH_P1	PO_MIN	1.013E+05	U. Brushy Can - Cherry C, Pay 1	Minimum Brine pressure (same for all materials)	Required for BRAGFLO	Analyst: DM Stoelzel
218	N/A	UBRSH_P1	PORE_DIS	7.000E-01	U. Brushy Can - Cherry C, Pay 1	Pore distribution (fraction)	Required for BRAGFLO	Analyst: DM Stoelzel
219	N/A	UBRSH_P1	POROSITY	2.900E-01	U. Brushy Can - Cherry C, Pay 1	Porosity (fraction)	Required for BRAGFLO	Analyst: DM Stoelzel
220	N/A	UBRSH_P1	PRESSURE	2.294E+07	U. Brushy Can - Cherry C, Pay 1	Hydrostatic initial pressure (Pa)	Not used	Analyst: DM Stoelzel
221	N/A	UBRSH_P1	PRMX_LOG	-1.290E+01	U. Brushy Can - Cherry C, Pay 1	Log x-direction permeability (from NM Bureau of Mines)	Intermediate value	Analyst: DM Stoelzel
222	N/A	UBRSH_P1	PRMY_LOG	-1.290E+01	U. Brushy Can - Cherry C, Pay 1	Log y-direction permeability	Intermediate value	Analyst: DM Stoelzel
223	N/A	UBRSH_P1	PRMZ_LOG	-1.290E+01	U. Brushy Can - Cherry C, Pay 1	Log z-direction permeability (BRAGFLO required input)	Not used - 2D model	Analyst: DM Stoelzel
224	N/A	UBRSH_P1	RELP_MOD	4.000E+00	U. Brushy Can - Cherry C, Pay 1	Relative permeability model number	Required for BRAGFLO	Analyst: DM Stoelzel
225	N/A	UBRSH_P1	SAT_RBRN	2.000E-01	U. Brushy Can - Cherry C, Pay 1	Residual Brine saturation	Required for BRAGFLO	Analyst: DM Stoelzel
226	N/A	UBRSH_P1	SAT_RGAS	1.000E-02	U. Brushy Can - Cherry C, Pay 1	Residual Gas saturation	Required for BRAGFLO	Analyst: DM Stoelzel
227	N/A	UBRSH_P1	PERM_X	1.268E-13	U. Brushy Can - Cherry C, Pay 1	X-direction permeability (m <sup>2</sup> ) from Log value (NM B of Mines)	Required for BRAGFLO	Analyst: DM Stoelzel
228	N/A	UBRSH_P1	PERM_Y	1.268E-13	U. Brushy Can - Cherry C, Pay 1	Y-direction permeability (m <sup>2</sup> ) from Log value	Required for BRAGFLO	Analyst: DM Stoelzel
229	N/A	UBRSH_P1	PERM_Z	1.268E-13	U. Brushy Can - Cherry C, Pay 1	Z-direction permeability (m <sup>2</sup> ) Not used in 2D	Required for BRAGFLO	Analyst: DM Stoelzel
230	N/A	UBRSH_P1	SB_MIN	2.100E-01	U. Brushy Can - Cherry C, Pay 1	Minimum saturation (SAT_RBRN * 1.05)	Required for BRAGFLO	Analyst: DM Stoelzel

Information Only

				Database Source: F1:[NOBACK2.DMS_WATERFLOOD.EPA.ALGEBRA]ALGEBRA_EPA_WF_RADIAL_R033.CDB;1 (Radial Case R5)					
ID Number	Material	Property	Value	Material Description	Property Value Description	Usage	Source		
231	N/A	UBRSH_P1	POR_COMP	6.020E-10	U. Brushy Can - Cherry C, Pay 1	Pore compress from petroleum literature as function of depth (1/Pa)	Required for BRAGFLO	Analyst: DM Stoelzel	
232	N/A	LBELLINP	CAP_MOD	2.000E+00	L. Bell Canyon-U. Cherry No Pay	Capillary Pressure Model Number (same as Culebra)	Required for BRAGFLO	Analyst: DM Stoelzel	
233	N/A	LBELLINP	COMP_RCK	6.767E-10	L. Bell Canyon-U. Cherry No Pay	Rock compressibility (also pore compress) from Petroleum literature	Not used	Analyst: DM Stoelzel	
234	N/A	LBELLINP	PC_MAX	1.000E+08	L. Bell Canyon-U. Cherry No Pay	Max capillary pressure (same as Culebra)	Required for BRAGFLO	Analyst: DM Stoelzel	
235	N/A	LBELLINP	PCT_A	2.600E-01	L. Bell Canyon-U. Cherry No Pay	Capillary pressure multiplier (same as Culebra)	Required for BRAGFLO	Analyst: DM Stoelzel	
236	N/A	LBELLINP	PCT_EXP	-3.480E-01	L. Bell Canyon-U. Cherry No Pay	Capillary pressure exponent (same as Culebra)	Required for BRAGFLO	Analyst: DM Stoelzel	
237	N/A	LBELLINP	KPT	0.000E+00	L. Bell Canyon-U. Cherry No Pay	Not used - placeholder	Not used	Analyst: DM Stoelzel	
238	N/A	LBELLINP	PO_MIN	1.013E+05	L. Bell Canyon-U. Cherry No Pay	Minimum Brine pressure (same for all materials)	Required for BRAGFLO	Analyst: DM Stoelzel	
239	N/A	LBELLINP	PORE_DIS	7.000E-01	L. Bell Canyon-U. Cherry No Pay	Pore distribution (fraction)	Required for BRAGFLO	Analyst: DM Stoelzel	
240	N/A	LBELLINP	POROSITY	1.400E-01	L. Bell Canyon-U. Cherry No Pay	Porosity (fraction)	Required for BRAGFLO	Analyst: DM Stoelzel	
241	N/A	LBELLINP	PRESSURE	1.962E+07	L. Bell Canyon-U. Cherry No Pay	Hydrostatic initial pressure (Pa)	Not used	Analyst: DM Stoelzel	
242	N/A	LBELLINP	PRMX_LOG	-1.601E+01	L. Bell Canyon-U. Cherry No Pay	Log x-direction permeability (from NM Bureau of Mines)	Intermediate value	Analyst: DM Stoelzel	
243	N/A	LBELLINP	PRMY_LOG	-1.601E+01	L. Bell Canyon-U. Cherry No Pay	Log y-direction permeability	Intermediate value	Analyst: DM Stoelzel	
244	N/A	LBELLINP	PRMZ_LOG	-1.601E+01	L. Bell Canyon-U. Cherry No Pay	Log z-direction permeability (BRAGFLO required input)	Not used - 2D model	Analyst: DM Stoelzel	
245	N/A	LBELLINP	RELP_MOD	4.000E+00	L. Bell Canyon-U. Cherry No Pay	Relative permeability model number	Required for BRAGFLO	Analyst: DM Stoelzel	
246	N/A	LBELLINP	SAT_RBRN	2.000E-01	L. Bell Canyon-U. Cherry No Pay	Residual Brine saturation	Required for BRAGFLO	Analyst: DM Stoelzel	
247	N/A	LBELLINP	SAT_RGAS	1.000E-02	L. Bell Canyon-U. Cherry No Pay	Residual Gas saturation	Required for BRAGFLO	Analyst: DM Stoelzel	
248	N/A	LBELLINP	PERM_X	9.863E-17	L. Bell Canyon-U. Cherry No Pay	X-direction permeability (m <sup>2</sup> ) from Log value (NM B of Mines)	Required for BRAGFLO	Analyst: DM Stoelzel	
249	N/A	LBELLINP	PERM_Y	9.863E-17	L. Bell Canyon-U. Cherry No Pay	Y-direction permeability (m <sup>2</sup> ) from Log value	Required for BRAGFLO	Analyst: DM Stoelzel	
250	N/A	LBELLINP	PERM_Z	9.863E-17	L. Bell Canyon-U. Cherry No Pay	Z-direction permeability (m <sup>2</sup> ) Not used in 2D	Required for BRAGFLO	Analyst: DM Stoelzel	
251	N/A	LBELLINP	SB_MIN	2.100E-01	L. Bell Canyon-U. Cherry No Pay	Minimum saturation (SAT_RBRN * 1.05)	Required for BRAGFLO	Analyst: DM Stoelzel	
252	N/A	LBELLINP	POR_COMP	6.767E-10	L. Bell Canyon-U. Cherry No Pay	Pore compress from petroleum literature as function of depth (1/Pa)	Required for BRAGFLO	Analyst: DM Stoelzel	
253	N/A	UBELL_P1	CAP_MOD	2.000E+00	U Bell Canyon Pay 1 (SWD zone)	Capillary Pressure Model Number (same as Culebra)	Required for BRAGFLO	Analyst: DM Stoelzel	
254	N/A	UBELL_P1	COMP_RCK	7.948E-10	U Bell Canyon Pay 1 (SWD zone)	Rock compressibility (also pore compress) from Petroleum literature	Not used	Analyst: DM Stoelzel	
255	N/A	UBELL_P1	PC_MAX	1.000E+08	U Bell Canyon Pay 1 (SWD zone)	Max capillary pressure (same as Culebra)	Required for BRAGFLO	Analyst: DM Stoelzel	
256	N/A	UBELL_P1	PCT_A	2.600E-01	U Bell Canyon Pay 1 (SWD zone)	Capillary pressure multiplier (same as Culebra)	Required for BRAGFLO	Analyst: DM Stoelzel	
257	N/A	UBELL_P1	PCT_EXP	-3.480E-01	U Bell Canyon Pay 1 (SWD zone)	Capillary pressure exponent (same as Culebra)	Required for BRAGFLO	Analyst: DM Stoelzel	
258	N/A	UBELL_P1	KPT	0.000E+00	U Bell Canyon Pay 1 (SWD zone)	Not used - placeholder	Not used	Analyst: DM Stoelzel	
259	N/A	UBELL_P1	PO_MIN	1.013E+05	U Bell Canyon Pay 1 (SWD zone)	Minimum Brine pressure (same for all materials)	Required for BRAGFLO	Analyst: DM Stoelzel	
260	N/A	UBELL_P1	PORE_DIS	7.000E-01	U Bell Canyon Pay 1 (SWD zone)	Pore distribution (fraction)	Required for BRAGFLO	Analyst: DM Stoelzel	
261	N/A	UBELL_P1	POROSITY	2.900E-01	U Bell Canyon Pay 1 (SWD zone)	Porosity (fraction)	Required for BRAGFLO	Analyst: DM Stoelzel	
262	N/A	UBELL_P1	PRESSURE	1.564E+07	U Bell Canyon Pay 1 (SWD zone)	Hydrostatic initial pressure (Pa)	Not used	Analyst: DM Stoelzel	
263	N/A	UBELL_P1	PRMX_LOG	-1.290E+01	U Bell Canyon Pay 1 (SWD zone)	Log x-direction permeability (from NM Bureau of Mines)	Intermediate value	Analyst: DM Stoelzel	
264	N/A	UBELL_P1	PRMY_LOG	-1.290E+01	U Bell Canyon Pay 1 (SWD zone)	Log y-direction permeability	Intermediate value	Analyst: DM Stoelzel	
265	N/A	UBELL_P1	PRMZ_LOG	-1.290E+01	U Bell Canyon Pay 1 (SWD zone)	Log z-direction permeability (BRAGFLO required input)	Not used - 2D model	Analyst: DM Stoelzel	
266	N/A	UBELL_P1	RELP_MOD	4.000E+00	U Bell Canyon Pay 1 (SWD zone)	Relative permeability model number	Required for BRAGFLO	Analyst: DM Stoelzel	
267	N/A	UBELL_P1	SAT_RBRN	2.000E-01	U Bell Canyon Pay 1 (SWD zone)	Residual Brine saturation	Required for BRAGFLO	Analyst: DM Stoelzel	
268	N/A	UBELL_P1	SAT_RGAS	1.000E-02	U Bell Canyon Pay 1 (SWD zone)	Residual Gas saturation	Required for BRAGFLO	Analyst: DM Stoelzel	
269	N/A	UBELL_P1	PERM_X	1.268E-13	U Bell Canyon Pay 1 (SWD zone)	X-direction permeability (m <sup>2</sup> ) from Log value (NM B of Mines)	Required for BRAGFLO	Analyst: DM Stoelzel	
270	N/A	UBELL_P1	PERM_Y	1.268E-13	U Bell Canyon Pay 1 (SWD zone)	Y-direction permeability (m <sup>2</sup> ) from Log value	Required for BRAGFLO	Analyst: DM Stoelzel	
271	N/A	UBELL_P1	PERM_Z	1.268E-13	U Bell Canyon Pay 1 (SWD zone)	Z-direction permeability (m <sup>2</sup> ) Not used in 2D	Required for BRAGFLO	Analyst: DM Stoelzel	
272	N/A	UBELL_P1	SB_MIN	2.100E-01	U Bell Canyon Pay 1 (SWD zone)	Minimum saturation (SAT_RBRN * 1.05)	Required for BRAGFLO	Analyst: DM Stoelzel	
273	N/A	UBELL_P1	POR_COMP	7.948E-10	U Bell Canyon Pay 1 (SWD zone)	Pore compress from petroleum literature as function of depth (1/Pa)	Required for BRAGFLO	Analyst: DM Stoelzel	
274	60	CASTILER	CAP_MOD	2.000E+00	Castile Formation - non reservoir	Capillary Pressure Model Number	Required for BRAGFLO	Database: CCA view 6	
275	61	CASTILER	COMP_RCK	-1.000E+01	Castile Formation - non reservoir	Rock compressibility (1/Pa)	Intermediate value	Database: CCA view 6	
276	62	CASTILER	PC_MAX	1.000E+08	Castile Formation - non reservoir	Max capillary pressure	Required for BRAGFLO	Database: CCA view 6	

Information Only



				Database Source: F1:[NOBACK2.DMS_WATERFLOOD.EPA.ALGEBRA]ALGEBRA_EPA_WF_RADIAL_R033.CDB;1 (Radial Case R5)				
ID Number	Material	Property	Value	Material Description	Property Value Description	Usage	Source	
277	2609	CASTILER	PCT_A	5.600E-01	Castile Formation - non reservoir	Capillary pressure multiplier	Required for BRAGFLO	Database: CCA view 6
278	2610	CASTILER	PCT_EXP	-3.460E-01	Castile Formation - non reservoir	Capillary pressure exponent	Required for BRAGFLO	Database: CCA view 6
279	2608	CASTILER	KPT	0.000E+00	Castile Formation - non reservoir	Not used - placeholder	Not used	Database: CCA view 6
280	65	CASTILER	PO_MIN	1.013E+05	Castile Formation - non reservoir	Minimum Brine pressure (same for all materials)	Required for BRAGFLO	Database: CCA view 6
281	63	CASTILER	PORE_DIS	7.000E-01	Castile Formation - non reservoir	Pore distribution (fraction)	Required for BRAGFLO	Database: CCA view 6
282	64	CASTILER	POROSITY	1.000E-02	Castile Formation - non reservoir	Porosity (fraction)	Required for BRAGFLO	Database: CCA view 6
283	66	CASTILER	PRESSURE	1.270E+07	Castile Formation - non reservoir	Hydrostatic initial pressure (Pa)	Not used	Database: CCA view 6
284	N/A	CASTILER	PRMX_LOG	-1.180E+01	Castile Formation - non reservoir	Log x-direction permeability	Not used	Analyst: DM Stoelzel
285	N/A	CASTILER	PRMY_LOG	-1.180E+01	Castile Formation - non reservoir	Log y-direction permeability	Not used	Analyst: DM Stoelzel
286	N/A	CASTILER	PRMZ_LOG	-1.180E+01	Castile Formation - non reservoir	Log z-direction permeability (BRAGFLO required input)	Not used	Analyst: DM Stoelzel
287	72	CASTILER	RELP_MOD	4.000E+00	Castile Formation - non reservoir	Relative permeability model number	Required for BRAGFLO	Database: CCA view 6
288	74	CASTILER	SAT_RBRN	2.000E-01	Castile Formation - non reservoir	Residual Brine saturation	Required for BRAGFLO	Database: CCA view 6
289	75	CASTILER	SAT_RGAS	2.000E-01	Castile Formation - non reservoir	Residual Gas saturation	Required for BRAGFLO	Database: CCA view 6
290	N/A	CASTILER	PERM_X	3.162E-23	Castile Formation - non reservoir	X-direction permeability (m <sup>2</sup> ) from Log value	Required for BRAGFLO	from S_HALITE
291	N/A	CASTILER	PERM_Y	3.162E-23	Castile Formation - non reservoir	Y-direction permeability (m <sup>2</sup> ) from Log value	Required for BRAGFLO	from S_HALITE
292	N/A	CASTILER	PERM_Z	3.162E-23	Castile Formation - non reservoir	Z-direction permeability (m <sup>2</sup> ) Not used in 2D	Required for BRAGFLO	from S_HALITE
293	N/A	CASTILER	SB_MIN	2.100E-01	Castile Formation - non reservoir	Minimum saturation (SAT_RBRN * 1.05)	Required for BRAGFLO	Calculated
294	N/A	CASTILER	POR_COMP	9.750E-09	Castile Formation - non reservoir	Pore compressibility COMP_RCK/POROSITY (1/Pa)	Required for BRAGFLO	Calculated
295	N/A	CAST_ANH	CAP_MOD	2.000E+00	Castile Anhydrite Composite	Capillary Pressure Model Number	Required for BRAGFLO	From MB139
296	N/A	CAST_ANH	COMP_RCK	7.948E-10	Castile Anhydrite Composite	Rock compressibility (1/Pa)	Required for BRAGFLO	From MB139
297	N/A	CAST_ANH	PC_MAX	1.000E+08	Castile Anhydrite Composite	Max capillary pressure	Required for BRAGFLO	From MB139
298	N/A	CAST_ANH	PCT_A	2.600E-01	Castile Anhydrite Composite	Capillary pressure multiplier	Required for BRAGFLO	From MB139
299	N/A	CAST_ANH	PCT_EXP	-3.480E-01	Castile Anhydrite Composite	Capillary pressure exponent	Required for BRAGFLO	From MB139
300	N/A	CAST_ANH	KPT	0.000E+00	Castile Anhydrite Composite	Not used - placeholder	Not used	From MB139
301	N/A	CAST_ANH	PO_MIN	1.013E+05	Castile Anhydrite Composite	Minimum Brine pressure (same for all materials)	Required for BRAGFLO	From MB139
302	N/A	CAST_ANH	PORE_DIS	6.436E-01	Castile Anhydrite Composite	Pore distribution (fraction)	Required for BRAGFLO	From MB139
303	N/A	CAST_ANH	POROSITY	1.100E-02	Castile Anhydrite Composite	Porosity (fraction)	Required for BRAGFLO	From MB139
304	N/A	CAST_ANH	PRMX_LOG	-1.190E+01	Castile Anhydrite Composite	Log x-direction permeability	Placeholder	Not used
305	N/A	CAST_ANH	PRMY_LOG	-1.990E+01	Castile Anhydrite Composite	Log y-direction permeability	Placeholder	Not used
306	N/A	CAST_ANH	PRMZ_LOG	-1.190E+01	Castile Anhydrite Composite	Log z-direction permeability (BRAGFLO required input)	Placeholder	Not used
307	N/A	CAST_ANH	RELP_MOD	4.000E+00	Castile Anhydrite Composite	Relative permeability model number	Required for BRAGFLO	From MB139
308	N/A	CAST_ANH	SAT_RBRN	8.363E-02	Castile Anhydrite Composite	Residual Brine saturation	Required for BRAGFLO	From MB139
309	N/A	CAST_ANH	SAT_RGAS	7.711E-02	Castile Anhydrite Composite	Residual Gas saturation	Required for BRAGFLO	From MB139
310	N/A	CAST_ANH	DPHIMAX	1.500E-03	Castile Anhydrite Composite	Maximum delta change in porosity for fracture model	Required for BRAGFLO	From MB139
311	N/A	CAST_ANH	PI_DELTA	3.189E+05	Castile Anhydrite Composite	Fracture initiation pressure - reference pressure (Pa)	Required for BRAGFLO	From MB139
312	N/A	CAST_ANH	PF_DELTA	6.070E+06	Castile Anhydrite Composite	Maximum final fracture pressure - reference pressure (Pa)	Required for BRAGFLO	From MB139
313	N/A	CAST_ANH	IFRX	1.000E+00	Castile Anhydrite Composite	X-direction fracturing flag (1 = true, 0 = false)	Required for BRAGFLO	From MB139
314	N/A	CAST_ANH	IFRY	1.000E+00	Castile Anhydrite Composite	Y-direction fracturing flag (1 = true, 0 = false)	Required for BRAGFLO	From MB139
315	N/A	CAST_ANH	IFRZ	0.000E+00	Castile Anhydrite Composite	Z-direction fracturing flag (1 = true, 0 = false)	Required for BRAGFLO	From MB139
316	N/A	CAST_ANH	KMAXFRAC	1.000E-10	Castile Anhydrite Composite	Maximum allowable permeability in fracturing model (m <sup>2</sup> )	Used to calc perm_exp	calculated: 10^kmaxlog
317	N/A	CAST_ANH	GRADSTAR	8.510E-01	Castile Anhydrite Composite	Fracture Starting Gradient (psi/ft)	Gradient applied to all anh layers	From MB139
318	N/A	CAST_ANH	GRADSTOP	1.106E+00	Castile Anhydrite Composite	Fracture Stopping Gradient (psi/ft)	Gradient applied to all anh layers	From MB139
319	N/A	CAST_ANH	KMAXLOG	-1.000E+01	Castile Anhydrite Composite	Log maximum allowable permeability in fracturing model log(m <sup>2</sup> )	Used for fracturing mod	Analyst: DM Stoelzel
320	N/A	CAST_ANH	PERM_X	1.288E-19	Castile Anhydrite Composite	X-direction permeability (from PRMX_LOG) (m <sup>2</sup> )	Required for BRAGFLO	From MB139

Information Only



Database				Database Source: F1:[NOBACK2.DMS_WATERFLOOD.EPA.ALGEBRA]ALGEBRA_EPA_WF_RADIAL_R033.CDB;1 (Radial Case R5)				
ID Number	Material	Property	Value	Material Description	Property Value Description	Usage	Source	
321	N/A	CAST_ANH	PERM_Y	1.288E-19	Castile Anhydrite Composite	Y-direction permeability (from PRMY_LOG) (m <sup>2</sup> )	Required for BRAGFLO	From MB139
322	N/A	CAST_ANH	PERM_Z	1.288E-19	Castile Anhydrite Composite	Z-direction permeability (from PRMZ_LOG) (m <sup>2</sup> )	Not used - 2D model	From MB139
323	N/A	CAST_ANH	SB_MIN	8.781E-02	Castile Anhydrite Composite	Minimum saturation (SAT_RBRN * 1.05)	Required for BRAGFLO	Calculated
324	N/A	CAST_ANH	POR_COMP	7.512E-09	Castile Anhydrite Composite	Calculated: = COMP_RCK/POROSITY	Required for BRAGFLO	Calculated
325	N/A	CAST_ANH	AVG_PRES	1.992E+07	Castile Anhydrite Composite	Average Init grid-block pressure in layer	Calculated in ALGEBRA: Not used	Analyst: DM Stoelzel
326	N/A	CAST_ANH	AVG_ELEV	-1.239E+01	Castile Anhydrite Composite	Average grid-block elevation in layer	Calculated in ALGEBRA: Not used	Analyst: DM Stoelzel
327	N/A	CAST_ANH	INI_GRAD	8.376E-01	Castile Anhydrite Composite	Initial gradient in layer (psi/ft)	Calculated in ALGEBRA: Not used	Analyst: DM Stoelzel
328	N/A	CAST_ANH	PRES_INI	2.024E+07	Castile Anhydrite Composite	Fracture initiation pressure (Pa)	Calculated in ALGEBRA based on GRADSTAR	Calculated
329	N/A	CAST_ANH	PRES_FIN	2.631E+07	Castile Anhydrite Composite	Fracture Stopping pressure (Pa)	Calculated in ALGEBRA based on GRADSTOP	Calculated
330	N/A	CAST_ANH	PHIMAX	1.250E-02	Castile Anhydrite Composite	Calculated: = POROSITY + DPHIMAX for fracturing model	Required for BRAGFLO	Analyst: DM Stoelzel
331	N/A	CAST_ANH	PERM_EXP	1.632E+02	Castile Anhydrite Composite	Calculated in Algebra	Required for BRAGFLO	Calculated
332	540	S_HALITE	CAP_MOD	2.000E+00	Salado Formation - impure halite	Capillary Pressure Model Number	Required for BRAGFLO	Database: CCA view 6
333	541	S_HALITE	COMP_RCK	9.750E-11	Salado Formation - impure halite	Rock compressibility (1/Pa)	Intermediate value	Database: CCA view 6
334	542	S_HALITE	PC_MAX	1.000E+08	Salado Formation - impure halite	Max capillary pressure	Required for BRAGFLO	Database: CCA view 6
335	2779	S_HALITE	PCT_A	5.600E-01	Salado Formation - impure halite	Capillary pressure multiplier	Required for BRAGFLO	Database: CCA view 6
336	2780	S_HALITE	PCT_EXP	-3.460E-01	Salado Formation - impure halite	Capillary pressure exponent	Required for BRAGFLO	Database: CCA view 6
337	2778	S_HALITE	KPT	0.000E+00	Salado Formation - impure halite	Not used - placeholder	Not used	Database: CCA view 6
338	545	S_HALITE	PO_MIN	1.013E+05	Salado Formation - impure halite	Minimum Brine pressure (same for all materials)	Required for BRAGFLO	Database: CCA view 6
339	543	S_HALITE	PORE_DIS	7.000E-01	Salado Formation - impure halite	Pore distribution (fraction)	Required for BRAGFLO	Database: CCA view 6
340	544	S_HALITE	POROSITY	1.000E-02	Salado Formation - impure halite	Porosity (fraction)	Required for BRAGFLO	Database: CCA view 6
341	546	S_HALITE	PRESSURE	1.247E+07	Salado Formation - impure halite	Initial pressure (Pa).	Initialize Salado grid blo	Database: CCA view 6
342	547	S_HALITE	PRMX_LOG	-2.250E+01	Salado Formation - impure halite	Log x-direction permeability	Intermediate value	Database: CCA view 6
343	548	S_HALITE	PRMY_LOG	-2.250E+01	Salado Formation - impure halite	Log y-direction permeability	Intermediate value	Database: CCA view 6
344	549	S_HALITE	PRMZ_LOG	-2.250E+01	Salado Formation - impure halite	Log z-direction permeability (BRAGFLO required input)	Not used - 2D model	Database: CCA view 6
345	553	S_HALITE	RELP_MOD	4.000E+00	Salado Formation - impure halite	Relative permeability model number	Required for BRAGFLO	Database: CCA view 6
346	555	S_HALITE	SAT_RBRN	3.000E-01	Salado Formation - impure halite	Residual Brine saturation	Required for BRAGFLO	Database: CCA view 6
347	556	S_HALITE	SAT_RGAS	2.000E-01	Salado Formation - impure halite	Residual Gas saturation	Required for BRAGFLO	Database: CCA view 6
348	N/A	S_HALITE	PERM_X	3.162E-23	Salado Formation - impure halite	X-direction permeability (m <sup>2</sup> ) from Log value	Required for BRAGFLO	Calculated
349	N/A	S_HALITE	PERM_Y	3.162E-23	Salado Formation - impure halite	Y-direction permeability (m <sup>2</sup> ) from Log value	Required for BRAGFLO	Calculated
350	N/A	S_HALITE	PERM_Z	3.162E-23	Salado Formation - impure halite	Z-direction permeability (m <sup>2</sup> ) Not used in 2D	Required for BRAGFLO	Calculated
351	N/A	S_HALITE	SB_MIN	3.150E-01	Salado Formation - impure halite	Minimum saturation (SAT_RBRN * 1.05)	Required for BRAGFLO	Calculated
352	N/A	S_HALITE	POR_COMP	9.750E-09	Salado Formation - impure halite	Pore compressibility COMP_RCK/POROSITY (1/Pa)	Required for BRAGFLO	Calculated
353	N/A	L_ANH_CP	CAP_MOD	2.000E+00	Lower Anhydrite Composite	Capillary Pressure Model Number	Required for BRAGFLO	From MB139
354	N/A	L_ANH_CP	COMP_RCK	7.948E-10	Lower Anhydrite Composite	Rock compressibility (1/Pa)	Required for BRAGFLO	From MB139
355	N/A	L_ANH_CP	PC_MAX	1.000E+08	Lower Anhydrite Composite	Max capillary pressure	Required for BRAGFLO	From MB139
356	N/A	L_ANH_CP	PCT_A	2.600E-01	Lower Anhydrite Composite	Capillary pressure multiplier	Required for BRAGFLO	From MB139
357	N/A	L_ANH_CP	PCT_EXP	-3.480E-01	Lower Anhydrite Composite	Capillary pressure exponent	Required for BRAGFLO	From MB139
358	N/A	L_ANH_CP	KPT	0.000E+00	Lower Anhydrite Composite	Not used - placeholder	Not used	From MB139
359	N/A	L_ANH_CP	PO_MIN	1.013E+05	Lower Anhydrite Composite	Minimum Brine pressure (same for all materials)	Required for BRAGFLO	From MB139
360	N/A	L_ANH_CP	PORE_DIS	6.436E-01	Lower Anhydrite Composite	Pore distribution (fraction)	Required for BRAGFLO	From MB139
361	N/A	L_ANH_CP	POROSITY	1.100E-02	Lower Anhydrite Composite	Porosity (fraction)	Required for BRAGFLO	From MB139

Information Only

Database Source: F1:[NOBACK2.DMS_WATERFLOOD.EPA.ALGEBRA]ALGEBRA_EPA_WF_RADIAL_R033.CDB;1 (Radial Case R5)								
ID Number	Material	Property	Value	Material Description	Property Value Description	Usage	Source	
362	N/A	L_ANH_CP	PRMX_LOG	-1.190E+01	Lower Anhydrite Composite	Log x-direction permeability	Placeholder	Not used
363	N/A	L_ANH_CP	PRMY_LOG	-1.990E+01	Lower Anhydrite Composite	Log y-direction permeability	Placeholder	Not used
364	N/A	L_ANH_CP	PRMZ_LOG	-1.190E+01	Lower Anhydrite Composite	Log z-direction permeability (BRAGFLO required input)	Placeholder	Not used
365	N/A	L_ANH_CP	REL_P_MOD	4.000E+00	Lower Anhydrite Composite	Relative permeability model number	Required for BRAGFLO	From MB139
366	N/A	L_ANH_CP	SAT_RBRN	8.363E-02	Lower Anhydrite Composite	Residual Brine saturation	Required for BRAGFLO	From MB139
367	N/A	L_ANH_CP	SAT_RGAS	7.711E-02	Lower Anhydrite Composite	Residual Gas saturation	Required for BRAGFLO	From MB139
368	N/A	L_ANH_CP	DPHIMAX	6.000E-03	Lower Anhydrite Composite	Maximum delta change in porosity for fracture model	Required for BRAGFLO	From MB139
369	N/A	L_ANH_CP	PI_DELTA	2.253E+05	Lower Anhydrite Composite	Fracture initiation pressure - reference pressure (Pa)	Required for BRAGFLO	From MB139
370	N/A	L_ANH_CP	PF_DELTA	4.290E+06	Lower Anhydrite Composite	Maximum final fracture pressure - reference pressure (Pa)	Required for BRAGFLO	From MB139
371	N/A	L_ANH_CP	IFRX	1.000E+00	Lower Anhydrite Composite	X-direction fracturing flag (1 = true, 0 = false)	Required for BRAGFLO	From MB139
372	N/A	L_ANH_CP	IFRY	1.000E+00	Lower Anhydrite Composite	Y-direction fracturing flag (1 = true, 0 = false)	Required for BRAGFLO	From MB139
373	N/A	L_ANH_CP	IFRZ	0.000E+00	Lower Anhydrite Composite	Z-direction fracturing flag (1 = true, 0 = false)	Required for BRAGFLO	From MB139
374	N/A	L_ANH_CP	KMAXFRAC	1.000E-10	Lower Anhydrite Composite	Maximum allowable permeability in fracturing model (m <sup>2</sup> )	Used to calc perm_exp	calculated: 10 <sup>k</sup> maxlog
375	N/A	L_ANH_CP	GRADSTAR	8.510E-01	Lower Anhydrite Composite	Fracture Starting Gradient (psi/ft)	Gradient applied to all anh layers	From MB139
376	N/A	L_ANH_CP	GRADSTOP	1.106E+00	Lower Anhydrite Composite	Fracture Stopping Gradient (psi/ft)	Gradient applied to all anh layers	From MB139
377	N/A	L_ANH_CP	KMAXLOG	-1.000E+01	Lower Anhydrite Composite	Log maximum allowable permeability in fracturing model log(m <sup>2</sup> )	Used for fracturing mod	Analyst: DM Stoelzel
378	N/A	L_ANH_CP	PERM_X	1.288E-19	Lower Anhydrite Composite	X-direction permeability (from PRMX_LOG) (m <sup>2</sup> )	Required for BRAGFLO	From MB139
379	N/A	L_ANH_CP	PERM_Y	1.288E-19	Lower Anhydrite Composite	Y-direction permeability (from PRMY_LOG) (m <sup>2</sup> )	Required for BRAGFLO	From MB139
380	N/A	L_ANH_CP	PERM_Z	1.288E-19	Lower Anhydrite Composite	Z-direction permeability (from PRMZ_LOG) (m <sup>2</sup> )	Not used - 2D model	From MB139
381	N/A	L_ANH_CP	SB_MIN	8.781E-02	Lower Anhydrite Composite	Minimum saturation (SAT_RBRN * 1.05)	Required for BRAGFLO	Calculated
382	N/A	L_ANH_CP	POR_COMP	7.512E-09	Lower Anhydrite Composite	Calculated: = COMP_RCK/POROSITY	Required for BRAGFLO	Calculated
383	N/A	L_ANH_CP	AVG_PRES	1.408E+07	Lower Anhydrite Composite	Average Init grid-block pressure in layer	Calculated in ALGEBRA: Not used	Analyst: DM Stoelzel
384	N/A	L_ANH_CP	AVG_ELEV	2.960E+02	Lower Anhydrite Composite	Average grid-block elevation in layer	Calculated in ALGEBRA: Not used	Analyst: DM Stoelzel
385	N/A	L_ANH_CP	INI_GRAD	8.376E-01	Lower Anhydrite Composite	Initial gradient in layer (psi/ft)	Calculated in ALGEBRA: Not used	Analyst: DM Stoelzel
386	N/A	L_ANH_CP	PRES_INI	1.430E+07	Lower Anhydrite Composite	Fracture initiation pressure (Pa)	Calculated in ALGEBRA based on GRADSTAR	Calculated
387	N/A	L_ANH_CP	PRES_FIN	1.859E+07	Lower Anhydrite Composite	Fracture Stopping pressure (Pa)	Calculated in ALGEBRA based on GRADSTOP	Calculated
388	N/A	L_ANH_CP	PHIMAX	1.700E-02	Lower Anhydrite Composite	Calculated: = POROSITY + DPHIMAX for fracturing model	Required for BRAGFLO	Analyst: DM Stoelzel
389	N/A	L_ANH_CP	PERM_EXP	4.721E+01	Lower Anhydrite Composite	Calculated in Algebra	Required for BRAGFLO	Calculated
390	579	S_MB139	CAP_MOD	2.000E+00	Interbed: Marker Bed 139	Capillary Pressure Model Number	Required for BRAGFLO	Database: CCA view 6
391	580	S_MB139	COMP_RCK	8.263E-11	Interbed: Marker Bed 139	Rock compressibility (1/Pa)	Intermediate value	Database: CCA view 6
392	582	S_MB139	PC_MAX	1.000E+08	Interbed: Marker Bed 139	Max capillary pressure	Required for BRAGFLO	Database: CCA view 6
393	2789	S_MB139	PCT_A	2.600E-01	Interbed: Marker Bed 139	Capillary pressure multiplier	Required for BRAGFLO	Database: CCA view 6
394	2790	S_MB139	PCT_EXP	-3.480E-01	Interbed: Marker Bed 139	Capillary pressure exponent	Required for BRAGFLO	Database: CCA view 6
395	2788	S_MB139	KPT	0.000E+00	Interbed: Marker Bed 139	Not used - placeholder	Not used	Database: CCA view 6
396	589	S_MB139	PO_MIN	1.013E+05	Interbed: Marker Bed 139	Minimum Brine pressure (same for all materials)	Required for BRAGFLO	Database: CCA view 6
397	587	S_MB139	PORE_DIS	6.436E-01	Interbed: Marker Bed 139	Pore distribution (fraction)	Required for BRAGFLO	Database: CCA view 6
398	588	S_MB139	POROSITY	1.100E-02	Interbed: Marker Bed 139	Porosity (fraction)	Required for BRAGFLO	Database: CCA view 6
399	591	S_MB139	PRMX_LOG	-1.889E+01	Interbed: Marker Bed 139	Log x-direction permeability	Intermediate value	Database: CCA view 6
400	592	S_MB139	PRMY_LOG	-1.889E+01	Interbed: Marker Bed 139	Log y-direction permeability	Intermediate value	Database: CCA view 6

Information Only

Database		Database Source: FI:[NOBACK2.DMS_WATERFLOOD.EPA.ALGEBRA]ALGEBRA_EPA_WF_RADIAL_R033.CDB;1 (Radial Case R5)						
ID Number	Material	Property	Value	Material Description	Property Value Description	Usage	Source	
401	593	S_MB139	PRMZ_LOG	-1.889E+01	Interbed: Marker Bed 139	Log z-direction permeability (BRAGFLO required input)	Not used - 2D model	Database: CCA view 6
402	596	S_MB139	RELP_MOD	4.000E+00	Interbed: Marker Bed 139	Relative permeability model number	Required for BRAGFLO	Database: CCA view 6
403	598	S_MB139	SAT_RBRN	8.363E-02	Interbed: Marker Bed 139	Residual Brine saturation	Required for BRAGFLO	Database: CCA view 6
404	599	S_MB139	SAT_RGAS	7.711E-02	Interbed: Marker Bed 139	Residual Gas saturation	Required for BRAGFLO	Database: CCA view 6
405	2177	S_MB139	DPHIMAX	3.900E-02	Interbed: Marker Bed 139	Maximum delta change in porosity for fracture model	Required for BRAGFLO	Database: CCA view 6
406	586	S_MB139	PI_DELTA	1.996E+05	Interbed: Marker Bed 139	Fracture initiation pressure - reference pressure (Pa)	Required for BRAGFLO	Database: CCA view 6
407	2180	S_MB139	PF_DELTA	3.799E+06	Interbed: Marker Bed 139	Maximum final fracture pressure - reference pressure (Pa)	Required for BRAGFLO	Database: CCA view 6
408	2811	S_MB139	IFRX	1.000E+00	Interbed: Marker Bed 139	X-direction fracturing flag (1 = true, 0 = false)	Required for BRAGFLO	Database: CCA view 6
409	2814	S_MB139	IFRY	1.000E+00	Interbed: Marker Bed 139	Y-direction fracturing flag (1 = true, 0 = false)	Required for BRAGFLO	Database: CCA view 6
410	2817	S_MB139	IFRZ	0.000E+00	Interbed: Marker Bed 139	Z-direction fracturing flag (1 = true, 0 = false)	Required for BRAGFLO	Database: CCA view 6
411	N/A	S_MB139	KMAXFRAC	1.000E-09	Interbed: Marker Bed 139	Maximum allowable permeability in fracturing model (m <sup>2</sup> )	Used to calc perm_exp	calculated: 10 <sup>4</sup> *kmaxlog
412	N/A	S_MB139	GRADSTAR	8.510E-01	Interbed: Marker Bed 139	Fracture Starting Gradient (psi/ft)	Gradient applied to all anh layers	Analyst: DM Stoezel
413	N/A	S_MB139	GRADSTOP	1.106E+00	Interbed: Marker Bed 139	Fracture Stopping Gradient (psi/ft)	Gradient applied to all anh layers	Analyst: DM Stoezel
414	2178	S_MB139	KMAXLOG	-9.000E+00	Interbed: Marker Bed 139	Log maximum allowable permeability in fracturing model log(m <sup>2</sup> )	Used for fracturing mod	Database: CCA view 6
415	2905	S_MB139	BKLINK	2.710E-01	Interbed: Marker Bed 139	Klinkenberg Effects multiplier	Not used	Database: CCA view 6
416	2903	S_MB139	EXPKLINK	-3.410E-01	Interbed: Marker Bed 139	Klinkenberg exponent	Not used	Database: CCA view 6
417	N/A	S_MB139	PERM_X	1.288E-19	Interbed: Marker Bed 139	X-direction permeability (from PRMX_LOG) (m <sup>2</sup> )	Required for BRAGFLO	Calculated
418	N/A	S_MB139	PERM_Y	1.288E-19	Interbed: Marker Bed 139	Y-direction permeability (from PRMY_LOG) (m <sup>2</sup> )	Required for BRAGFLO	Calculated
419	N/A	S_MB139	PERM_Z	1.288E-19	Interbed: Marker Bed 139	Z-direction permeability (from PRMZ_LOG) (m <sup>2</sup> )	Not used - 2D model	Calculated
420	N/A	S_MB139	SB_MIN	8.781E-02	Interbed: Marker Bed 139	Minimum saturation (SAT_RBRN * 1.05)	Required for BRAGFLO	Calculated
421	N/A	S_MB139	POR_COMP	7.512E-09	Interbed: Marker Bed 139	Calculated: = COMP_RCK/POROSITY	Required for BRAGFLO	Calculated
422	N/A	S_MB139	AVG_PRES	1.247E+07	Interbed: Marker Bed 139	Average Init grid-block pressure in layer	Calculated in ALGEBRA: Not used	Analyst: DM Stoezel
423	N/A	S_MB139	AVG_ELEV	3.809E+02	Interbed: Marker Bed 139	Average grid-block elevation in layer	Calculated in ALGEBRA: Not used	Analyst: DM Stoezel
424	N/A	S_MB139	INI_GRAD	8.376E-01	Interbed: Marker Bed 139	Initial gradient in layer (psi/ft)	Calculated in ALGEBRA: Not used	Analyst: DM Stoezel
425	N/A	S_MB139	PRES_INI	1.267E+07	Interbed: Marker Bed 139	Fracture initiation pressure (Pa)	Calculated in ALGEBRA: Not used	Analyst: DM Stoezel
426	N/A	S_MB139	PRES_FIN	1.647E+07	Interbed: Marker Bed 139	Fracture Stopping pressure (Pa)	Calculated in ALGEBRA: Not used	Analyst: DM Stoezel
427	N/A	S_MB139	PHIMAX	5.000E-02	Interbed: Marker Bed 139	Calculated: = POROSITY + DPHIMAX for fracturing model	Required for BRAGFLO	Analyst: DM Stoezel
428	N/A	S_MB139	PERM_EXP	1.506E+01	Interbed: Marker Bed 139	Calculated in Algebra	Required for BRAGFLO	Calculated
429	559	S_MB138	CAP_MOD	2.000E+00	Interbed: Marker Bed 138+A&B	Capillary Pressure Model Number	Required for BRAGFLO	From MB139
430	560	S_MB138	COMP_RCK	8.263E-11	Interbed: Marker Bed 138+A&B	Rock compressibility (1/Pa)	Required for BRAGFLO	From MB139
431	561	S_MB138	PC_MAX	1.000E+08	Interbed: Marker Bed 138+A&B	Max capillary pressure	Required for BRAGFLO	From MB139
432	2784	S_MB138	PCT_A	2.600E-01	Interbed: Marker Bed 138+A&B	Capillary pressure multiplier	Required for BRAGFLO	From MB139
433	2785	S_MB138	PCT_EXP	-3.480E-01	Interbed: Marker Bed 138+A&B	Capillary pressure exponent	Required for BRAGFLO	From MB139
434	2783	S_MB138	KPT	0.000E+00	Interbed: Marker Bed 138+A&B	Not used - placeholder	Not used	From MB139
435	568	S_MB138	PO_MIN	1.013E+05	Interbed: Marker Bed 138+A&B	Minimum Brine pressure (same for all materials)	Required for BRAGFLO	From MB139
436	566	S_MB138	PORE_DIS	6.436E-01	Interbed: Marker Bed 138+A&B	Pore distribution (fraction)	Required for BRAGFLO	From MB139
437	567	S_MB138	POROSITY	1.100E-02	Interbed: Marker Bed 138+A&B	Porosity (fraction)	Required for BRAGFLO	From MB139
438	570	S_MB138	PRMX_LOG	-1.889E+01	Interbed: Marker Bed 138+A&B	Log x-direction permeability	Placeholder	Not used
439	571	S_MB138	PRMY_LOG	-1.889E+01	Interbed: Marker Bed 138+A&B	Log y-direction permeability	Placeholder	Not used

Information Only



Database		Database Source: F1:[NOBACK2.DMS_WATERFLOOD.EPA_ALGEBRA]ALGEBRA_EPA_WF_RADIAL_R033.CDB;1 (Radial Case R5)						
ID Number	Material	Property	Value	Material Description	Property Value Description	Usage	Source	
440	572	S_MB138	PRMZ_LOG	-1.889E+01	Interbed: Marker Bed 138+A&B	Log z-direction permeability (BRAGFLO required input)	Placeholder	Not used
441	575	S_MB138	RELP_MOD	4.000E+00	Interbed: Marker Bed 138+A&B	Relative permeability model number	Required for BRAGFLO	From MB139
442	577	S_MB138	SAT_RBRN	8.363E-02	Interbed: Marker Bed 138+A&B	Residual Brine saturation	Required for BRAGFLO	From MB139
443	578	S_MB138	SAT_RGAS	7.711E-02	Interbed: Marker Bed 138+A&B	Residual Gas saturation	Required for BRAGFLO	From MB139
444	N/A	S_MB138	DPHIMAX	5.900E-02	Interbed: Marker Bed 138+A&B	Maximum delta change in porosity for fracture model	Required for BRAGFLO	From MB139
445	N/A	S_MB138	PI_DELTA	1.986E+05	Interbed: Marker Bed 138+A&B	Fracture initiation pressure - reference pressure (Pa)	Required for BRAGFLO	From MB139
446	N/A	S_MB138	PF_DELTA	3.780E+06	Interbed: Marker Bed 138+A&B	Maximum final fracture pressure - reference pressure (Pa)	Required for BRAGFLO	From MB139
447	2810	S_MB138	IFRX	1.000E+00	Interbed: Marker Bed 138+A&B	X-direction fracturing flag (1 = true, 0 = false)	Required for BRAGFLO	From MB139
448	2813	S_MB138	IFRY	1.000E+00	Interbed: Marker Bed 138+A&B	Y-direction fracturing flag (1 = true, 0 = false)	Required for BRAGFLO	From MB139
449	2816	S_MB138	IFRZ	0.000E+00	Interbed: Marker Bed 138+A&B	Z-direction fracturing flag (1 = true, 0 = false)	Required for BRAGFLO	From MB139
450	N/A	S_MB138	KMAXFRAC	1.000E-10	Interbed: Marker Bed 138+A&B	Maximum allowable permeability in fracturing model (m <sup>2</sup> )	Used to calc perm_exp	calculated: 10 <sup>4</sup> kmaxlog
451	N/A	S_MB138	GRADSTAR	8.510E-01	Interbed: Marker Bed 138+A&B	Fracture Starting Gradient (psi/ft)	Gradient applied to all anh layers	From MB139
452	N/A	S_MB138	GRADSTOP	1.106E+00	Interbed: Marker Bed 138+A&B	Fracture Stopping Gradient (psi/ft)	Gradient applied to all anh layers	From MB139
453	N/A	S_MB138	KMAXLOG	-1.000E+01	Interbed: Marker Bed 138+A&B	Log maximum allowable permeability in fracturing model log(m <sup>2</sup> )	Used for fracturing mod	Analyst: DM Stoezel
454	N/A	S_MB138	PERM_X	1.288E-19	Interbed: Marker Bed 138+A&B	X-direction permeability (from PRMX_LOG) (m <sup>2</sup> )	Required for BRAGFLO	From MB139
455	N/A	S_MB138	PERM_Y	1.288E-19	Interbed: Marker Bed 138+A&B	Y-direction permeability (from PRMY_LOG) (m <sup>2</sup> )	Required for BRAGFLO	From MB139
456	N/A	S_MB138	PERM_Z	1.288E-19	Interbed: Marker Bed 138+A&B	Z-direction permeability (from PRMZ_LOG) (m <sup>2</sup> )	Not used - 2D model	From MB139
457	N/A	S_MB138	SB_MIN	8.781E-02	Interbed: Marker Bed 138+A&B	Minimum saturation (SAT_RBRN * 1.05)	Required for BRAGFLO	Calculated
458	N/A	S_MB138	POR_COMP	7.512E-09	Interbed: Marker Bed 138+A&B	Calculated: = COMP_RCK/POROSITY	Required for BRAGFLO	Calculated
459	N/A	S_MB138	AVG_PRES	1.241E+07	Interbed: Marker Bed 138+A&B	Average Init grid-block pressure in layer	Calculated in ALGEBRA: Not used	Analyst: DM Stoezel
460	N/A	S_MB138	AVG_ELEV	3.842E+02	Interbed: Marker Bed 138+A&B	Average grid-block elevation in layer	Calculated in ALGEBRA: Not used	Analyst: DM Stoezel
461	N/A	S_MB138	INI_GRAD	8.376E-01	Interbed: Marker Bed 138+A&B	Initial gradient in layer (psi/ft)	Calculated in ALGEBRA: Not used	Analyst: DM Stoezel
462	N/A	S_MB138	PRES_INI	1.261E+07	Interbed: Marker Bed 138+A&B	Fracture initiation pressure (Pa)	Calculated in ALGEBRA based on GRADSTAR	Calculated
463	N/A	S_MB138	PRES_FIN	1.639E+07	Interbed: Marker Bed 138+A&B	Fracture Stopping pressure (Pa)	Calculated in ALGEBRA based on GRADSTOP	Calculated
464	N/A	S_MB138	PHIMAX	7.000E-02	Interbed: Marker Bed 138+A&B	Calculated: = POROSITY + DPHIMAX for fracturing model	Required for BRAGFLO	Analyst: DM Stoezel
465	N/A	S_MB138	PERM_EXP	1.107E+01	Interbed: Marker Bed 138+A&B	Calculated in Algebra	Required for BRAGFLO	Calculated
466	N/A	U_ANH_CP	CAP_MOD	2.000E+00	Upper Anhydrite Composite	Capillary Pressure Model Number	Required for BRAGFLO	From MB139
467	N/A	U_ANH_CP	COMP_RCK	7.948E-10	Upper Anhydrite Composite	Rock compressibility (1/Pa)	Required for BRAGFLO	From MB139
468	N/A	U_ANH_CP	PC_MAX	1.000E+08	Upper Anhydrite Composite	Max capillary pressure	Required for BRAGFLO	From MB139
469	N/A	U_ANH_CP	PCT_A	2.600E-01	Upper Anhydrite Composite	Capillary pressure multiplier	Required for BRAGFLO	From MB139
470	N/A	U_ANH_CP	PCT_EXP	-3.480E-01	Upper Anhydrite Composite	Capillary pressure exponent	Required for BRAGFLO	From MB139
471	N/A	U_ANH_CP	KPT	0.000E+00	Upper Anhydrite Composite	Not used - placeholder	Not used	From MB139
472	N/A	U_ANH_CP	PO_MIN	1.013E+05	Upper Anhydrite Composite	Minimum Brine pressure (same for all materials)	Required for BRAGFLO	From MB139
473	N/A	U_ANH_CP	PORE_DIS	6.436E-01	Upper Anhydrite Composite	Pore distribution (fraction)	Required for BRAGFLO	From MB139
474	N/A	U_ANH_CP	POROSITY	1.100E-02	Upper Anhydrite Composite	Porosity (fraction)	Required for BRAGFLO	From MB139
475	N/A	U_ANH_CP	PRMX_LOG	-1.190E+01	Upper Anhydrite Composite	Log x-direction permeability	Placeholder	Not used
476	N/A	U_ANH_CP	PRMY_LOG	-1.990E+01	Upper Anhydrite Composite	Log y-direction permeability	Placeholder	Not used
477	N/A	U_ANH_CP	PRMZ_LOG	-1.190E+01	Upper Anhydrite Composite	Log z-direction permeability (BRAGFLO required input)	Placeholder	Not used
478	N/A	U_ANH_CP	RELP_MOD	4.000E+00	Upper Anhydrite Composite	Relative permeability model number	Required for BRAGFLO	From MB139

Information Only

				Database Source: F1:[NOBACK2.DMS_WATERFLOOD.EPA.ALGEBRA]ALGEBRA_EPA_WF_RADIAL_R033.CDB;1 (Radial Case R5)				
ID Number	Material	Property	Value	Material Description	Property Value Description	Usage	Source	
479	N/A	U_ANH_CP	SAT_RBRN	8.363E-02	Upper Anhydrite Composite	Residual Brine saturation	Required for BRAGFLO	From MB139
480	N/A	U_ANH_CP	SAT_RGAS	7.711E-02	Upper Anhydrite Composite	Residual Gas saturation	Required for BRAGFLO	From MB139
481	N/A	U_ANH_CP	DPHIMAX	7.000E-03	Upper Anhydrite Composite	Maximum delta change in porosity for fracture model	Required for BRAGFLO	From MB139
482	N/A	U_ANH_CP	PI_DELTA	1.477E+05	Upper Anhydrite Composite	Fracture initiation pressure - reference pressure (Pa)	Required for BRAGFLO	From MB139
483	N/A	U_ANH_CP	PF_DELTA	2.812E+06	Upper Anhydrite Composite	Maximum final fracture pressure - reference pressure (Pa)	Required for BRAGFLO	From MB139
484	N/A	U_ANH_CP	IFRX	1.000E+00	Upper Anhydrite Composite	X-direction fracturing flag (1 = true, 0 = false)	Required for BRAGFLO	From MB139
485	N/A	U_ANH_CP	IFRY	1.000E+00	Upper Anhydrite Composite	Y-direction fracturing flag (1 = true, 0 = false)	Required for BRAGFLO	From MB139
486	N/A	U_ANH_CP	IFRZ	0.000E+00	Upper Anhydrite Composite	Z-direction fracturing flag (1 = true, 0 = false)	Required for BRAGFLO	From MB139
487	N/A	U_ANH_CP	KMAXFRAC	1.000E-11	Upper Anhydrite Composite	Maximum allowable permeability in fracturing model (m <sup>2</sup> )	Used to calc perm_exp	calculated: 10 <sup>^</sup> kmaxlog
488	N/A	U_ANH_CP	GRADSTAR	8.510E-01	Upper Anhydrite Composite	Fracture Starting Gradient (psi/ft)	Gradient applied to all anh layers	From MB139
489	N/A	U_ANH_CP	GRADSTOP	1.106E+00	Upper Anhydrite Composite	Fracture Stopping Gradient (psi/ft)	Gradient applied to all anh layers	From MB139
490	N/A	U_ANH_CP	KMAXLOG	-1.100E+01	Upper Anhydrite Composite	Log maximum allowable permeability in fracturing model log(m <sup>2</sup> )	Used for fracturing mod	Analyst: DM Stoelzel
491	N/A	U_ANH_CP	PERM_X	1.288E-19	Upper Anhydrite Composite	X-direction permeability (from PRMX_LOG) (m <sup>2</sup> )	Required for BRAGFLO	From MB139
492	N/A	U_ANH_CP	PERM_Y	1.288E-19	Upper Anhydrite Composite	Y-direction permeability (from PRMY_LOG) (m <sup>2</sup> )	Required for BRAGFLO	From MB139
493	N/A	U_ANH_CP	PERM_Z	1.288E-19	Upper Anhydrite Composite	Z-direction permeability (from PRMZ_LOG) (m <sup>2</sup> )	Not used - 2D model	From MB139
494	N/A	U_ANH_CP	SB_MIN	8.781E-02	Upper Anhydrite Composite	Minimum saturation (SAT_RBRN * 1.05)	Required for BRAGFLO	Calculated
495	N/A	U_ANH_CP	POR_COMP	7.512E-09	Upper Anhydrite Composite	Calculated: = COMP_RCK/POROSITY	Required for BRAGFLO	Calculated
496	N/A	U_ANH_CP	AVG_PRES	9.230E+06	Upper Anhydrite Composite	Average Init grid-block pressure in layer	Calculated in ALGEBRA: Not used	Analyst: DM Stoelzel
497	N/A	U_ANH_CP	AVG_ELEV	5.519E+02	Upper Anhydrite Composite	Average grid-block elevation in layer	Calculated in ALGEBRA: Not used	Analyst: DM Stoelzel
498	N/A	U_ANH_CP	INI_GRAD	8.376E-01	Upper Anhydrite Composite	Initial gradient in layer (psi/ft)	Calculated in ALGEBRA: Not used	Analyst: DM Stoelzel
499	N/A	U_ANH_CP	PRES_INI	9.377E+06	Upper Anhydrite Composite	Fracture initiation pressure (Pa)	Calculated in ALGEBRA based on GRADSTAR	Calculated
500	N/A	U_ANH_CP	PRES_FIN	1.219E+07	Upper Anhydrite Composite	Fracture Stopping pressure (Pa)	Calculated in ALGEBRA based on GRADSTOP	Calculated
501	N/A	U_ANH_CP	PHIMAX	1.800E-02	Upper Anhydrite Composite	Calculated: = POROSITY + DPHIMAX for fracturing model	Required for BRAGFLO	Analyst: DM Stoelzel
502	N/A	U_ANH_CP	PERM_EXP	3.697E+01	Upper Anhydrite Composite	Calculated in Algebra	Required for BRAGFLO	Calculated
503	2217	UNNAMED	CAP_MOD	1.000E+00	Un-named member of Rustler	Capillary Pressure Model Number	Required for BRAGFLO	Database: CCA view 6
504	2218	UNNAMED	COMP_RCK	0.000E+00	Un-named member of Rustler	Rock compressibility (1/Pa)	Intermediate value	Database: CCA view 6
505	2247	UNNAMED	PC_MAX	1.000E+08	Un-named member of Rustler	Max capillary pressure	Required for BRAGFLO	Database: CCA view 6
506	2800	UNNAMED	PCT_A	0.000E+00	Un-named member of Rustler	Capillary pressure multiplier (placeholder)	Not used	Database: CCA view 6
507	2801	UNNAMED	PCT_EXP	0.000E+00	Un-named member of Rustler	Capillary pressure exponent (placeholder)	Not used	Database: CCA view 6
508	2799	UNNAMED	KPT	0.000E+00	Un-named member of Rustler	Not used - placeholder	Not used	Database: CCA view 6
509	2802	UNNAMED	PO_MIN	1.013E+05	Un-named member of Rustler	Minimum Brine pressure (same for all materials)	Required for BRAGFLO	Database: CCA view 6
510	2219	UNNAMED	PORE_DIS	7.000E-01	Un-named member of Rustler	Pore distribution (fraction)	Required for BRAGFLO	Database: CCA view 6
511	2220	UNNAMED	POROSITY	1.810E-01	Un-named member of Rustler	Porosity (fraction)	Required for BRAGFLO	Database: CCA view 6
512	2911	UNNAMED	PRMX_LOG	-3.500E+01	Un-named member of Rustler	Log x-direction permeability	Intermediate value	Database: CCA view 6
513	2912	UNNAMED	PRMY_LOG	-3.500E+01	Un-named member of Rustler	Log y-direction permeability	Intermediate value	Database: CCA view 6
514	2913	UNNAMED	PRMZ_LOG	-3.500E+01	Un-named member of Rustler	Log z-direction permeability (BRAGFLO required input)	Not used - 2D model	Database: CCA view 6
515	2225	UNNAMED	REL_P_MOD	4.000E+00	Un-named member of Rustler	Relative permeability model number	Required for BRAGFLO	Database: CCA view 6
516	2248	UNNAMED	SAT_RBRN	2.000E-01	Un-named member of Rustler	Residual Brine saturation	Required for BRAGFLO	Database: CCA view 6
517	2226	UNNAMED	SAT_RGAS	2.000E-01	Un-named member of Rustler	Residual Gas saturation	Required for BRAGFLO	Database: CCA view 6

Information Only

Database Source: F1:[NOBACK2.DMS_WATERFLOOD.EPA.ALGEBRA]ALGEBRA_EPA_WF_RADIAL_R033.CDB;1 (Radial Case R5)								
ID Number	Material	Property	Value	Material Description	Property Value Description	Usage	Source	
518	N/A	UNNAMED	PERM_X	1.000E-35	Un-named member of Rustler	X-direction permeability (m <sup>2</sup> ) from Log value (impermeable)	Required for BRAGFLO	Calculated
519	N/A	UNNAMED	PERM_Y	1.000E-35	Un-named member of Rustler	Y-direction permeability (m <sup>2</sup> ) from Log value (impermeable)	Required for BRAGFLO	Calculated
520	N/A	UNNAMED	PERM_Z	1.000E-35	Un-named member of Rustler	Z-direction permeability (m <sup>2</sup> ) Not used in 2D	Required for BRAGFLO	Calculated
521	N/A	UNNAMED	SB_MIN	2.100E-01	Un-named member of Rustler	Minimum saturation (SAT_RBRN * 1.05)	Required for BRAGFLO	Calculated
522	N/A	UNNAMED	POR_COMP	0.000E+00	Un-named member of Rustler	Pore compressibility COMP_RCK/POROSITY (1/Pa)	Required for BRAGFLO	Calculated
523	229	IMPERM_Z	CAP_MOD	1.000E+00	Becomes Culebra @ time 0	Capillary Pressure Model Number	Required for BRAGFLO	Database: CCA view 6
524	230	IMPERM_Z	COMP_RCK	0.000E+00	Becomes Culebra @ time 0	Rock compressibility (1/Pa)	Intermediate value	Database: CCA view 6
525	231	IMPERM_Z	PC_MAX	1.000E+08	Becomes Culebra @ time 0	Max capillary pressure	Required for BRAGFLO	Database: CCA view 6
526	2721	IMPERM_Z	PCT_A	0.000E+00	Becomes Culebra @ time 0	Capillary pressure multiplier (placeholder)	Not used	Database: CCA view 6
527	2722	IMPERM_Z	PCT_EXP	0.000E+00	Becomes Culebra @ time 0	Capillary pressure exponent (placeholder)	Not used	Database: CCA view 6
528	2720	IMPERM_Z	KPT	0.000E+00	Becomes Culebra @ time 0	Not used - placeholder	Not used	Database: CCA view 6
529	234	IMPERM_Z	PO_MIN	1.013E+05	Becomes Culebra @ time 0	Minimum Brine pressure (same for all materials)	Required for BRAGFLO	Database: CCA view 6
530	232	IMPERM_Z	PORE_DIS	7.000E-01	Becomes Culebra @ time 0	Pore distribution (fraction)	Required for BRAGFLO	Database: CCA view 6
531	233	IMPERM_Z	POROSITY	5.000E-03	Becomes Culebra @ time 0	Porosity (fraction)	Required for BRAGFLO	Database: CCA view 6
532	236	IMPERM_Z	PRMX_LOG	-3.500E+01	Becomes Culebra @ time 0	Log x-direction permeability	Intermediate value	Database: CCA view 6
533	237	IMPERM_Z	PRMY_LOG	-3.500E+01	Becomes Culebra @ time 0	Log y-direction permeability	Intermediate value	Database: CCA view 6
534	238	IMPERM_Z	PRMZ_LOG	-3.500E+01	Becomes Culebra @ time 0	Log z-direction permeability (BRAGFLO required input)	Not used - 2D model	Database: CCA view 6
535	241	IMPERM_Z	REL_P_MOD	4.000E+00	Becomes Culebra @ time 0	Relative permeability model number	Required for BRAGFLO	Database: CCA view 6
536	243	IMPERM_Z	SAT_RBRN	0.000E+00	Becomes Culebra @ time 0	Residual Brine saturation	Required for BRAGFLO	Database: CCA view 6
537	244	IMPERM_Z	SAT_RGAS	0.000E+00	Becomes Culebra @ time 0	Residual Gas saturation	Required for BRAGFLO	Database: CCA view 6
538	N/A	IMPERM_Z	PERM_X	1.000E-35	Becomes Culebra @ time 0	X-direction permeability (m <sup>2</sup> ) from Log value (impermeable)	Required for BRAGFLO	Calculated
539	N/A	IMPERM_Z	PERM_Y	1.000E-35	Becomes Culebra @ time 0	Y-direction permeability (m <sup>2</sup> ) from Log value (impermeable)	Required for BRAGFLO	Calculated
540	N/A	IMPERM_Z	PERM_Z	1.000E-35	Becomes Culebra @ time 0	Z-direction permeability (m <sup>2</sup> ) Not used in 2D	Required for BRAGFLO	Calculated
541	N/A	IMPERM_Z	SB_MIN	0.000E+00	Becomes Culebra @ time 0	Minimum saturation (SAT_RBRN * 1.05)	Required for BRAGFLO	Calculated
542	N/A	IMPERM_Z	POR_COMP	0.000E+00	Becomes Culebra @ time 0	Pore compressibility COMP_RCK/POROSITY (1/Pa)	Required for BRAGFLO	Calculated
543	119	CULEBRA	CAP_MOD	2.000E+00	Replaces IMPERM_Z @ t=0	Capillary Pressure Model Number	Required for BRAGFLO	Database: CCA view 6
544	120	CULEBRA	COMP_RCK	1.000E-10	Replaces IMPERM_Z @ t=0	Rock compressibility (1/Pa)	Intermediate value	Database: CCA view 6
545	137	CULEBRA	PC_MAX	1.000E+08	Replaces IMPERM_Z @ t=0	Max capillary pressure	Required for BRAGFLO	Database: CCA view 6
546	2692	CULEBRA	PCT_A	2.600E-01	Replaces IMPERM_Z @ t=0	Capillary pressure multiplier	Required for BRAGFLO	Database: CCA view 6
547	2693	CULEBRA	PCT_EXP	-3.480E-01	Replaces IMPERM_Z @ t=0	Capillary pressure exponent	Required for BRAGFLO	Database: CCA view 6
548	2691	CULEBRA	KPT	0.000E+00	Replaces IMPERM_Z @ t=0	Not used - placeholder	Not used	Database: CCA view 6
549	141	CULEBRA	PO_MIN	1.013E+05	Replaces IMPERM_Z @ t=0	Minimum Brine pressure (same for all materials)	Required for BRAGFLO	Database: CCA view 6
550	139	CULEBRA	PORE_DIS	6.436E-01	Replaces IMPERM_Z @ t=0	Pore distribution (fraction)	Required for BRAGFLO	Database: CCA view 6
551	140	CULEBRA	POROSITY	1.510E-01	Replaces IMPERM_Z @ t=0	Porosity (fraction)	Required for BRAGFLO	Database: CCA view 6
552	142	CULEBRA	PRESSURE	8.220E+05	Replaces IMPERM_Z @ t=0	Initial pressure for Culebra, Unnamed formations (Pa)	In ALGEBRA step	Database: CCA view 6
553	143	CULEBRA	PRMX_LOG	-1.368E+01	Replaces IMPERM_Z @ t=0	Log x-direction permeability	Intermediate value	Analyst: DM Stoelzel
554	144	CULEBRA	PRMY_LOG	-1.368E+01	Replaces IMPERM_Z @ t=0	Log y-direction permeability	Intermediate value	Analyst: DM Stoelzel
555	145	CULEBRA	PRMZ_LOG	-1.368E+01	Replaces IMPERM_Z @ t=0	Log z-direction permeability (BRAGFLO required input)	Not used - 2D model	Analyst: DM Stoelzel
556	148	CULEBRA	REL_P_MOD	4.000E+00	Replaces IMPERM_Z @ t=0	Relative permeability model number	Required for BRAGFLO	Database: CCA view 6
557	150	CULEBRA	SAT_RBRN	8.363E-02	Replaces IMPERM_Z @ t=0	Residual Brine saturation	Required for BRAGFLO	Database: CCA view 6
558	151	CULEBRA	SAT_RGAS	7.711E-02	Replaces IMPERM_Z @ t=0	Residual Gas saturation	Required for BRAGFLO	Database: CCA view 6
559	N/A	CULEBRA	PERM_X	2.099E-14	Replaces IMPERM_Z @ t=0	X-direction permeability (m <sup>2</sup> ) from Log value	Required for BRAGFLO	Calculated
560	N/A	CULEBRA	PERM_Y	2.099E-14	Replaces IMPERM_Z @ t=0	Y-direction permeability (m <sup>2</sup> ) from Log value	Required for BRAGFLO	Calculated
561	N/A	CULEBRA	PERM_Z	2.099E-14	Replaces IMPERM_Z @ t=0	Z-direction permeability (m <sup>2</sup> ) Not used in 2D	Required for BRAGFLO	Calculated
562	N/A	CULEBRA	SB_MIN	8.781E-02	Replaces IMPERM_Z @ t=0	Minimum saturation (SAT_RBRN * 1.05)	Required for BRAGFLO	Calculated
563	N/A	CULEBRA	POR_COMP	6.623E-10	Replaces IMPERM_Z @ t=0	Pore compressibility COMP_RCK/POROSITY (1/Pa)	Required for BRAGFLO	Calculated

Information Only



Database Source: F1:[NOBACK2.DMS_WATERFLOOD.EPA.ALGEBRA]ALGEBRA_EPA_WF_RADIAL_R033.CDB;1 (Radial Case R5)								
ID Number	Material	Property	Value	Material Description	Property Value Description	Usage	Source	
564	44	BRINESAL	DNSFLUID	1.220E+03	Salado Brine	Density (kg/m <sup>3</sup> )	BRAGFLO input	Database: CCA view 6
565	57	BRINESAL	WTF	3.240E-01	Salado Brine	Salinity	BRAGFLO input	Database: CCA view 6
566	48	BRINESAL	COMPRES	3.100E-10	Salado Brine	Fluid compressibility (1/Pa)	BRAGFLO input	Database: CCA view 6
567	55	BRINESAL	VISCO	2.100E-03	Salado Brine	Brine viscosity (Pa-s)	BRAGFLO input	Database: CCA view 6
568	51	BRINESAL	REF_TEMP	3.002E+02	Salado Brine	Brine reference temperature (deg Kelvin)	BRAGFLO input	Database: CCA view 6
569	50	BRINESAL	REF_PRES	1.013E+05	Salado Brine	Brine reference pressure (Pa)	BRAGFLO input	Database: CCA view 6
570	N/A	BRINESAL	COMP	3.100E-10	Salado Brine	Set equal to compressibility: COMP = COMPRES (1/Pa)	BRAGFLO key word	Calculated
571	28	H2	VISCO	8.934E-06	Hydrogen gas	Gas viscosity (Pa-s)	BRAGFLO key word	Database: CCA view 6
572	2889	REFCON	GRAVACC	9.807E+00	Reference props or conversions	Acceleration due to gravity	ALGEBRA: Chem mod	Database: CCA view 6
573	2896	REFCON	PI	3.142E+00	Reference props or conversions	constant PI	ALGEBRA: Chem mod	Database: CCA view 6
574	3107	REFCON	VPANLEX	4.610E+04	Reference props or conversions	Conversion used in gas generation rates (see task 1 WPO# 40514)	ALGEBRA: Chem mod	Database: CCA view 6
575	3105	REFCON	VROOM	3.644E+03	Reference props or conversions	Conversion used in gas generation rates (see task 1 WPO# 40514)	ALGEBRA: Chem mod	Database: CCA view 6
576	3108	REFCON	VREPOS	4.360E+05	Reference props or conversions	Conversion used in gas generation rates (see task 1 WPO# 40514)	ALGEBRA: Chem mod	Database: CCA view 6
577	3132	REFCON	DRROOM	6.804E+03	Reference props or conversions	Conversion used in gas generation rates (see task 1 WPO# 40514)	ALGEBRA: Chem mod	Database: CCA view 6
578	2888	REFCON	YRSEC	3.156E+07	Reference props or conversions	Years to seconds conversion	ALGEBRA: Chem mod	Database: CCA view 6
579	3112	REFCON	SECYR	3.169E-08	Reference props or conversions	Seconds to year conversion	ALGEBRA: Chem mod	Database: CCA view 6
580	3106	REFCON	ASDRUM	6.000E+00	Reference props or conversions	Conversion used in gas generation rates (see task 1 WPO# 40514)	ALGEBRA: Chem mod	Database: CCA view 6
581	2890	REFCON	ATMPA	1.013E+05	Reference props or conversions	Atmospheric pressure (Pa)	ALGEBRA: Chem mod	Database: CCA view 6
582	3150	CONC_PLG	CAP_MOD	1.000E+00	Concrete Plug	Capillary Pressure Model Number	U Bell & Rustler: 50-250 yrs	Database: CCA view 6
583	3148	CONC_PLG	COMP_RCK	1.200E-09	Concrete Plug	Rock compressibility (1/Pa)	U Bell & Rustler: 50-250 yrs	Database: CCA view 6
584	3151	CONC_PLG	PC_MAX	1.000E+08	Concrete Plug	Max capillary pressure	U Bell & Rustler: 50-250 yrs	Database: CCA view 6
585	3157	CONC_PLG	PCT_A	0.000E+00	Concrete Plug	Capillary pressure multiplier (placeholder)	U Bell & Rustler: 50-250 yrs	Database: CCA view 6
586	3158	CONC_PLG	PCT_EXP	0.000E+00	Concrete Plug	Capillary pressure exponent (placeholder)	U Bell & Rustler: 50-250 yrs	Database: CCA view 6
587	3156	CONC_PLG	KPT	0.000E+00	Concrete Plug	Not used - placeholder	U Bell & Rustler: 50-250 yrs	Database: CCA view 6
588	3155	CONC_PLG	PO_MIN	1.013E+05	Concrete Plug	Minimum Brine pressure (same for all materials)	U Bell & Rustler: 50-250 yrs	Database: CCA view 6
589	3154	CONC_PLG	PORE_DIS	9.400E-01	Concrete Plug	Pore distribution (fraction)	U Bell & Rustler: 50-250 yrs	Database: CCA view 6
590	3147	CONC_PLG	POROSITY	3.200E-01	Concrete Plug	Porosity (fraction)	U Bell & Rustler: 50-250 yrs	Database: CCA view 6
591	3185	CONC_PLG	PRMX_LOG	-1.630E+01	Concrete Plug	Log x-direction permeability	U Bell & Rustler: 50-250 yrs	Database: CCA view 6
592	3192	CONC_PLG	PRMY_LOG	-1.630E+01	Concrete Plug	Log y-direction permeability	U Bell & Rustler: 50-250 yrs	Database: CCA view 6
593	3193	CONC_PLG	PRMZ_LOG	-1.630E+01	Concrete Plug	Log z-direction permeability (BRAGFLO required input)	U Bell & Rustler: 50-250 yrs	Database: CCA view 6
594	3149	CONC_PLG	RELP_MOD	4.000E+00	Concrete Plug	Relative permeability model number	U Bell & Rustler: 50-250 yrs	Database: CCA view 6
595	3152	CONC_PLG	SAT_RBRN	0.000E+00	Concrete Plug	Residual Brine saturation	U Bell & Rustler: 50-250 yrs	Database: CCA view 6

Information Only



				Database Source: F1:[NOBACK2.DMS_WATERFLOOD.EPA_ALGEBRA]ALGEBRA_EPA_WF_RADIAL_R033.CDB;1 (Radial Case R5)				
ID Number	Material	Property	Value	Material Description	Property Value Description	Usage	Source	
596	3153	CONC_PLG	SAT_RGAS	0.000E+00	Concrete Plug	Residual Gas saturation	U Bell & Rustler: 50-250 yrs	Database: CCA view 6
597	N/A	CONC_PLG	PERM_X	5.000E-17	Concrete Plug	X-direction permeability (m <sup>2</sup> ) from Log value	U Bell & Rustler: 50-250 yrs	Calculated
598	N/A	CONC_PLG	PERM_Y	5.000E-17	Concrete Plug	Y-direction permeability (m <sup>2</sup> ) from Log value	U Bell & Rustler: 50-250 yrs	Calculated
599	N/A	CONC_PLG	PERM_Z	5.000E-17	Concrete Plug	Z-direction permeability (m <sup>2</sup> ) Not used in 2D	U Bell & Rustler: 50-250 yrs	Calculated
600	N/A	CONC_PLG	SB_MIN	0.000E+00	Concrete Plug	Minimum saturation (SAT_RBRN * 1.05)	U Bell & Rustler: 50-250 yrs	Calculated
601	N/A	CONC_PLG	POR_COMP	1.200E-09	Concrete Plug	Pore compressibility COMP_RCK/POROSITY (1/Pa)	U Bell & Rustler: 50-250 yrs	Calculated
602	3138	BH_OPEN	CAP_MOD	1.000E+00	Open or channel borehole props	Capillary Pressure Model Number	For leaky boreholes	Database: CCA view 6
603	3136	BH_OPEN	COMP_RCK	0.000E+00	Open or channel borehole props	Rock compressibility (1/Pa)	For leaky boreholes	Database: CCA view 6
604	3139	BH_OPEN	PC_MAX	1.000E+08	Open or channel borehole props	Max capillary pressure	For leaky boreholes	Database: CCA view 6
605	3145	BH_OPEN	PCT_A	0.000E+00	Open or channel borehole props	Capillary pressure multiplier (placeholder)	For leaky boreholes	Database: CCA view 6
606	3146	BH_OPEN	PCT_EXP	0.000E+00	Open or channel borehole props	Capillary pressure exponent (placeholder)	For leaky boreholes	Database: CCA view 6
607	3144	BH_OPEN	KPT	0.000E+00	Open or channel borehole props	Not used - placeholder	For leaky boreholes	Database: CCA view 6
608	3143	BH_OPEN	PO_MIN	1.013E+05	Open or channel borehole props	Minimum Brine pressure (same for all materials)	For leaky boreholes	Database: CCA view 6
609	3142	BH_OPEN	PORE_DIS	7.000E-01	Open or channel borehole props	Pore distribution (fraction)	For leaky boreholes	Database: CCA view 6
610	3135	BH_OPEN	POROSITY	3.200E-01	Open or channel borehole props	Porosity (fraction)	For leaky boreholes	Database: CCA view 6
611	3134	BH_OPEN	PRMX_LOG	-9.000E+00	Open or channel borehole props	Log x-direction permeability	For leaky boreholes	Database: CCA view 6
612	3186	BH_OPEN	PRMY_LOG	-9.000E+00	Open or channel borehole props	Log y-direction permeability	For leaky boreholes	Database: CCA view 6
613	3187	BH_OPEN	PRMZ_LOG	-9.000E+00	Open or channel borehole props	Log z-direction permeability (BRAGFLO required input)	For leaky boreholes	Database: CCA view 6
614	3137	BH_OPEN	RELP_MOD	5.000E+00	Open or channel borehole props	Relative permeability model number	For leaky boreholes	Database: CCA view 6
615	3140	BH_OPEN	SAT_RBRN	0.000E+00	Open or channel borehole props	Residual Brine saturation	For leaky boreholes	Database: CCA view 6
616	3141	BH_OPEN	SAT_RGAS	0.000E+00	Open or channel borehole props	Residual Gas saturation	For leaky boreholes	Database: CCA view 6
617	N/A	BH_OPEN	PERM_X	1.000E-09	Open or channel borehole props	X-direction permeability (m <sup>2</sup> ) from Log value	For leaky boreholes	Calculated
618	N/A	BH_OPEN	PERM_Y	1.000E-09	Open or channel borehole props	Y-direction permeability (m <sup>2</sup> ) from Log value	For leaky boreholes	Calculated
619	N/A	BH_OPEN	PERM_Z	1.000E-09	Open or channel borehole props	Z-direction permeability (m <sup>2</sup> ) Not used in 2D	For leaky boreholes	Calculated
620	N/A	BH_OPEN	SB_MIN	0.000E+00	Open or channel borehole props	Minimum saturation (SAT_RBRN * 1.05)	For leaky boreholes	Calculated
621	N/A	BH_OPEN	POR_COMP	0.000E+00	Open or channel borehole props	Pore compressibility COMP_RCK/POROSITY (1/Pa)	For leaky boreholes	Calculated
622	3162	BH_SAND	CAP_MOD	1.000E+00	Sand-filled Borehole properties	Capillary Pressure Model Number	For abandoned boreholes	Database: CCA view 6
623	3160	BH_SAND	COMP_RCK	0.000E+00	Sand-filled Borehole properties	Rock compressibility (1/Pa)	For abandoned boreholes	Database: CCA view 6
624	3163	BH_SAND	PC_MAX	1.000E+08	Sand-filled Borehole properties	Max capillary pressure	For abandoned boreholes	Database: CCA view 6
625	3169	BH_SAND	PCT_A	0.000E+00	Sand-filled Borehole properties	Capillary pressure multiplier (placeholder)	For abandoned boreholes	Database: CCA view 6
626	3170	BH_SAND	PCT_EXP	0.000E+00	Sand-filled Borehole properties	Capillary pressure exponent (placeholder)	For abandoned boreholes	Database: CCA view 6
627	3168	BH_SAND	KPT	0.000E+00	Sand-filled Borehole properties	Not used - placeholder	For abandoned boreholes	Database: CCA view 6
628	3167	BH_SAND	PO_MIN	1.013E+05	Sand-filled Borehole properties	Minimum Brine pressure (same for all materials)	For abandoned boreholes	Database: CCA view 6
629	3166	BH_SAND	PORE_DIS	9.400E-01	Sand-filled Borehole properties	Pore distribution (fraction)	For abandoned boreholes	Database: CCA view 6
630	3159	BH_SAND	POROSITY	3.200E-01	Sand-filled Borehole properties	Porosity (fraction)	For abandoned boreholes	Database: CCA view 6
631	3184	BH_SAND	PRMX_LOG	-1.250E+01	Sand-filled Borehole properties	Log x-direction permeability	For abandoned boreholes	Database: CCA view 6
632	3190	BH_SAND	PRMY_LOG	-1.250E+01	Sand-filled Borehole properties	Log y-direction permeability	For abandoned boreholes	Database: CCA view 6
633	3191	BH_SAND	PRMZ_LOG	-1.250E+01	Sand-filled Borehole properties	Log z-direction permeability (BRAGFLO required input)	For abandoned boreholes	Database: CCA view 6
634	3161	BH_SAND	RELP_MOD	4.000E+00	Sand-filled Borehole properties	Relative permeability model number	For abandoned boreholes	Database: CCA view 6
635	3164	BH_SAND	SAT_RBRN	0.000E+00	Sand-filled Borehole properties	Residual Brine saturation	For abandoned boreholes	Database: CCA view 6

Information Only

ID Number	Database	Material	Property	Value	Material Description	Property Value Description	Usage	Source
636	N/A	BH_SAND	SAT_RGAS	0.000E+00	Sand-filled Borehole properties	Residual Gas saturation	For abandoned boreholes	Database: CCA view 6
637	N/A	BH_SAND	PERM_X	3.162E-13	Sand-filled Borehole properties	X-direction permeability (m^2)	For abandoned boreholes	Calculated
638	N/A	BH_SAND	PERM_Y	3.162E-13	Sand-filled Borehole properties	Y-direction permeability (m^2)	For abandoned boreholes	Calculated
639	N/A	BH_SAND	PERM_Z	3.162E-13	Sand-filled Borehole properties	Z-direction permeability (m^2)	For abandoned boreholes	Calculated
640	N/A	BH_SAND	SB_MIN	0.000E+00	Sand-filled Borehole properties	Minimum saturation (SAT_RBRN * 1.05)	For abandoned boreholes	Calculated
641	N/A	BH_SAND	POR_COMP	0.000E+00	Sand-filled Borehole properties	Pore compressibility (1/Pa)	For abandoned boreholes	Calculated
642	3174	BH_CREEP	CAP_MOD	1.000E+00	BH props for lower part after 1k yrs	Capillary Pressure Model Number	Salt creep portion of BH	Database: CCA view 6
643	3172	BH_CREEP	COMP_RCK	0.000E+00	BH props for lower part after 1k yrs	Rock compressibility (1/Pa)	Salt creep portion of BH	Database: CCA view 6
644	3175	BH_CREEP	PC_MAX	1.000E+08	BH props for lower part after 1k yrs	Max capillary pressure	Salt creep portion of BH	Database: CCA view 6
645	3181	BH_CREEP	PCT_A	0.000E+00	BH props for lower part after 1k yrs	Capillary pressure multiplier (placeholder)	Salt creep portion of BH	Database: CCA view 6
646	3182	BH_CREEP	PCT_EXP	0.000E+00	BH props for lower part after 1k yrs	Capillary pressure exponent (placeholder)	Salt creep portion of BH	Database: CCA view 6
647	3180	BH_CREEP	KPT	0.000E+00	BH props for lower part after 1k yrs	Not used - placeholder	Salt creep portion of BH	Database: CCA view 6
648	3179	BH_CREEP	PO_MIN	1.013E+05	BH props for lower part after 1k yrs	Minimum Brine pressure (same for all materials)	Salt creep portion of BH	Database: CCA view 6
649	3178	BH_CREEP	PORE_DIS	9.400E-01	BH props for lower part after 1k yrs	Pore distribution (fraction)	Salt creep portion of BH	Database: CCA view 6
650	3171	BH_CREEP	POROSITY	3.200E-01	BH props for lower part after 1k yrs	Porosity (fraction)	Salt creep portion of BH	Database: CCA view 6
651	3183	BH_CREEP	PRMX_LOG	-1.350E+01	BH props for lower part after 1k yrs	Log x-direction permeability	Salt creep portion of BH	Database: CCA view 6
652	3188	BH_CREEP	PRMY_LOG	-1.350E+01	BH props for lower part after 1k yrs	Log y-direction permeability	Salt creep portion of BH	Database: CCA view 6
653	3189	BH_CREEP	PRMZ_LOG	-1.350E+01	BH props for lower part after 1k yrs	Log z-direction permeability (BRAGFLO required input)	Salt creep portion of BH	Database: CCA view 6
654	3173	BH_CREEP	RELP_MOD	4.000E+00	BH props for lower part after 1k yrs	Relative permeability model number	Salt creep portion of BH	Database: CCA view 6
655	3176	BH_CREEP	SAT_RBRN	0.000E+00	BH props for lower part after 1k yrs	Residual Brine saturation	Salt creep portion of BH	Database: CCA view 6
656	3177	BH_CREEP	SAT_RGAS	0.000E+00	BH props for lower part after 1k yrs	Residual Gas saturation	Salt creep portion of BH	Database: CCA view 6
657	N/A	BH_CREEP	PERM_X	3.162E-14	BH props for lower part after 1k yrs	X-direction permeability (m^2)	Salt creep portion of BH	Calculated
658	N/A	BH_CREEP	PERM_Y	3.162E-14	BH props for lower part after 1k yrs	Y-direction permeability (m^2)	Salt creep portion of BH	Calculated
659	N/A	BH_CREEP	PERM_Z	3.162E-14	BH props for lower part after 1k yrs	Z-direction permeability (m^2)	Salt creep portion of BH	Calculated
660	N/A	BH_CREEP	SB_MIN	0.000E+00	BH props for lower part after 1k yrs	Minimum saturation (SAT_RBRN * 1.05)	Salt creep portion of BH	Calculated
661	N/A	BH_CREEP	POR_COMP	0.000E+00	BH props for lower part after 1k yrs	Pore compressibility (1/Pa)	Salt creep portion of BH	Calculated
662	N/A	LEAKY_K	CASE_LK	-5.000E+00	Leaky Injector permeabilities	Log(m^2)	Used in CASE_LK material	Analyst: DMStoelzel
663	N/A	LEAKY_K	CMT_LK	-1.365E+01	Leaky Injector permeabilities	Log(m^2)	Used in CMT_LK material	Analyst: DMStoelzel
664	N/A	SCENARIO	SPR_BELL	7.250E-01	Defines Injection Pressures for Cases	U Bell Inj gradient (psi/ft)	South well	Analyst: DMStoelzel
665	N/A	SCENARIO	SPR_CHER	1.000E+00	Defines Injection Pressures for Cases	Cherry C Inj gradient (psi/ft)	South well	Analyst: DMStoelzel
666	N/A	SCENARIO	SPR_BRSH	1.000E+00	Defines Injection Pressures for Cases	Brushy C Inj gradient (psi/ft)	South well	Analyst: DMStoelzel
667	N/A	SCENARIO	SPR_BSPR	1.000E+00	Defines Injection Pressures for Cases	Bonespr Inj gradient (psi/ft)	South well	Analyst: DMStoelzel
668	N/A	SCENARIO	UBELL_FT	4.259E+03	Defines Injection Pressures for Cases	Mid-cell depth fr surface (ft)	To Upper Bell Canyon	From BRAGFLO mesh
669	N/A	SCENARIO	CHERY_FT	6.247E+03	Defines Injection Pressures for Cases	Mid-cell depth fr surface (ft)	To Cherry Canyon	From BRAGFLO mesh
670	N/A	SCENARIO	BRUSH_FT	7.965E+03	Defines Injection Pressures for Cases	Mid-cell depth fr surface (ft)	To Brushy Canyon	From BRAGFLO mesh
671	N/A	SCENARIO	BSPRG_FT	9.708E+03	Defines Injection Pressures for Cases	Mid-cell depth fr surface (ft)	To Bone Spring	From BRAGFLO mesh
672	N/A	SCENARIO	STRWN_FT	1.306E+04	Defines Injection Pressures for Cases	Mid-cell depth fr surface (ft)	To Strawn	From BRAGFLO mesh
673	N/A	SCENARIO	ATOKA_FT	1.371E+04	Defines Injection Pressures for Cases	Mid-cell depth fr surface (ft)	To Atoka	From BRAGFLO mesh
674	N/A	SCENARIO	MORRO_FT	1.441E+04	Defines Injection Pressures for Cases	Mid-cell depth fr surface (ft)	To Morrow	From BRAGFLO mesh
675	N/A	SCENARIO	SPRBELL1	2.129E+07	Defines Injection Pressures for Cases	B.C. pressure to Bell Canyon (Pa)	South: 0 to 50 yrs	Calc fr depth and grad
676	N/A	SCENARIO	SWBELL1	1.000E-10	Defines Injection Pressures for Cases	Well Pl to Bell Canyon (Pa)	South: 0 to 50 yrs	Analyst: DMStoelzel
677	N/A	SCENARIO	SPRBELL2	1.527E+07	Defines Injection Pressures for Cases	B.C. pressure to Bell Canyon (Pa)	South: 100 to 150 yrs	Calc fr depth and grad
678	N/A	SCENARIO	SWBELL2	1.000E-20	Defines Injection Pressures for Cases	Well Pl to Bell Canyon (Pa)	South: 100 to 150 yrs	Analyst: DMStoelzel
679	N/A	SCENARIO	SPRCHER1	4.307E+07	Defines Injection Pressures for Cases	B.C. pressure to Cherry Canyon (Pa)	South: 0 to 50 yrs	Calc fr depth and grad
680	N/A	SCENARIO	SWCHER1	1.000E-10	Defines Injection Pressures for Cases	Well Pl to Cherry Canyon (Pa)	South: 0 to 50 yrs	Analyst: DMStoelzel

				Database Source: F1:[NOBACK2.DMS_WATERFLOOD.EPA_ALGEBRA]ALGEBRA_EPA_WF_RADIAL_R033.CDB;1 (Radial Case R5)				
ID Number	Material	Property	Value	Material Description	Property Value Description	Usage	Source	
681	N/A	SCENARIO	SPRCHER2	2.240E+07	Defines Injection Pressures for Cases	B.C. pressure to Cherry Canyon (Pa)	Not Used	Calc fr depth and grad
682	N/A	SCENARIO	SWICHER2	1.000E-20	Defines Injection Pressures for Cases	Well PI to Cherry Canyon (Pa)	Not Used	Analyst: DMStoelzel
683	N/A	SCENARIO	SPRBRSH1	5.492E+07	Defines Injection Pressures for Cases	B.C. pressure to Brushy Canyon (Pa)	South: 0 to 50 yrs	Calc fr depth and grad
684	N/A	SCENARIO	SWIBRSH1	1.000E-10	Defines Injection Pressures for Cases	Well PI to Brushy Canyon (Pa)	South: 0 to 50 yrs	Analyst: DMStoelzel
685	N/A	SCENARIO	SPRBRSH2	2.856E+07	Defines Injection Pressures for Cases	B.C. pressure to Brushy Canyon (Pa)	Not Used	Calc fr depth and grad
686	N/A	SCENARIO	SWIBRSH2	1.000E-20	Defines Injection Pressures for Cases	Well PI to Brushy Canyon (Pa)	Not Used	Analyst: DMStoelzel
687	N/A	SCENARIO	SPRBSPR1	6.694E+07	Defines Injection Pressures for Cases	B.C. pressure to Bone Spring (Pa)	South: 0 to 50 yrs	Calc fr depth and grad
688	N/A	SCENARIO	SWIBSPR1	1.000E-10	Defines Injection Pressures for Cases	Well PI to Bone Spring (Pa)	South: 0 to 50 yrs	Analyst: DMStoelzel
689	N/A	SCENARIO	SPRBSPR2	3.481E+07	Defines Injection Pressures for Cases	B.C. pressure to Bone Spring (Pa)	Not Used	Calc fr depth and grad
690	N/A	SCENARIO	SWIBSPR2	1.000E-20	Defines Injection Pressures for Cases	Well PI to Bone Spring (Pa)	Not Used	Analyst: DMStoelzel
691	N/A	CASE_LK	CAP_MOD	1.000E+00	BH props for Casing leak	Capillary Pressure Model Number	Assigned to BH sections of leak	Same as BH_OPEN
692	N/A	CASE_LK	PC_MAX	1.000E+08	BH props for Casing leak	Max capillary pressure	Assigned to BH sections of leak	Same as BH_OPEN
693	N/A	CASE_LK	PCT_A	0.000E+00	BH props for Casing leak	Capillary pressure multiplier (placeholder)	Assigned to BH sections of leak	Same as BH_OPEN
694	N/A	CASE_LK	PCT_EXP	0.000E+00	BH props for Casing leak	Capillary pressure exponent (placeholder)	Assigned to BH sections of leak	Same as BH_OPEN
695	N/A	CASE_LK	KPT	0.000E+00	BH props for Casing leak	Not used - placeholder	Assigned to BH sections of leak	Same as BH_OPEN
696	N/A	CASE_LK	PO_MIN	1.013E+05	BH props for Casing leak	Minimum Brine pressure (same for all materials)	Assigned to BH sections of leak	Same as BH_OPEN
697	N/A	CASE_LK	PORE_DIS	7.000E-01	BH props for Casing leak	Pore distribution (fraction)	Assigned to BH sections of leak	Same as BH_OPEN
698	N/A	CASE_LK	POROSITY	3.200E-01	BH props for Casing leak	Porosity (fraction)	Assigned to BH sections of leak	Same as BH_OPEN
699	N/A	CASE_LK	RELP_MOD	5.000E+00	BH props for Casing leak	Relative permeability model number	Assigned to BH sections of leak	Same as BH_OPEN
700	N/A	CASE_LK	SAT_RBRN	0.000E+00	BH props for Casing leak	Residual Brine saturation	Assigned to BH sections of leak	Same as BH_OPEN
701	N/A	CASE_LK	SAT_RGAS	0.000E+00	BH props for Casing leak	Residual Gas saturation	Assigned to BH sections of leak	Same as BH_OPEN
702	N/A	CASE_LK	PERM_X	1.000E-05	BH props for Casing leak	X-direction permeability (m <sup>2</sup> ) from Log value	Assigned to BH sections of leak	10^LEAKY_K:CASE_
703	N/A	CASE_LK	PERM_Y	1.000E-05	BH props for Casing leak	Y-direction permeability (m <sup>2</sup> ) from Log value	Assigned to BH sections of leak	10^LEAKY_K:CASE_
704	N/A	CASE_LK	PERM_Z	1.000E-05	BH props for Casing leak	Z-direction permeability (m <sup>2</sup> ) Not used in 2D	Assigned to BH sections of leak	10^LEAKY_K:CASE_
705	N/A	CASE_LK	SB_MIN	0.000E+00	BH props for Casing leak	Minimum saturation (SAT_RBRN * 1.05)	Assigned to BH sections of leak	Same as BH_OPEN
706	N/A	CASE_LK	POR_COMP	0.000E+00	BH props for Casing leak	Pore compressibility COMP_RCK/POROSITY (1/Pa)	Assigned to BH sections of leak	Same as BH_OPEN
707	N/A	CMT_LK	CAP_MOD	1.000E+00	BH props for Cement leak	Capillary Pressure Model Number	Assigned to BH sections of leak	Same as BH_OPEN
708	N/A	CMT_LK	PC_MAX	1.000E+08	BH props for Cement leak	Max capillary pressure	Assigned to BH sections of leak	Same as BH_OPEN

Information Only

				Database Source: F1:[NOBACK2.DMS_WATERFLOOD.EPA.ALGEBRA]ALGEBRA_EPA_WF_RADIAL_R033.CDB;1 (Radial Case R5)				
ID Number	Material	Property	Value	Material Description	Property Value Description	Usage	Source	
709	N/A	CMT_LK	PCT_A	0.000E+00	BH props for Cement leak	Capillary pressure multiplier (placeholder)	Assigned to BH sections of leak	Same as BH_OPEN
710	N/A	CMT_LK	PCT_EXP	0.000E+00	BH props for Cement leak	Capillary pressure exponent (placeholder)	Assigned to BH sections of leak	Same as BH_OPEN
711	N/A	CMT_LK	KPT	0.000E+00	BH props for Cement leak	Not used - placeholder	Assigned to BH sections of leak	Same as BH_OPEN
712	N/A	CMT_LK	PO_MIN	1.013E+05	BH props for Cement leak	Minimum Brine pressure (same for all materials)	Assigned to BH sections of leak	Same as BH_OPEN
713	N/A	CMT_LK	PORE_DIS	7.000E-01	BH props for Cement leak	Pore distribution (fraction)	Assigned to BH sections of leak	Same as BH_OPEN
714	N/A	CMT_LK	POROSITY	3.200E-01	BH props for Cement leak	Porosity (fraction)	Assigned to BH sections of leak	Same as BH_OPEN
715	N/A	CMT_LK	RELP_MOD	5.000E+00	BH props for Cement leak	Relative permeability model number	Assigned to BH sections of leak	Same as BH_OPEN
716	N/A	CMT_LK	SAT_RBRN	0.000E+00	BH props for Cement leak	Residual Brine saturation	Assigned to BH sections of leak	Same as BH_OPEN
717	N/A	CMT_LK	SAT_RGAS	0.000E+00	BH props for Cement leak	Residual Gas saturation	Assigned to BH sections of leak	Same as BH_OPEN
718	N/A	CMT_LK	PERM_X	2.239E-14	BH props for Cement leak	X-direction permeability (m <sup>2</sup> ) from Log value	Assigned to BH sections of leak	10 <sup>^</sup> LEAKY_K:CMT_L
719	N/A	CMT_LK	PERM_Y	2.239E-14	BH props for Cement leak	Y-direction permeability (m <sup>2</sup> ) from Log value	Assigned to BH sections of leak	10 <sup>^</sup> LEAKY_K:CMT_L
720	N/A	CMT_LK	PERM_Z	2.239E-14	BH props for Cement leak	Z-direction permeability (m <sup>2</sup> ) Not used in 2D	Assigned to BH sections of leak	10 <sup>^</sup> LEAKY_K:CMT_L
721	N/A	CMT_LK	SB_MIN	0.000E+00	BH props for Cement leak	Minimum saturation (SAT_RBRN * 1.05)	Assigned to BH sections of leak	Same as BH_OPEN
722	N/A	CMT_LK	POR_COMP	0.000E+00	BH props for Cement leak	Pore compressibility COMP_RCK/POROSITY (1/Pa)	Assigned to BH sections of leak	Same as BH_OPEN

Information Only



## **Appendix D: Complete Listing of Parameters Used for the Cross-Sectional Model**

The following table lists the parameters used for the cross-sectional model, which are in addition to the those used for the radial models (Appendix C). These additional parameters pertain mainly to the material regions that represent the repository.

Database Source: F1:[NOBACK2.DMS_WATERFLOOD.EPA.ALGEBRA]ALGEBRA_EPA_WF_DUMBELL_R001.CDB;2 (Cross-sectional Model)								
ID Number	Material	Property	Value	Material Description	Property Value Description	Usage	Source	
723	91	CAVITY_2	CAP_MOD	1.000E+00	Becomes Waste area @ time 0	Capillary Pressure Model Number	Required for BRAGFLO	Database: CCA view 6
724	92	CAVITY_2	COMP_RCK	0.000E+00	Becomes Waste area @ time 0	Rock compressibility (1/Pa)	Intermediate value	Database: CCA view 6
725	93	CAVITY_2	PC_MAX	1.000E+08	Becomes Waste area @ time 0	Max capillary pressure	Required for BRAGFLO	Database: CCA view 6
726	2617	CAVITY_2	PCT_A	0.000E+00	Becomes Waste area @ time 0	Capillary pressure multiplier (placeholder)	Not used	Database: CCA view 6
727	2618	CAVITY_2	PCT_EXP	0.000E+00	Becomes Waste area @ time 0	Capillary pressure exponent (placeholder)	Not used	Database: CCA view 6
728	2616	CAVITY_2	KPT	0.000E+00	Becomes Waste area @ time 0	Not used - placeholder	Not used	Database: CCA view 6
729	96	CAVITY_2	PO_MIN	1.013E+05	Becomes Waste area @ time 0	Minimum Brine pressure (same for all materials)	Required for BRAGFLO	Database: CCA view 6
730	94	CAVITY_2	PORE_DIS	7.000E-01	Becomes Waste area @ time 0	Pore distribution (fraction)	Required for BRAGFLO	Database: CCA view 6
731	95	CAVITY_2	POROSITY	1.000E+00	Becomes Waste area @ time 0	Porosity (fraction)	Required for BRAGFLO	Database: CCA view 6
732	97	CAVITY_2	PRESSURE	1.013E+05	Becomes Waste area @ time 0	Initial brine pressure (Pa)	Used in ICSET	Database: CCA view 6
733	98	CAVITY_2	PRMX_LOG	-1.000E+01	Becomes Waste area @ time 0	Log x-direction permeability	Intermediate value	Database: CCA view 6
734	99	CAVITY_2	PRMY_LOG	-1.000E+01	Becomes Waste area @ time 0	Log y-direction permeability	Intermediate value	Database: CCA view 6
735	100	CAVITY_2	PRMZ_LOG	-1.000E+01	Becomes Waste area @ time 0	Log z-direction permeability (BRAGFLO required input)	Not used - 2D model	Database: CCA view 6
736	103	CAVITY_2	REL_P_MOD	4.000E+00	Becomes Waste area @ time 0	Relative permeability model number	Required for BRAGFLO	Database: CCA view 6
737	104	CAVITY_2	SAT_RBRN	0.000E+00	Becomes Waste area @ time 0	Residual Brine saturation	Required for BRAGFLO	Database: CCA view 6
738	105	CAVITY_2	SAT_RGAS	0.000E+00	Becomes Waste area @ time 0	Residual Gas saturation	Required for BRAGFLO	Database: CCA view 6
739	3100	CAVITY_2	SAT_IBRN	0.000E+00	Becomes Waste area @ time 0	Initial brine saturation @ t = -5 years	Used in ICSET	Database: CCA view 6
740	N/A	CAVITY_2	PERM_X	1.000E-10	Becomes Waste area @ time 0	X-direction permeability (m <sup>2</sup> ) from Log value	Required for BRAGFLO	Calculated
741	N/A	CAVITY_2	PERM_Y	1.000E-10	Becomes Waste area @ time 0	Y-direction permeability (m <sup>2</sup> ) from Log value	Required for BRAGFLO	Calculated
742	N/A	CAVITY_2	PERM_Z	1.000E-10	Becomes Waste area @ time 0	Z-direction permeability (m <sup>2</sup> ) Not used in 2D	Required for BRAGFLO	Calculated
743	N/A	CAVITY_2	SB_MIN	0.000E+00	Becomes Waste area @ time 0	Minimum saturation (SAT_RBRN * 1.05)	Required for BRAGFLO	Calculated
744	N/A	CAVITY_2	POR_COMP	0.000E+00	Becomes Waste area @ time 0	Pore compressibility COMP_RCK/POROSITY (1/Pa)	Required for BRAGFLO	Calculated
745	2049	CAVITY_3	CAP_MOD	1.000E+00	Becomes Exp. & Oper. areas t=0	Capillary Pressure Model Number	Required for BRAGFLO	Database: CCA view 6
746	2051	CAVITY_3	COMP_RCK	0.000E+00	Becomes Exp. & Oper. areas t=0	Rock compressibility (1/Pa)	Intermediate value	Database: CCA view 6
747	2234	CAVITY_3	PC_MAX	1.000E+08	Becomes Exp. & Oper. areas t=0	Max capillary pressure	Required for BRAGFLO	Database: CCA view 6
748	2621	CAVITY_3	PCT_A	0.000E+00	Becomes Exp. & Oper. areas t=0	Capillary pressure multiplier (placeholder)	Not used	Database: CCA view 6
749	2622	CAVITY_3	PCT_EXP	0.000E+00	Becomes Exp. & Oper. areas t=0	Capillary pressure exponent (placeholder)	Not used	Database: CCA view 6
750	2620	CAVITY_3	KPT	0.000E+00	Becomes Exp. & Oper. areas t=0	Not used - placeholder	Not used	Database: CCA view 6
751	2623	CAVITY_3	PO_MIN	1.013E+05	Becomes Exp. & Oper. areas t=0	Minimum Brine pressure (same for all materials)	Required for BRAGFLO	Database: CCA view 6
752	2052	CAVITY_3	PORE_DIS	7.000E-01	Becomes Exp. & Oper. areas t=0	Pore distribution (fraction)	Required for BRAGFLO	Database: CCA view 6
753	2053	CAVITY_3	POROSITY	1.000E+00	Becomes Exp. & Oper. areas t=0	Porosity (fraction)	Required for BRAGFLO	Database: CCA view 6
754	3101	CAVITY_3	PRESSURE	1.013E+05	Becomes Exp. & Oper. areas t=0	Initial brine pressure (Pa)	Used in ICSET	Database: CCA view 6
755	2054	CAVITY_3	PRMX_LOG	-1.000E+01	Becomes Exp. & Oper. areas t=0	Log x-direction permeability	Intermediate value	Database: CCA view 6
756	2055	CAVITY_3	PRMY_LOG	-1.000E+01	Becomes Exp. & Oper. areas t=0	Log y-direction permeability	Intermediate value	Database: CCA view 6
757	2056	CAVITY_3	PRMZ_LOG	-1.000E+01	Becomes Exp. & Oper. areas t=0	Log z-direction permeability (BRAGFLO required input)	Not used - 2D model	Database: CCA view 6
758	2058	CAVITY_3	REL_P_MOD	4.000E+00	Becomes Exp. & Oper. areas t=0	Relative permeability model number	Required for BRAGFLO	Database: CCA view 6
759	2235	CAVITY_3	SAT_RBRN	0.000E+00	Becomes Exp. & Oper. areas t=0	Residual Brine saturation	Required for BRAGFLO	Database: CCA view 6
760	2059	CAVITY_3	SAT_RGAS	0.000E+00	Becomes Exp. & Oper. areas t=0	Residual Gas saturation	Required for BRAGFLO	Database: CCA view 6
761	3102	CAVITY_3	SAT_IBRN	0.000E+00	Becomes Exp. & Oper. areas t=0	Initial brine saturation @ t = -5 years	Used in ICSET	Database: CCA view 6
762	N/A	CAVITY_3	PERM_X	1.000E-10	Becomes Exp. & Oper. areas t=0	X-direction permeability (m <sup>2</sup> ) from Log value	Required for BRAGFLO	Calculated
763	N/A	CAVITY_3	PERM_Y	1.000E-10	Becomes Exp. & Oper. areas t=0	Y-direction permeability (m <sup>2</sup> ) from Log value	Required for BRAGFLO	Calculated
764	N/A	CAVITY_3	PERM_Z	1.000E-10	Becomes Exp. & Oper. areas t=0	Z-direction permeability (m <sup>2</sup> ) Not used in 2D	Required for BRAGFLO	Calculated
765	N/A	CAVITY_3	SB_MIN	0.000E+00	Becomes Exp. & Oper. areas t=0	Minimum saturation (SAT_RBRN * 1.05)	Required for BRAGFLO	Calculated
766	N/A	CAVITY_3	POR_COMP	0.000E+00	Becomes Exp. & Oper. areas t=0	Pore compressibility COMP_RCK/POROSITY (1/Pa)	Required for BRAGFLO	Calculated
767	2060	CAVITY_4	CAP_MOD	1.000E+00	Becomes shaft & seals @ t=0	Capillary Pressure Model Number	Required for BRAGFLO	Database: CCA view 6
768	2062	CAVITY_4	COMP_RCK	0.000E+00	Becomes shaft & seals @ t=0	Rock compressibility (1/Pa)	Intermediate value	Database: CCA view 6

Information Only



Database		Database Source: F1:[NOBACK2.DMS_WATERFLOOD.EPA.ALGEBRA]ALGEBRA_EPA_WF_DUMBELL_R001.CDB;2 (Cross-sectional Model)						
ID Number	Material	Property	Value	Material Description	Property Value Description	Usage	Source	
769	2236	CAVITY_4	PC_MAX	1.000E+08	Becomes shaft & seals @ t=0	Max capillary pressure	Required for BRAGFLO	Database: CCA view 6
770	2626	CAVITY_4	PCT_A	0.000E+00	Becomes shaft & seals @ t=0	Capillary pressure multiplier (placeholder)	Not used	Database: CCA view 6
771	2627	CAVITY_4	PCT_EXP	0.000E+00	Becomes shaft & seals @ t=0	Capillary pressure exponent (placeholder)	Not used	Database: CCA view 6
772	2625	CAVITY_4	KPT	0.000E+00	Becomes shaft & seals @ t=0	Not used - placeholder	Not used	Database: CCA view 6
773	2628	CAVITY_4	PO_MIN	1.013E+05	Becomes shaft & seals @ t=0	Minimum Brine pressure (same for all materials)	Required for BRAGFLO	Database: CCA view 6
774	2063	CAVITY_4	PORE_DIS	7.000E-01	Becomes shaft & seals @ t=0	Pore distribution (fraction)	Required for BRAGFLO	Database: CCA view 6
775	2064	CAVITY_4	POROSITY	1.000E+00	Becomes shaft & seals @ t=0	Porosity (fraction)	Required for BRAGFLO	Database: CCA view 6
776	3103	CAVITY_4	PRESSURE	1.013E+05	Becomes shaft & seals @ t=0	Initial brine pressure (Pa)	Used in ICSET	Database: CCA view 6
777	2065	CAVITY_4	PRMX_LOG	-1.000E+01	Becomes shaft & seals @ t=0	Log x-direction permeability	Intermediate value	Database: CCA view 6
778	2066	CAVITY_4	PRMY_LOG	-1.000E+01	Becomes shaft & seals @ t=0	Log y-direction permeability	Intermediate value	Database: CCA view 6
779	2067	CAVITY_4	PRMZ_LOG	-1.000E+01	Becomes shaft & seals @ t=0	Log z-direction permeability (BRAGFLO required input)	Not used - 2D model	Database: CCA view 6
780	2069	CAVITY_4	REL_P_MOD	4.000E+00	Becomes shaft & seals @ t=0	Relative permeability model number	Required for BRAGFLO	Database: CCA view 6
781	2237	CAVITY_4	SAT_RBRN	0.000E+00	Becomes shaft & seals @ t=0	Residual Brine saturation	Required for BRAGFLO	Database: CCA view 6
782	2070	CAVITY_4	SAT_RGAS	0.000E+00	Becomes shaft & seals @ t=0	Residual Gas saturation	Required for BRAGFLO	Database: CCA view 6
783	N/A	CAVITY_4	PERM_X	1.000E-10	Becomes shaft & seals @ t=0	X-direction permeability (m <sup>2</sup> ) from Log value	Required for BRAGFLO	Calculated
784	N/A	CAVITY_4	PERM_Y	1.000E-10	Becomes shaft & seals @ t=0	Y-direction permeability (m <sup>2</sup> ) from Log value	Required for BRAGFLO	Calculated
785	N/A	CAVITY_4	PERM_Z	1.000E-10	Becomes shaft & seals @ t=0	Z-direction permeability (m <sup>2</sup> ) Not used in 2D	Required for BRAGFLO	Calculated
786	N/A	CAVITY_4	SB_MIN	0.000E+00	Becomes shaft & seals @ t=0	Minimum saturation (SAT_RBRN * 1.05)	Required for BRAGFLO	Calculated
787	N/A	CAVITY_4	POR_COMP	0.000E+00	Becomes shaft & seals @ t=0	Pore compressibility COMP_RCK/POROSITY (1/Pa)	Required for BRAGFLO	Calculated
788	174	DRZ_0	CAP_MOD	1.000E+00	DRZ @ -5 to 0 years	Capillary Pressure Model Number	Required for BRAGFLO	Database: CCA view 6
789	175	DRZ_0	COMP_RCK	7.410E-10	DRZ @ -5 to 0 years	Rock compressibility (1/Pa)	Intermediate value	Database: CCA view 6
790	176	DRZ_0	PC_MAX	1.000E+08	DRZ @ -5 to 0 years	Max capillary pressure	Required for BRAGFLO	Database: CCA view 6
791	2702	DRZ_0	PCT_A	0.000E+00	DRZ @ -5 to 0 years	Capillary pressure multiplier (placeholder)	Not used	Database: CCA view 6
792	2703	DRZ_0	PCT_EXP	0.000E+00	DRZ @ -5 to 0 years	Capillary pressure exponent (placeholder)	Not used	Database: CCA view 6
793	2701	DRZ_0	KPT	0.000E+00	DRZ @ -5 to 0 years	Not used - placeholder	Not used	Database: CCA view 6
794	179	DRZ_0	PO_MIN	1.013E+05	DRZ @ -5 to 0 years	Minimum Brine pressure (same for all materials)	Required for BRAGFLO	Database: CCA view 6
795	177	DRZ_0	PORE_DIS	7.000E-01	DRZ @ -5 to 0 years	Pore distribution (fraction)	Required for BRAGFLO	Database: CCA view 6
796	N/A	DRZ_0	POROSITY	1.290E-02	DRZ @ -5 to 0 years	Porosity (Fraction) (Halite porosity plus 0.0029)	Required for BRAGFLO	Calculated
797	181	DRZ_0	PRMX_LOG	-1.700E+01	DRZ @ -5 to 0 years	Log x-direction permeability	Intermediate value	Database: CCA view 6
798	182	DRZ_0	PRMY_LOG	-1.700E+01	DRZ @ -5 to 0 years	Log y-direction permeability	Intermediate value	Database: CCA view 6
799	183	DRZ_0	PRMZ_LOG	-1.700E+01	DRZ @ -5 to 0 years	Log z-direction permeability (BRAGFLO required input)	Not used - 2D model	Database: CCA view 6
800	186	DRZ_0	REL_P_MOD	4.000E+00	DRZ @ -5 to 0 years	Relative permeability model number	Required for BRAGFLO	Database: CCA view 6
801	188	DRZ_0	SAT_RBRN	0.000E+00	DRZ @ -5 to 0 years	Residual Brine saturation	Required for BRAGFLO	Database: CCA view 6
802	189	DRZ_0	SAT_RGAS	0.000E+00	DRZ @ -5 to 0 years	Residual Gas saturation	Required for BRAGFLO	Database: CCA view 6
803	N/A	DRZ_0	PERM_X	1.000E-17	DRZ @ -5 to 0 years	X-direction permeability (m <sup>2</sup> ) from Log value	Required for BRAGFLO	Calculated
804	N/A	DRZ_0	PERM_Y	1.000E-17	DRZ @ -5 to 0 years	Y-direction permeability (m <sup>2</sup> ) from Log value	Required for BRAGFLO	Calculated
805	N/A	DRZ_0	PERM_Z	1.000E-17	DRZ @ -5 to 0 years	Z-direction permeability (m <sup>2</sup> ) Not used in 2D	Required for BRAGFLO	Calculated
806	N/A	DRZ_0	SB_MIN	0.000E+00	DRZ @ -5 to 0 years	Minimum saturation (SAT_RBRN * 1.05)	Required for BRAGFLO	Calculated
807	N/A	DRZ_0	POR_COMP	5.744E-08	DRZ @ -5 to 0 years	Pore compressibility COMP_RCK/POROSITY (1/Pa)	Required for BRAGFLO	Calculated
808	190	DRZ_1	CAP_MOD	1.000E+00	DRZ @ time = 0	Capillary Pressure Model Number	Required for BRAGFLO	Database: CCA view 6
809	191	DRZ_1	COMP_RCK	7.410E-10	DRZ @ time = 0	Rock compressibility (1/Pa)	Intermediate value	Database: CCA view 6
810	193	DRZ_1	PC_MAX	1.000E+08	DRZ @ time = 0	Max capillary pressure	Required for BRAGFLO	Database: CCA view 6
811	3128	DRZ_1	PCT_A	0.000E+00	DRZ @ time = 0	Capillary pressure multiplier (placeholder)	Not used	Database: CCA view 6
812	3129	DRZ_1	PCT_EXP	0.000E+00	DRZ @ time = 0	Capillary pressure exponent (placeholder)	Not used	Database: CCA view 6
813	3116	DRZ_1	KPT	0.000E+00	DRZ @ time = 0	Not used - placeholder	Not used	Database: CCA view 6
814	196	DRZ_1	PO_MIN	1.013E+05	DRZ @ time = 0	Minimum Brine pressure (same for all materials)	Required for BRAGFLO	Database: CCA view 6

Information Only

Database		Database Source: F1:[NOBACK2.DMS_WATERFLOOD.EPA_ALGEBRA]ALGEBRA_EPA_WF_DUMBELL_R001.CDB;2 (Cross-sectional Model)						
ID Number	Material	Property	Value	Material Description	Property Value Description	Usage	Source	
815	194	DRZ_1	PORE_DIS	7.000E-01	DRZ @ time = 0	Pore distribution (fraction)	Required for BRAGFLO	Database: CCA view 6
816	N/A	DRZ_1	POROSITY	1.290E-02	DRZ @ time = 0	Porosity (Fraction) (Halite porosity plus 0.0029)	Required for BRAGFLO	Calculated
817	198	DRZ_1	PRMX_LOG	-1.500E+01	DRZ @ time = 0	Log x-direction permeability	Intermediate value	Database: CCA view 6
818	199	DRZ_1	PRMY_LOG	-1.500E+01	DRZ @ time = 0	Log y-direction permeability	Intermediate value	Database: CCA view 6
819	200	DRZ_1	PRMZ_LOG	-1.500E+01	DRZ @ time = 0	Log z-direction permeability (BRAGFLO required input)	Not used - 2D model	Database: CCA view 6
820	203	DRZ_1	RELP_MOD	4.000E+00	DRZ @ time = 0	Relative permeability model number	Required for BRAGFLO	Database: CCA view 6
821	205	DRZ_1	SAT_RBRN	0.000E+00	DRZ @ time = 0	Residual Brine saturation	Required for BRAGFLO	Database: CCA view 6
822	206	DRZ_1	SAT_RGAS	0.000E+00	DRZ @ time = 0	Residual Gas saturation	Required for BRAGFLO	Database: CCA view 6
823	N/A	DRZ_1	PERM_X	1.000E-15	DRZ @ time = 0	X-direction permeability (m <sup>2</sup> ) from Log value	Required for BRAGFLO	Calculated
824	N/A	DRZ_1	PERM_Y	1.000E-15	DRZ @ time = 0	Y-direction permeability (m <sup>2</sup> ) from Log value	Required for BRAGFLO	Calculated
825	N/A	DRZ_1	PERM_Z	1.000E-15	DRZ @ time = 0	Z-direction permeability (m <sup>2</sup> ) Not used in 2D	Required for BRAGFLO	Calculated
826	N/A	DRZ_1	SB_MIN	0.000E+00	DRZ @ time = 0	Minimum saturation (SAT_RBRN * 1.05)	Required for BRAGFLO	Calculated
827	N/A	DRZ_1	POR_COMP	5.744E-08	DRZ @ time = 0	Pore compressibility COMP_RCK/POROSITY (1/Pa)	Required for BRAGFLO	Calculated
828	652	WAS_AREA	CAP_MOD	1.000E+00	Replaces CAVITY_2 @ t=0	Capillary Pressure Model Number	Required for BRAGFLO	Database: CCA view 6
829	653	WAS_AREA	COMP_RCK	0.000E+00	Replaces CAVITY_2 @ t=0	Rock compressibility (1/Pa)	Intermediate value	Database: CCA view 6
830	658	WAS_AREA	PC_MAX	1.000E+08	Replaces CAVITY_2 @ t=0	Max capillary pressure	Required for BRAGFLO	Database: CCA view 6
831	2805	WAS_AREA	PCT_A	0.000E+00	Replaces CAVITY_2 @ t=0	Capillary pressure multiplier (placeholder)	Not used	Database: CCA view 6
832	2806	WAS_AREA	PCT_EXP	0.000E+00	Replaces CAVITY_2 @ t=0	Capillary pressure exponent (placeholder)	Not used	Database: CCA view 6
833	2804	WAS_AREA	KPT	0.000E+00	Replaces CAVITY_2 @ t=0	Not used - placeholder	Not used	Database: CCA view 6
834	661	WAS_AREA	PO_MIN	1.013E+05	Replaces CAVITY_2 @ t=0	Minimum Brine pressure (same for all materials)	Required for BRAGFLO	Database: CCA view 6
835	659	WAS_AREA	PORE_DIS	2.890E+00	Replaces CAVITY_2 @ t=0	Pore distribution (fraction)	Required for BRAGFLO	Database: CCA view 6
836	660	WAS_AREA	POROSITY	8.480E-01	Replaces CAVITY_2 @ t=0	Porosity (fraction)	Required for BRAGFLO	Database: CCA view 6
837	663	WAS_AREA	PRMX_LOG	-1.277E+01	Replaces CAVITY_2 @ t=0	Log x-direction permeability	Intermediate value	Database: CCA view 6
838	664	WAS_AREA	PRMY_LOG	-1.277E+01	Replaces CAVITY_2 @ t=0	Log y-direction permeability	Intermediate value	Database: CCA view 6
839	665	WAS_AREA	PRMZ_LOG	-1.277E+01	Replaces CAVITY_2 @ t=0	Log z-direction permeability (BRAGFLO required input)	Not used - 2D model	Database: CCA view 6
840	668	WAS_AREA	RELP_MOD	4.000E+00	Replaces CAVITY_2 @ t=0	Relative permeability model number	Required for BRAGFLO	Database: CCA view 6
841	670	WAS_AREA	SAT_RBRN	2.760E-01	Replaces CAVITY_2 @ t=0	Residual Brine saturation	Required for BRAGFLO	Database: CCA view 6
842	671	WAS_AREA	SAT_RGAS	7.500E-02	Replaces CAVITY_2 @ t=0	Residual Gas saturation	Required for BRAGFLO	Database: CCA view 6
843	669	WAS_AREA	SAT_IBRN	1.500E-02	Replaces CAVITY_2 @ t=0	Initial brine saturation @ t = -5 years	Used in ICSET	Database: CCA view 6
844	657	WAS_AREA	GRATMICI	3.709E-09	Replaces CAVITY_2 @ t=0	Variable for gas generation stoichiometry (see Task 1, WPO# 40514)	Gas generation sub-mod	Database: CCA view 6
845	656	WAS_AREA	GRATMICH	1.290E-01	Replaces CAVITY_2 @ t=0	Variable for gas generation stoichiometry (see Task 1, WPO# 40514)	Gas generation sub-mod	Database: CCA view 6
846	2401	WAS_AREA	DCELLCHW	5.400E+01	Replaces CAVITY_2 @ t=0	Variable for gas generation stoichiometry (see Task 1, WPO# 40514)	Gas generation sub-mod	Database: CCA view 6
847	2274	WAS_AREA	DCELLRHW	1.700E+01	Replaces CAVITY_2 @ t=0	Variable for gas generation stoichiometry (see Task 1, WPO# 40514)	Gas generation sub-mod	Database: CCA view 6
848	2040	WAS_AREA	DIRONCHW	1.700E+02	Replaces CAVITY_2 @ t=0	Variable for gas generation stoichiometry (see Task 1, WPO# 40514)	Gas generation sub-mod	Database: CCA view 6
849	2044	WAS_AREA	DIRONRHW	1.000E+02	Replaces CAVITY_2 @ t=0	Variable for gas generation stoichiometry (see Task 1, WPO# 40514)	Gas generation sub-mod	Database: CCA view 6
850	2043	WAS_AREA	DPLASCHW	3.400E+01	Replaces CAVITY_2 @ t=0	Variable for gas generation stoichiometry (see Task 1, WPO# 40514)	Gas generation sub-mod	Database: CCA view 6
851	2275	WAS_AREA	DPLASRHW	1.500E+01	Replaces CAVITY_2 @ t=0	Variable for gas generation stoichiometry (see Task 1, WPO# 40514)	Gas generation sub-mod	Database: CCA view 6
852	2042	WAS_AREA	DRUBBCHW	1.000E+01	Replaces CAVITY_2 @ t=0	Variable for gas generation stoichiometry (see Task 1, WPO# 40514)	Gas generation sub-mod	Database: CCA view 6
853	2046	WAS_AREA	DRUBBRHW	3.300E+00	Replaces CAVITY_2 @ t=0	Variable for gas generation stoichiometry (see Task 1, WPO# 40514)	Gas generation sub-mod	Database: CCA view 6
854	1992	WAS_AREA	DIRNCCHW	1.390E+03	Replaces CAVITY_2 @ t=0	Variable for gas generation stoichiometry (see Task 1, WPO# 40514)	Gas generation sub-mod	Database: CCA view 6
855	1993	WAS_AREA	DIRNCRHW	2.591E+03	Replaces CAVITY_2 @ t=0	Variable for gas generation stoichiometry (see Task 1, WPO# 40514)	Gas generation sub-mod	Database: CCA view 6
856	1995	WAS_AREA	DPLSCCHW	2.600E+01	Replaces CAVITY_2 @ t=0	Variable for gas generation stoichiometry (see Task 1, WPO# 40514)	Gas generation sub-mod	Database: CCA view 6
857	2228	WAS_AREA	DPLSCRHW	3.100E+00	Replaces CAVITY_2 @ t=0	Variable for gas generation stoichiometry (see Task 1, WPO# 40514)	Gas generation sub-mod	Database: CCA view 6
858	2232	WAS_AREA	VOLCHW	1.690E+05	Replaces CAVITY_2 @ t=0	Variable for gas generation stoichiometry (see Task 1, WPO# 40514)	Gas generation sub-mod	Database: CCA view 6
859	2233	WAS_AREA	VOLRHW	7.080E+03	Replaces CAVITY_2 @ t=0	Variable for gas generation stoichiometry (see Task 1, WPO# 40514)	Gas generation sub-mod	Database: CCA view 6
860	2231	WAS_AREA	SAT_WICK	5.000E-01	Replaces CAVITY_2 @ t=0	Variable for gas generation stoichiometry (see Task 1, WPO# 40514)	Gas generation sub-mod	Database: CCA view 6

Information Only

Database Source: F1:[NOBACK2.DMS_WATERFLOOD.EPA.ALGEBRA]ALGEBRA_EPA_WF_DUMBELL_R001.CDB;2 (Cross-sectional Model)								
ID Number	Material	Property	Value	Material Description	Property Value Description	Usage	Source	
861	2823	WAS_AREA	PROBDEG	2.000E+00	Replaces CAVITY_2 @ t=0	Variable for gas generation stoichiometry (see Task 1, WPO# 40514)	Gas generation sub-mod	Database: CCA view 6
862	N/A	WAS_AREA	PERM_X	1.702E-13	Replaces CAVITY_2 @ t=0	X-direction permeability (m <sup>2</sup> ) from Log value	Required for BRAGFLO	Calculated
863	N/A	WAS_AREA	PERM_Y	1.702E-13	Replaces CAVITY_2 @ t=0	Y-direction permeability (m <sup>2</sup> ) from Log value	Required for BRAGFLO	Calculated
864	N/A	WAS_AREA	PERM_Z	1.702E-13	Replaces CAVITY_2 @ t=0	Z-direction permeability (m <sup>2</sup> ) Not used in 2D	Required for BRAGFLO	Calculated
865	N/A	WAS_AREA	SB_MIN	2.898E-01	Replaces CAVITY_2 @ t=0	Minimum saturation (SAT_RBRN * 1.05)	Required for BRAGFLO	Calculated
866	N/A	WAS_AREA	POR_COMP	0.000E+00	Replaces CAVITY_2 @ t=0	Pore compressibility COMP_RCK/POROSITY (1/Pa)	Required for BRAGFLO	Calculated
867	N/A	WAS_AREA	STOICOR	1.000E+00	Replaces CAVITY_2 @ t=0	Variable for gas generation stoichiometry (see Task 1, WPO# 40514)	Reaction chemistry mod	Calculated in ALGEBRA
868	N/A	WAS_AREA	SCOR_H2	1.000E+00	Replaces CAVITY_2 @ t=0	Variable for gas generation stoichiometry (see Task 1, WPO# 40514)	Reaction chemistry mod	Calculated in ALGEBRA
869	N/A	WAS_AREA	SCOR_H2O	2.000E+00	Replaces CAVITY_2 @ t=0	Variable for gas generation stoichiometry (see Task 1, WPO# 40514)	Reaction chemistry mod	Calculated in ALGEBRA
870	N/A	WAS_AREA	SCOR_FE	1.000E+00	Replaces CAVITY_2 @ t=0	Variable for gas generation stoichiometry (see Task 1, WPO# 40514)	Reaction chemistry mod	Calculated in ALGEBRA
871	N/A	WAS_AREA	DRH_METL	2.691E+03	Replaces CAVITY_2 @ t=0	Variable for gas generation stoichiometry (see Task 1, WPO# 40514)	Reaction chemistry mod	Calculated in ALGEBRA
872	N/A	WAS_AREA	DRH_RUPL	3.407E+01	Replaces CAVITY_2 @ t=0	Variable for gas generation stoichiometry (see Task 1, WPO# 40514)	Reaction chemistry mod	Calculated in ALGEBRA
873	N/A	WAS_AREA	DRH_BIO	5.107E+01	Replaces CAVITY_2 @ t=0	Variable for gas generation stoichiometry (see Task 1, WPO# 40514)	Reaction chemistry mod	Calculated in ALGEBRA
874	N/A	WAS_AREA	DCH_METL	3.090E+02	Replaces CAVITY_2 @ t=0	Variable for gas generation stoichiometry (see Task 1, WPO# 40514)	Reaction chemistry mod	Calculated in ALGEBRA
875	N/A	WAS_AREA	DCH_RUPL	1.120E+02	Replaces CAVITY_2 @ t=0	Variable for gas generation stoichiometry (see Task 1, WPO# 40514)	Reaction chemistry mod	Calculated in ALGEBRA
876	N/A	WAS_AREA	DCH_BIO	1.660E+02	Replaces CAVITY_2 @ t=0	Variable for gas generation stoichiometry (see Task 1, WPO# 40514)	Reaction chemistry mod	Calculated in ALGEBRA
877	N/A	WAS_AREA	WTFETOT	7.127E+07	Replaces CAVITY_2 @ t=0	Variable for gas generation stoichiometry (see Task 1, WPO# 40514)	Reaction chemistry mod	Calculated in ALGEBRA
878	N/A	WAS_AREA	WTCELTOT	9.246E+06	Replaces CAVITY_2 @ t=0	Variable for gas generation stoichiometry (see Task 1, WPO# 40514)	Reaction chemistry mod	Calculated in ALGEBRA
879	N/A	WAS_AREA	WTRPLTOT	1.917E+07	Replaces CAVITY_2 @ t=0	Variable for gas generation stoichiometry (see Task 1, WPO# 40514)	Reaction chemistry mod	Calculated in ALGEBRA
880	N/A	WAS_AREA	PLASIDX	1.000E+00	Replaces CAVITY_2 @ t=0	Variable for gas generation stoichiometry (see Task 1, WPO# 40514)	Reaction chemistry mod	Calculated in ALGEBRA
881	N/A	WAS_AREA	BIOIDX	1.000E+00	Replaces CAVITY_2 @ t=0	Variable for gas generation stoichiometry (see Task 1, WPO# 40514)	Reaction chemistry mod	Calculated in ALGEBRA
882	N/A	WAS_AREA	WTBIOTOT	2.842E+07	Replaces CAVITY_2 @ t=0	Variable for gas generation stoichiometry (see Task 1, WPO# 40514)	Reaction chemistry mod	Calculated in ALGEBRA
883	N/A	WAS_AREA	CONCFE	1.635E+02	Replaces CAVITY_2 @ t=0	Variable for gas generation stoichiometry (see Task 1, WPO# 40514)	Reaction chemistry mod	Calculated in ALGEBRA
884	N/A	WAS_AREA	CONCBIO	6.517E+01	Replaces CAVITY_2 @ t=0	Variable for gas generation stoichiometry (see Task 1, WPO# 40514)	Reaction chemistry mod	Calculated in ALGEBRA
885	N/A	WAS_AREA	CH20CONC	2.121E+01	Replaces CAVITY_2 @ t=0	Variable for gas generation stoichiometry (see Task 1, WPO# 40514)	Reaction chemistry mod	Calculated in ALGEBRA
886	N/A	WAS_AREA	DRUMVOL	1.867E+00	Replaces CAVITY_2 @ t=0	Variable for gas generation stoichiometry (see Task 1, WPO# 40514)	Reaction chemistry mod	Calculated in ALGEBRA
887	N/A	WAS_AREA	DRUMTOT	8.140E+05	Replaces CAVITY_2 @ t=0	Variable for gas generation stoichiometry (see Task 1, WPO# 40514)	Reaction chemistry mod	Calculated in ALGEBRA
888	N/A	WAS_AREA	DRPANEL	8.606E+04	Replaces CAVITY_2 @ t=0	Variable for gas generation stoichiometry (see Task 1, WPO# 40514)	Reaction chemistry mod	Calculated in ALGEBRA
889	N/A	WAS_AREA	A1	1.052E+09	Replaces CAVITY_2 @ t=0	Variable for gas generation stoichiometry (see Task 1, WPO# 40514)	Reaction chemistry mod	Calculated in ALGEBRA
890	N/A	WAS_AREA	A2	4.407E+10	Replaces CAVITY_2 @ t=0	Variable for gas generation stoichiometry (see Task 1, WPO# 40514)	Reaction chemistry mod	Calculated in ALGEBRA
891	N/A	WAS_AREA	MAX_CELL	1.052E+09	Replaces CAVITY_2 @ t=0	Variable for gas generation stoichiometry (see Task 1, WPO# 40514)	Reaction chemistry mod	Calculated in ALGEBRA
892	N/A	WAS_AREA	B1	1.273E+09	Replaces CAVITY_2 @ t=0	Variable for gas generation stoichiometry (see Task 1, WPO# 40514)	Reaction chemistry mod	Calculated in ALGEBRA
893	N/A	WAS_AREA	B2	2.242E+10	Replaces CAVITY_2 @ t=0	Variable for gas generation stoichiometry (see Task 1, WPO# 40514)	Reaction chemistry mod	Calculated in ALGEBRA
894	N/A	WAS_AREA	MAX_FE	1.273E+09	Replaces CAVITY_2 @ t=0	Variable for gas generation stoichiometry (see Task 1, WPO# 40514)	Reaction chemistry mod	Calculated in ALGEBRA
895	N/A	WAS_AREA	NUM1	4.568E+07	Replaces CAVITY_2 @ t=0	Variable for gas generation stoichiometry (see Task 1, WPO# 40514)	Reaction chemistry mod	Calculated in ALGEBRA
896	N/A	WAS_AREA	NUM2	1.977E+07	Replaces CAVITY_2 @ t=0	Variable for gas generation stoichiometry (see Task 1, WPO# 40514)	Reaction chemistry mod	Calculated in ALGEBRA
897	N/A	WAS_AREA	NUM3	1.007E+09	Replaces CAVITY_2 @ t=0	Variable for gas generation stoichiometry (see Task 1, WPO# 40514)	Reaction chemistry mod	Calculated in ALGEBRA
898	N/A	WAS_AREA	YMAX	1.019E+00	Replaces CAVITY_2 @ t=0	Variable for gas generation stoichiometry (see Task 1, WPO# 40514)	Reaction chemistry mod	Calculated in ALGEBRA
899	N/A	WAS_AREA	C1	5.557E+08	Replaces CAVITY_2 @ t=0	Variable for gas generation stoichiometry (see Task 1, WPO# 40514)	Reaction chemistry mod	Calculated in ALGEBRA
900	N/A	WAS_AREA	C2	1.273E+09	Replaces CAVITY_2 @ t=0	Variable for gas generation stoichiometry (see Task 1, WPO# 40514)	Reaction chemistry mod	Calculated in ALGEBRA
901	N/A	WAS_AREA	G	5.557E+08	Replaces CAVITY_2 @ t=0	Variable for gas generation stoichiometry (see Task 1, WPO# 40514)	Reaction chemistry mod	Calculated in ALGEBRA
902	N/A	WAS_AREA	YMIN	4.906E-01	Replaces CAVITY_2 @ t=0	Variable for gas generation stoichiometry (see Task 1, WPO# 40514)	Reaction chemistry mod	Calculated in ALGEBRA
903	N/A	WAS_AREA	STOIMIC	7.547E-01	Replaces CAVITY_2 @ t=0	Variable for gas generation stoichiometry (see Task 1, WPO# 40514)	Reaction chemistry mod	Calculated in ALGEBRA
904	N/A	WAS_AREA	KCGSI	1.630E-07	Replaces CAVITY_2 @ t=0	Variable for gas generation stoichiometry (see Task 1, WPO# 40514)	Reaction chemistry mod	Calculated in ALGEBRA
905	N/A	WAS_AREA	KCGSH	0.000E+00	Replaces CAVITY_2 @ t=0	Variable for gas generation stoichiometry (see Task 1, WPO# 40514)	Reaction chemistry mod	Calculated in ALGEBRA
906	N/A	WAS_AREA	GRATCORI	1.455E-08	Replaces CAVITY_2 @ t=0	Variable for gas generation stoichiometry (see Task 1, WPO# 40514)	Reaction chemistry mod	Calculated in ALGEBRA

Information Only



Database Source: F1:[NOBACK2.DMS_WATERFLOOD.EPA.ALGEBRA]ALGEBRA_EPA_WF_DUMBELL_R001.CDB;2 (Cross-sectional Model)								
ID Number	Material	Property	Value	Material Description	Property Value Description	Usage	Source	
907	N/A	WAS_AREA	GRATCORH	0.000E+00	Replaces CAVITY_2 @ t=0	Variable for gas generation stoichiometry (see Task 1, WPO# 40514)	Reaction chemistry mod	Calculated in ALGEBRA
908	N/A	WAS_AREA	KBGSI	3.203E-07	Replaces CAVITY_2 @ t=0	Variable for gas generation stoichiometry (see Task 1, WPO# 40514)	Reaction chemistry mod	Calculated in ALGEBRA
909	N/A	WAS_AREA	KBGSH	4.133E-08	Replaces CAVITY_2 @ t=0	Variable for gas generation stoichiometry (see Task 1, WPO# 40514)	Reaction chemistry mod	Calculated in ALGEBRA
910	7	OPS_AREA	CAP_MOD	1.000E+00	Resets Oper area of CAVITY_3	Capillary Pressure Model Number	Required for BRAGFLO	Database: CCA view 6
911	8	OPS_AREA	COMP_RCK	0.000E+00	Resets Oper area of CAVITY_3	Rock compressibility (1/Pa)	Intermediate value	Database: CCA view 6
912	9	OPS_AREA	PC_MAX	1.000E+08	Resets Oper area of CAVITY_3	Max capillary pressure	Required for BRAGFLO	Database: CCA view 6
913	2605	OPS_AREA	PCT_A	0.000E+00	Resets Oper area of CAVITY_3	Capillary pressure multiplier (placeholder)	Not used	Database: CCA view 6
914	2606	OPS_AREA	PCT_EXP	0.000E+00	Resets Oper area of CAVITY_3	Capillary pressure exponent (placeholder)	Not used	Database: CCA view 6
915	2604	OPS_AREA	KPT	0.000E+00	Resets Oper area of CAVITY_3	Not used - placeholder	Not used	Database: CCA view 6
916	12	OPS_AREA	PO_MIN	1.013E+05	Resets Oper area of CAVITY_3	Minimum Brine pressure (same for all materials)	Required for BRAGFLO	Database: CCA view 6
917	10	OPS_AREA	PORE_DIS	7.000E-01	Resets Oper area of CAVITY_3	Pore distribution (fraction)	Required for BRAGFLO	Database: CCA view 6
918	11	OPS_AREA	POROSITY	1.800E-01	Resets Oper area of CAVITY_3	Porosity (fraction)	Required for BRAGFLO	Database: CCA view 6
919	14	OPS_AREA	PRMX_LOG	-1.100E+01	Resets Oper area of CAVITY_3	Log x-direction permeability	Intermediate value	Database: CCA view 6
920	15	OPS_AREA	PRMY_LOG	-1.100E+01	Resets Oper area of CAVITY_3	Log y-direction permeability	Intermediate value	Database: CCA view 6
921	16	OPS_AREA	PRMZ_LOG	-1.100E+01	Resets Oper area of CAVITY_3	Log z-direction permeability (BRAGFLO required input)	Not used - 2D model	Database: CCA view 6
922	19	OPS_AREA	REL_P_MOD	4.000E+00	Resets Oper area of CAVITY_3	Relative permeability model number	Required for BRAGFLO	Database: CCA view 6
923	21	OPS_AREA	SAT_RBRN	0.000E+00	Resets Oper area of CAVITY_3	Residual Brine saturation	Required for BRAGFLO	Database: CCA view 6
924	22	OPS_AREA	SAT_RGAS	0.000E+00	Resets Oper area of CAVITY_3	Residual Gas saturation	Required for BRAGFLO	Database: CCA view 6
925	N/A	OPS_AREA	PERM_X	1.000E-11	Resets Oper area of CAVITY_3	X-direction permeability (m <sup>2</sup> ) from Log value	Required for BRAGFLO	Calculated
926	N/A	OPS_AREA	PERM_Y	1.000E-11	Resets Oper area of CAVITY_3	Y-direction permeability (m <sup>2</sup> ) from Log value	Required for BRAGFLO	Calculated
927	N/A	OPS_AREA	PERM_Z	1.000E-11	Resets Oper area of CAVITY_3	Z-direction permeability (m <sup>2</sup> ) Not used in 2D	Required for BRAGFLO	Calculated
928	N/A	OPS_AREA	SB_MIN	0.000E+00	Resets Oper area of CAVITY_3	Minimum saturation (SAT_RBRN * 1.05)	Required for BRAGFLO	Calculated
929	N/A	OPS_AREA	POR_COMP	0.000E+00	Resets Oper area of CAVITY_3	Pore compressibility COMP_RCK/POROSITY (1/Pa)	Required for BRAGFLO	Calculated
930	207	EXP_AREA	CAP_MOD	1.000E+00	Resets Exp area of CAVITY_3	Capillary Pressure Model Number	Required for BRAGFLO	Database: CCA view 6
931	208	EXP_AREA	COMP_RCK	0.000E+00	Resets Exp area of CAVITY_3	Rock compressibility (1/Pa)	Intermediate value	Database: CCA view 6
932	209	EXP_AREA	PC_MAX	1.000E+08	Resets Exp area of CAVITY_3	Max capillary pressure	Required for BRAGFLO	Database: CCA view 6
933	2712	EXP_AREA	PCT_A	0.000E+00	Resets Exp area of CAVITY_3	Capillary pressure multiplier (placeholder)	Not used	Database: CCA view 6
934	2713	EXP_AREA	PCT_EXP	0.000E+00	Resets Exp area of CAVITY_3	Capillary pressure exponent (placeholder)	Not used	Database: CCA view 6
935	2711	EXP_AREA	KPT	0.000E+00	Resets Exp area of CAVITY_3	Not used - placeholder	Not used	Database: CCA view 6
936	212	EXP_AREA	PO_MIN	1.013E+05	Resets Exp area of CAVITY_3	Minimum Brine pressure (same for all materials)	Required for BRAGFLO	Database: CCA view 6
937	210	EXP_AREA	PORE_DIS	7.000E-01	Resets Exp area of CAVITY_3	Pore distribution (fraction)	Required for BRAGFLO	Database: CCA view 6
938	211	EXP_AREA	POROSITY	1.800E-01	Resets Exp area of CAVITY_3	Porosity (fraction)	Required for BRAGFLO	Database: CCA view 6
939	214	EXP_AREA	PRMX_LOG	-1.100E+01	Resets Exp area of CAVITY_3	Log x-direction permeability	Intermediate value	Database: CCA view 6
940	215	EXP_AREA	PRMY_LOG	-1.100E+01	Resets Exp area of CAVITY_3	Log y-direction permeability	Intermediate value	Database: CCA view 6
941	216	EXP_AREA	PRMZ_LOG	-1.100E+01	Resets Exp area of CAVITY_3	Log z-direction permeability (BRAGFLO required input)	Not used - 2D model	Database: CCA view 6
942	219	EXP_AREA	REL_P_MOD	4.000E+00	Resets Exp area of CAVITY_3	Relative permeability model number	Required for BRAGFLO	Database: CCA view 6
943	221	EXP_AREA	SAT_RBRN	0.000E+00	Resets Exp area of CAVITY_3	Residual Brine saturation	Required for BRAGFLO	Database: CCA view 6
944	222	EXP_AREA	SAT_RGAS	0.000E+00	Resets Exp area of CAVITY_3	Residual Gas saturation	Required for BRAGFLO	Database: CCA view 6
945	N/A	EXP_AREA	PERM_X	1.000E-11	Resets Exp area of CAVITY_3	X-direction permeability (m <sup>2</sup> ) from Log value	Required for BRAGFLO	Calculated
946	N/A	EXP_AREA	PERM_Y	1.000E-11	Resets Exp area of CAVITY_3	Y-direction permeability (m <sup>2</sup> ) from Log value	Required for BRAGFLO	Calculated
947	N/A	EXP_AREA	PERM_Z	1.000E-11	Resets Exp area of CAVITY_3	Z-direction permeability (m <sup>2</sup> ) Not used in 2D	Required for BRAGFLO	Calculated
948	N/A	EXP_AREA	SB_MIN	0.000E+00	Resets Exp area of CAVITY_3	Minimum saturation (SAT_RBRN * 1.05)	Required for BRAGFLO	Calculated
949	N/A	EXP_AREA	POR_COMP	0.000E+00	Resets Exp area of CAVITY_3	Pore compressibility COMP_RCK/POROSITY (1/Pa)	Required for BRAGFLO	Calculated
950	252	PAN_SEAL	CAP_MOD	2.000E+00	Resets Panel seals @ t=0	Capillary Pressure Model Number	Required for BRAGFLO	Database: CCA view 6
951	253	PAN_SEAL	COMP_RCK	2.640E-09	Resets Panel seals @ t=0	Rock compressibility (1/Pa)	Intermediate value	Database: CCA view 6
952	254	PAN_SEAL	PC_MAX	1.000E+08	Resets Panel seals @ t=0	Max capillary pressure	Required for BRAGFLO	Database: CCA view 6

Information Only

Database Source: F1:[NOBACK2.DMS_WATERFLOOD.EPA.ALGEBRA]ALGEBRA_EPA_WF_DUMBELL_R001.CDB;2 (Cross-sectional Model)								
ID Number	Material	Property	Value	Material Description	Property Value Description	Usage	Source	
953	2732	PAN_SEAL	PCT_A	5.600E-01	Resets Panel seals @ t=0	Capillary pressure multiplier (placeholder)	Not used	Database: CCA view 6
954	2733	PAN_SEAL	PCT_EXP	-3.460E-01	Resets Panel seals @ t=0	Capillary pressure exponent (placeholder)	Not used	Database: CCA view 6
955	2731	PAN_SEAL	KPT	0.000E+00	Resets Panel seals @ t=0	Not used - placeholder	Not used	Database: CCA view 6
956	257	PAN_SEAL	PO_MIN	1.013E+05	Resets Panel seals @ t=0	Minimum Brine pressure (same for all materials)	Required for BRAGFLO	Database: CCA view 6
957	255	PAN_SEAL	PORE_DIS	9.400E-01	Resets Panel seals @ t=0	Pore distribution (fraction)	Required for BRAGFLO	Database: CCA view 6
958	256	PAN_SEAL	POROSITY	7.500E-02	Resets Panel seals @ t=0	Porosity (fraction)	Required for BRAGFLO	Database: CCA view 6
959	259	PAN_SEAL	PRMX_LOG	-1.500E+01	Resets Panel seals @ t=0	Log x-direction permeability	Intermediate value	Database: CCA view 6
960	260	PAN_SEAL	PRMY_LOG	-1.500E+01	Resets Panel seals @ t=0	Log y-direction permeability	Intermediate value	Database: CCA view 6
961	261	PAN_SEAL	PRMZ_LOG	-1.500E+01	Resets Panel seals @ t=0	Log z-direction permeability (BRAGFLO required input)	Not used - 2D model	Database: CCA view 6
962	264	PAN_SEAL	RELP_MOD	4.000E+00	Resets Panel seals @ t=0	Relative permeability model number	Required for BRAGFLO	Database: CCA view 6
963	265	PAN_SEAL	SAT_RBRN	2.000E-01	Resets Panel seals @ t=0	Residual Brine saturation	Required for BRAGFLO	Database: CCA view 6
964	266	PAN_SEAL	SAT_RGAS	2.000E-01	Resets Panel seals @ t=0	Residual Gas saturation	Required for BRAGFLO	Database: CCA view 6
965	2734	PAN_SEAL	SAT_IBRN	1.000E+00	Resets Panel seals @ t=0	Initial brine saturation @ t = -5 years	Used in ICSET	Database: CCA view 6
966	N/A	PAN_SEAL	PERM_X	1.000E-15	Resets Panel seals @ t=0	X-direction permeability (m <sup>2</sup> ) from Log value	Required for BRAGFLO	Calculated
967	N/A	PAN_SEAL	PERM_Y	1.000E-15	Resets Panel seals @ t=0	Y-direction permeability (m <sup>2</sup> ) from Log value	Required for BRAGFLO	Calculated
968	N/A	PAN_SEAL	PERM_Z	1.000E-15	Resets Panel seals @ t=0	Z-direction permeability (m <sup>2</sup> ) Not used in 2D	Required for BRAGFLO	Calculated
969	N/A	PAN_SEAL	SB_MIN	2.100E-01	Resets Panel seals @ t=0	Minimum saturation (SAT_RBRN * 1.05)	Required for BRAGFLO	Calculated
970	N/A	PAN_SEAL	POR_COMP	2.640E-09	Resets Panel seals @ t=0	Pore compressibility COMP_RCK/POROSITY (1/Pa)	Required for BRAGFLO	Calculated
971	2909	SULFATE	QINIT	6.590E+06	Sulfate	Initial Moles of Sulfate for reaction chemistry model	Used in ALGEBRA	Database: CCA view 6
972	2906	NITRATE	QINIT	2.610E+07	Nitrate	Initial Moles of Sulfate for reaction chemistry model	Used in ALGEBRA	Database: CCA view 6
973	2907	STEEL	CORRMC02	7.937E-15	Steel properties	INUNDATED STEEL CORROSION RATE [M/SEC] W/OUT microb	ALGEBRA: Chem mod	Database: CCA view 6
974	2908	STEEL	CORRWCO2	1.032E-13	Steel properties	INUNDATED STEEL CORROSION RATE [M/SEC] WITH microb	ALGEBRA: Chem mod	Database: CCA view 6
975	2910	STEEL	HUMCORR	0.000E+00	Steel properties	HUMID STEEL CORROSION RATE	ALGEBRA: Chem mod	Database: CCA view 6
976	2898	STEEL	STOIFX	1.000E+00	Steel properties	IRON-CORROSION STOCHIO. FACTOR (Y.WANG MEMO)	ALGEBRA: Chem mod	Database: CCA view 6
977	2994	CELLULS	FBETA	5.000E-01	Cellulosics property	Stoichiometry factor used in Reaction Chemistry model	ALGEBRA: Chem mod	Database: CCA view 6
978	N/A	LEAKY_K	CASE_LK	-5.000E+00	Leaky Injector permeabilities	Log(m <sup>2</sup> )	Used in CASE_LK material	Analyst: DMStoelzel
979	N/A	LEAKY_K	CMT_LK	-1.365E+01	Leaky Injector permeabilities	Log(m <sup>2</sup> )	Used in CMT_LK material	Analyst: DMStoelzel
980	N/A	SCENARIO	SPR_BELL	7.250E-01	Defines Injection Pressures	U Bell Inj gradient (psi/ft)	South well	Analyst: DMStoelzel
981	N/A	SCENARIO	SPR_CHER	1.000E+00	Defines Injection Pressures	Cherry C Inj gradient (psi/ft)	South well	Analyst: DMStoelzel
982	N/A	SCENARIO	SPR_BRSH	1.000E+00	Defines Injection Pressures	Brushy C Inj gradient (psi/ft)	South well	Analyst: DMStoelzel
983	N/A	SCENARIO	SPR_BSPR	1.000E+00	Defines Injection Pressures	Bonespr Inj gradient (psi/ft)	South well	Analyst: DMStoelzel
984	N/A	SCENARIO	NPR_BELL	7.250E-01	Defines Injection Pressures	U Bell Inj gradient (psi/ft)	North Well	Analyst: DMStoelzel
985	N/A	SCENARIO	NPR_CHER	5.120E-01	Defines Injection Pressures	Cherry C Inj gradient (psi/ft)	North Well	Analyst: DMStoelzel
986	N/A	SCENARIO	NPR_BRSH	5.120E-01	Defines Injection Pressures	Brushy C Inj gradient (psi/ft)	North Well	Analyst: DMStoelzel
987	N/A	SCENARIO	NPR_BSPR	5.120E-01	Defines Injection Pressures	Bonespr Inj gradient (psi/ft)	North Well	Analyst: DMStoelzel
988	N/A	SCENARIO	NPR_STRA	3.580E+06	Defines Prod Pressures for deep units	Strawn Production Pressure (Pa)	North Well	Analyst: DMStoelzel
989	N/A	SCENARIO	NPR_ATOK	3.580E+06	Defines Prod Pressures for deep units	Atoka Production Pressure (Pa)	North Well	Analyst: DMStoelzel
990	N/A	SCENARIO	NPR_MORR	3.580E+06	Defines Prod Pressures for deep units	Morrow Production Pressure (Pa)	North Well	Analyst: DMStoelzel
991	N/A	SCENARIO	UBELL_FT	4.259E+03	Defines Injection Pressures	Mid-cell depth fr surface (ft)	To Upper Bell Canyon	From BRAGFLO mesh
992	N/A	SCENARIO	CHERY_FT	6.247E+03	Defines Injection Pressures	Mid-cell depth fr surface (ft)	To Cherry Canyon	From BRAGFLO mesh
993	N/A	SCENARIO	BRUSH_FT	7.965E+03	Defines Injection Pressures	Mid-cell depth fr surface (ft)	To Brushy Canyon	From BRAGFLO mesh
994	N/A	SCENARIO	BSPRG_FT	9.708E+03	Defines Injection Pressures	Mid-cell depth fr surface (ft)	To Bone Spring	From BRAGFLO mesh
995	N/A	SCENARIO	STRWN_FT	1.306E+04	Defines Production Pressures	Mid-cell depth fr surface (ft)	To Strawn	From BRAGFLO mesh
996	N/A	SCENARIO	ATOKA_FT	1.371E+04	Defines Production Pressures	Mid-cell depth fr surface (ft)	To Atoka	From BRAGFLO mesh
997	N/A	SCENARIO	MORRO_FT	1.441E+04	Defines Production Pressures	Mid-cell depth fr surface (ft)	To Morrow	From BRAGFLO mesh

Information Only



ID Number	Material	Property	Value	Material Description	Property Value Description	Usage	Source
998	N/A	SCENARIO	2.129E+07	Defines Injection Pressures	B.C. pressure to Bell Canyon (Pa)	South: 0 to 50 yrs, 100 to 150 yrs	Calc fr depth and grad
999	N/A	SCENARIO	1.000E-10	Defines Injection Pressures	Well PI to Bell Canyon (Pa)	South: 0 to 50 yrs, 100 to 150 yrs	Analyst: DMSstoelzel
1000	N/A	SCENARIO	1.527E+07	Defines Injection Pressures	B.C. pressure to Bell Canyon (Pa)	Not Used	Calc fr depth and grad
1001	N/A	SCENARIO	1.000E-20	Defines Injection Pressures	Well PI to Bell Canyon (Pa)	Not Used	Analyst: DMSstoelzel
1002	N/A	SCENARIO	4.307E+07	Defines Injection Pressures	B.C. pressure to Cherry Canyon (Pa)	South: 0 to 50 yrs	Calc fr depth and grad
1003	N/A	SCENARIO	1.000E-10	Defines Injection Pressures	Well PI to Cherry Canyon (Pa)	South: 0 to 50 yrs	Analyst: DMSstoelzel
1004	N/A	SCENARIO	2.240E+07	Defines Injection Pressures	B.C. pressure to Cherry Canyon (Pa)	Not Used	Calc fr depth and grad
1005	N/A	SCENARIO	1.000E-20	Defines Injection Pressures	Well PI to Cherry Canyon (Pa)	Not Used	Analyst: DMSstoelzel
1006	N/A	SCENARIO	5.492E+07	Defines Injection Pressures	B.C. pressure to Brushy Canyon (Pa)	South: 50 to 100 yrs	Calc fr depth and grad
1007	N/A	SCENARIO	1.000E-10	Defines Injection Pressures	Well PI to Brushy Canyon (Pa)	South: 50 to 100 yrs	Analyst: DMSstoelzel
1008	N/A	SCENARIO	2.856E+07	Defines Injection Pressures	B.C. pressure to Brushy Canyon (Pa)	Not Used	Calc fr depth and grad
1009	N/A	SCENARIO	1.000E-20	Defines Injection Pressures	Well PI to Brushy Canyon (Pa)	Not Used	Analyst: DMSstoelzel
1010	N/A	SCENARIO	6.694E+07	Defines Injection Pressures	B.C. pressure to Bone Spring (Pa)	South: 100 to 150 yrs	Calc fr depth and grad
1011	N/A	SCENARIO	1.000E-10	Defines Injection Pressures	Well PI to Bone Spring (Pa)	South: 100 to 150 yrs	Analyst: DMSstoelzel
1012	N/A	SCENARIO	3.481E+07	Defines Injection Pressures	B.C. pressure to Bone Spring (Pa)	Not Used	Calc fr depth and grad
1013	N/A	SCENARIO	1.000E-20	Defines Injection Pressures	Well PI to Bone Spring (Pa)	Not Used	Analyst: DMSstoelzel
1014	N/A	SCENARIO	2.129E+07	Defines Injection Pressures	B.C. pressure to Bell Canyon (Pa)	North: 50 to 100 yrs	Calc fr depth and grad
1015	N/A	SCENARIO	1.000E-10	Defines Injection Pressures	Well PI to Bell Canyon (Pa)	North: 50 to 100 yrs	Analyst: DMSstoelzel
1016	N/A	SCENARIO	1.527E+07	Defines Injection Pressures	B.C. pressure to Bell Canyon (Pa)	Not Used	Calc fr depth and grad
1017	N/A	SCENARIO	1.000E-20	Defines Injection Pressures	Well PI to Bell Canyon (Pa)	Not Used	Analyst: DMSstoelzel
1018	N/A	SCENARIO	2.205E+07	Defines Production Pressures	B.C. pressure to Cherry Canyon (Pa)	North: 0 to 50 yrs	Analyst: DMSstoelzel
1019	N/A	SCENARIO	1.000E-10	Defines Production Pressures	Well PI to Cherry Canyon (Pa)	North: 0 to 50 yrs	Analyst: DMSstoelzel
1020	N/A	SCENARIO	2.240E+07	Defines Production Pressures	B.C. pressure to Cherry Canyon (Pa)	Not Used	Analyst: DMSstoelzel
1021	N/A	SCENARIO	1.000E-20	Defines Production Pressures	Well PI to Cherry Canyon (Pa)	Not Used	Analyst: DMSstoelzel
1022	N/A	SCENARIO	2.812E+07	Defines Production Pressures	B.C. pressure to Brushy Canyon (Pa)	North: 50 to 100 yrs	Analyst: DMSstoelzel
1023	N/A	SCENARIO	1.000E-10	Defines Production Pressures	Well PI to Brushy Canyon (Pa)	North: 50 to 100 yrs	Analyst: DMSstoelzel
1024	N/A	SCENARIO	2.856E+07	Defines Production Pressures	B.C. pressure to Brushy Canyon (Pa)	Not Used	Analyst: DMSstoelzel
1025	N/A	SCENARIO	1.000E-20	Defines Production Pressures	Well PI to Brushy Canyon (Pa)	Not Used	Analyst: DMSstoelzel
1026	N/A	SCENARIO	3.427E+07	Defines Production Pressures	B.C. pressure to Bone Spring (Pa)	North: 100 to 150 yrs	Analyst: DMSstoelzel
1027	N/A	SCENARIO	1.000E-10	Defines Production Pressures	Well PI to Bone Spring (Pa)	North: 100 to 150 yrs	Analyst: DMSstoelzel
1028	N/A	SCENARIO	3.480E+07	Defines Production Pressures	B.C. pressure to Bone Spring (Pa)	Not Used	Analyst: DMSstoelzel
1029	N/A	SCENARIO	1.000E-20	Defines Production Pressures	Well PI to Bone Spring (Pa)	Not Used	Analyst: DMSstoelzel
1030	N/A	SCENARIO	1.000E-10	Defines Well PI for deep units	Strawn well Productivity Index during production (m <sup>3</sup> /Pa-s)	North Well	Analyst: DMSstoelzel
1031	N/A	SCENARIO	1.000E-20	Defines Well PI for deep units	Strawn well Productivity Index for no production (m <sup>3</sup> /Pa-s)	North Well	Analyst: DMSstoelzel
1032	N/A	SCENARIO	1.000E-10	Defines Well PI for deep units	Atoka well Productivity Index during production (m <sup>3</sup> /Pa-s)	North Well	Analyst: DMSstoelzel
1033	N/A	SCENARIO	1.000E-20	Defines Well PI for deep units	Atoka well Productivity Index for no production (m <sup>3</sup> /Pa-s)	North Well	Analyst: DMSstoelzel
1034	N/A	SCENARIO	1.000E-10	Defines Well PI for deep units	Morrow well Productivity Index during production (m <sup>3</sup> /Pa-s)	North Well	Analyst: DMSstoelzel
1035	N/A	SCENARIO	1.000E-20	Defines Well PI for deep units	Morrow well Productivity Index for no production (m <sup>3</sup> /Pa-s)	North Well	Analyst: DMSstoelzel

**Attachment 1: Injection Methods: Current Practices and Failure Rates in  
the Delaware Basin**

**Information Only**

DOE/WIPP-97-2240

# **Injection Methods: Current Practices and Failure Rates in the Delaware Basin**



June 1997

## **United States Department of Energy Waste Isolation Pilot Plant**

**Carlsbad Area Office  
Carlsbad, New Mexico**

Processing and final preparation of this report were performed by the Westinghouse Electric Corporation's Waste Isolation Division, the management and operating contractor for the Waste Isolation Pilot Plant, under U.S. Department of Energy contract DE-AC04-86AL31950.

**Information Only**

**Injection Methods: Current Practices and  
Failure Rates in the Delaware Basin**

**June 1997**

Prepared by

G. Ross Kirkes,  
Westinghouse Electric Corporation  
Waste Isolation Division

Ronald D. Evans, PhD., P.E.,  
Petroleum Consultant

## Table of Contents

1.0	Introduction .....	1
2.0	Regulatory Requirements .....	3
2.1	Testing .....	3
2.2	Injection Volume .....	4
3.0	Data Acquisition .....	4
4.0	Potential Failures of Injection Wells .....	7
4.1	Types of Failures .....	7
5.0	Injection and Salt Water Disposal Wells Assessment .....	11
5.1	The Nine-Township Study Area .....	11
5.1.2	Injection Pressures .....	12
5.1.3	Radioactive Tracer Tests at Todd 26 and David Ross SWDs .....	13
5.2	The Remainder of Eddy and Lea Counties Within the Delaware Basin .....	14
6.0	Carbon Dioxide (CO <sub>2</sub> ) Miscible Flooding .....	16
7.0	Duration of Leaks .....	18
8.0	Failure Rates .....	18
8.1	Failure Rate Calculations .....	19
9.0	Conclusions .....	20
10.0	References .....	22
Attachment 1	Permitted SWD and WI Wells in the Nine Township Area Surrounding the WIPP Site	
Attachment 2	Wellbore Diagrams for the Active and Inactive SWD and WI Wells in the Nine Township Area Surrounding the WIPP Site	
Attachment 3	Permitted SWD and WI Wells in New Mexico Outside the Nine Township Area Surrounding the WIPP But Within the Delaware Basin	
Attachment 4	New Mexico Injection Rules, Section 701 - 708	
Attachment 5	Determining Months of Regulated Service for Salt Water Disposal and Water Injection Wells	



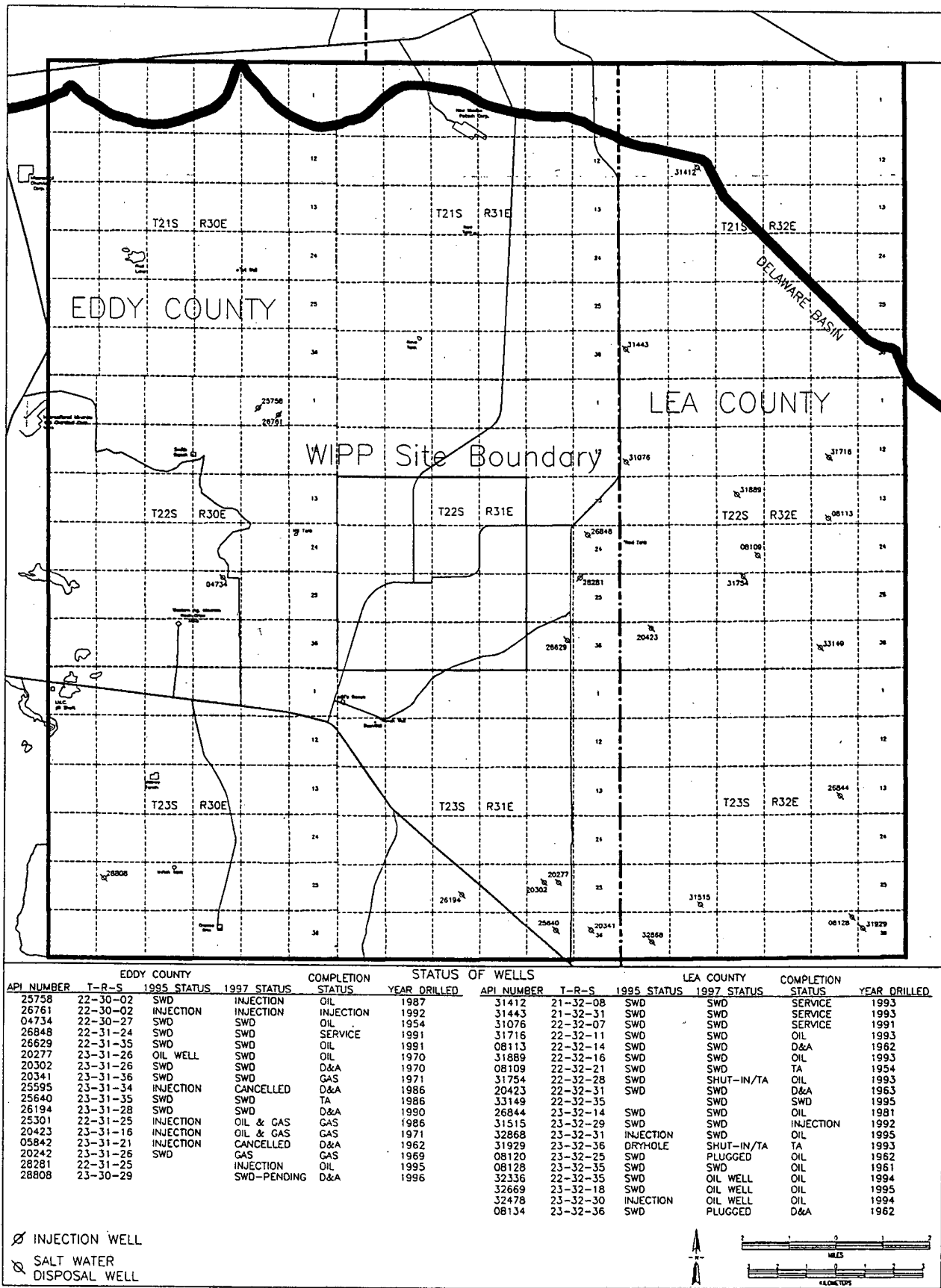
## List of Figures

Figure 1	Permitted Injection and Salt Water Disposal Wells in the Nine Township Area	2
Figure 2	Typical Injection Well and General Stratigraphy Near the WIPP Site .....	5
Figure 3	Typical Wellhead and Casing Schematic for an Injection Well .....	6
Figure 4	Tubing, Casing, Packer, and Cement Sheath Failures in a Typical Injection Well .....	8

## List of Tables

Table 1	SWD or WI Well Failures Within the Nine Township Area Surrounding the WIPP .....	12
Table 2	SWD or WI Well Failures in Eddy County, Outside the Nine Township Area Surrounding the WIPP .....	15
Table 3	SWD or WI Well Failures in Lea County, Outside the Nine Township Area Surrounding the WIPP .....	16





EDDY COUNTY					STATUS OF WELLS					LEA COUNTY							
API NUMBER	T-R-S	1995 STATUS	1997 STATUS	COMPLETION STATUS	YEAR DRILLED	API NUMBER	T-R-S	1995 STATUS	1997 STATUS	COMPLETION STATUS	YEAR DRILLED	API NUMBER	T-R-S	1995 STATUS	1997 STATUS	COMPLETION STATUS	YEAR DRILLED
25758	22-30-02	SWD	INJECTION	OIL	1987	31412	21-32-08	SWD	SWD	SERVICE	1993	31412	21-32-08	SWD	SWD	SERVICE	1993
26761	22-30-02	INJECTION	INJECTION	INJECTION	1992	31443	21-32-31	SWD	SWD	SERVICE	1993	31076	22-32-07	SWD	SWD	SERVICE	1991
04734	22-30-27	SWD	SWD	OIL	1954	31076	22-32-07	SWD	SWD	SERVICE	1991	31716	22-32-11	SWD	SWD	OIL	1993
26848	22-31-24	SWD	SWD	SERVICE	1991	08113	22-32-14	SWD	SWD	OIL	1962	31716	22-32-11	SWD	SWD	OIL	1993
26629	22-31-35	SWD	SWD	OIL	1970	31889	22-32-16	SWD	SWD	D&A	1993	08109	22-32-21	SWD	SWD	TA	1954
20277	23-31-26	OIL WELL	SWD	OIL	1991	08109	22-32-21	SWD	SWD	TA	1993	20423	22-32-28	SWD	SHUT-IN/TA	OIL	1963
20302	23-31-26	SWD	SWD	D&A	1986	20423	22-32-28	SWD	SWD	D&A	1963	20423	22-32-31	SWD	SWD	SWD	1995
20341	23-31-36	SWD	SWD	TA	1986	33149	22-32-35	SWD	SWD	SWD	1981	31515	23-32-29	SWD	SWD	INJECTION	1992
25595	23-31-34	INJECTION	CANCELLED	D&A	1986	26844	23-32-14	SWD	SWD	OIL	1981	32868	23-32-31	INJECTION	SWD	OIL	1995
25640	23-31-35	SWD	SWD	TA	1986	31515	23-32-29	SWD	SWD	INJECTION	1992	32868	23-32-31	INJECTION	SWD	OIL	1995
26194	23-31-28	SWD	SWD	D&A	1990	31754	22-32-28	SWD	SHUT-IN/TA	TA	1993	31929	23-32-36	DRYHOLE	SWD	OIL	1962
25301	22-31-25	INJECTION	OIL & GAS	GAS	1986	20423	22-32-31	SWD	SWD	PLUGGED	1962	08120	23-32-25	SWD	SWD	OIL	1961
20423	23-31-16	INJECTION	OIL & GAS	GAS	1971	31929	23-32-36	DRYHOLE	SHUT-IN/TA	TA	1993	08128	23-32-35	SWD	SWD	OIL	1961
05842	23-31-21	INJECTION	CANCELLED	D&A	1962	08120	23-32-25	SWD	PLUGGED	OIL	1962	32336	22-32-35	SWD	SWD	OIL	1994
20242	23-31-26	SWD	GAS	GAS	1969	08128	23-32-35	SWD	SWD	OIL	1961	32669	23-32-18	SWD	SWD	OIL	1995
28281	22-31-25	INJECTION	INJECTION	OIL	1995	32478	23-32-30	INJECTION	OIL WELL	OIL	1994	32478	23-32-30	INJECTION	OIL WELL	OIL	1994
28808	23-30-29	SWD	SWD-PENDING	D&A	1996	08134	23-32-36	SWD	PLUGGED	D&A	1962	32668	23-32-36	SWD	SWD	OIL	1994

- ⊗ INJECTION WELL
- ⊗ SALT WATER DISPOSAL WELL

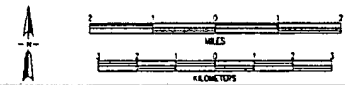


Figure 1. Permitted Injection and Salt Water Disposal Wells - Nine Township Area

## 2.0 Regulatory Requirements

The area surrounding WIPP used in this analysis lies exclusively within the State of New Mexico and is subject to the Uniform Injection Code (UIC) (EPA 1983), which is administered by the New Mexico Oil Conservation Division (NMOCD). The UIC requirements apply to SWD and WI activities conducted on all lands in New Mexico whether owned by the Federal government, State of New Mexico, or private individuals.

The NMOCD regulations applicable to injection wells are stated in Rules 701 through 708 (19 NMAC 15.I.701-708)<sup>1</sup>. These regulations are provided in Attachment 4 of this report. The rules apply to injection for secondary or other enhanced recovery, pressure maintenance, salt water disposal, and underground storage. A permit must be obtained from the NMOCD for the injection of gas, air, water, or any other medium into any oil or gas reservoir in order to maintain pressure for secondary or other enhanced recovery (Rule 701-A). A permit is also required for injection of water for disposal or for underground storage.

In pressure maintenance projects, fluids are injected into the oil- or gas-producing horizon in order to increase or maintain reservoir pressure in an area that has not reached the stripper-well degree of depletion. Although not prescribed by NMOCD regulations, practice is to limit all injection well pressures to 0.2 pounds per square inch (psi) (1,379 pascals) for each linear foot of well depth to the top of the injection zone. The maximum injection pressure is prescribed for each well in the permit. Permit conditions are set by the NMOCD based on consideration of site-specific characteristics (i.e., nearby groundwater sources, nearby production wells, lithology). Operators may exceed this pressure only with NMOCD authorization (see discussion in Section 4.1).

### 2.1 Testing

The NMOCD requires periodic scheduled testing of SWD and WI wells (19 NMAC 15.I.704.A) (see Attachment 4). Typically, a Bradenhead Test (BHT) is conducted annually and a Mechanical Integrity Test (MIT) is conducted at five-year intervals or anytime that a well is taken off-line for repairs, however the actual frequency of these tests may vary based on permit conditions. The well records (Appendices A through D) show consistent evidence of periodic and routine testing. A description of these tests follows.

The BHT is performed by opening the bradenhead valve to the atmosphere. If gas or water flow is observed or indicated, flow through the bradenhead valve is allowed to continue for a minimum of fifteen minutes. During this period, pressures are recorded at five-minute

---

<sup>1</sup> The NMOCD began the administration of the UIC March 7, 1982 (47 FR 5412).

1 intervals on the production, intermediate, and surface casing. Any fluids flowing from the  
2 bradenhead valve, including measured or estimated rates of flow, are described in detail.  
3

4 The BHT tests the integrity of the tubing and packer. The tubing annulus is typically filled  
5 with a corrosion-inhibiting fluid. If a leak in the tubing or packer is present, this annulus  
6 becomes pressurized, and flow occurs when the valve is opened. If the casing is defective, the  
7 annular space created by the loss of fluid may be at a partial vacuum. This annular space is  
8 not required to be open to the atmosphere, but if closed, a pressure gauge must be installed.  
9 Operators typically prefer to close this annulus to prevent evaporation of the fluid, thereby  
10 limiting corrosion of casing and tubing.  
11

12 The MIT tests the integrity of the casing and must be performed prior to commencement of  
13 injection and/or any time the tubing is pulled or the packer is resealed. In this test, the casing-  
14 tubing annulus is pressurized to a minimum of 300 psi. A pressure recorder is used to show  
15 any loss of pressure over a 30-minute period. Copies of the pressure recorder chart must be  
16 submitted to the NMOCD within 30 days of the test date. If a well fails a test,<sup>2</sup> it is shut-in  
17 and the operator must take corrective action before returning the well to service. The testing  
18 dates for the last four years for permitted (active and shut-in) SWD and WI wells in the nine  
19 township study area are provided in Attachment 1. The typical wellbore schematic and general  
20 stratigraphy near the WIPP are shown in Figure 2. The typical wellhead hardware associated  
21 with each of the tests described above is depicted in Figure 3.  
22  
23

## 24 2.2 Injection Volume

25  
26 The NMOCD does not place specific limits on total quantities of salt water to be injected over  
27 the entire life of the well. Instead, maximum monthly or daily volumes are specified in the  
28 permit.  
29

## 30 3.0 Data Acquisition

31  
32  
33 In an effort to obtain the most accurate and current data available, the NMOCD permit list was  
34 used as the primary data source. This list contains all permitted SWD, WI wells, including  
35 those that are currently active and shut-in. From this list, the actual well records were  
36 obtained and evaluation was based on the status given in the NMOCD permit list. In many  
37 cases, information in the well records superseded that given in the permit list. For example,  
38 the list may have shown a well as pending, however an inspection of the well record would  
39 reveal that injection operations have begun. Through this verification process, an accurate data

---

<sup>2</sup> A failed MIT is identified by an anomalous drop in pressure.



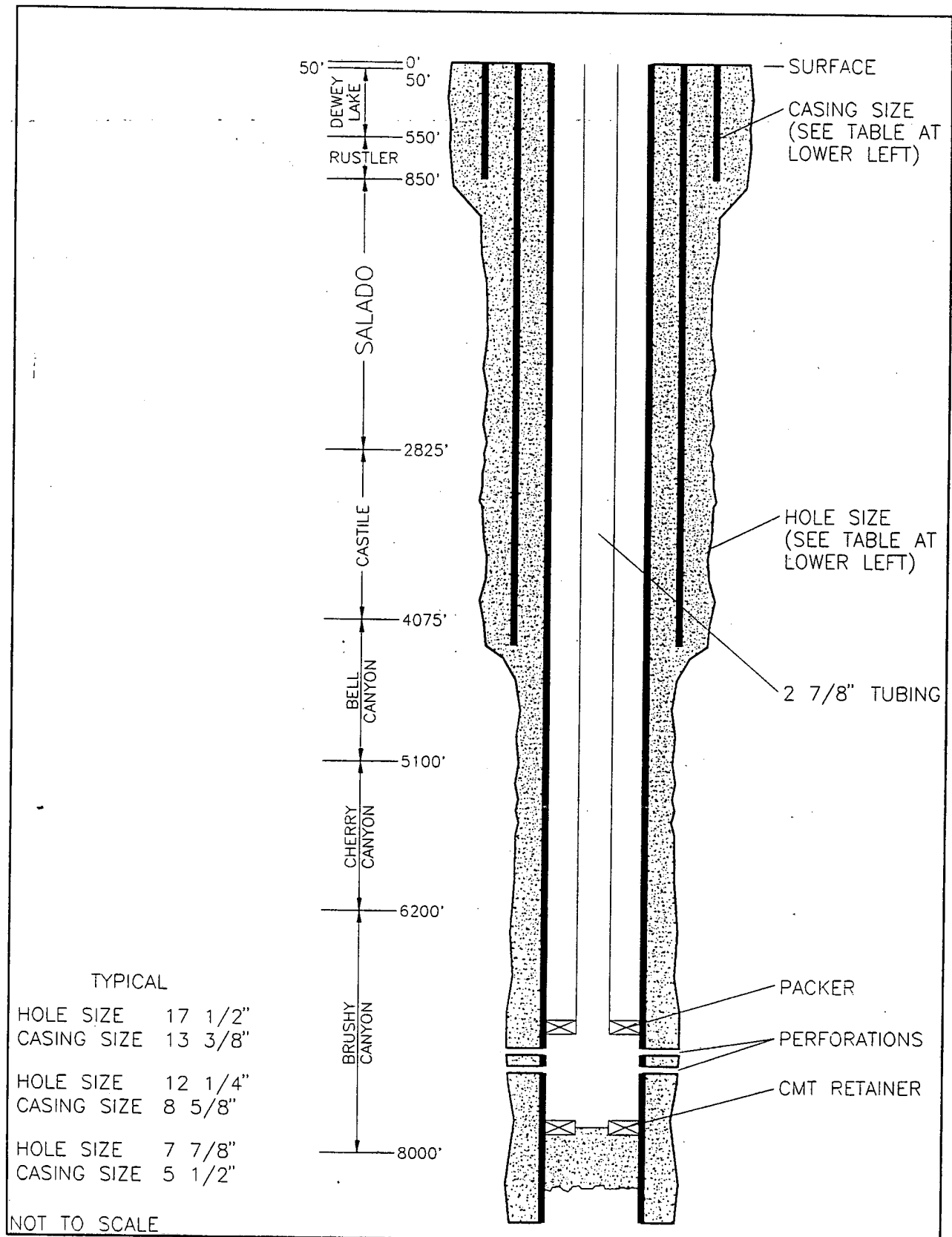


Figure 2. Typical Injection Well and General Stratigraphy Near the WIPP Site

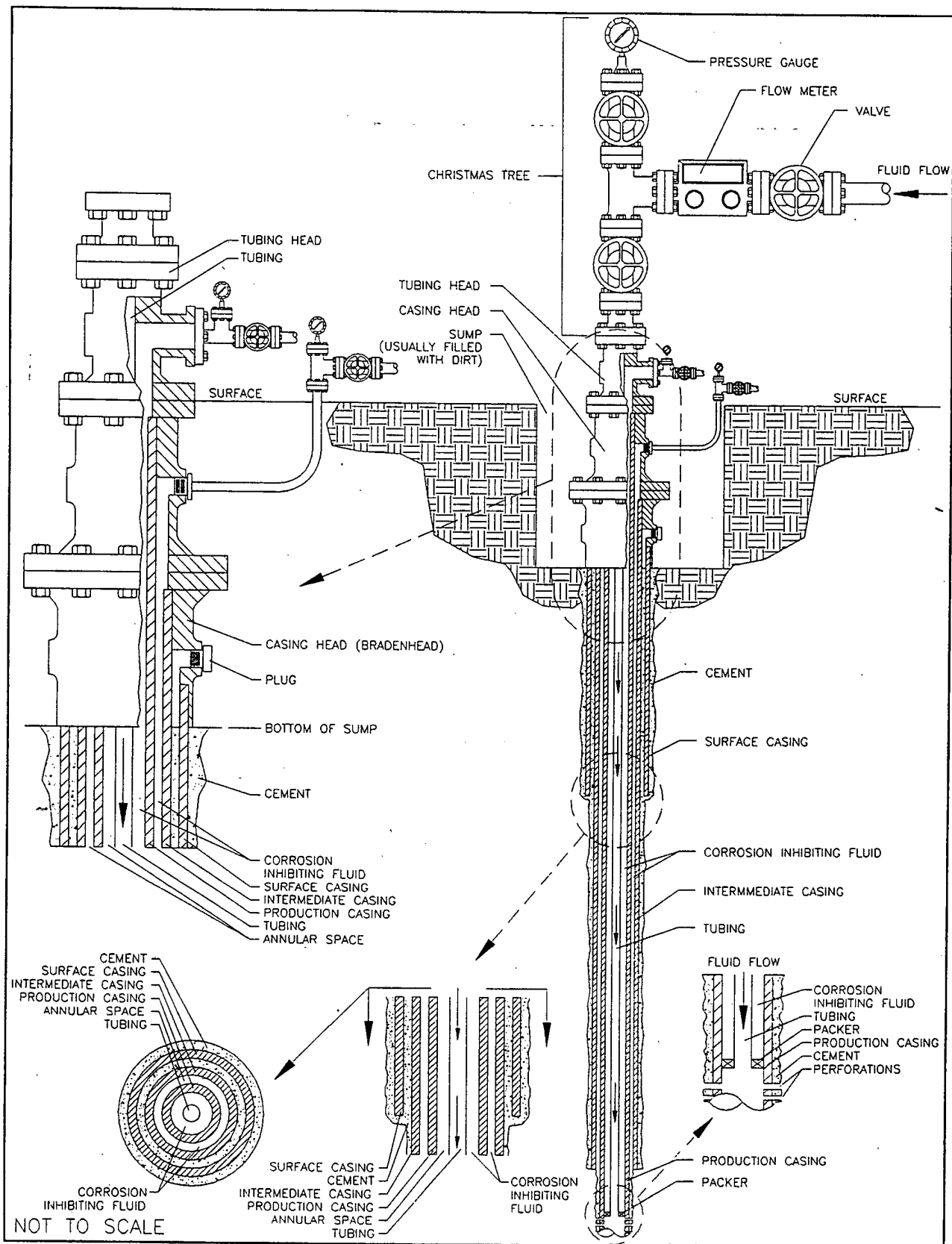


Figure 3. Typical Wellhead and Casing Schematic for an Injection Well

Information Only

1 set was obtained. As an additional safeguard, the *Petroleum Information Corporation*  
2 *Database* (Petroleum Information Corp., 1997) was also used as a cross-verification tool.

3  
4 A listing of the permitted and shut-in SWD and WI wells located in the nine township study  
5 area is provided in Attachment 1. Wellbore diagrams for these wells are provided in  
6 Attachment 2. Permitted SWD and WI wells located in New Mexico and the Delaware Basin,  
7 but outside the nine township study area, are listed in Attachment 3. Specific well records are  
8 provided in appendices A through D.

#### 11 **4.0 Potential Failures of Injection Wells**

12  
13 The equipping, operating, and monitoring of WI and SWD wells are essentially the same:  
14 each is normally a previously producing oil or gas well that is no longer economical to produce  
15 or a dry hole that is completed as an WI or SWD well.

#### 18 **4.1 Types of Failures**

19  
20 Four types of potential wellbore failure scenarios are possible:

- 21  
22 Type 1. Tubing leak;  
23  
24 Type 2. Packer leak;  
25  
26 Type 3. Casing leak;  
27  
28 Type 4. Breakdown of casing cement sheath  
29

30 One potential formation failure scenario is possible:

- 31  
32 Type 5. The creation of a fluid path by hydraulically fracturing the injection zone by  
33 injecting above fracture pressure for a given formation.  
34

35 Figure 4 illustrates the flow paths for leak types.

36  
37 The BHT and the MIT are able to determine the occurrence of failure types 1, 2, and 3;  
38 tubing, packer, and casing leaks. Tubing and packer leaks are of no consequence because the  
39 leak is contained within the production casing (assuming it has mechanical integrity). In  
40 addition, the casing leak has no consequence as well, unless it is coupled by a tubing or a  
41 packer leak; thereby pressurizing the annulus, resulting in migration of fluid through the casing  
42 leak. Given the infrequency of tubing and packer leaks (see Section 7.0), and the infrequency  
43

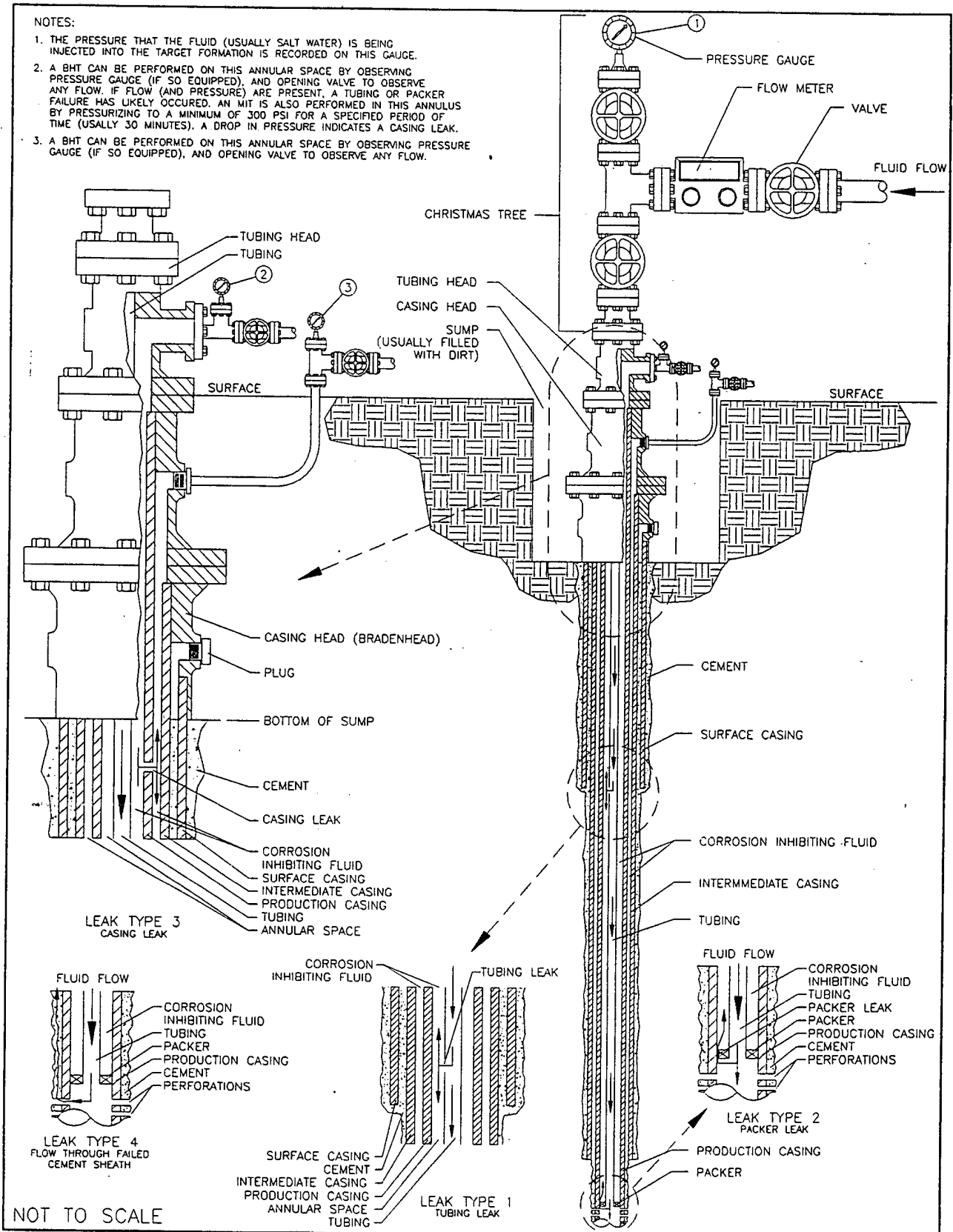


Figure 4. Tubing, Casing, Packer, and Cement Sheath Failures in a Typical Injection Well

Information Only

1 of casing leaks, the probability of these two type of leaks occurring simultaneously is very,  
2 very low. In addition, in the rare instances in which the coupled leak scenario occurs, the leak  
3 would likely be contained by the next larger casing string (when present). Each of these leak  
4 types are easily identified, and easily repaired. As such, these types of failures would not  
5 impact the WIPP since the failure is contained within the tubing/casing annulus or the  
6 production casing/surface casing annulus.  
7

8 The fourth failure type, the breakdown of the cement sheath between the casing and/or the  
9 borehole wall, is the only leak scenario that has the potential to impact the WIPP repository.  
10 This type of failure can only be detected by a radioactive tracer test (RTT) survey conducted  
11 inside the cased wellbore. This type of test is not a normal regulatory requirement, but may be  
12 conducted if it appears there may be fluid migration behind casing. For example, if a WI well  
13 operated to enhance oil production (i.e., waterflood operations) caused migration out of zone,  
14 anticipated recovery would not meet the predetermined expectations of the operator, thereby  
15 affecting the economics of the waterflood project. Prudent operators of waterflood projects  
16 will not allow injected fluids to migrate out of zone. Further, it is a violation of NMOCD  
17 regulations to allow migration of fluid out of the target zone.  
18

19 If the cement sheath in an SWD well is compromised by the injection process and fluid  
20 migrates upward, it is more likely that this event would go undetected for a greater period of  
21 time than for a WI well. However, the low permeability of cement will preclude the migration  
22 of injected water through the cement sheath. One-hundred percent bonding between  
23 cement/casing and cement/formation is not necessary to insure a hydraulic seal. Sixty to  
24 eighty percent cement bonding over a distance of 25 - 50 feet for 5.5 inch casing and 60 - 125  
25 feet bonding for 8.625 inch casing is adequate to insure a hydraulic seal for injection purposes  
26 (Schlumberger 1989). Note that the minimum length of any cement sheath (production casing)  
27 within the study area is 140 feet (Prohibition Federal Unit #2, Attachment 2); this is roughly 3  
28 times the minimum needed for an adequate hydraulic seal.  
29

30 The remaining potential failure, Type 5, the creation of a vertical hydraulic pathway between  
31 the injection zone and an upper zone such as the Salado Formation, could only occur if the  
32 injection pressure of a well at the perforations is much greater than the breakdown pressure of  
33 the injection zone. Since the NMOCD requires that the surface injection pressure be no more  
34 than 0.2 psi/ft. of depth to the top of the perforated interval, it is impossible to create a vertical  
35 fracture in the injection zone because injection pressure at the perforations is less than the  
36 pressure required to fracture the formation. The exception to this is a NMOCD provision that  
37 allows an operator to perform a step-rate test to determine the fracturing pressure of the  
38 formation. The step-rate test is a well-established industry procedure that, when interpreted  
39 correctly, allows the surface injection pressure to be safely increased in excess of the standard  
40 0.2 psi/ft value used for initial permitting. Even if a surface injection pressure exceeds the 0.2  
41 psi/ft limit, this does not infer that the operator of an SWD or WI well is exceeding fracturing  
42 pressure at the perforations. The new surface injection pressure allowed after conducting the  
43 step-rate test is still set below fracturing pressure.



1 In the hydraulic fracturing process, a fluid is pumped down the wellbore (tubing or casing) and  
2 the bottom hole pressure is increased until the formation of interest breaks down, (parts). The  
3 pressure at which the formation breaks down is called the fracture initiation pressure. The  
4 formation will fracture perpendicular to the least principle stress. If the least principal stress is  
5 vertical, a horizontal or 'pancake' fracture will occur.  
6

7 To extend the fracture vertically and horizontally away from the wellbore, the bottom hole  
8 pressure must be maintained at a level such that the pressure at the fracture tip is maintained  
9 above fracture initiation pressure of the formation. Hence, during the fracturing process, the  
10 bottom hole pressure must be elevated so as to increase the frictional pressure drop along the  
11 created fracture. At a given injection rate (normally tens of barrels per minute), given fluid  
12 rheological properties, and a fixed bottom hole injection pressure, an equilibrium will be  
13 reached and propagation of fractures will cease due to fluid leakoff and friction losses. This  
14 situation is indicative of WI and SWD wells; the injection rate is normally constant, the  
15 rheology of the saltwater is fixed, and the bottom hole injection pressure is fixed relative to the  
16 surface injection pressure.  
17

18 Over time microscopic fines entrained in the injected saltwater may result in partial plugging of  
19 the formation. When this occurs, an increase in surface injection pressure is required to  
20 maintain a constant injection rate. To increase the injectivity of the formation the operator can  
21 design and conduct a hydraulic fracture treatment to increase the area available to take fluid.  
22 In this case, a proppant is placed in the fracture to keep it open so the injected fluid will have  
23 the larger flow area. In this manner the WI or SWD well can be returned to injection at the  
24 same rate (or even a higher rate) at a surface injection pressure at or below the permitted value  
25 set by the NMOCD. An alternative to hydraulically fracturing the formation to maintain  
26 injectivity is to conduct a step-rate test. The step-rate test is used by the operator to obtain a  
27 higher permitted surface injection pressure. Such an increase in the permit conditions for  
28 maximum pressure does not exceed the level which is required to fracture the formation.  
29

30 As the fracture is initiated and propagates away from the wellbore, some of the fluid leaks off  
31 into the surrounding formation across the two faces of the created fracture. The rest of the  
32 fracturing fluid continues to create fracture volume, (i.e., fracture length, height, and width).  
33 In order to create the desired fracture geometry, fracturing fluids used to increase production  
34 in oil and gas wells or increase injectivity in WI or SWD wells require fluids with high  
35 viscosity and very low leakoff characteristics. To minimize leakoff, the fracturing fluid is  
36 chemically treated with an additive that deposits a thin, impermeable cake on the fracture faces  
37 during the pumping of the fracturing fluid. The high viscosity is required to transport the  
38 proppant, (i.e., sand, centered bauxite, ceramic beads.), which is blended in the fracturing  
39 fluid and used to prop open the fracture once the pumping process is terminated.  
40

41 Saltwater injected for enhanced recovery or disposal purposes is an extremely poor fracturing  
42 fluid. Its viscosity (approximately 0.60 centipoise at 140°F) (Amyx, et al., 1960), is almost  
43 two orders of magnitude below typical fracturing fluids, (20-150 centipoise) (Halliburton

1 1986). Because saltwater is compatible with reservoir rocks, it has very poor leakoff  
2 characteristics. Most of the injected saltwater will leakoff into the surrounding formation  
3 resulting in very little fracture volume being created by the remaining saltwater in the event the  
4 surface injection pressure creates a bottom hole pressure greater than the fracturing pressure of  
5 the formation.  
6

7 In addition, the stress differential between bounding formations and the injection zone makes  
8 the creation of a vertical fracture (with height in excess of a few tens of feet) highly  
9 improbable at injection rates and surface injection pressures of the WI and SWD wells  
10 investigated in this study. The shallowest injection zone within the study area is 3,820 feet,  
11 which provides a minimum vertical separation between this zone and the WIPP repository  
12 horizon of 1,670 feet. The mean injection depth in the study area is 5,179 feet, providing  
13 3,029 feet of vertical separation.  
14

## 16 5.0 Injection and Salt Water Disposal Wells Assessment

17  
18 The data used as a basis for evaluating WI and SWD wells consists of well records obtained  
19 from the NMOCD (Appendices A through D). For this analysis, these records were compiled  
20 and reviewed to determine the number of SWD and WI well failures that have occurred in the  
21 region. This information, coupled with the total number of years in which wells in the study  
22 area have operated under the current regulatory program, are used to derive a frequency at  
23 which SWD and WI wells have failed. The method for determining this probability is  
24 described in Section 7.0 of this report.  
25

### 27 5.1 Wellbore Failures Within the Nine Township Study Area

28  
29 As of April 1997, there are three active WI wells and 21 active SWD wells within this area.  
30 There are two temporarily abandoned or inactive SWD wells. In addition, one application for  
31 an SWD well is pending. Among these wells, only three BHT and MIT failures have been  
32 identified during the fifteen-year study period (Table 1). It should be noted that none of the  
33 three failures were detected during a regularly scheduled BHT or MIT. This indicates that the  
34 operators maintain an active presence at these well locations and proactively mitigate wellbore  
35 failures.  
36

37 The 21 SWD wells are previously producing oil and gas wells or non-commercial oil and gas  
38 wells completed as SWD wells. These wellbores were drilled and completed between  
39 May 1954 and April 1994. The dates of first water injection range from May 1969, to  
40 April 1996. According to existing records one of the older wells, the Todd 26 Federal #3  
41 (converted to injection in 1971) failed a MIT on November 22, 1993. The casing leak was  
42 repaired by removing the casing from 338 feet below grade, back to the surface. This portion  
43 of the casing was replaced with 338 feet of new casing cemented to the surface. Hence, based

on existing records, this well was in service as an SWD well for 22 years without a failure.

Two other SWD wells failed a BHT or an MIT. The Flamenco Federal #1 SWD well failed an MIT on November 11, 1995. The problem was corrected and the casing tubing annulus subsequently passed an MIT on this date. The James Federal #1 well deserves some special attention since it was originally permitted on April 23, 1969, as a WI well in a pilot waterflood. This was a former oil-producing well that was converted to an SWD well on May 16, 1969. The tubing casing annulus was pressure tested on this date and the well was taking saltwater on a vacuum. Apparently, it was the intent of the operator to use this well as an SWD well even though originally permitted as a WI well. A BHT was conducted on January 27, 1987, and a hairline leak in the bradenhead line was reported and repaired the same day. Since 1990, five BHTs and two MITs have been conducted on this well. The well passed each of these tests indicating the casing possesses good integrity even though it was run and cemented in place 28 years ago.

**Table 1. Salt Water Disposal/Injection Well Failures - Eddy and Lea County, New Mexico - Delaware Basin - Inside the Nine Townships Surrounding the Waste Isolation Pilot Plant**

Well Name / Date of Conversion	Location	API #	Problem	Repairs	Date Returned to Injection
Flamenco Fed. #1 Converted to SWD 7/91	S07-T22S- R32E (Lea County)	30- 025- 31076	1. Packer Leak 11/9/95	1. New Packer Installed; also replaced 2 jts. 3.5" tubing; Passed MIT	1. 11/11/95
Todd 26 Fed. #3 Converted to SWD 7/71	S26-T23S- R31E (Eddy County)	30- 015- 20302	1. Casing Leak; Tubing upgrade (failed MIT 11/22/93)	1. Replaced 8 jts. casing; cemented to surface; Ran 134 jts. new 2.378" plastic coated tubing and 4.5" tension packer;	1. 12/1/93
James Fed. #1 Converted to SWD 5/69	S35-T23S- R32E (Lea County)	30- 025- 08128	1. Bradenhead hairline leak 1/27/87	1. Re-plumbed Bradenhead; Passed MIT	1. 1/27/87

### 5.1.2 Injection Pressures

Currently, all but one SWD and WI wells in the 9 township are surrounding the WIPP site are injecting at or below the original NMOCD permitted pressure. The exception is the Cal-Mon #5 SWD well. This well was originally permitted at a maximum surface injection pressure of 897 psi. The NMOCD approved an increase to 998 psi based on a step-rate test performed on October 12, 1993, by John West

1 Engineering, Hobbs, New Mexico. This increase in surface injection pressure is 12 psi above the  
2 NMOCD-specified initial maximum of 0.2psi/ft at the top of the perforated interval (4,931 feet at this  
3 well).  
4

### 5 *5.1.3 Radioactive Tracer Tests at Todd 26 and David Ross SWDs*

6

7 On June 13, 1995, a workshop entitled "Fluid Injection for Salt Water Disposal and Enhanced Oil  
8 Recovery as a Potential Problem for the WIPP" was held in Albuquerque, New Mexico. A paper  
9 presented at this workshop by researchers from the New Mexico Environmental Evaluation Group,  
10 (EEG), Albuquerque, New Mexico, alleged that injected waters from the Todd 26 Federal #3 SWD  
11 well and the David Ross AIT Federal #1 SWD well may have migrated vertically upward to the  
12 Culebra interval located at a depth of 600-800 feet. The allegation was based upon observed increases  
13 in water levels of two monitor wells completed in the Culebra.  
14

15 The Todd 26 Federal #3 SWD well injects water below the tubing/casing packer over a perforated  
16 interval from 4,379-5,700 feet. Similarly, the David Ross AIT Federal #1 SWD well injects water  
17 over a perforated interval from 4,500-5,670 feet. Hence, to communicate with the Culebra would  
18 require the injected water from these two SWD wells to travel a vertical distance in excess of 3,579  
19 feet. This could occur only if there were to be a fluid conduit created within the cemented annulus  
20 between casing and formation or via a vertical fluid path in the formations penetrated by the wellbore.  
21 To assume the injected water at the sand face could create a fluid path by a hydraulically created  
22 vertical fracture and propagated it upward over 3,500 feet is totally unrealistic since the bottom hole  
23 injection pressure of these two SWD wells is at least 28 percent below fracture initiation pressures.  
24 Regardless, an RTT survey will detect a fluid path created by either of these scenarios.  
25

26 As a result of these allegations, the NMOCD requested the operators of the Todd 26 Federal #3 SWD  
27 well and the David Ross AIT Federal #1 SWD well to run an RTT to determine if injected fluids were  
28 migrating out of zone. On November 13, 1995, an RTT was conducted on the Todd 26 Federal #3  
29 SWD well by Cardinal Surveys Company, Hobbs, New Mexico. The survey was witnessed by a  
30 NMOCD representative. The RTT survey indicated no upward flow of fluids above the injection zone.  
31 On November 20, 1995, an RTT and a temperature survey were conducted on the David Ross AIT  
32 Federal #1 SWD well by Cardinal Surveys Company. The survey was witnessed by two NMOCD  
33 representatives. The results of the RTT and temperature survey indicated no vertical movement of  
34 water out of zone and that injected water was entering the perforated interval from 4,500-5,670 feet.  
35

36 A previous RTT was conducted on the David Ross AIT Federal #1 SWD on October 22, 1992 by  
37 Cardinal Surveys Company. Available records do not indicate the reason this survey was conducted.  
38 However, a copy of the RTT survey was available for evaluation. The survey results clearly indicate  
39 no upward movement of fluids above the perforated interval (4,500-5,670 feet). The perforated  
40 interval in this well was hydraulically fractured on September 24, 1991, and again on October 30-  
41 November 1, 1991 (additional perforations were added prior to the latter fracture treatment). It is clear  
42 that neither the cement sheath was compromised nor was a vertical fluid path was created above the  
43 perforated interval as a result of these fracture treatments. If such a near-wellbore fluid path had been  
44 created by the fracturing process it would have been detected by the subsequent RTT surveys  
45 conducted on October 22, 1992, and November 20, 1995.  
46  
47

1 **5.2 The Remainder of Eddy and Lea Counties Within the Delaware Basin**

2  
3 To enhance the validity of the failure analysis performed relative to the nine township area surrounding  
4 the WIPP, the study was expanded to cover the same types of wells outside the nine township area  
5 surrounding the WIPP in Lea and Eddy counties within the Delaware Basin. Within this expanded area  
6 are 25 active WI wells and 46 active SWD wells. There are 33 temporarily abandoned or inactive WI  
7 wells and 8 temporarily abandoned or inactive SWD wells. In addition, three applications for SWD  
8 wells are pending.

9  
10 Well records were obtained for this area on the total number of failures by type (i.e., tubing, packer,  
11 casing, or cement). During the past fifteen years, only 24 failures were identified. These failures are  
12 similar in nature and do not occur at a significantly different rate than those which occurred inside the  
13 nine township study area. (See Tables 2 and 3).

14  
15  
16 **Table 2. Salt Water Disposal/Injection Well Failures - Eddy County, New Mexico - Delaware Basin -**  
17 **Outside the Nine Townships Surrounding to the WIPP**

Well Name / Date of Conversion	Location	API #	Problem	Repairs	Date Returned to Injection
Sulphate Sister Converted to SWD 1/24/78	S13-T25S- R26E	30-015- 21029	1. Packer leak	1. Replaced packer; Passed MIT	1. 9/29/86
Federal AZ Converted to SWD 11/85	S29-T26S- R30E	30-015- 23324	1. Casing cement repaired	1. Re-cemented from 370' to the cellar after cement bond log indicated inadequate cement; Passed MIT	1. 12/17/89
Old Indian Draw Unit # 4 Converted to injection 2/76	S18-T22S- R28E	30-015- 21505	1. Packer leak	1. Repaired packer leakage; passed MIT	1. 8/19/92
Old Indian Draw Unit # 6 Converted to injection 11/84	S18-T22S- R28E	30-015- 21619	1. Tubing leak	1. Repaired tubing leaks; passed MIT	1. 7/9/93
Old Indian Draw Unit # 5 Converted to injection 3/85	S18-T22S- 28E	30-015- 21618	1. Tubing leak 2. Packer leak	1. Replaced 3 jts. Returned to injection; 2. Repaired packer leaks; Passed MIT	1. 10/25/91 2. 6/17/92
Salty Bill #1 Converted to SWD 2/26/72	S36-T22S- 26E	30-015- 10908	1. Tubing leak	1. Repair parted tubing	1. 7/29/95



1  
2  
3  
4  
5  
6  
7  
8  
9  
10  
11  
12  
13  
14  
15  
16  
17  
18  
19  
20  
21  
22  
23  
24  
25  
26  
27  
28  
29  
30  
31  
32  
33  
34

**Table 2. Salt Water Disposal/Injection Well Failures - Eddy County, New Mexico - Delaware Basin - Outside the Nine Townships Surrounding to the WIPP (Continued)**

Well Name / Date of Conversion	Location	API #	Problem	Repairs	Date Returned to Injection
Old Indian Draw Unit # 35 Converted to SWD 11/8/84	S7-T22S- R28E	30-015- 22182	1. Casing leaks	1. Repaired casing; Passed MIT	1. 12/17/96
Old Indian Draw Unit # 10 Converted to injection 12/83	S18-T22S- 28E	30-015- 21843	1. Tubing leak 2. Packer leak	1. Repaired packer leak 2. Repaired tubing leak; Passed MIT	1. 8/19/92 2. 8/19/92
Rohmer # 1 Converted to SWD 7/1/93	S23-T22S- R27E	30-015- 25722	1. Tubing leak	1. Ran string of new tubing; Passed MIT	1. 12/8/95
New Mexico DU # 1 Converted to SWD 12/93	S36-T22S- 27E	30-015- 24531	1. Tubing leak 2. Tubing repair	1. Repaired tubing leakage; Passed MIT 2. Repaired tubing due to metal loss and erosion; Passed MIT	1. 2/19/97 2. 7/03/96
Gourley Federal # 4 Converted to SWD 7/30/79	S31-T22S- R28E	30-015- 22661	1. casing leak 7' to 10' from surface	1. Repaired casing leaks by casing replacement and replacing one jt. of tubing; Passed MIT	1. 1/17/95
Russell Federal # 2 Converted to SWD 4/8/92	S35-T26S- R31E	30-015- 05891	1. Packer leak 2. Tubing leak	1. Ran new packer. Passed MIT 2. Ran one new jt. of tubing; Passed MIT.	1. 9/04/92 2. 8/30/95
McKenna Federal #2 Converted to SWD 12/9/69	S18-T26S- R30E	30-015- 20222	1. Casing leak @ 1202' - 1225'	1. Repaired Casing by squeezing cement; Passed MIT	1. 3/21/86

1  
2  
3  
4  
5  
6  
7  
8  
9  
10  
11

**Table 3. Salt Water Disposal/Injection Well Failures - Lea County, New Mexico - Delaware Basin - Outside the Nine Townships Directly Adjacent to the WIPP**

Well Name / Date of Conversion	Location	API #	Problem	Repairs	Date Returned to Injection
Thompson 19 Federal #2 Converted to SWD 11/26/68	S19-T26S-R32E	30-025-08266	1. Casing leak 2. Casing leak	1. Casing repaired; Passed MIT 2. Casing Repaired; Passed MIT	1. 1/10/90 2. 1/26/90
Jennings Federal #1 Converted to SWD 10/87	S14-T24S-R32E	30-025-08148	1. Tubing leak 2. Tubing leak 3. Packer leak 4. Casing leaks at 535' to 567'	1. Tubing leak repaired; Passed MIT 2. Tubing leak repaired; Passed MIT 3. Packer leak repaired; Passed MIT 4. Casing leaks repaired; Passed MIT	1. 5/30/90 2. 5/04/91 3. 5/04/91 4. 4/22/93
Ingram "O" State #2 Converted to SWD 9/4/74	S7-T24S-R33E	30-025-24432	1. Casing leak	1. Casing repaired; Passed MIT	1. 3/24/83
North El Mar Unit #50 Converted to SWD 5/12/77	S34-T26S-R2E	30-025-08305	1. Tubing leak	1. Repaired 2 jts of 2.378" tubing; Passed MIT	1. 5/16/90

12  
13  
14  
15  
16  
17  
18  
19  
20  
21

## 6.0 Carbon Dioxide (CO<sub>2</sub>) Miscible Flooding

22 The use of Carbon Dioxide (CO<sub>2</sub>) as an injection fluid to enhance the recovery of oil from below-  
23 ground reservoirs is a potential recovery process that could be used in both carbonate and sandstone  
24 reservoirs located in the Delaware Basin. The CO<sub>2</sub> enhanced recovery process consists of injecting a  
25 slug (a prescribed amount of CO<sub>2</sub>) into the reservoir followed by an injection of water and  
26 subsequent injection of a second CO<sub>2</sub> slug. This process is called the water-alternating-gas (WAG)  
27 injection method. Although CO<sub>2</sub> can be injected continuously, it is not cost effective to implement  
28 this type of process. Simultaneous injection of carbonated water has been tested in the laboratory  
29 and in the field, but the incremental oil recovery is less than that for the WAG process. The WAG  
30 process is the preferred method for using CO<sub>2</sub> as an enhanced oil recovery process.

31  
32 The miscibility of CO<sub>2</sub> in crude oil is a function of temperature, pressure, and impurities that may be  
33 present in the CO<sub>2</sub>, as well as the molecular weight of the heavy fraction of the crude oil. In CO<sub>2</sub>  
34 enhanced recovery processes, the ultimate oil recovery by this process is normally defined in terms  
35 of a minimum miscibility pressure (MMP). Technically, the MMP is defined as the pressure at  
36 which 80 percent of the oil in place is recovered at CO<sub>2</sub> breakthrough at a gas oil ratio (GOR) of  
37 40,000 standard cubic feet per barrel. The MMP does not represent the actual minimum miscibility  
38 pressure. However, it does represent a miscibility pressure that can be used in designing a CO<sub>2</sub>  
39 flood to have the greatest potential for economic success. From a practical standpoint, the MMP for  
40 a given reservoir of crude oil is that pressure above which a further increase produces only a

1 minimal increase in oil recovery. The MMP will dictate the maximum pressure at which CO<sub>2</sub> will be  
2 injected at the sand face (i.e., bottom hole injection pressure) to achieve miscibility of the CO<sub>2</sub> in the  
3 crude oil phase. It would not be economical to inject CO<sub>2</sub> at sand face pressures greater than the  
4 MMP. The type of crude oil (paraffinic or aromatic) also effects the MMP of CO<sub>2</sub> in crude oils.  
5 The determination of the MMP for a given reservoir oil must be experimentally determined prior to  
6 designing and implementing a CO<sub>2</sub> recovery project. An upper limit, however, can be estimated for  
7 the MMP for crude oils in reservoirs identified in the Delaware Basin of New Mexico. Oil  
8 reservoirs in the Delaware Basin of New Mexico that may be candidates for a CO<sub>2</sub> enhanced  
9 recovery process are at depths between 4,500-8,000 feet. The temperatures at these depths would  
10 vary between 105°-140°F (Davis and Faulk 1957). Using the accepted Holm-Josendal dynamic  
11 miscibility displacement correlation for CO<sub>2</sub> the MMP for the previous temperature ranges would be  
12 between 1,500-2,000 psi (Holm and Josendal, 1980).

13  
14 Existing bottom hole injection pressures (BHIP) for WI and SWD wells located in the nine township  
15 area surrounding the WIPP site vary between 2,284 psi and 3,778 psi. These bottom hole injection  
16 pressures were calculated based upon NMOCD permitted surface injection pressures and water  
17 injection rates. Fluid friction was taken into account in the calculations. It was further assumed that  
18 the tubing in the well was new, resulting in a lower friction pressure drop than would be the case for  
19 used tubulars. The average bottom hole injection pressure of these 24 active WI and SWD wells  
20 located within the nine township area surrounding the WIPP was calculated to be 3,197 psi. Hence,  
21 all SWD and WI wells located in the nine township area surrounding the WIPP currently operate at a  
22 BHIP greater than the MMP for CO<sub>2</sub> for oil reservoirs in the Delaware Basin of New Mexico that  
23 may be candidates for implementation of this type of enhanced oil recovery process.

24  
25 During the process of injecting the CO<sub>2</sub>, the surface well head pressure will be higher than when  
26 water is being injected in order to achieve the design MMP at the bottom of the hole. However, the  
27 MMP at the bottom of the hole will be less than the BHIP calculated for the existing active WI and  
28 SWD wells located in the nine township area surrounding the WIPP site. Hence, it is more likely a  
29 downhole failure of the tubing, packer, casing, etc. will occur during water injection than during  
30 CO<sub>2</sub> injection since the BHIP will be higher.

31  
32 As an example, the SACROC Unit of the Kelly-Snyder Field, Scurry County, Texas is the largest  
33 CO<sub>2</sub> flood ever implemented. The unit produces from the Canyon Reef reservoir at a depth of from  
34 6,600 - 6,900 feet. The reservoir temperature is 135°F and the reservoir pressure was 2,400 psi at  
35 the start of the CO<sub>2</sub> flood. The MMP for the crude oil in the reservoir is 1,850 psi (IOCC 1974).  
36 This particular CO<sub>2</sub> flood continues to be an economic success.

37  
38 From a mechanical equipment and operations standpoint, injection wells in a CO<sub>2</sub> recovery process  
39 do not differ substantially from an WI well in a water flood process or a SWD well. However, due  
40 to the corrosive nature of CO<sub>2</sub>, more attention is given to the selection of corrosion-inhibitive pipe,  
41 wellhead equipment, flowlines, and valves and fittings that are installed in CO<sub>2</sub> injection wells.  
42 Further, to minimize the amount of CO<sub>2</sub> lost in the recovery process, more sophisticated monitoring  
43 equipment is installed at the wellhead to identify potential downhole problems associated with  
44 tubing, packer, and casing leaks. Most of the CO<sub>2</sub> that is injected into the producing formations is  
45 recovered with the oil and water by the producing wells, separated at the surface treating facilities,

1 mixed with additional ("make-up") CO<sub>2</sub>, compressed, and reinjected into the reservoir. Make-up  
2 CO<sub>2</sub> represents the amount of CO<sub>2</sub> that is lost in the reservoir or escaped via a downhole or surface  
3 leak. Given the associated expense, and the need to comply with the UIC, the operator of a CO<sub>2</sub>  
4 enhanced oil recovery project will conduct more frequent testing to identify and correct downhole  
5 failures. Additionally, the operator will be far more concerned about fluids migrating out of zone  
6 through a cement sheath failure or a vertically created fracture as a result of injecting at pressures  
7 considerably above formation fracturing pressures. The latter is highly unlikely due to the low  
8 miscibility of CO<sub>2</sub> in crude oil and salt water. A prudent operator of a CO<sub>2</sub> recovery project cannot  
9 afford to allow this to happen.

10  
11 Although there are no CO<sub>2</sub> recovery projects in operation (nor are any planned for the foreseeable  
12 future) in the area surrounding the WIPP, it is unlikely that failure rates for CO<sub>2</sub> injection wells  
13 would be higher than for the SWD and WI wells discussed previously. Regardless, the response  
14 time for correcting a failure will be much shorter for CO<sub>2</sub> injection wells than in conventional WI  
15 and SWD wells, primarily due to the economics associated with CO<sub>2</sub> recovery processes. The  
16 failure rate for CO<sub>2</sub> injection wells will be defined by the failure rate for existing WI and SWD  
17 wells.

## 18 19 20 **7.0 Duration of Leaks**

21  
22 The records show that when leaks are identified they are repaired very quickly. Operators visit these  
23 wells one to two times a week, and will notice obvious problems (leak types 1 and 2) and take  
24 corrective action. However, some leaks may not be identified during a routine check. For example,  
25 if a casing leak were to exist (leak type 3), but the packer and tubing were intact and functioning  
26 properly, a BHT may not identify a casing leak, however an MIT would. In addition, as discussed  
27 previously in Section 4.1, a failure of the cement sheath (leak type 4) would not be identifiable by a  
28 BHT or an MIT and could continue for longer periods of time.

29  
30 It is recommended that the duration of leak types 1 and 2 be conservatively estimated at one year.  
31 This is based on the regulatory requirement to perform a BHT no less frequently than once annually.  
32 This is reasonable because in no instances did the records show that the required annual tests were  
33 not performed. In addition, it is recommended that casing leaks (leak type 3) will have no more than  
34 a five year duration. This is based on the requirement to conduct an MIT no less frequently than  
35 once every five years.

## 36 37 38 **8.0 Failure Rates**

39  
40 Failures were determined by evidence in the well records on file at the NMOCDC offices.

41  
42 Of the 28 failures identified, 8 were casing failures, 11 were tubing failures, 7 were packer failures,  
43 1 bradenhead line leak, and 1 remedial cement operation (squeeze job).

44  
45 Failure rates were based upon the following criteria:

1. The failure rate is defined to be the ratio of the number of actual well failures to the number of years of regulated service.
2. The maximum period of regulated service a well can have is fifteen years (1982 - 1996). The regulated service value was determined by counting months of service since 1982 on currently active SWD and WI wells and dividing by 12. The period of service (in months) for each well in this analysis is provided in Attachment 5.
3. Well failures mean actual incidences of mechanical failure and do not include such operations as acidizing, casing upgrades, or other normal preventative maintenance or modernization activities.
4. Failure rates were computed for the following cases:
  - a) Eddy County portion inside the nine township area
  - b) Eddy County portion outside the nine township area but within the Delaware Basin
  - c) Lea County portion inside the nine township area
  - d) Lea County portion outside the nine township area but within the Delaware Basin
  - e) Total failure rate for Eddy County inside the Delaware Basin
  - f) Total failure rate for Lea County inside the Delaware Basin
  - g) Total failure rate for the nine township area
  - h) Total failure rate for the New Mexico portion of the Delaware Basin

The equation used to determine the failure rate is:

$$\text{Failure Rate} = \frac{\Sigma (\text{Failures})}{\Sigma (\text{Number of years of regulated operation})}$$

### 8.1 -- Failure Rate Calculations:

a. Eddy County portion inside the nine Townships of the Delaware Basin

$$\text{a. } \frac{1 \text{ Casing Leak}}{51 \text{ years of Regulated Operation}} = .020$$

b. Eddy County portion outside the nine Townships in the Delaware Basin

$$\text{b. } \frac{(8 \text{ Tubing Leaks} + 5 \text{ Packer Leaks} + 3 \text{ Casing Leaks} + 1 \text{ Cement})}{372 \text{ years of Regulated Operation}} = .045$$

c. Lea County portion inside the nine Townships of the Delaware Basin

$$\text{c. } \frac{(1 \text{ Hairline crack of Bradenhead line} + 1 \text{ Tubing Leak})}{55 \text{ years of Regulated Operation}} = .036$$



1  
2 d. Lea County portion outside the nine Townships in the Delaware Basin  
3

4 d. 
$$\frac{(4 \text{ Casing Leaks} + 3 \text{ Tubing Leaks} + 1 \text{ Packer Leak})}{294 \text{ years of Regulated Operation}} = .027$$
  
5  
6

7 e. Total Failure Rate for Eddy County  
8

9 e. 
$$\frac{18 \text{ Failures}}{423 \text{ years of Regulated Operation}} = .043$$
  
10  
11

12 f. Total Failure Rate for Lea County  
13

14 f. 
$$\frac{10 \text{ Failures}}{350 \text{ years of Regulated Operation}} = .029$$
  
15  
16

17 g. Total Failure Rate for the nine Townships  
18

19 g. 
$$\frac{3 \text{ Failures}}{106 \text{ years of Regulated Operation}} = .028$$
  
20  
21

22 h. Total Failure Rate for the New Mexico Portion of the Delaware Basin  
23

24 h. 
$$\frac{28 \text{ Failures}}{772 \text{ years of Regulated Operation}} = .036$$
  
25  
26

## 27 28 9.0 Conclusions 29

30 The most plausible explanation for the low failure rate observed for injection wells in the vicinity of  
31 the WIPP relates directly to the region's geology. The Delaware Basin is a mature geologic basin  
32 with little tectonic activity over the past 240 million years. Since there is little or no uplifting or  
33 faulting in this region, and due to the nature of the formations encountered, wellbores are drilled  
34 with little difficulty and result in reasonably gauged straight holes. Therefore, there is little evidence  
35 that operators have to resort to remedial cementing procedures (referred to as squeeze cementing) to  
36 repair a bad primary cement job. Of the 24 wells evaluated within the nine townships, only one  
37 squeeze cementing operation was done to repair a casing leak. It should be noted that this casing  
38 leak was discovered *before* the well had begun disposal operations. The casing integrity is also  
39 prolonged by the NMOCD requirement that drilling fluids must be salt saturated when drilling  
40 through the Salado Formation. In addition, salt treated cement slurries are used for cementing  
41 intermediate or production strings across the salt formation. This also helps maintain the integrity of  
42 the casing. Further, the use of corrosion inhibiting fluids in the annular space between casing and  
43 injection tubing (see Figures 3 and 4) also adds to this longevity, thereby minimizing casing failures.  
44

45 From an evaluation of the data for the 24 wells within the nine township area, it can be concluded  
46 that the failures identified by scheduled and unscheduled BHTs and MITs (tubing, packer, and

1 production casing failures) will have no effect upon the integrity of the WIPP.

2  
3 A failure mechanism more difficult to assess, however, is the creation of a fluid path through the  
4 cement sheath between wellbore and casing. As discussed previously, detection of a fluid path  
5 behind casing can be determined by conducting an RTT as was done for the Todd 26 Federal #3  
6 SWD. Because this is not a regularly scheduled test, a fluid path created in the cement sheath would  
7 probably go undetected for a much longer period of time than a failure detected by a BHT or MIT.  
8 This would be particularly true for an SWD well, whereas, it would more likely be discovered in a  
9 WI well since the oil recovery of nearby producing wells would be adversely affected by the loss of  
10 injection fluids. For this reason, it is this type of leak (Type 4) that merits additional consideration.  
11 The potential impacts of this scenario will be evaluated through computer modeling.

12  
13 Investigation of the 24 WI and SWD wells located in the nine townships surrounding the WIPP  
14 indicate there is an average probability of .028 per year that a given well will have a failure that can  
15 be detected by a BHT or MIT. Although there is no known test (other than the RTT survey) to  
16 identify a failure in the cement sheath, the lack of a statistically significant number of squeeze  
17 cement operations conducted in the study area indicates cement sheath failure is unlikely.

18  
19 Results from the analysis conducted on SWD and WI wells located in Eddy and Lea counties that are  
20 outside the targeted nine township area surrounding the WIPP validate results from the same analysis  
21 conducted for those wells located inside the targeted area. Combining all the failures associated with  
22 SWD and WI wells located in the New Mexico portion of the Delaware Basin, there is a .036 per  
23 year probability that a given SWD or WI well will experience a failure.

24  
25 This low probability for failure can be attributed to the following:

- 26
- 27 • The NMOCDC is responsive and efficient to insure that oil and gas producers comply with the  
28 regulations.
  - 29
  - 30 • Oil and gas producers in the Delaware Basin of New Mexico appear to be prudent operators;  
31 they readily identify and correct failures that may have a negative effect upon the  
32 environment as well as their own operations and reputations.
  - 33
  - 34 • The geology of the Delaware Basin of New Mexico is conducive to the drilling of straight  
35 wellbores insuring quality primary cement jobs. Adherence to good practice when drilling  
36 through salt formations like the Salado, and methods of setting and cementing casing  
37 compatible with a salt environment contribute to the low failure rates.
  - 38
  - 39 • Adherence to surface injection pressures of WI and SWD wells as specified by the NMOCDC  
40 (0.2 psi/ft depth) insures injected water is confined to the permitted injection interval and  
41 does not migrate vertically upward through a hydraulically created vertical fracture or  
42 compromise the cement sheath between casing and formation.
  - 43

44 It is likely that this probability for failure will decrease in the future. Operators will continue to  
45 comply with applicable regulatory requirements. Advances in processes, technologies, and materials  
46 will make the operation of WI and SWD wells more predictable in the future.

1 10.0 References

2  
3  
4  
5  
6  
7  
8  
9  
10  
11  
12  
13  
14  
15  
16  
17  
18  
19  
20  
21  
22  
23  
24  
25  
26  
27  
28  
29  
30  
31  
32  
33  
34  
35  
36  
37  
38  
39  
40  
41  
42

Amyx, J.W., D.M. Bass, and R.L. Whiting, 1960. Petroleum Reservoir Engineering - Physical Properties. McGraw - Hill: New York, New York.

Davis, S.H. and J.H. Faulk, 1957. *Have Waiting on Cement Practices Kept Pace with Technology?* Journal of Drilling and Production Practices. American Petroleum Institute: Dallas, Texas

EPA (U.S. Environmental Protection Agency), 1997. Letter from E. Ramona Trovato, Director Office of Radiation and Indoor Air to Alvin Alm, Assistant Secretary for Environmental Management, U.S. Department of Energy: March 19, 1997.

EPA (U.S. Environmental Protection Agency), 1993. 40 CFR Part 191, Environmental Radiation Protection Standards for the Management and Disposal of Spent Nuclear Fuel, High-Level and Transuranic Radioactive Wastes; Final Rule. Federal Register, Vol. 58, No. 242, jpp. 66398 - 66416, December 20, 1993. Office of Radiation and Indoor Air: Washington, D.C.

EPA (U.S. Environmental Protection Agency), 1983. 40 CFR Part 144, Underground Injection Control Program. Federal Register, Vol. 48, pp. 14189, April 1, 1983. Environmental Protection Agency: Washington, D.C.

Halliburton Energy Services, 1986. FRACBOOK II - Design/Data Manual for Hydraulic Fracturing. Halliburton Energy Services: Duncan, Oklahoma.

Holm, L.W. and V. A. Josendal, 1980. *Effect of Oil Composition on Miscible-Type Displacement by Carbon Dioxide*, Proceedings SPE/DOE Symposium on Enhanced Oil Recovery, Tulsa, Oklahoma, April 20-23, 1980. (SPE Paper #8814). Society of Petroleum Engineers: Richardson, Texas.

IOCC (Interstate Oil Compact Commission), 1974. *Secondary and Tertiary Oil Recovery Processes, Second Edition*. December, 1974. Oklahoma City, Oklahoma.

Petroleum Information Corporation, 1997. *PetroROM: Permian Basin 7C, 8, 8A-November 1996. Southeast New Mexico-September 1996*. Production Data. Houston, Texas.

Schlumberger Educational Services, 1989. *Schlumberger Cased Hole Log Interpretation: Principles/Applications*. Schlumberger: Houston, Texas.

1  
2  
3  
4  
5  
6  
7  
8  
9  
10  
11  
12  
13  
14  
15  
16  
17  
18  
19  
20  
21

**Attachment 1**

**Permitted SWD and WI Wells in the  
Nine Township Area Surrounding the WIPP Site**

**Information Only**

**ACTIVE INJECTION WELLS  
IN THE NINE TOWNSHIP AREA SURROUNDING THE WIPP  
(EDDY COUNTY PORTION).**

	Well name location API # County Elevation at KB Elevation at GL	Well Type	Injection or Disposal Intervals (location of perforations)	Permitted Injection Pressure  [actual if avail]	Well Status	Test Information	Average barrels per month
EJ-1	James A # 3 22S/30E/02 API# 30-015-25758 Eddy County Elevation at KB 3178' Elevation at GL 3167'	Injection	4802' top perfs 5136' lower perfs 493 shots over a 334' span	945 psi  [660 - 910]	Active	converted to injection 3/93; BHT dates: 5/94, 5/96, passed MIT dates: 9/95, passed	48,276 bbls/mo average (6/93 to 2/97)
EJ-2	James A # 12 22S/30E'02 API# 30-015-26761 Eddy County Elevation at KB 3196' Elevation at GL 3197'	Injection	5388' top perfs 7408' lower perfs 286 shots over a 2020' span	1120 psi  [380 - 910]	Active	converted to injection 5/91 BHT dates: 5/94, 5/96 passed MIT dates: 5/95 passed	60,835 bbls/mo average (1/94 to 2/97)
EJ-3	Neff Fed. #3 22S/31E/25 API # 30-015-28281 Eddy County Elevation at KB Elevation at GL 3572'	Injection	7050' to 7068'	1410 psi  [vacuum]	Active	Converted to injection 3/96 BHT dates: 3/96, 7/96	N/A



**ACTIVE SALT WATER DISPOSAL WELLS  
IN THE NINE TOWNSHIP AREA SURROUNDING THE WIPP  
(EDDY COUNTY PORTION) (Continued)**

	Well name location API # County Elevation at KB Elevation at GL	Well Type	Injection or Disposal Intervals (location of perforations)	Permitted Injection Pressure  [actual if avail]	Well Status	Test Information	Average barrels per month
ES-1	Legg Fed. # 1 22S/30E/27 API # 30-015-04734 Eddy County Elevation at KB 3309' Elevation at GL 3328'	SWD	3820' upper 3915' lower 3915' - 3990' 4125' - 4185' 4220' - 4280' 4295' - 4335' 4430' - 4470' 4485' - 4505' 4580' - 4620'	764 psi  [500 - 750]	Active	converted to SWD 3/94 MIT dates: 5/94, 8/94, 9/95 passed BHT dates: 5/95, 7/96 passed	14,735 bbls/mo. average 8/95 to 2/97)
ES-2	Getty 24 Fed #5 22S/31E/24 API # 30-015-26848 Eddy County Elevation at KB 3574' Elevation at GL 3556'	SWD	4519' to 4568' 4582' to 4688' 4832' to 4868' 4946' to 4970' 5034' to 5110'	904 psi  [615-900]	Active	converted to SWD 9/91 MIT dates: 8/95 passed BHT dates: 7/93, 6/94, 6/96 passed	56,482 bbls/mo average (1/94 to 2/97)
ES-3	Davis Ross AIT Federal # 1 API # 30-015-26629 Eddy County Elevation at KB Elevation at GL 3463'	SWD	4500' to 4590 4866' - 4907' 4944' - 4975' 5108' - 5120' 5158' - 5180' 5328' - 5346' 5401' - 5421' 5460' - 5670'	900 psi  [175 - 900]	Active	converted to SWD 5/91 MIT dates: 8/95 passed BHT dates: 6/94, 6/96 passed	71,561 bbls/mo average (1/94 to 1/97)

**ACTIVE SALT WATER DISPOSAL WELLS  
IN THE NINE TOWNSHIP AREA SURROUNDING THE WIPP  
(EDDY COUNTY PORTION) (Continued)**

	Well name location API # County Elevation at KB Elevation at GL	Well Type	Injection or Disposal Intervals (location of perforations)	Permitted Injection Pressure  [actual if avail]	Well Status	Test Information	Average barrels per month
ES-4	Todd 26 Fed #3 23S/31E/26 API # 30-015-20302 Eddy County Elevation at KB Elevation at GL 3416'	SWD	4379' to 5700'	878 psi  [240-875]  (This well has been injecting since 1971 before UIC)	Active	converted to SWD 7/71 BHT dates: 7/93, 6/94, 10/95, 6/96 passed MIT dates: 8/95 passed	53,758 bbls/mo average (1/94 to 12/96)
ES-5	Todd 26 G Fed#2 API# 30-015-20277 Eddy County Elevation at KB 3454' Elevation at GL 3443'	SWD	4460' to 5134' 408 shots over 670'	892 psi  [257 - 812]	Active	converted to SWD 11/92 MIT dates: 1/93, 8/95 passed BHT dates: 6/94, 6/96 passed	29,448 bbls/mo average (1/94 to 12/96)
ES-6	Sand Dunes 28 Federal #1 API # 30-015-26194 Eddy County Elevation at KB 3397' Elevation at GL 3368'	SWD	5500' to 5550' 200 shots over 50'	859 psi  [N/A]	Active	converted to SWD 5/93 BHT dates: 7/94, 7/96 passed MIT dates: 9/95 passed	34,720 bbls/mo average (1/95 to 1/97)

**ACTIVE SALT WATER DISPOSAL WELLS  
IN THE NINE TOWNSHIP AREA SURROUNDING THE WIPP  
(EDDY COUNTY PORTION) (Continued)**

	Well name location API # County Elevation at KB Elevation at GL	Well Type	Injection or Disposal Intervals (location of perforations)	Permitted Injection Pressure  [actual if avail]	Well Status	Test Information	Average barrels per month
ES-7	Calmon # 5 23S/31E/35 API # 30-015-25640 Eddy County Elevation at KB 3486' Elevation at GL 3475	SWD	4931' to 4973' 4994' to 5090' 5117' to 5148' 676 holes	897 psi (original pressure)  Increased to 998 psi 12/93  [700 - 900]	Active	converted to SWD 5/93 BHT dates: 7/94, 7/96 passed MIT dates: 9/95 passed	18,418 bbls/mo average (1/94 to 1/97)
ES-8	Todd 36 State 1 23S/31E/36 API # 30-015-20341 Eddy County Elevation at KB Elevation at GL 3499'	SWD	5980' to 6030' 6130' to 6200' 6360' to 6560'	1196 psi  [377-720]	Active	converted to SWD 4/94 MIT dates: 7/94, 8/95 passed BHT dates: 6/96 passed	48,916 bbls/mo average (12/94 to 5/96)

**ACTIVE SALT WATER DISPOSAL WELLS  
IN THE NINE TOWNSHIP AREA SURROUNDING THE WIPP  
(LEA COUNTY PORTION)**

	Well name location API # County Elevation at KB Elevation at GL	Well Type	Injection or Disposal Intervals (location of perforations)	Permitted Injection Pressure  [actual if avail]	Well Status	Test Information	Average barrels per month
LS-1	Union AJS Fed#1 21S32E/08 API# 30-025-31412 Lea County Elevation at KB Elevation at GL 3685'	SWD	4826' to 4838' 4996' to 5190' 5308' to 5616' 5794' to 5798'  (operator ran 6197' of new 5.5" casing and circulated cement to the surface when converting to SWD)	965 psi  [650 - 700]	Active	converted to SWD 1/92 Date of first injection 11/93 MIT date: 7/93 BHT dates: 11/94, 11/95, 11/96 test info to be obtained	37,075 bbls/mo average (1/94 to 6/96)
LS-2	Luke Fed.#1 21S/32E/31 API# 30-025-31443 Lea County Elevation at KB Elevation at GL 3646'  Renamed: Lost Tank #1	SWD	5296' to 5326' 5373' to 5386' 5442' to 5462' 5496' to 5506' 5552' to 5573' 5604' to 5636' 5654' to 5666' 5716' to 5748' 5776' to 5792' 5820' to 5830' 5838' to 5878' 5892' to 5916' 5930' to 5966' 5982' to 6012'	924 psi  [300]	Active	converted to SWD 5/92 MIT date: 5/92, 12/94 passed BHT dates: 12/93, 12/94, 12/96, passed	1,549 bbls/mo (one month of data: 9/96)

**ACTIVE SALT WATER DISPOSAL WELLS  
IN THE NINE TOWNSHIP AREA SURROUNDING THE WIPP  
(LEA COUNTY PORTION) (Continued)**

	Well name location API # County Elevation at KB Elevation at GL	Well Type	Injection or Disposal Intervals (location of perforations)	Permitted Injection Pressure  [actual if avail]	Well Status	Test Information	Average barrels per month
LS-3	Prohibition Fed Unit #2 22S/32E/11 API# 30-025-31716 Lea County Elevation at KB Elevation at GL 3746'	SW D	5220' - 5386' 32 holes  5804' - 5942' 34 holes	1044 psi  [450 - 600]	Active	converted to SWD 9/ 94 MIT dates: 3/95 passed BHT dates: 3/96, 11/96 passed	13,202 bbls/mo average (from 4/95 to 5/96)
LS-4	Red Tank Fed#2 22S/32E/14 API# 30-025-08113 Lea County Elevation at KB Elevation at GL 3733'	SWD	5382' to 5602'	1150 psi  [200]	Active	converted to SWD 6/94 BHT dates: 3/96, 3/97 passed MIT dates: 7/94 passed (While converting to an SWD, found hole in casing between 100' and 40'. Squeezed with 150 sx cement; ran new casing from surface to 6215' and circulated cement to surface.) (Note: This is not considered an injection well failure because injection had not yet commenced.)	41,490 bbls/mo average (7/94 to 2/96)



**ACTIVE SALT WATER DISPOSAL WELLS  
IN THE NINE TOWNSHIP AREA SURROUNDING THE WIPP  
(LEA COUNTY PORTION) (Continued)**

	Well name location API # County Elevation at KB Elevation at GL	Well Type	Injection or Disposal Intervals (location of perforations)	Permitted Injection Pressure  [actual if avail]	Well Status	Test Information	Average barrels per month
LS-5	Kiwi AKX State well #8 22S/32E/16 API# 30-025-31889 Lea County Elevation at KB Elevation at GL 3746'	SWD	8443' to 8470' 8539' to 8562' 8653' to 8710'	1048 psi  [40 - 300]	Active	Converted to SWD 4/93 BHT dates: 11/95, 11/96 passed MIT dates: 11/94 passed	46,932 bbls/mo average (2/95 to 6/96)
LS-6	Gilmore FED #1 22S/32E/21 API# 30-025-08109 Lea County Elevation at KB Elevation at GL 3678'	SWD	4807' to 5110'	951 psi  [650]	Active	Converted to SWD 4/92 MIT date: 5/92, 3/97 passed BHT dates 3/93, 3/94, 3/95, 3/96 passed	25,558 bbls/mo average (1/94 to 10/96)
LS-7	Proximity 31 Federal #4 22S/32E/31 API# 30-025-20423 Lea County Elevation at KB Elevation at GL 3527'	SWD	5174' - 5202' 5212' - 5230' 5310' - 5324' 5526' - 5554'	932 psi	Active	Converted to SWD 1/94 MIT dates 3/94 passed BHT dates: 3/95, 3/96, 3/97 passed  (new 5.5" casing and cement to surface when converted to SWD)	56,454 bbls/mo (one month of data [10/95])

**ACTIVE SALT WATER DISPOSAL WELLS  
IN THE NINE TOWNSHIP AREA SURROUNDING THE WIPP  
(LEA COUNTY PORTION) (Continued)**

	Well name location API # County Elevation at KB Elevation at GL	Well Type	Injection or Disposal Intervals (location of perforations)	Permitted Injection Pressure  [actual if avail]	Well Status	Test Information	Average barrels per month
LS-8	Red Tank 35 Federal #3 22S/32E/35 API# 30-025-33149 Lea County Elevation at KB Elevation at GL 3726'	SWD	6048' to 6252'	990 psi	Active	converted to SWD 12/95 MIT date 11/95 passed BHT dates: 4/96, 3/97 passed  (new 5.5" casing and cement to surface when converted to SWD)	N/A
LS-9	Cuervo Fed #1 23S/32E/14 API# 30-025-26844 Lea County Elevation at KB Elevation at GL 3705'	SWD	5520' to 5549' 5598' to 5592' 5686' to 5671' 5871' to 5858' 5998' to 5987'	1100 psi  [650]	Active	Converted to SWD 7/91 MIT date 8/92, 3/96 passed BHT dates: 3/93, 3/94, 3/95, 3/96, 3/97 passed	10.452 bbls/mo average (1/94 to 10/96)
LS-10	James Fed #1 23S/32E/29 API# 30-025-31515 Lea County Elevation at KB 3659' Elevation at GL 3664'	SWD	4844' to 6160'	969 psi  [650]	Active	Converted to SWD 8/92 BHt dates 10/93, 1/94, 12/95 passed Tracer run 8/92	20,605 bbls/mo average (1/93 to 6/96)

**ACTIVE SALT WATER DISPOSAL WELLS  
IN THE NINE TOWNSHIP AREA SURROUNDING THE WIPP  
(LEA COUNTY PORTION) (Continued)**

	Well name location API # County Elevation at KB Elevation at GL	Well Type	Injection or Disposal Intervals (location of perforations)	Permitted Injection Pressure  [actual if avail]	Well Status	Test Information	Average barrels per month
LS-11	James Fed #1 23S/32E/35 API# 30-025-08128 Lea County Elevation at KB Elevation at GL 3692'	SWD	5070' to 5097	1014 psi  [850]	Active	converted to SWD 5/69 MIT date: 1/87, 12/96 passed BHT dates 1/87, 12/90, 12/91, 11/92, 1/94, 11/95, passed	934 bbls/mo average (1/94 to 5/96)
LS-12	SDE 31 Fed # 9 23S/32E/31 API# 30-025-32868 Lea County Elevation at KB 3602' Elevation at GL 3591'	SWD	5178' - 5724'	1020 psi	Active	converted to SWD 4/96 MIT date: 12/96 passed	N/A
LS-13	Flamenco Fed. #1 22S/32E/07 API# 30-025-31076 Lea County Elevation at KB Elevation at GL 3642'	SWD	4676' to 4792' 5114' to 5306' 5575' to 5670' 5776' to 5814'	920 psi	Active	Converted to SWD 6/91 MIT dates: 11/95, 6/91 passed BHT dates : 12/92, 12/93, 11/94, 11/95, 11/96 passed  (11/95 test identified leak, was repaired with 2 joints 3.5" tubing; resumed injection)	500 bbls per day (permitted)

**SHUT-IN / TEMPORARILY ABANDONED  
SALT WATER DISPOSAL AND INJECTION WELLS  
IN THE NINE TOWNSHIP AREA SURROUNDING THE WIPP**

	Well name location API # County Elevation at KB Elevation at GL	Well Type	Injection or Disposal intervals (location of perforations)	Permitted Injection Pressure	Well Status	Test Information	Average barrels per month
TA-1	Triste Draw 36 State # 1 23S/32E/36 API# 30-025-31929 Lea County Elevation at KB Elevation at GL 3682'	SWD	5268' to 6294'	1073 psi	Shut-in	Converted to SWD 10/95 MIT date 10/95 passed BHT date: 12/96 passed	Records dating 4/96 to 10/96 show no injection
TA-2	Red Tank 28 Fed #3-B 22S/32E/28 API# 30-025-31754 Lea County Elevation at KB Elevation at GL 3621'	SWD	4674' to 4698' 5434' to 5748'	938 psi	Shut-in	Converted to SWD 9/94 MIT date: 3/94 passed BHT dates: 3/95, 4/96, 3/97 passed	N/A

**PENDING SALT WATER DISPOSAL AND INJECTION WELLS  
IN THE NINE TOWNSHIP AREA SURROUNDING THE WIPP**

	Well name location API # County Elevation at KB Elevation at GL	Well Type	Injection or Disposal intervals (location of perforations)	Permitted Injection Pressure  [actual]	Well Status	Test Information	Average barrels per month
PE-1	Charger 29 Fed#1 23S/30E/29 API# 30-015-28808 Eddy County Elevation at KB Elevation at GL 3088'	SWD	5479' to 7220'	1096 psi	Pending	Converted to SWD 6/96  MIT and BHT dates must be obtained	N/A



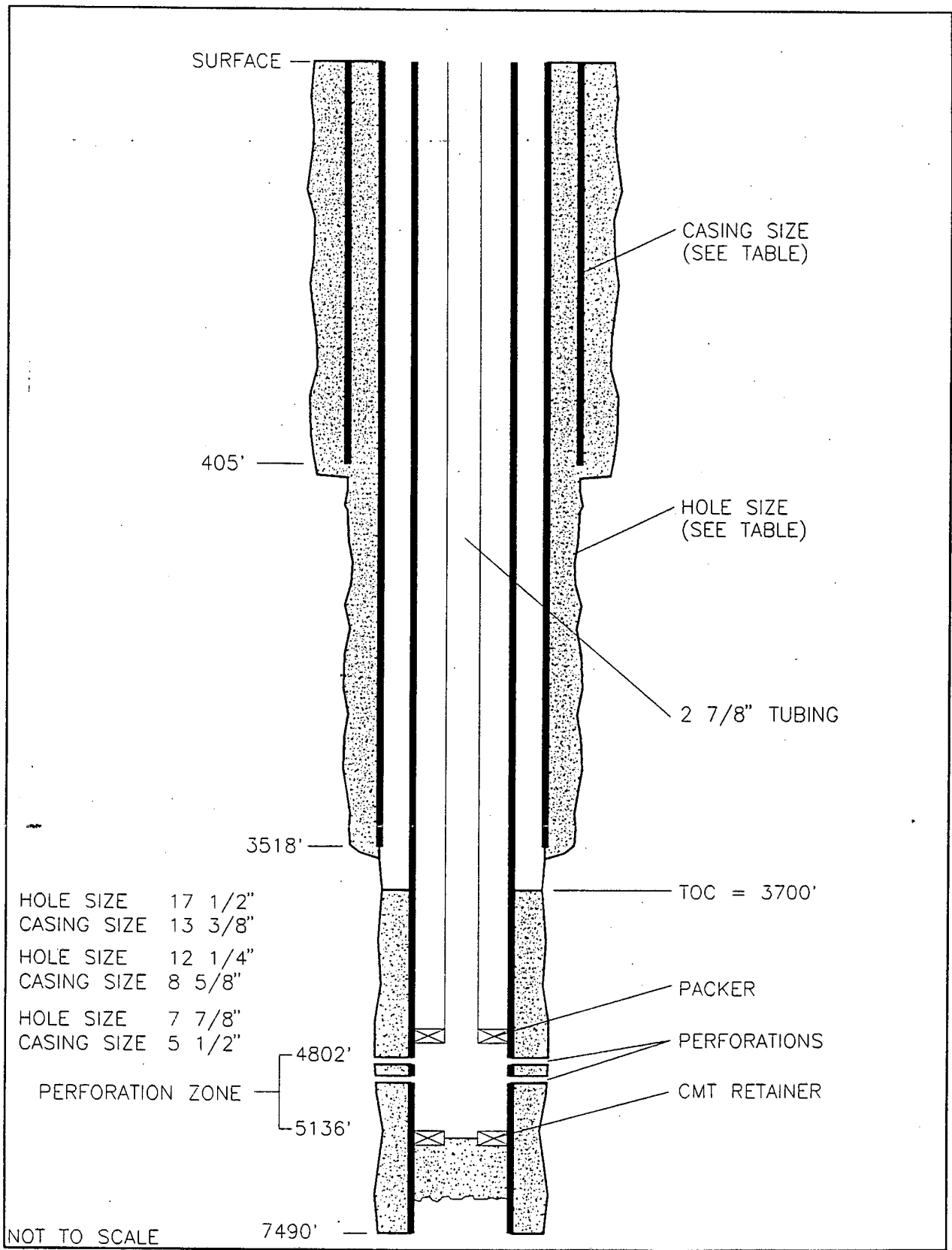
1  
2  
3  
4  
5  
6  
7  
8  
9  
10  
11  
12  
13  
14  
15  
16  
17  
18  
19  
20  
21  
22  
23

**Attachment 2**

**Wellbore Diagrams for the Active and Inactive**

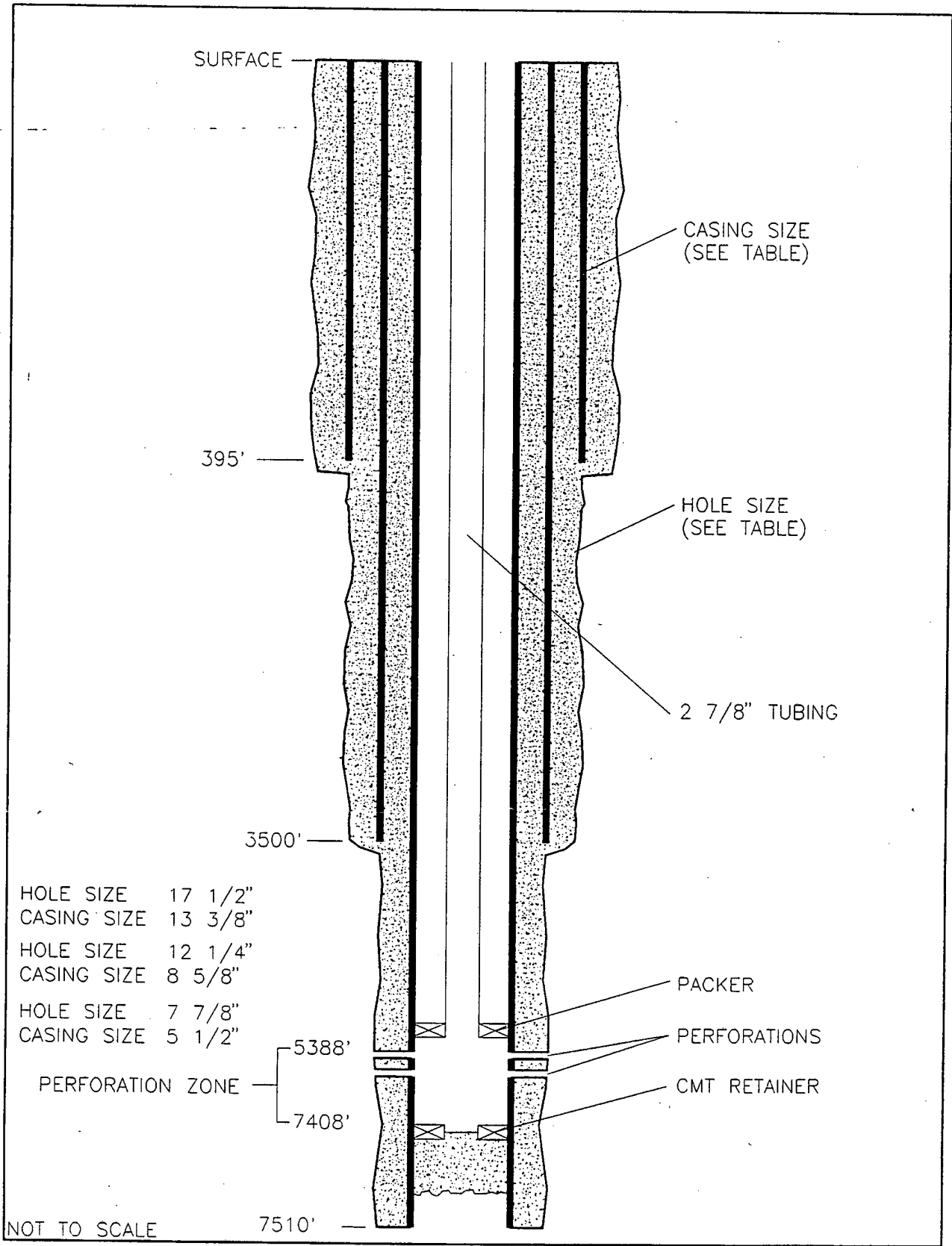
**SWD and WI Wells in the**

**Nine Township Area Surrounding the WIPP Site**



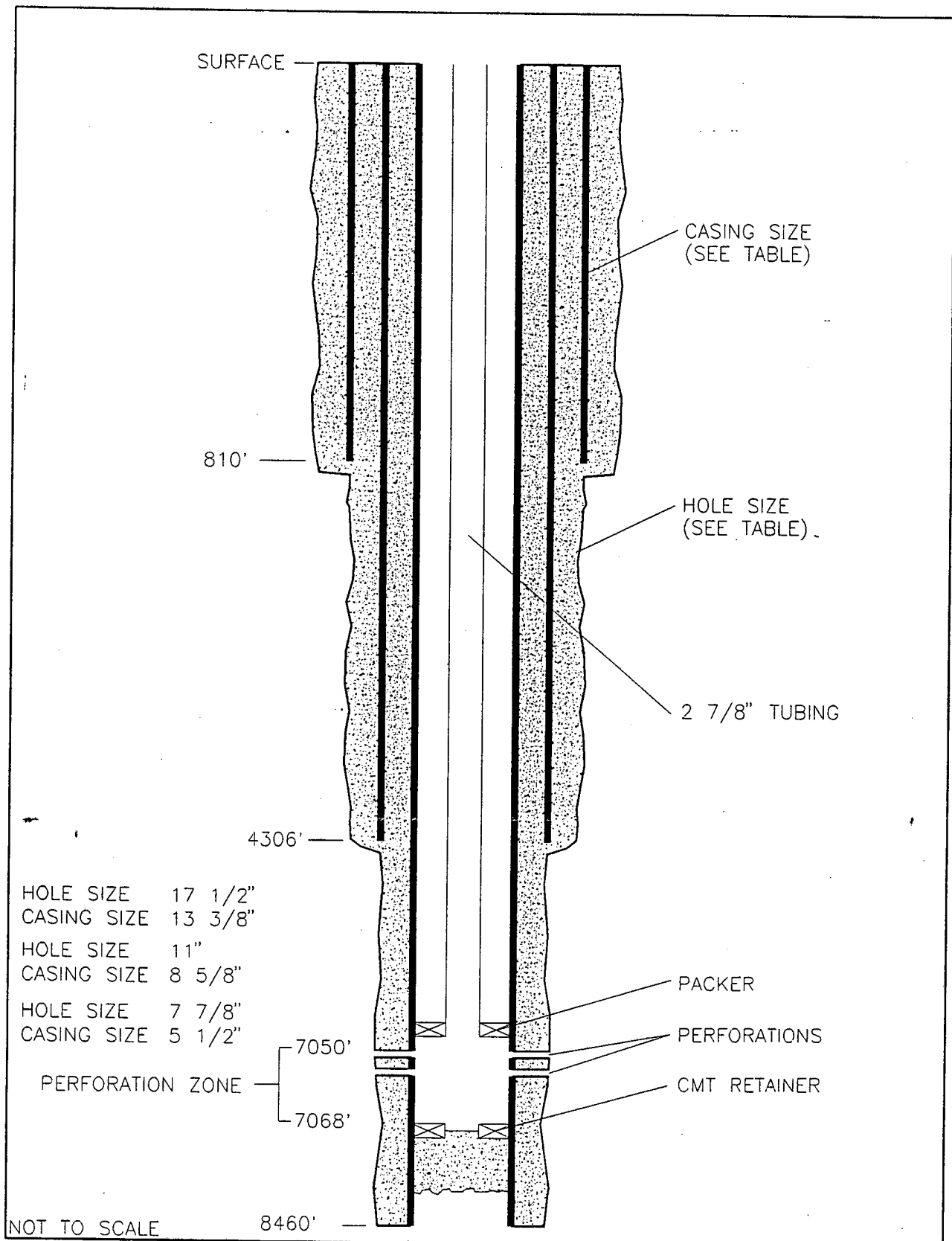
CASING AND TUBING FOR WELL # 30015257580000  
 JAMES A #3 - 225-30E-02

Information Only



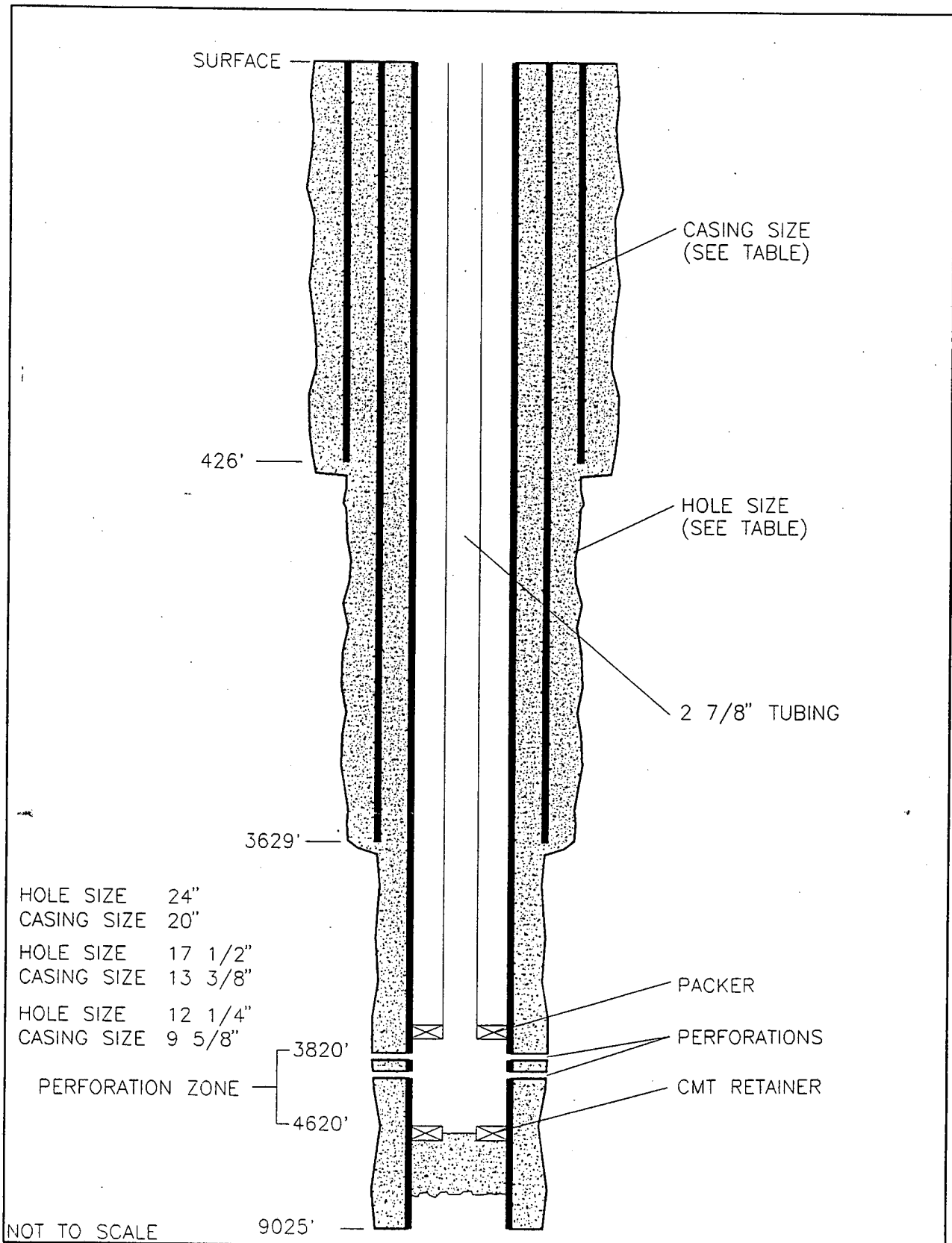
CASING AND TUBING FOR WELL # 30015267610000  
 JAMES A #12 - 22S-30E-02

Information Only



CASING AND TUBING FOR WELL # 30015282810000  
 NEFF FEDERAL #3 - 22S-31E-25

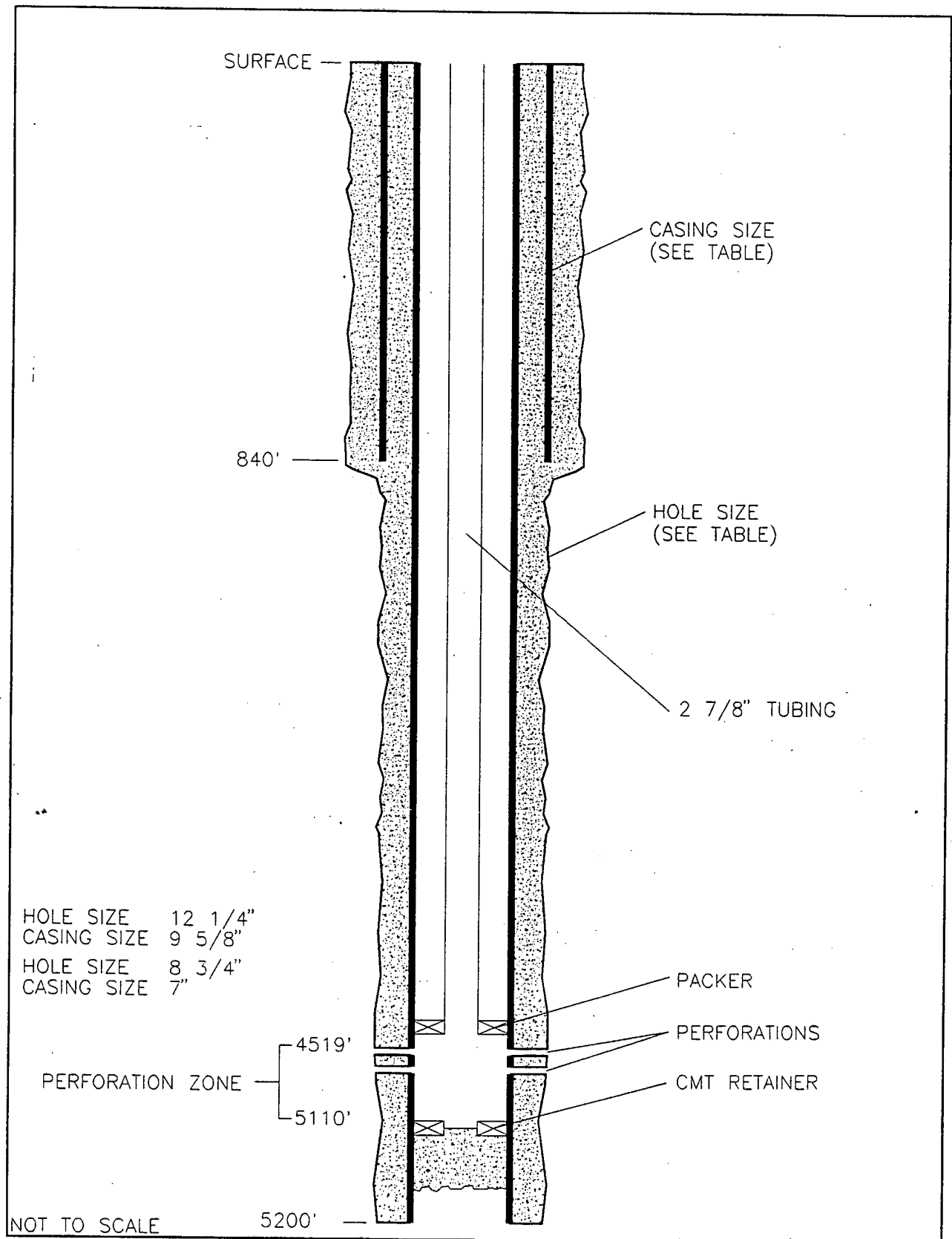
Information Only



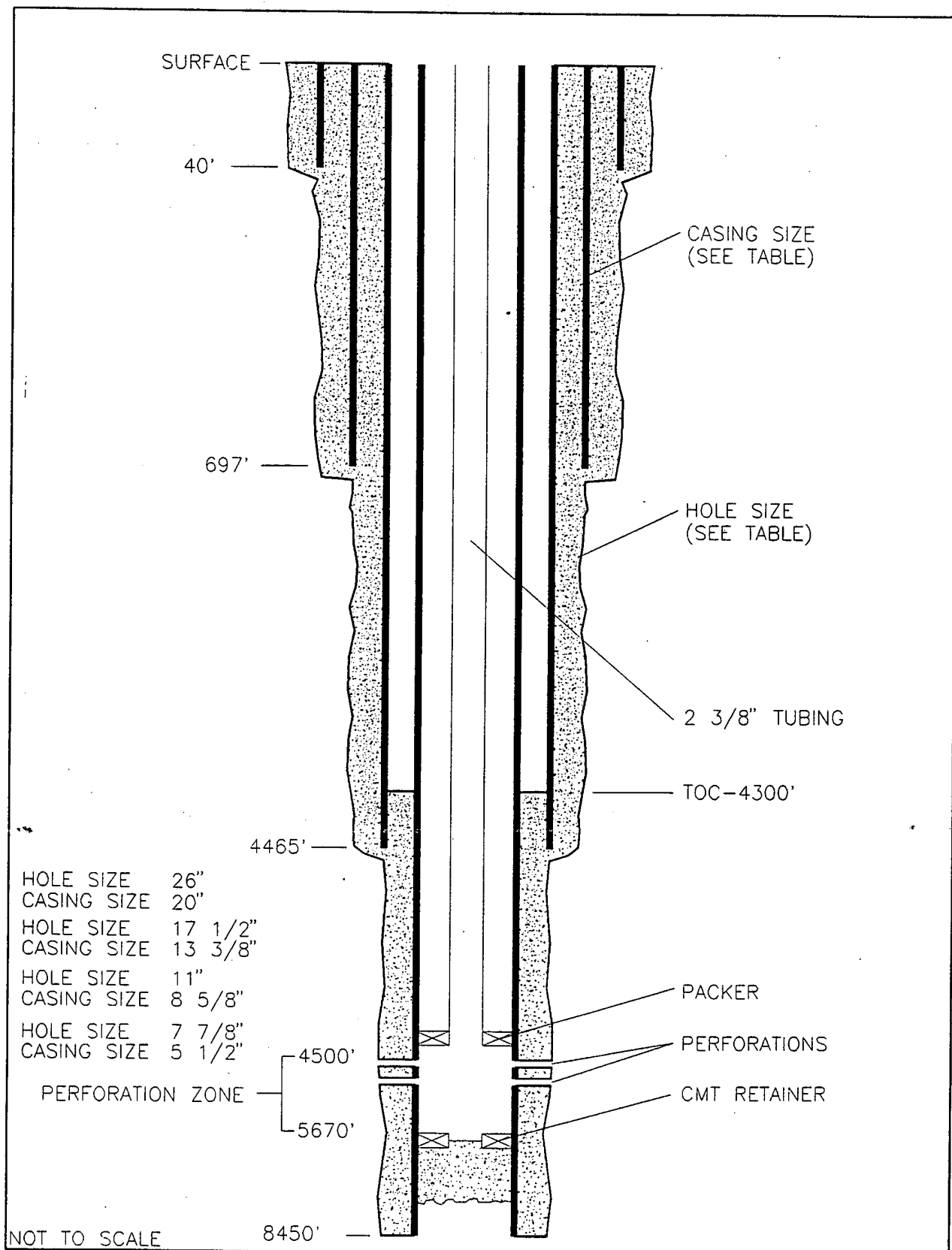
CASING AND TUBING FOR WELL # 30015047340000  
 LEGG FEDERAL #1 - 22S-30E-27

Information Only

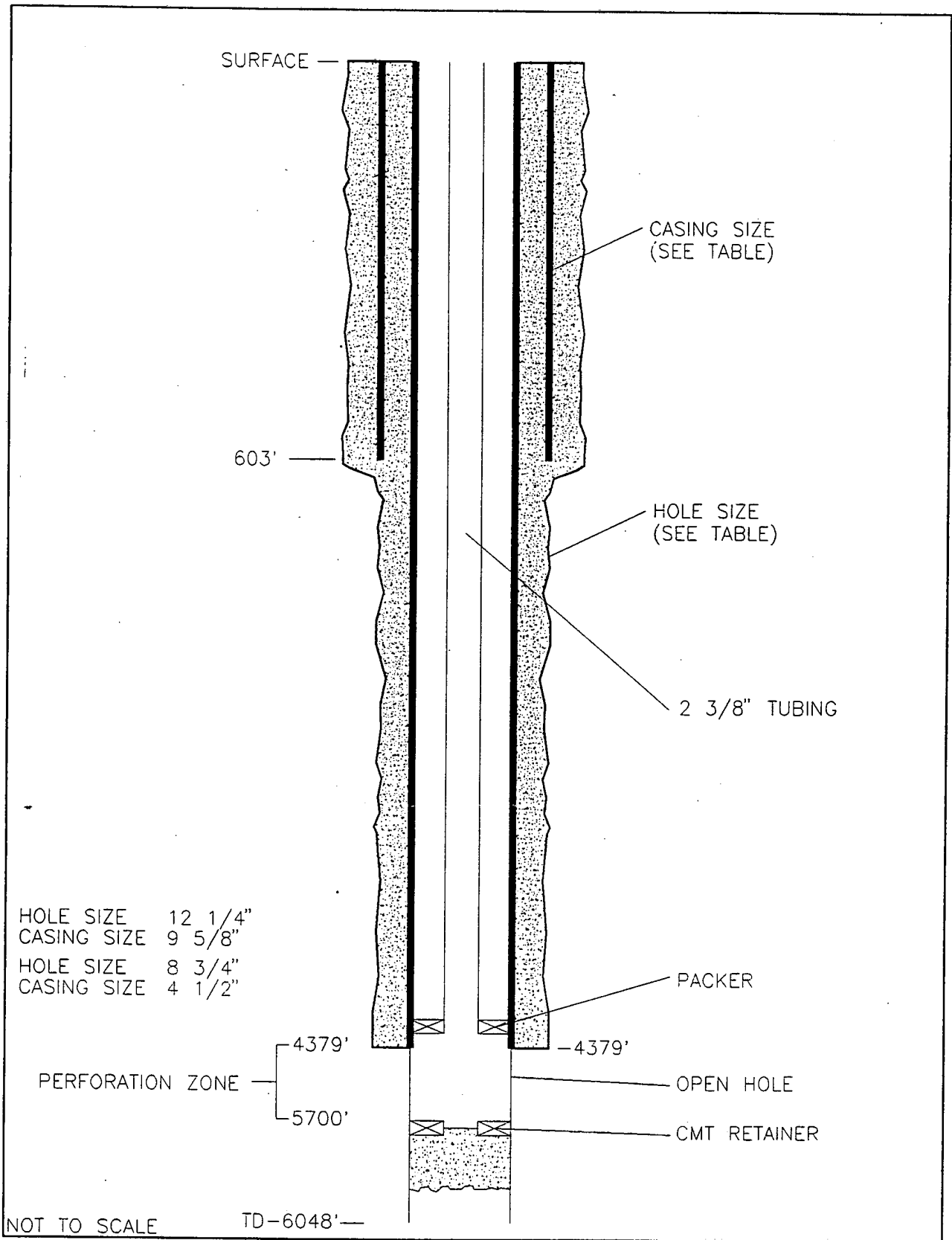




CASING AND TUBING FOR WELL # 30015268480000  
 GETTY 24 FEDERAL #5 - 22S-31E-21

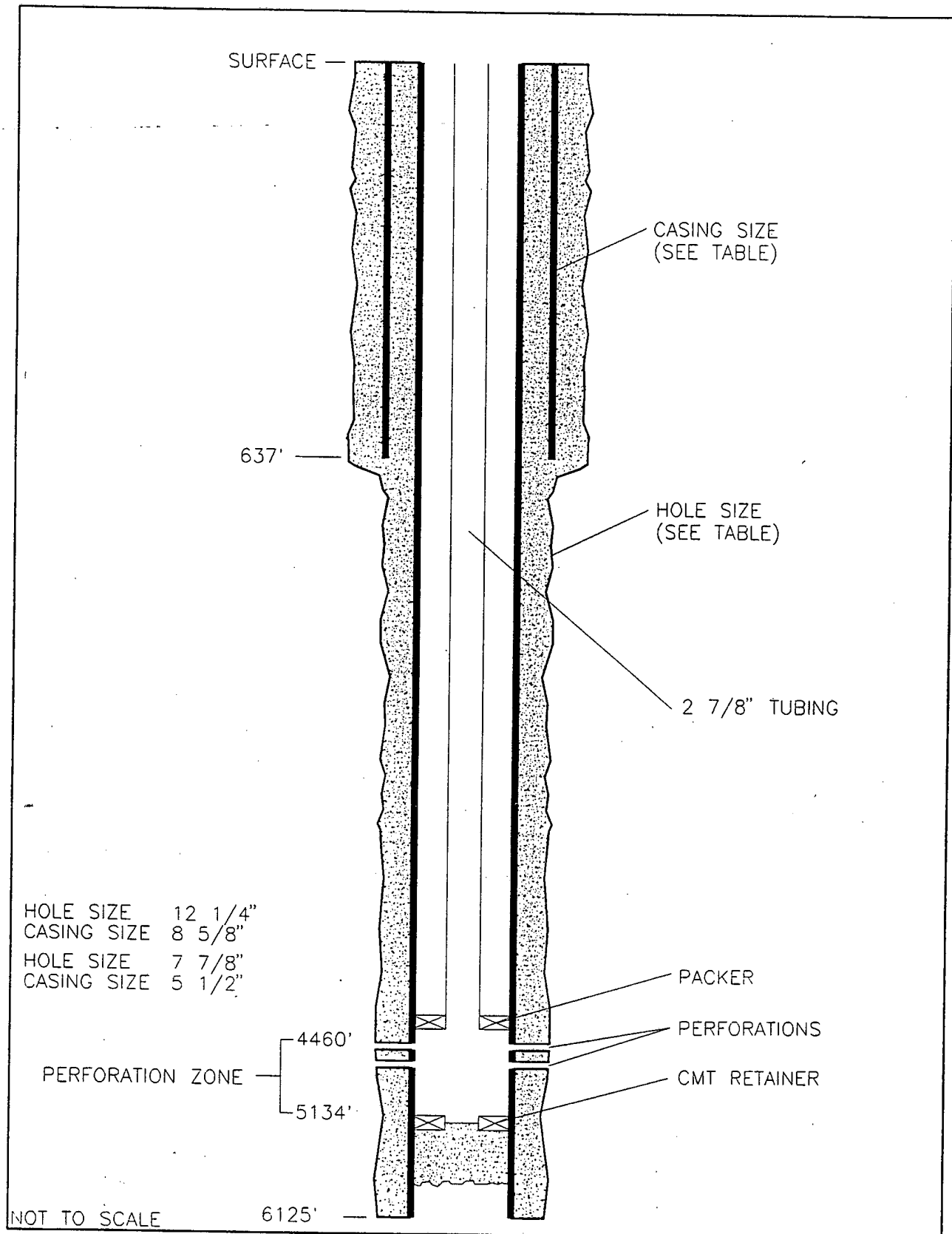


CASING AND TUBING FOR WELL # 30015266290000  
 DAVID ROSS AIT FEDERAL #1 - 22S-31E-35

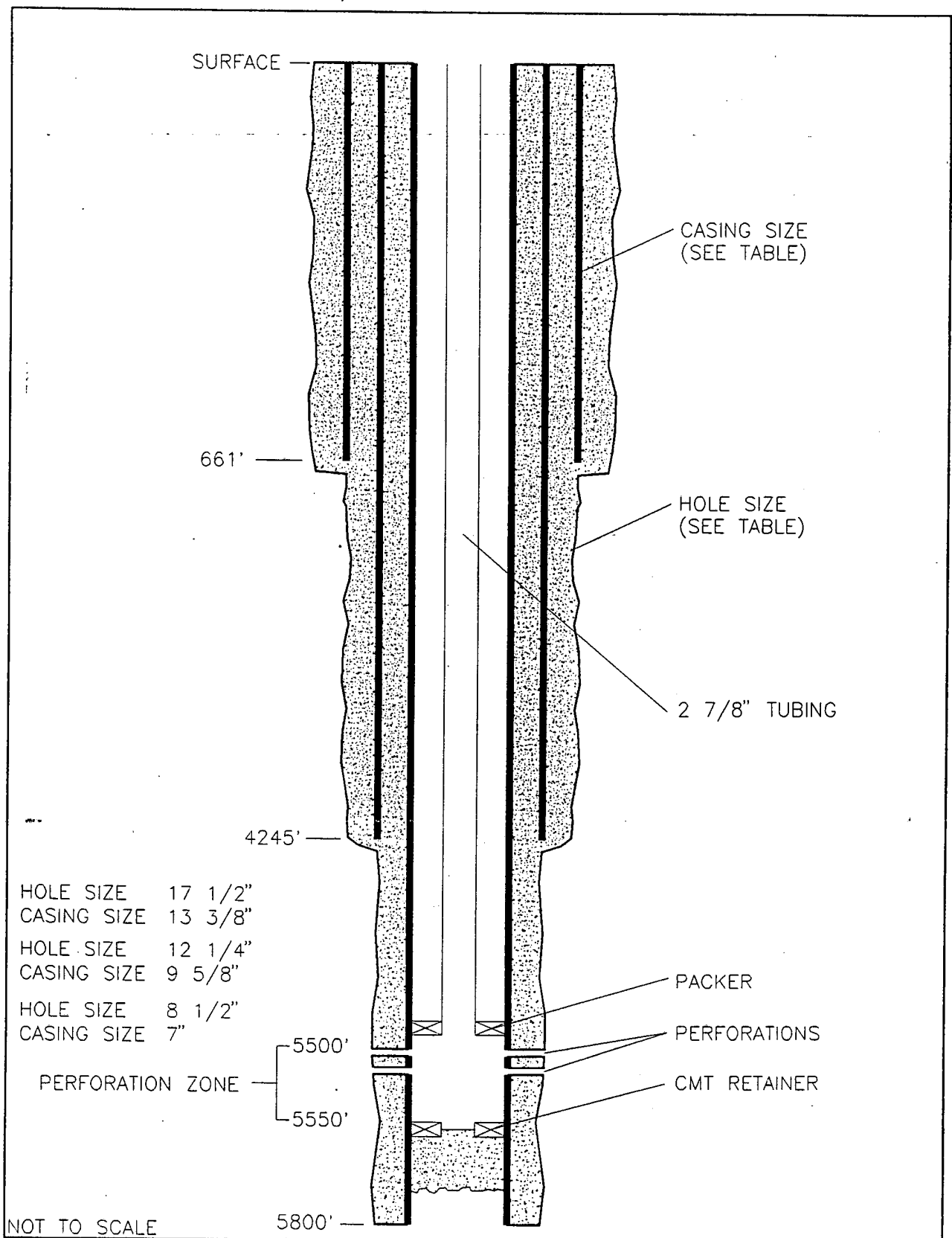


CASING AND TUBING FOR WELL # 30015203020000  
 TODD 26 FEDERAL #3 - 23S-31E-26

Information Only



CASING AND TUBING FOR WELL # 30015202770000  
 TODD 26 G FEDERAL #2 - 23S-31E-26



CASING AND TUBING FOR WELL # 30015261940000  
SAND DUNES 28 FEDERAL #1 - 23S-31E-28

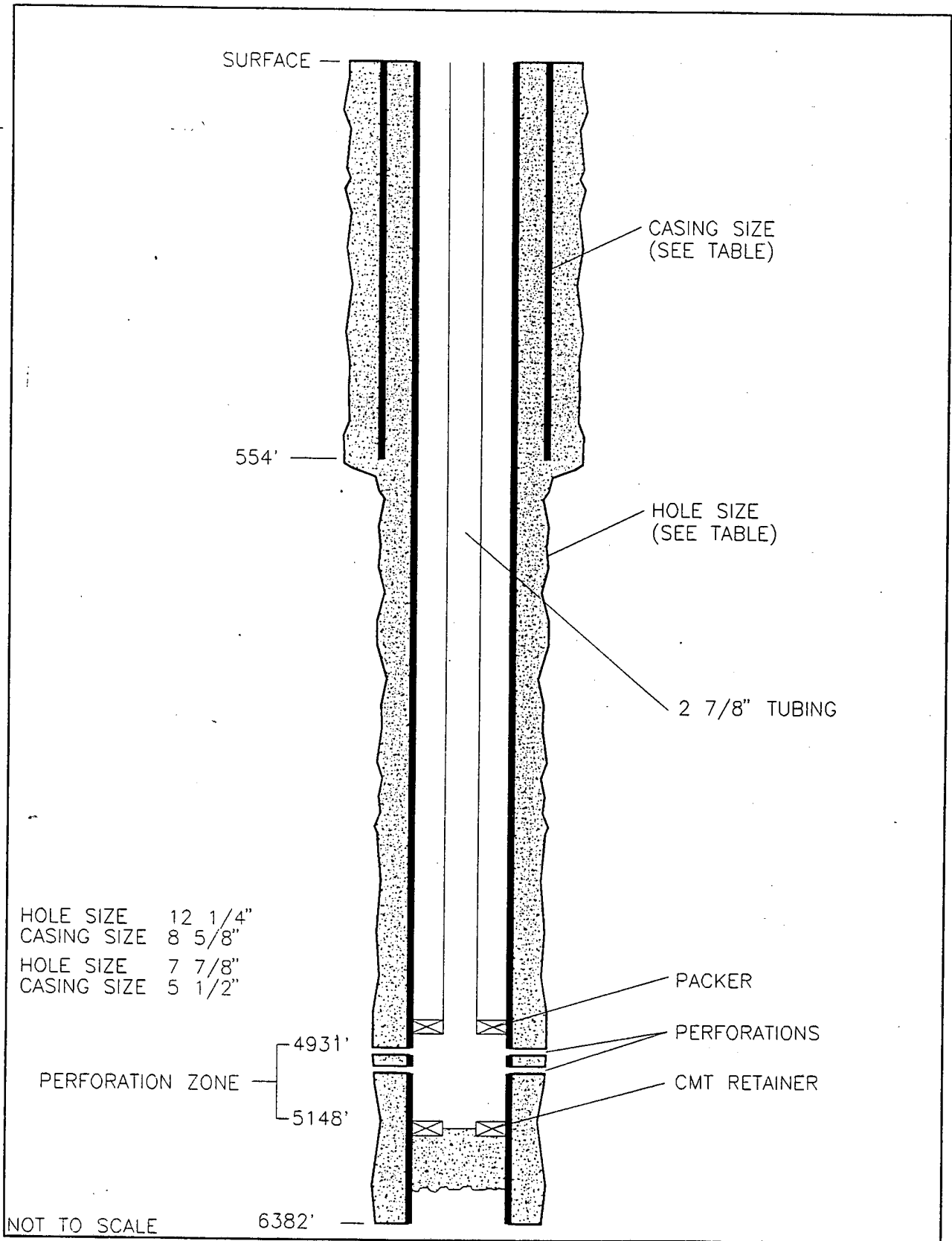
June 1997

Information Only

Attachment 2

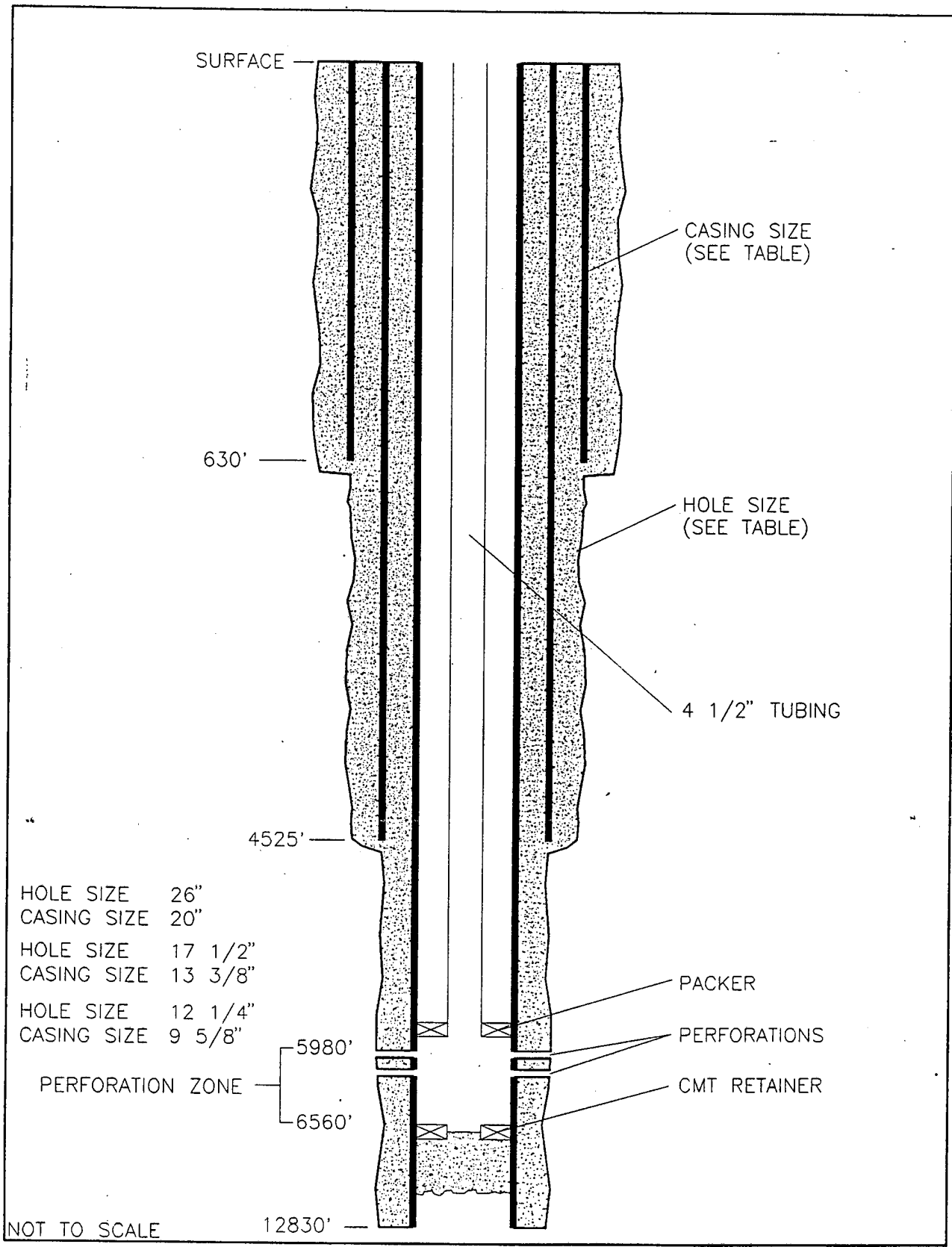
RK-6





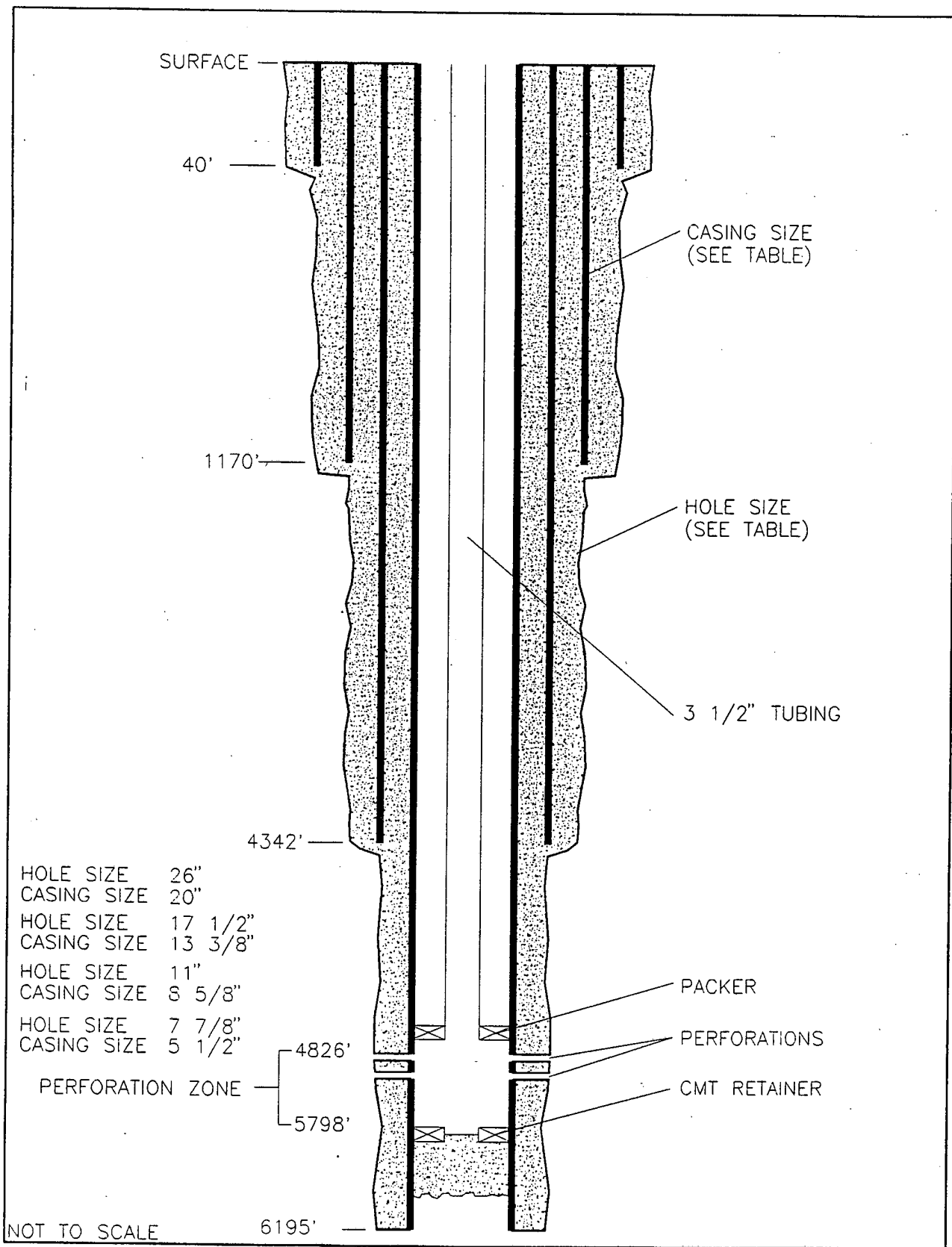
CASING AND TUBING FOR WELL # 3001525640000  
 CALMON #5 - 23S-31E-35

Information Only



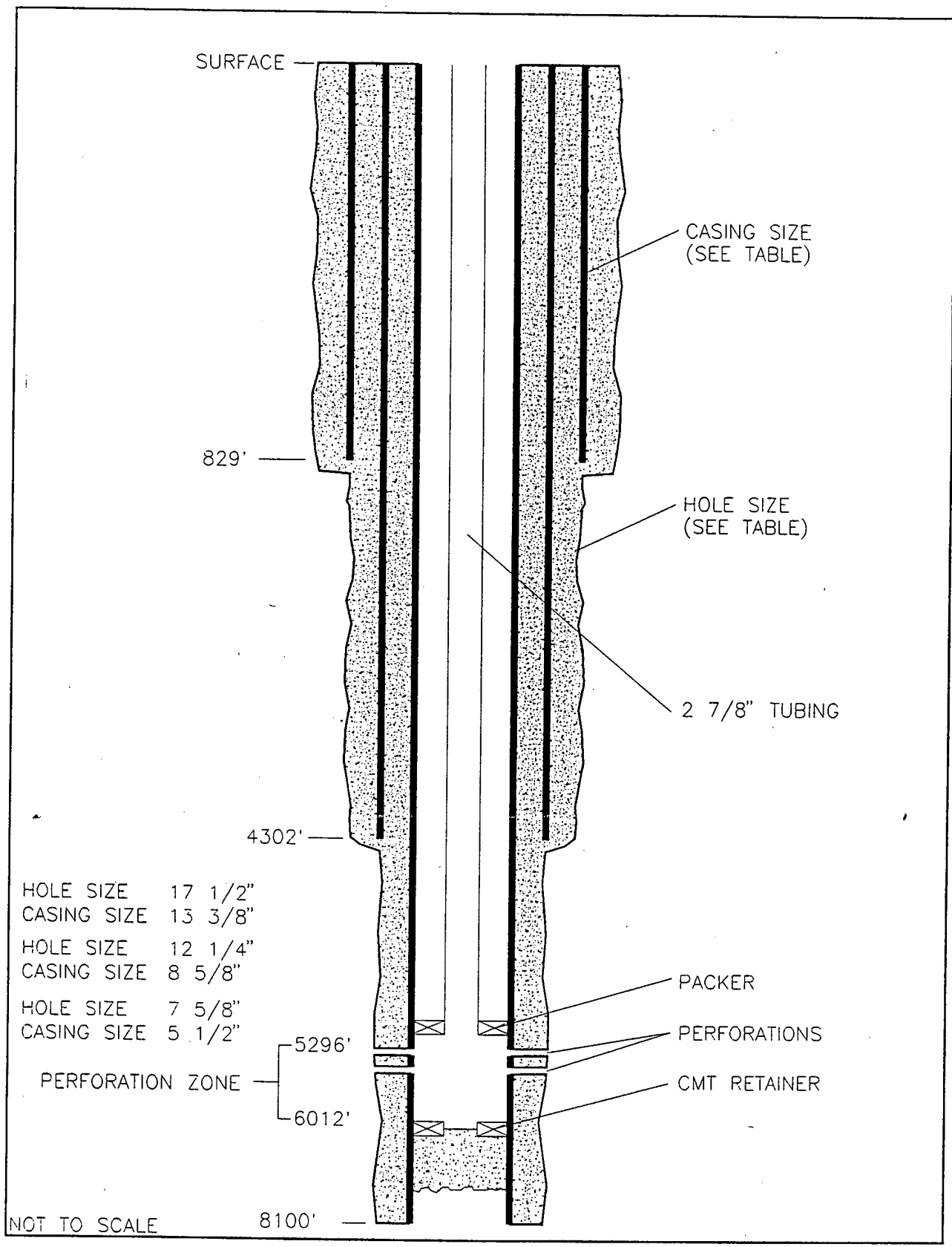
CASING AND TUBING FOR WELL # 30015203410000  
 TODD 36 STATE 1 - 23S-31E-36

Information Only

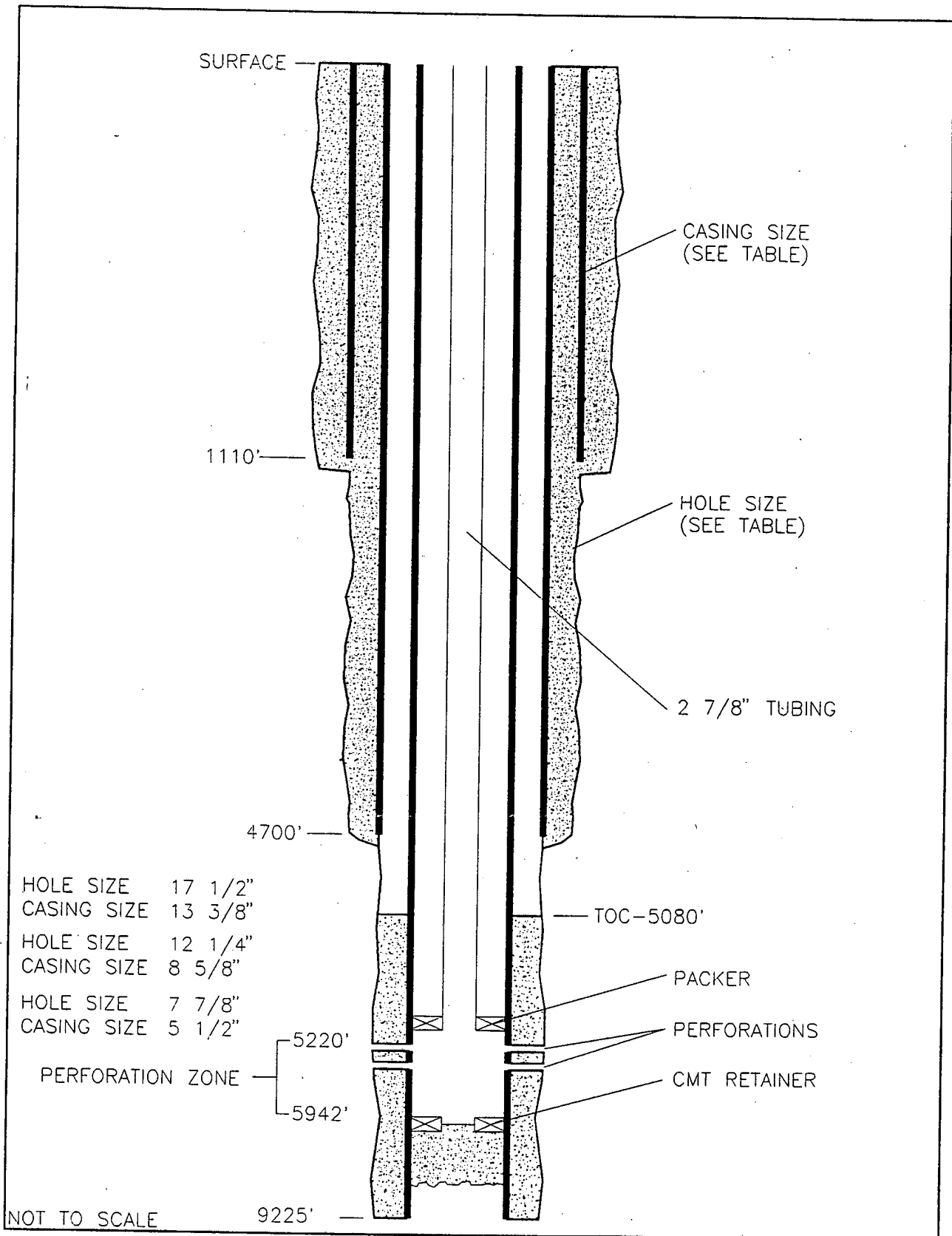


CASING AND TUBING FOR WELL # 30025314120000  
 UNION AJS FEDERAL #1 - 21S-32E-08

Information Only

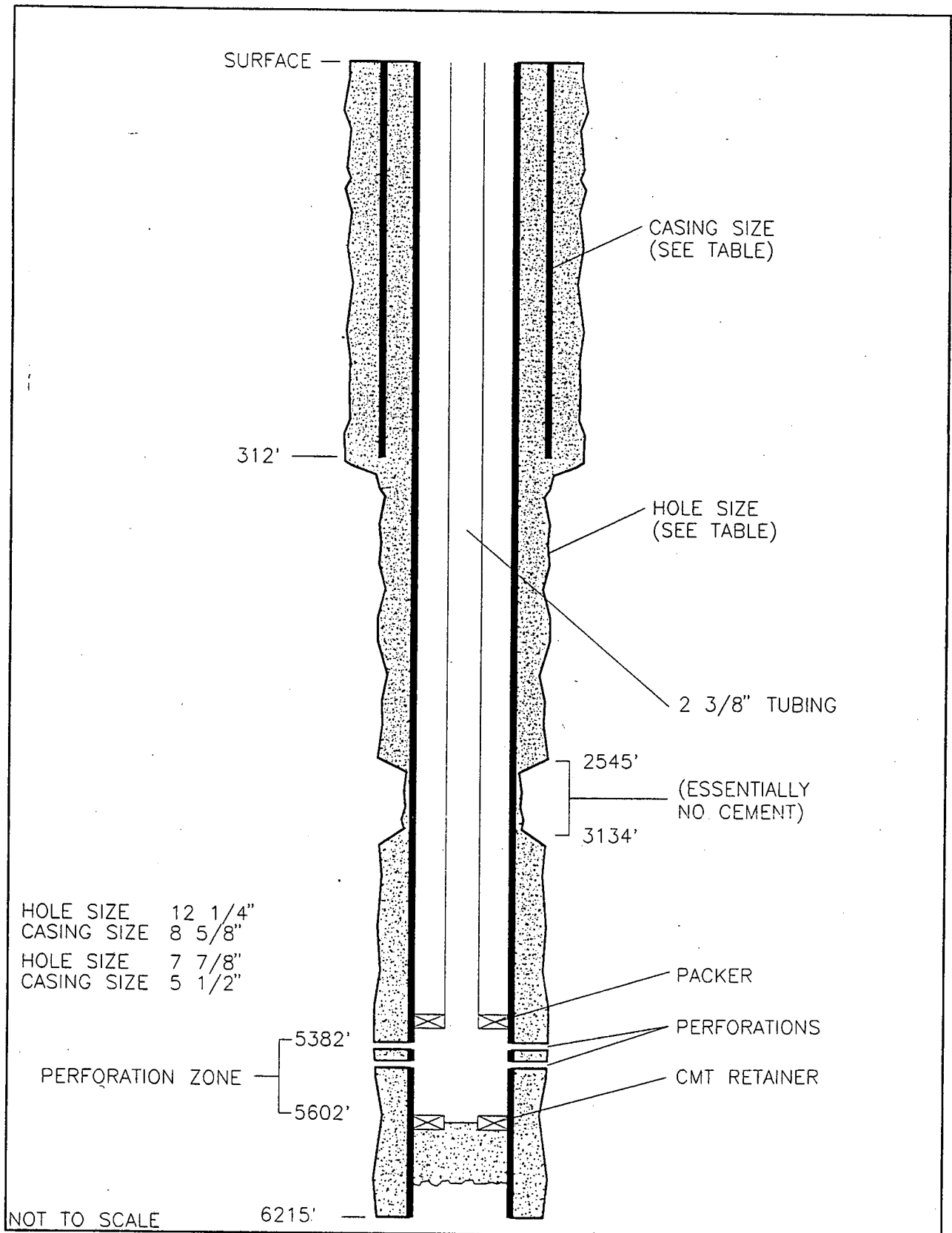


CASING AND TUBING FOR WELL # 30025314430000  
 LUKE FEDERAL (LOST TANK) #1 - 21S-32E-31



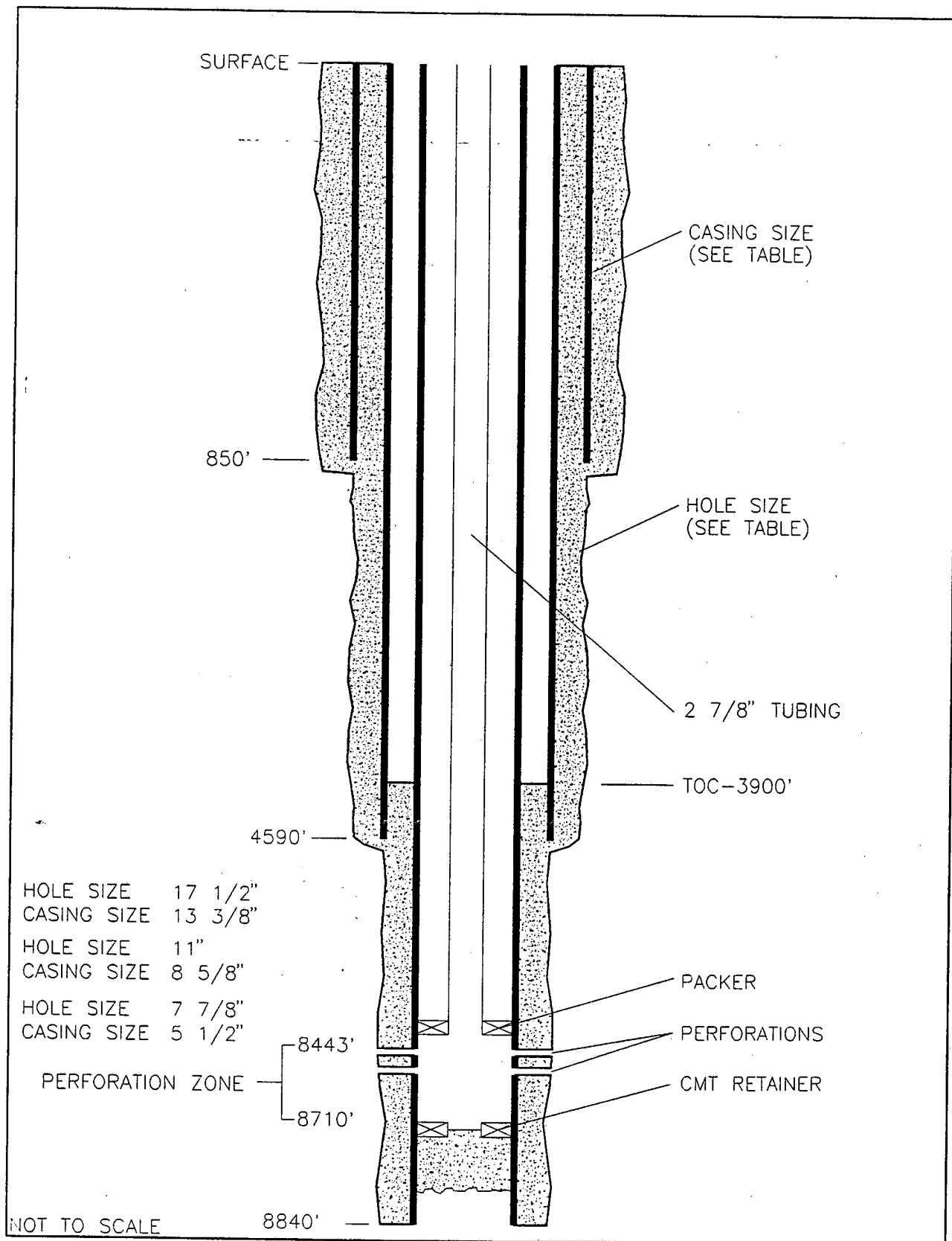
CASING AND TUBING FOR WELL # 30025317160000  
 PROHIBITION FEDERAL UNIT #2 - 22S-32E-11





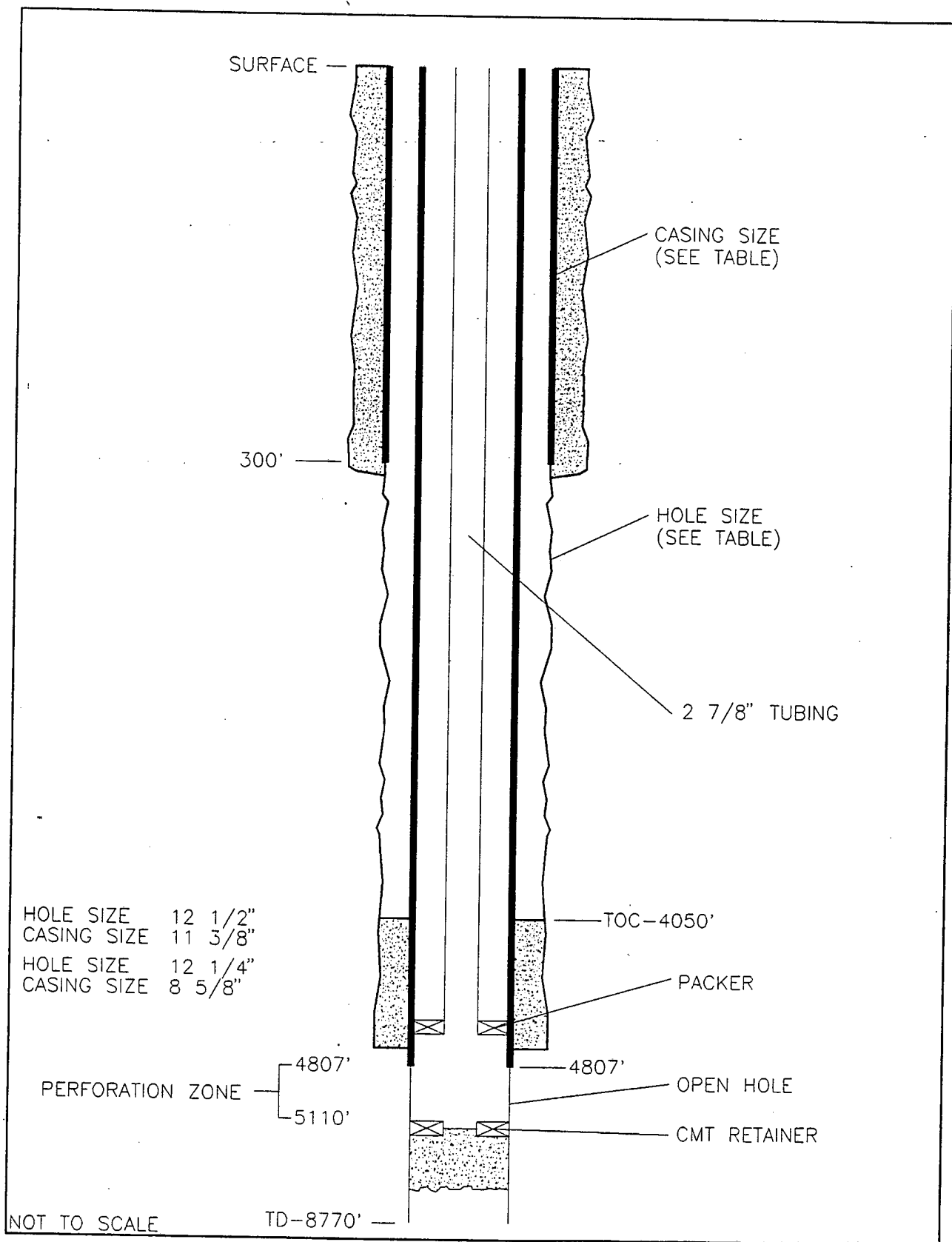
CASING AND TUBING FOR WELL # 30025081130000  
 RED TANK FEDERAL #2 - 22S-32E-14

Information Only

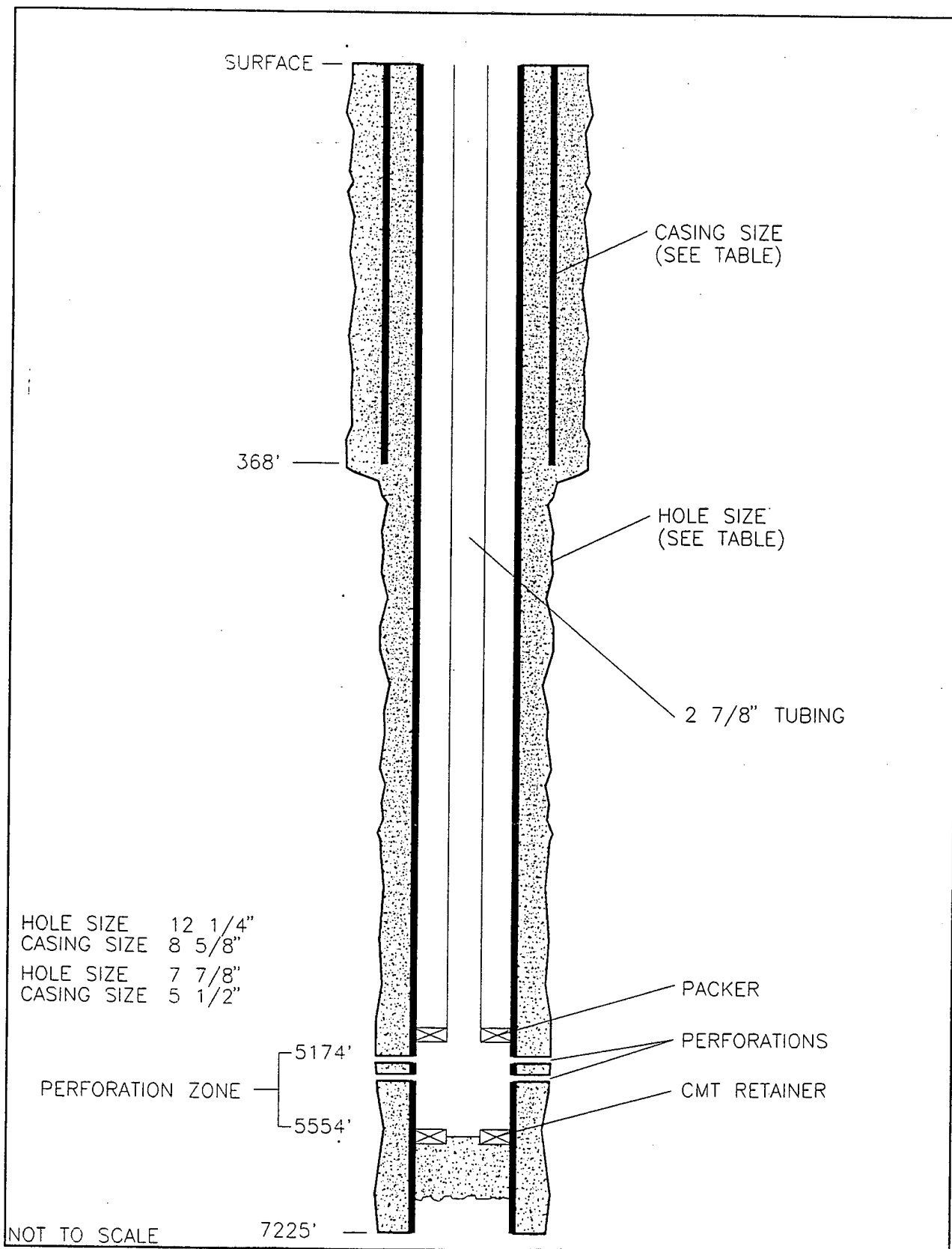


CASING AND TUBING FOR WELL # 30025318890000  
 KIWI AKX STATE #8 - 22S-32E-16

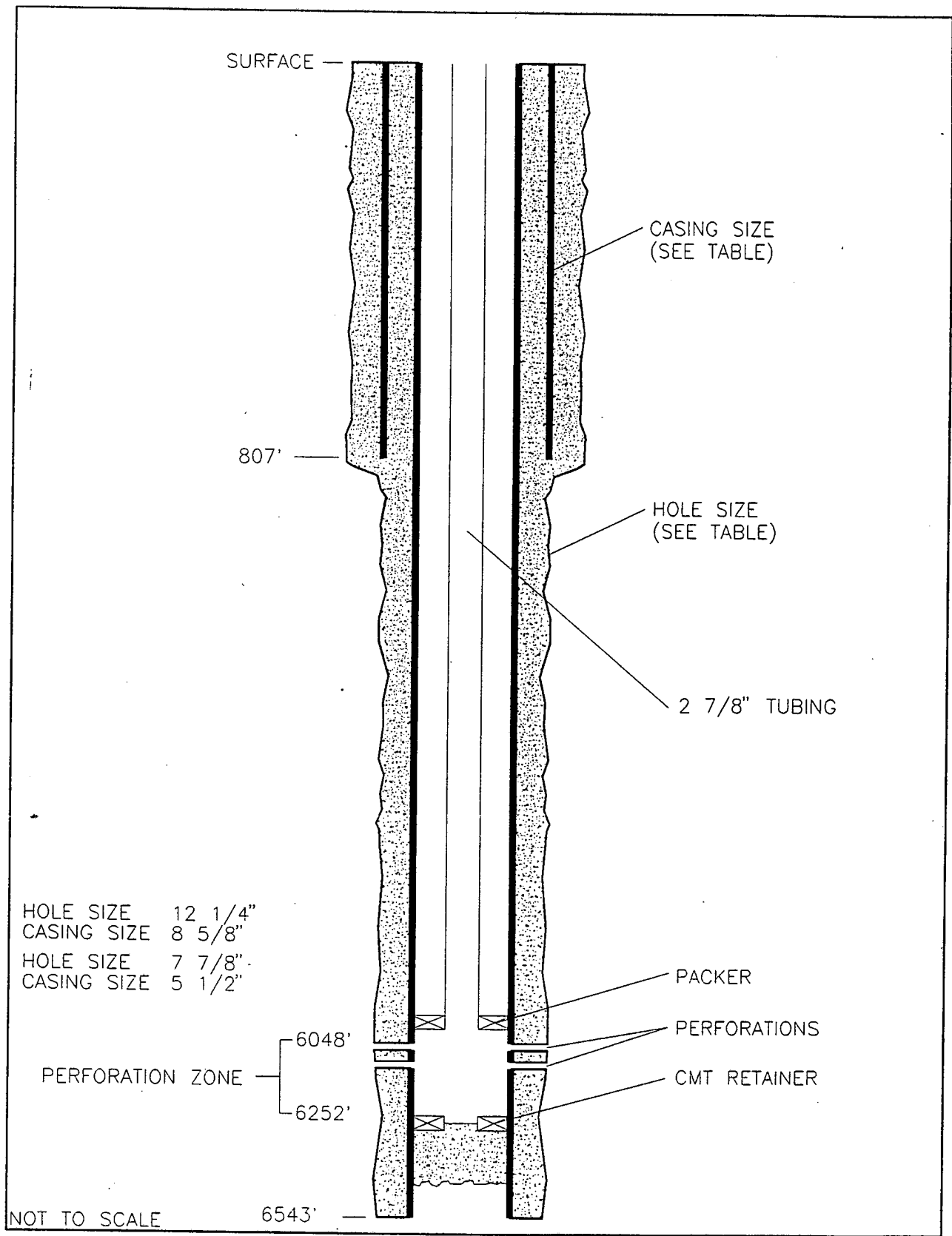
Information Only



CASING AND TUBING FOR WELL # 30025081090000  
GILMORE FEDERAL #1 - 22S-32E-21

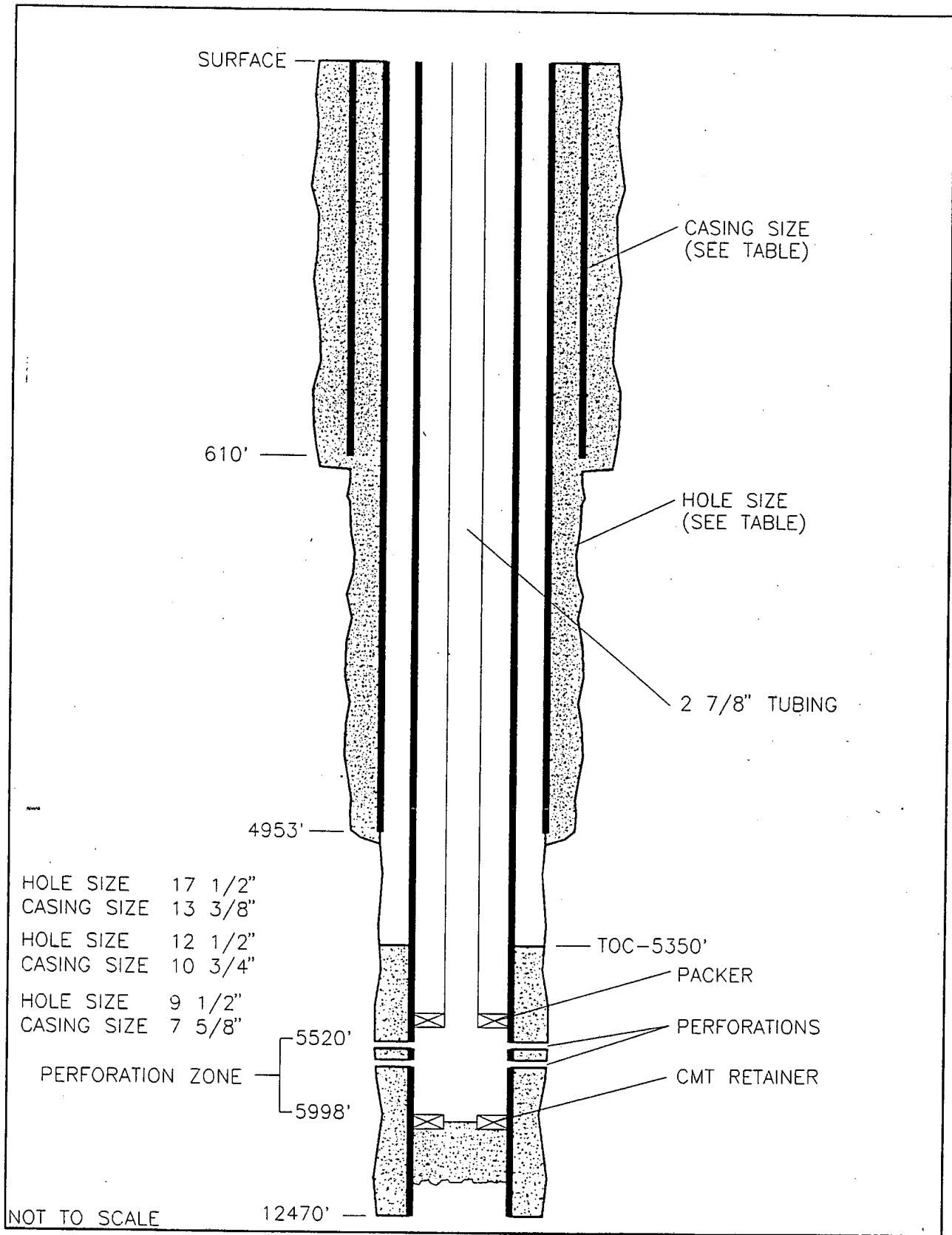


CASING AND TUBING FOR WELL # 30025204230000  
 PROXIMITY 31 FEDERAL #4 - 22S-32E-31



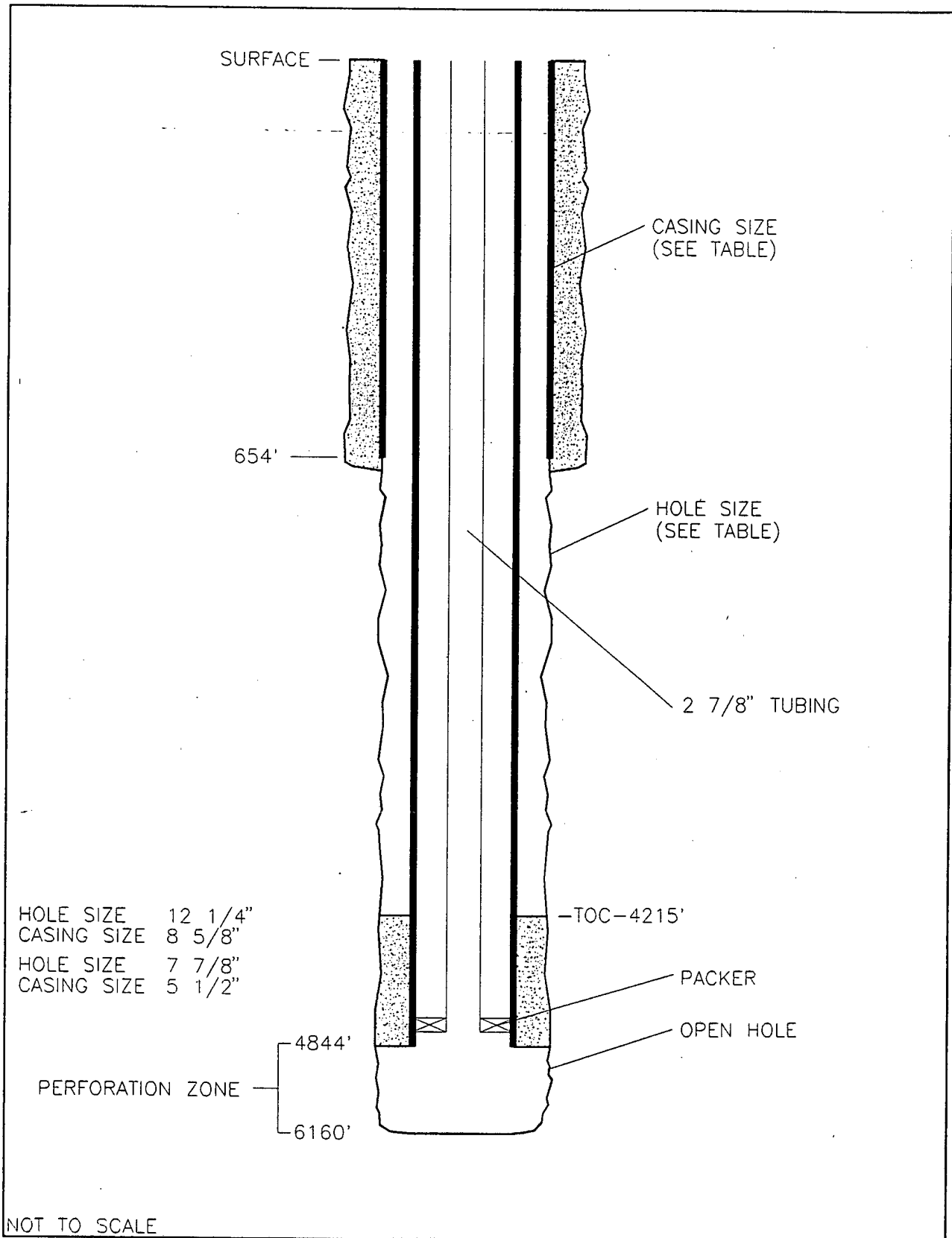
HOLE SIZE 12 1/4"  
 CASING SIZE 8 5/8"  
 HOLE SIZE 7 7/8"  
 CASING SIZE 5 1/2"

CASING AND TUBING FOR WELL # 30025331490000  
 RED TANK 35 FEDERAL #3 - 22S-32E-35

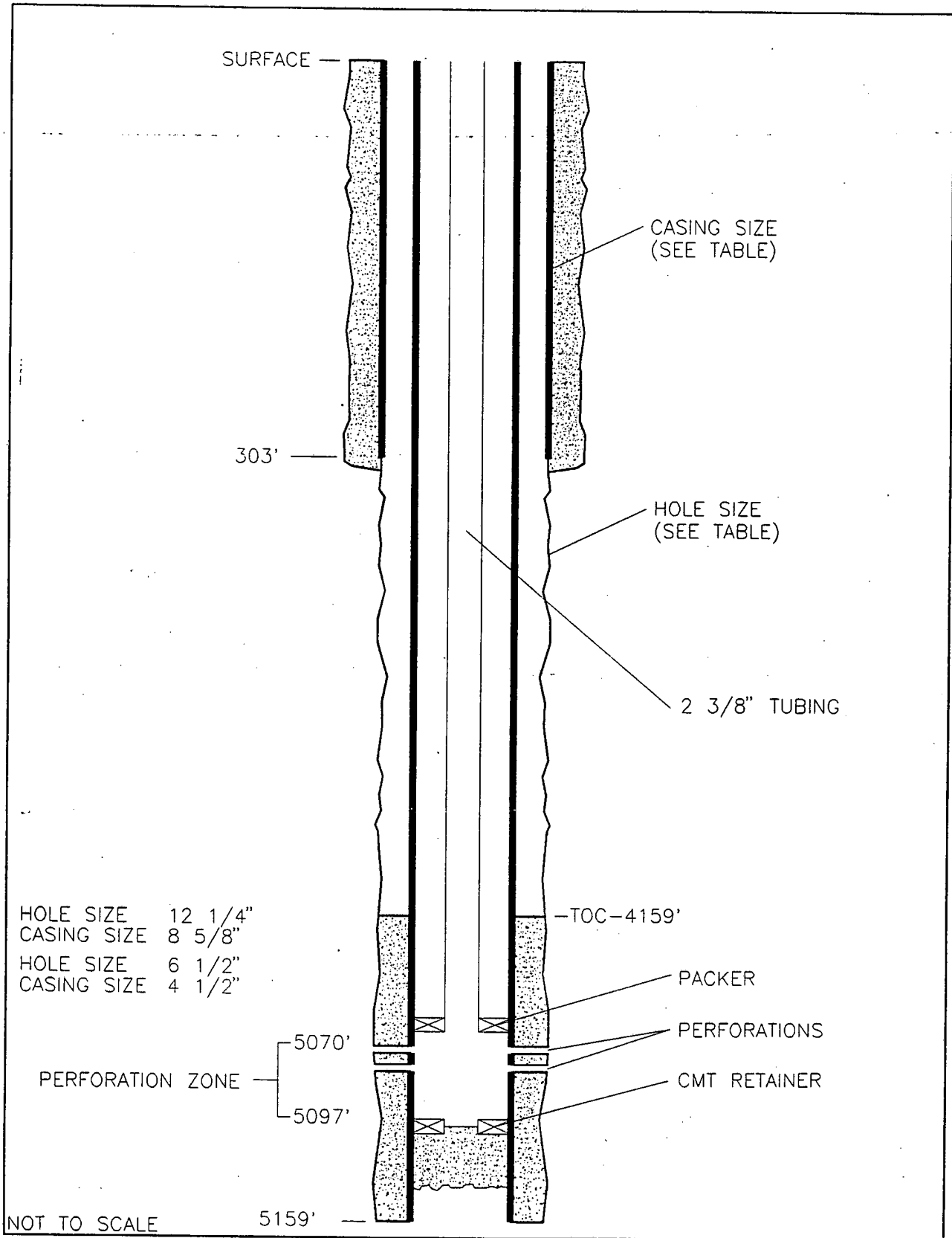


CASING AND TUBING FOR WELL # 30025268440000  
 CUERVO FEDERAL #1 - 23S-32E-14

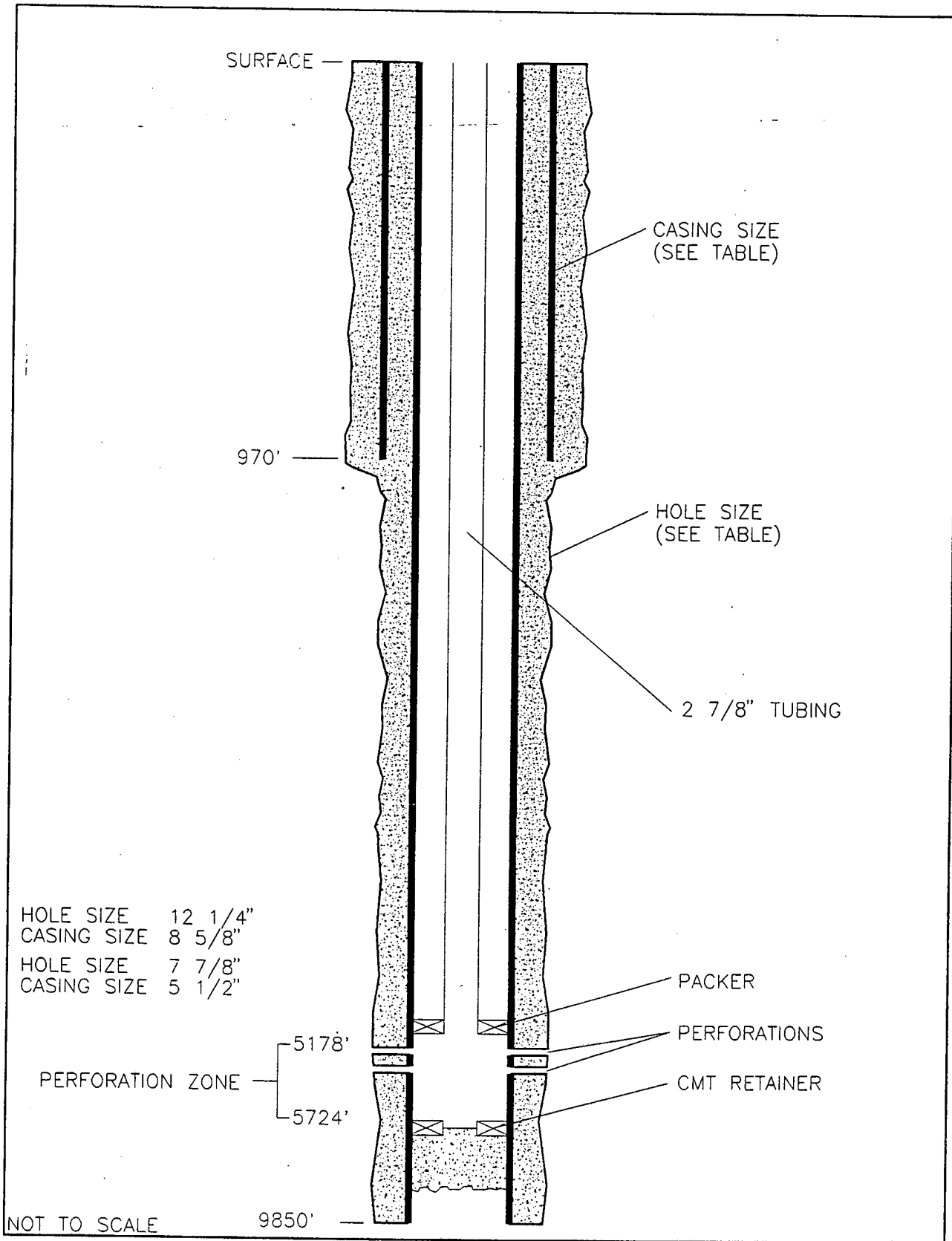




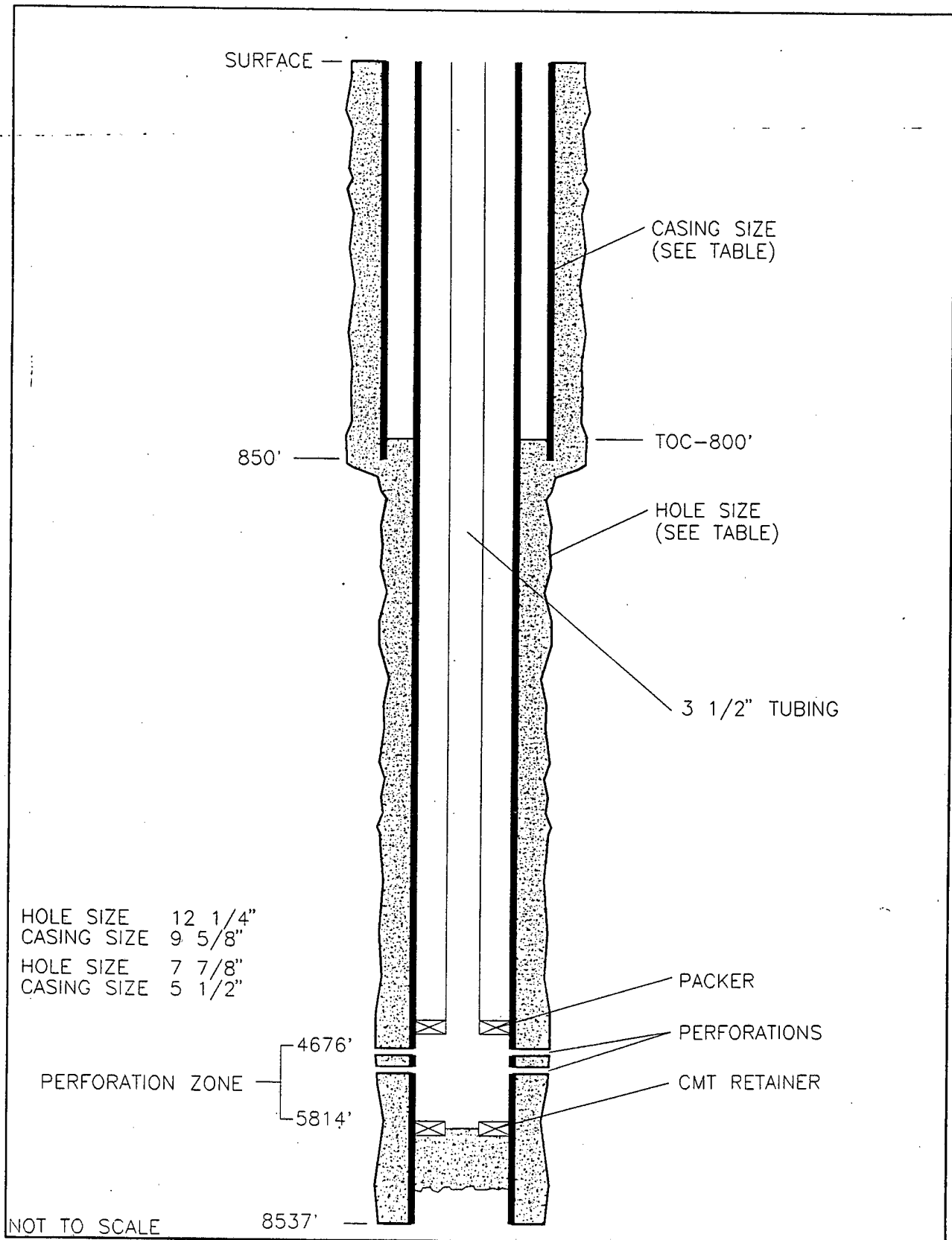
CASING AND TUBING FOR WELL # 30025315150000  
 JAMES FEDERAL #1 - 23S-32E-29



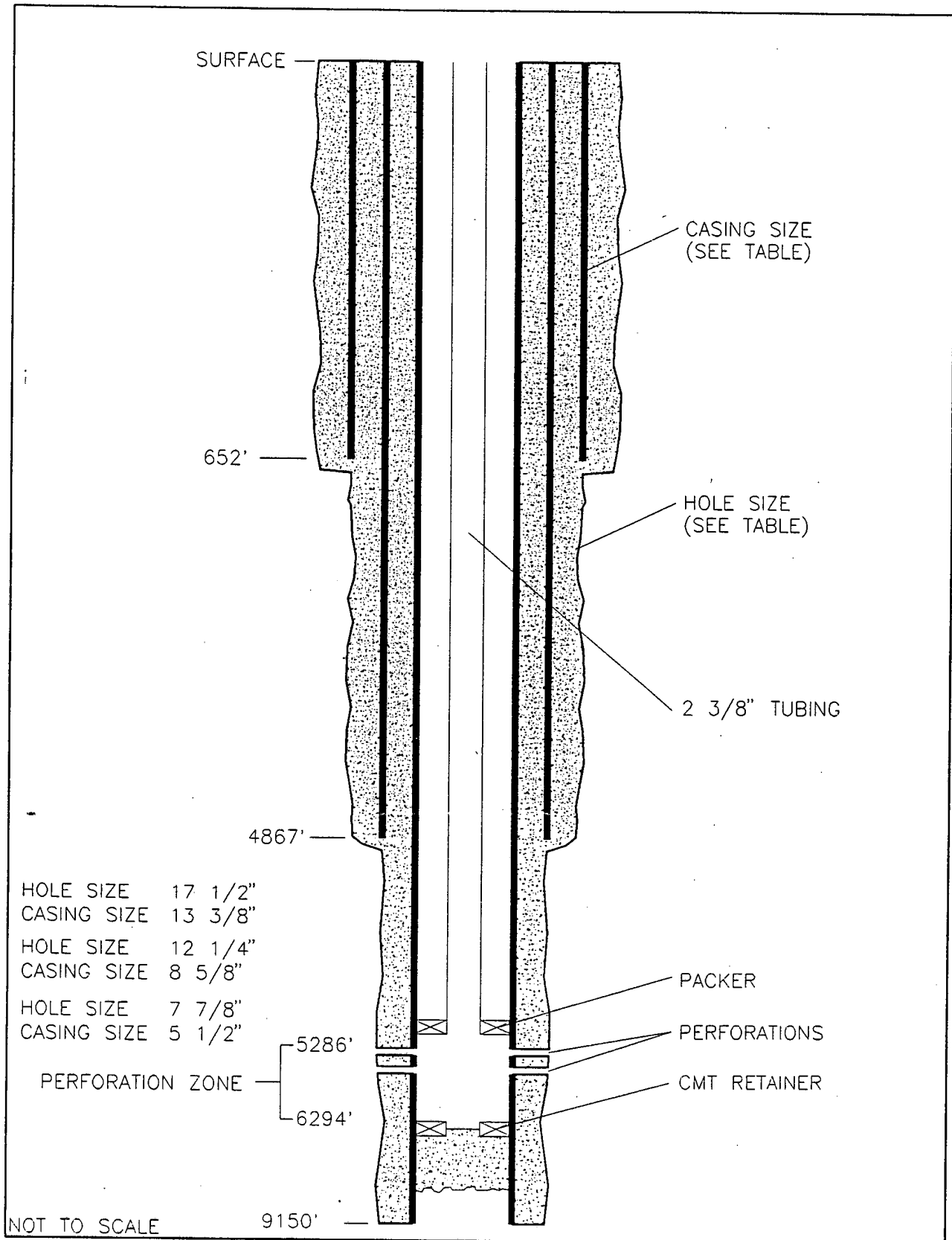
CASING AND TUBING FOR WELL # 30025081280000  
 JAMES FEDERAL #1 - 23S-32E-35



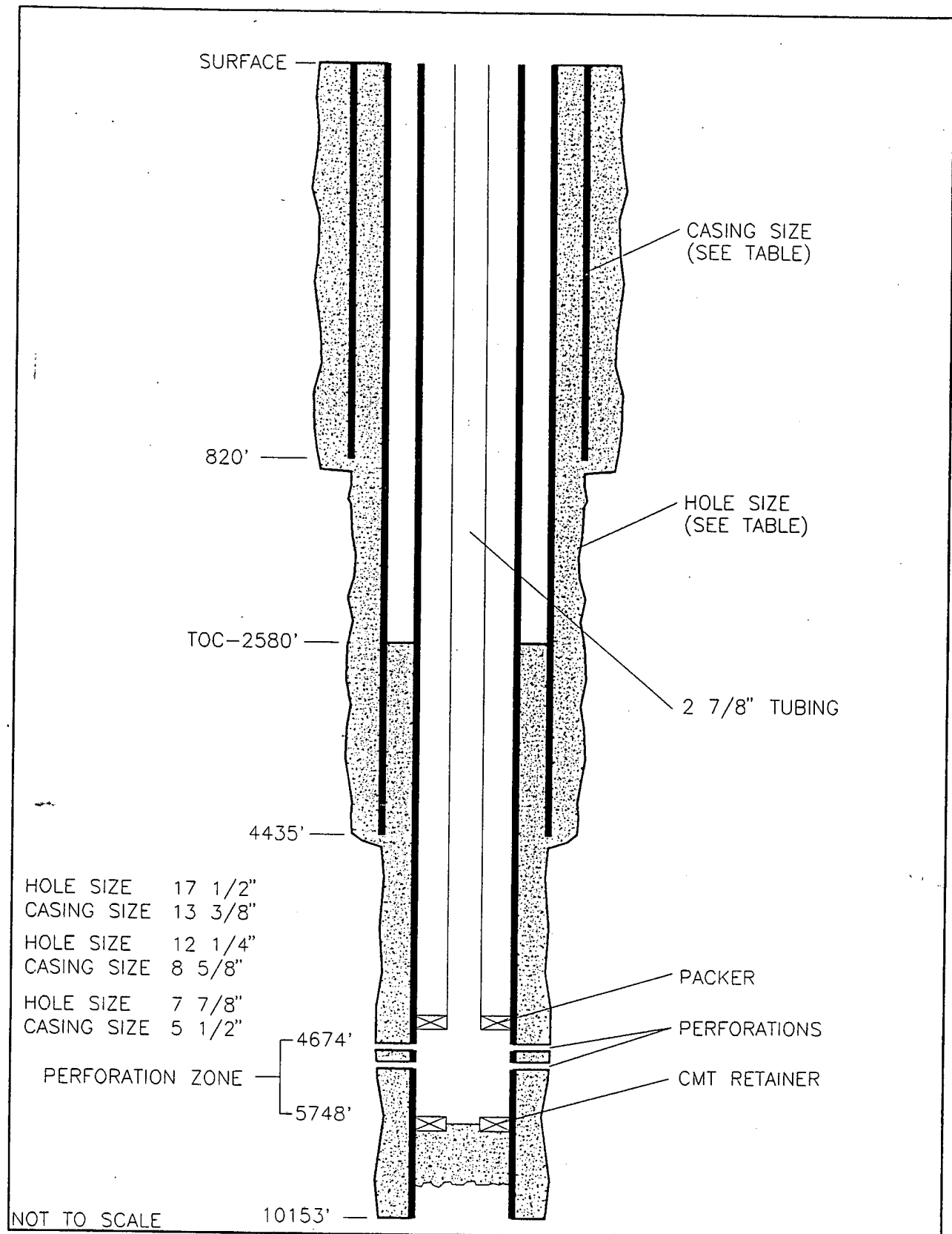
CASING AND TUBING FOR WELL # 30025328680000  
 SDE 31 FEDERAL 19 - 233-32E-31



CASING AND TUBING FOR WELL # 30025310760000  
FLAMENCO FEDERAL #1 - 22S-32E-07



CASING AND TUBING FOR WELL # 30025319290000  
 TRISTE DRAW 36 STATE #1 - 23S-32E-36



CASING AND TUBING FOR WELL # 30025317540000  
 RED TANK 28 FEDERAL #3-B - 22S 32E-28



1  
2  
3  
4  
5  
6  
7  
8  
9  
10  
11  
12  
13  
14  
15  
16  
17  
18  
19  
20  
21  
22

**Attachment 3**

**Permitted SWD and WI Wells in New Mexico**

**Outside the Nine Township Area Surrounding WIPP**

**But Within the Delaware Basin**

**Information Only**

**PERMITTED INJECTION AND SALT WATER DISPOSAL WELLS FOR  
EDDY COUNTY AS IDENTIFIED BY THE STATE THAT LIE OUTSIDE THE  
NINE TOWNSHIP AREA BUT WITHIN THE DELAWARE BASIN**

	<u>API NUMBER</u>	<u>T-R-S</u>	<u>TYPE</u>	<u>STATUS</u>
1.	30015222220000	21S-28E-35	SWD	ACTIVE
2.	30015272830000	21S-29E-08	WIW	ACTIVE
3.	30015229800000	22S-26E-24	SWD	ACTIVE
4.	30015253520000	22S-26E-32	SWD	PENDING
5.	30015275580000	22S-26E-32	SWD	ACTIVE
6.	30015109080000	22S-26E-36	SWD	ACTIVE
7.	30015257220000	22S-27E-23	SWD	ACTIVE
8.	30015245310000	22S-27E-36	SWD	ACTIVE
9.	30015221820000	22S-28E-07	WIW	ACTIVE
10.	30015219590000	22S-28E-07	WIW	ACTIVE
11.	30015221010000	22S-28E-07	WIW	ACTIVE
12.	30015218430000	22S-28E-18	WIW	ACTIVE
13.	30015218450000	22S-28E-18	WIW	ACTIVE
14.	30015216180000	22S-28E-18	WIW	ACTIVE
15.	30015215050000	22S-28E-18	WIW	ACTIVE
16.	30015216190000	22S-28E-18	WIW	ACTIVE
17.	30015213910000	22S-28E-18	WIW	ACTIVE
18.	30015218440000	22S-28E-19	WIW	ACTIVE
19.	30015272610000	22S-28E-25	SWD	ACTIVE
20.	30015226610000	22S-28E-31	SWD	ACTIVE
21.	30015234930000	23S-27E-13	SWD	ACTIVE
22.	30015227540000	23S-28E-02	SWD	ACTIVE
23.	30015244240000	23S-28E-09	SWD	INACTIVE
24.	30015263410000	23S-28E-11	SWD	ACTIVE
25.	30015267640000	23S-28E-15	SWD	ACTIVE
26.	30015226110000	23S-28E-16	SWD	ACTIVE
27.	30015261220000	23S-28E-27	SWD	ACTIVE
28.	30015217770000	23S-29E-13	SWD	ACTIVE
29.	30015003860000	24S-26E-11	SWD	INACTIVE
30.	30015024910000	24S-28E-12	WIW	INACTIVE
31.	30015037020000	24S-29E-07	WIW	INACTIVE
32.	30015283900000	24S-29E-23	SWD	PENDING
33.	30015280570000	24S-30E-13	SWD	PENDING
34.	30015102590000	24S-31E-11	SWD	ACTIVE

	<u>API NUMBER</u>	<u>T-R-S</u>	<u>TYPE</u>	<u>STATUS</u>
35.	30015276270000	24S-31E-11	SWD	ACTIVE
36.	30015217000000	24S-31E-21	SWD	ACTIVE
37.	30015108590000	24S-31E-28	SWD	ACTIVE
38.	30015210290000	25S-26E-13	SWD	ACTIVE
39.	30015237090000	25S-28E-03	SWD	ACTIVE
40.	30015237280000	25S-28E-27	SWD	INACTIVE
41.	30015214250000	25S-29E-22	SWD	ACTIVE
42.	30015273980000	25S-29E-36	SWD	ACTIVE
43.	30015025230000	26S-28E-03	SWD	INACTIVE
44.	30015269300000	26S-29E-16	SWD	INACTIVE
45.	30015253210000	26S-29E-22	WIW	ACTIVE
46.	30015244660000	26S-29E-27	SWD	ACTIVE
47.	30015037510000	26S-29E-34	SWD	ACTIVE
48.	30015202220000	26S-30E-18	SWD	ACTIVE
49.	30015257450000	26S-30E-25	SWD	ACTIVE
50.	30015233240000	26S-30E-29	SWD	ACTIVE
51.	30015236800000	26S-30E-33	SWD	ACTIVE
52.	30015232240000	26S-30E-34	SWD	ACTIVE
53.	30015058680000	26S-31E-24	SWD	ACTIVE
54.	30015058770000	26S-31E-25	SWD	ACTIVE
55.	30015058910000	26S-31E-35	SWD	ACTIVE

**PERMITTED INJECTION AND SALT WATER DISPOSAL WELLS FOR  
LEA COUNTY AS IDENTIFIED BY THE STATE THAT LIE OUTSIDE THE  
NINE TOWNSHIP AREA BUT WITHIN THE DELAWARE BASIN**

	<u>API NUMBER</u>	<u>T-R-S</u>	<u>TYPE</u>	<u>STATUS</u>
1.	30025286970000	23S-33E-17	WIW	ACTIVE
2.	30025083590000	23S-33E-19	SWD	ACTIVE
3.	30025083580000	23S-33E-19	SWD	INACTIVE
4.	30025217400000	23S-34E-22	SWD	ACTIVE
5.	30025084890000	23S-34E-30	SWD	ACTIVE
6.	30025290690000	23S-34E-30	SWD	ACTIVE
7.	30025249160000	23S-34E-33	SWD	ACTIVE
8.	30025081480000	24S-32E-14	SWD	ACTIVE
9.	30025081610000	24S-32E-22	SWD	ACTIVE
10.	30025282020000	24S-32E-27	SWD	ACTIVE
11.	30025083670000	24S-33E-01	SWD	INACTIVE
12.	30025243810000	24S-33E-06	SWD	INACTIVE
13.	30025244320000	24S-33E-07	SWD	ACTIVE
14.	30025288730000	24S-34E-30	SWD	ACTIVE
15.	30025081700000	25S-32E-10	WIW	ACTIVE
16.	30025081750000	25S-32E-10	WIW	ACTIVE
17.	30025081900000	25S-32E-15	WIW	ACTIVE
18.	30025081830000	25S-32E-15	WIW	ACTIVE
19.	30025081870000	25S-32E-15	WIW	ACTIVE
20.	30025081940000	25S-32E-16	WIW	INACTIVE
21.	30025236020000	25S-32E-16	WIW	INACTIVE
22.	30025081980000	25S-32E-16	WIW	INACTIVE
23.	30025082130000	25S-32E-21	WIW	INACTIVE
24.	30025082080000	25S-32E-21	WIW	INACTIVE
25.	30025082170000	25S-32E-21	WIW	ACTIVE
26.	30025082040000	25S-32E-21	WIW	ACTIVE
27.	30025082220000	25S-32E-22	WIW	ACTIVE
28.	30025282590000	26S-32E-09	SWD	ACTIVE
29.	30025082660000	26S-32E-19	WIW	ACTIVE
30.	30025223900000	26S-32E-20	SWD	ACTIVE
31.	30025082690000	26S-32E-24	WIW	INACTIVE
32.	30025082800000	26S-32E-25	WIW	INACTIVE
33.	30025082870000	26S-32E-25	WIW	INACTIVE
34.	30025082770000	26S-32E-25	WIW	INACTIVE
35.	30025082810000	26S-32E-25	WIW	INACTIVE
36.	30025082780000	26S-32E-25	WIW	ACTIVE
37.	30025082750000	26S-32E-25	WIW	INACTIVE

	<u>API NUMBER</u>	<u>T-R-S</u>	<u>TYPE</u>	<u>STATUS</u>
38.	30025082740000	26S-32E-25	WIW	INACTIVE
39.	30025082830000	26S-32E-25	WIW	INACTIVE
40.	30025082990000	26S-32E-26	WIW	INACTIVE
41.	30025082940000	26S-32E-26	WIW	INACTIVE
42.	30025082930000	26S-32E-26	WIW	ACTIVE
43.	30025082960000	26S-32E-26	WIW	INACTIVE
44.	30025082920000	26S-32E-26	WIW	INACTIVE
45.	30025082880000	26S-32E-26	WIW	INACTIVE
46.	30025083000000	26S-32E-27	WIW	INACTIVE
47.	30025083050000	26S-32E-34	WIW	ACTIVE
48.	30025083090000	26S-32E-35	WIW	INACTIVE
49.	30025083120000	26S-32E-35	WIW	INACTIVE
50.	30025083130000	26S-32E-35	WIW	INACTIVE
51.	30025249080000	26S-32E-36	WIW	INACTIVE
52.	30025083180000	26S-32E-36	WIW	INACTIVE
53.	30025084160000	26S-33E-15	SWD	ACTIVE
54.	30025084360000	26S-33E-30	WIW	INACTIVE
55.	30025084340000	26S-33E-30	WIW	INACTIVE
56.	30025084310000	26S-33E-30	WIW	INACTIVE
57.	30025084350000	26S-33E-30	WIW	INACTIVE
58.	30025084370000	26S-33E-31	WIW	INACTIVE
59.	30025084400000	26S-33E-31	WIW	INACTIVE

1  
2  
3  
4  
5  
6  
7  
8  
9  
10  
11  
12  
13  
14  
15

**Attachment 4**  
**New Mexico Injection Rules**  
**Section 701 - 708**

**Information Only**



Enhanced Recovery Disposal and Storage  
TITLE 19 NATURAL RESOURCES & WILDLIFE  
CHAPTER 15 OIL AND GAS

PART I SECONDARY OR OTHER ENHANCED RECOVERY, PRESSURE  
MAINTENANCE, SALT WATER DISPOSAL, AND UNDERGROUND STORAGE

ISSUING AGENCY: Energy, Minerals and Natural Resources Dept.  
Oil Conservation Division  
2040 S. Pacheco  
Santa Fe, New Mexico 87505  
(505) 827-7131. [2-1-96]

SCOPE: All persons/entities engaged in oil and gas development and production within  
New Mexico. [2-1-96]

STATUTORY AUTHORITY: Sections 70-2-1 through 70-2-38 NMSA 1978 sets forth the Oil  
and Gas Act which grants the Oil Conservation Division jurisdiction and authority over all  
matters relating to the conservation of oil and gas, the prevention of waste of oil and gas and of  
potash as a result of oil and gas operations, the protection of correlative rights, and the  
disposition of wastes resulting from oil and gas operations. [2-1-96]

DURATION: Permanent [2-1-96] EFFECTIVE DATE: February 1, 1996. [2-1-96]

OBJECTIVE: To regulate secondary or other enhanced recovery, pressure maintenance, salt  
water disposal, and underground storage to prevent waste, protect correlative rights  
and protect public health and the environment pursuant to the Oil and Gas Act. [2-1-96]

-7-700 RESERVED

INJECTION OF FLUIDS INTO RESERVOIRS

701.A. Permit for Injection Required

(1) The injection of gas, liquefied petroleum gas, air, water, or any other medium into any  
reservoir for the purpose of maintaining reservoir pressure or for the purpose of secondary or  
other enhanced recovery or for storage or the injection of water into any formation for the  
purpose of water disposal shall be permitted only by order of the Division after notice and  
hearing, unless otherwise provided herein. [1-1-50...2-1-96]

701.B. Method of Making Application

(1) Application for authority for the injection of gas, liquefied petroleum gas, air, water or

any other medium into any formation for any reason, including but not necessarily limited to the establishment of or the expansion of water flood projects, enhanced recovery projects, pressure maintenance projects, and salt water disposal, shall be by submittal of Division Form C-108 complete with all attachments. [7-1-81...2-1-96]

(2) The Applicant shall furnish, by certified or registered mail, a copy of the application to the owner of the surface of the land on which each injection or disposal well is to be located and to each leasehold operator within one-half mile of the well. [7-1-81...2-1-96]

#### 701.C. Administrative Approval

(1) If the application is for administrative approval rather than for a hearing, it must also be accompanied by a copy of a legal publication published by the applicant in a newspaper of general circulation in the county in which the proposed injection well is located. (The details required in such legal notice are listed on Side 2 of Form C-108). [7-1-81...2-1-96]

(2) No application for administrative approval may be approved until 15 days following receipt by the Division of Form C-108 complete with all attachments including evidence of mailing as required under paragraph B (2) above and proof of publication as required by paragraph C (1) above. [7-1-81...2-1-96]

(3) If no objection is received within said 15-day period, and a hearing is not otherwise required, the application may be approved administratively. [7-1-81...2-1-96]

#### 701.D. Hearings

(1) If a written objection to any application for administrative approval of an injection well is filed within 15 days after receipt of a complete application, or if a hearing is required by these rules or deemed advisable by the Division Director, the application shall be set for hearing and notice thereof given by the Division. [7-1-81...2-1-96]

#### 701.E. Salt Water Disposal Wells

(1) The Division Director shall have authority to grant an exception to the requirements of Rule 701-A for water disposal wells only, without hearing, when the waters to be disposed of are mineralized to such a degree as to be unfit for domestic, stock, irrigation, or other general use, and when said waters are to be disposed of into a formation older than Triassic (Lea County only) and provided no objections are received pursuant to Rule 701-C. [5-28-63...2-1-96]

(2) Disposal will not be permitted into zones containing waters having total dissolved solids concentrations of 10,000 mg/l or less except after notice and hearing, provided however, that

the Division may establish exempted aquifers for such zones wherein such injection may be approved administratively. [7-1-81...2-1-96]

(3) Notwithstanding the provisions of Paragraph (2) above, the Division Director may authorize disposal into such zones if the waters to be disposed of are of higher quality than the native water in the disposal zone. [7-1-81...2-1-96]

#### Pressure Maintenance Projects

(1) Pressure maintenance projects are defined as those projects in which fluids are injected into the producing horizon in an effort to build up and/or maintain the reservoir pressure in an area which has not reached the advanced or "stripper" state of depletion. [7-1-81...2-1-96]

(2) All applications for establishment of pressure maintenance projects shall be set for hearing. The project area and the allowable formula for any pressure maintenance project shall be fixed by the Division on an individual basis after notice and hearing. [7-1-81.2-1-96]

(3) Pressure maintenance projects may be expanded and additional wells placed on injection only upon authority from the Division after notice and hearing or by administrative approval. [7-1-81...2-1-96]

(4) The Division Director shall have authority to grant an exception to the hearing requirements of Rule 701-A for the conversion to injection of additional wells within a project area provided that any such well is necessary to develop or maintain efficient pressure maintenance within such project and provided that no objections are received pursuant to Rule 701-C. [7-1-81...2-1-96]

#### Water Flood Projects

(1) Water flood projects are defined as those projects in which water is injected into a producing horizon in sufficient quantities and under sufficient pressure to stimulate the production of oil from other wells in the area, and shall be limited to those areas in which the wells have reached an advanced state of depletion and are regarded as what is commonly referred to as "stripper" wells. [9-1-72...2-1-96]

(2) All applications for establishment of water flood projects shall be set for hearing. [7-1-81...2-1-96]

(3) The project area of a water flood project shall comprise the proration units owned or operated by a given operator upon which injection wells are located plus all proration units owned or operated by the same operator which directly or diagonally offset the injection tracts and have producing wells completed on them in the same formation; provided however, that

additional proration units not directly nor diagonally offsetting an injection tract may be included in the project area if, after notice and hearing, it has been established that such additional units have wells completed thereon which have experienced a substantial response to water injection. [9-1-72...2-1-96]

(4) The allowable assigned to wells in a water flood project area shall be equal to the ability of the wells to produce and shall not be subject to the depth bracket allowable for the pool nor to the market demand percentage factor. [7-1-81...2-1-96]

(5) Nothing herein contained shall be construed as prohibiting the assignment of special allowables to wells in buffer zones after notice and hearing. Special allowables may also be assigned in the limited instances where it is established at a hearing that it is imperative for the protection of correlative rights to do so. [7-1-81...2-1-96]

(6) Water flood projects may be expanded and additional wells placed on injection only upon authority from the Division after notice and hearing or by administrative approval. [9-1-72...2-1-96]

(7) The Division Director shall have authority to grant an exception to the hearing requirements of Rule 701-A for conversion to injection of additional wells provided that any such well is necessary to develop or maintain thorough and efficient water flood injection for any authorized project and provided that no objections are received pursuant to Rule 701-C. [7-1-81...2-1-96]

#### 701.H. Storage Wells

(1) The Division Director shall have authority to grant an exception to the hearing requirements of Rule 701-A for the underground storage of liquefied petroleum gas or liquid hydrocarbons in secure caverns within massive salt beds, and provided no objections are received pursuant to Rule 701-C. [2-1-78...2-1-96]

(2) In addition to the filing requirements of Rule 701-B, the applicant for approval of a storage well under this rule shall file the following:

(a) With the Division Director:

(i) A plugging bond in accordance with the provisions of Rule 101;

(b) With the appropriate district office of the Division in TRIPLICATE:

(i) Form C-101, Application for Permit to Drill, Deepen, or Plug Back;

(ii) Form C-102, Well Location and Acreage Dedication Plat; and

(iii) Form C-105, Well Completion or Recompletion Report and Log. [7-1-81...2-1-96]

### CASING AND CEMENTING OF INJECTION WELLS

Wells used for injection of gas, air, water, or any other medium into any formation shall be cased with safe and adequate casing or tubing so as to prevent leakage, and such casing or tubing shall be so set and cemented as to prevent the movement of formation or injected fluid from the injection zone into any other zone or to the surface around the outside of any casing string. [1-1-50...2-1-96]

### OPERATION AND MAINTENANCE

703.A. Injection wells shall be equipped, operated, monitored, and maintained to facilitate periodic testing and to assure continued mechanical integrity which will result in no significant leak in the tubular goods and packing materials used and no significant fluid movement through vertical channels adjacent to the well bore. [7-1-81...2-1-96]

703.B. Injection project, including injection wells and producing wells and all related surface facilities shall be operated and maintained at all times in such a manner as will confine the injected fluids to the interval or intervals approved and prevent surface damage or pollution resulting from leaks, breaks, or spills. [7-1-81...2-1-96]

703.C. Failure of any injection well, producing well, or surface facility, which failure may endanger underground sources of drinking water, shall be reported under the "Immediate Notification" procedure of Rule 116. [7-1-81...2-1-96]

703.D. Injection well or producing well failures requiring casing repair or cementing are to be reported to the Division prior to commencement of workover operations. [7-1-81...2-1-96]

703.E. Injection wells or projects which have exhibited failure to confine injected fluids to the authorized injection zone or zones may be subject to restriction of injection volume and pressure, or shut-in, until the failure has been identified and corrected. [7-1-81...2-1-96]

### TESTING, MONITORING, STEP-RATE TESTS, NOTICE TO THE DIVISION, REQUESTS FOR PRESSURE INCREASES

#### 704.A. Testing

(1) Prior to commencement of injection and any time tubing is pulled or the packer is resealed, wells shall be tested to assure the integrity of the casing and the tubing and packer, if used, including pressure testing of the casing-tubing annulus to a minimum of 300 psi for 30 minutes or such other pressure and/or time as may be approved by the appropriate district supervisor. A pressure recorder shall be used and copies of the chart shall be submitted to the

appropriate Division district office within 30 days following the test date. [7-1-81...2-1-96]

(2) At least once every five years thereafter, injection wells shall be tested to assure their continued mechanical integrity. Tests demonstrating continued mechanical integrity shall include the following:

- (a) measurement of annular pressures in wells injecting at positive pressure under a packer or a balanced fluid seal; or,
- (b) pressure testing of the casing-tubing annulus for wells injecting under vacuum conditions; or,
- (c) such other tests which are demonstrably effective and which may be approved for use by the Division. [7-1-81...2-1-96]

(3) Notwithstanding the test procedures outlined above, the Division may require more comprehensive testing of the injection wells when deemed advisable, including the use of tracer surveys, noise logs, temperature logs, or other test procedures or devices. [7-1-81...2-1-96]

(4) In addition, the Division may order special tests to be conducted prior to the expiration of five years if conditions are believed to so warrant. Any such special test which demonstrates continued mechanical integrity of a well shall be considered the equivalent of an initial test for test scheduling purposes, and the regular five-year testing schedule shall be applicable thereafter. [7-1-81...2-1-96]

(5) The injection well operator shall advise the Division of the date and time any initial, five-year, or special tests are to be commenced in order that such tests may be witnessed. [7-1-81...2-1-96]

#### 704.B. Monitoring

Injection wells shall be so equipped that the injection pressure and annular pressure may be determined at the wellhead and the injected volume may be determined at least monthly. [7-1-81...2-1-96]

#### 704.C. Step-Rate Tests, Notice to the Division, Requests for Injection Pressure Limit Increases

(1) Whenever an operator shall conduct a step-rate test for the purpose of increasing an authorized injection or disposal well pressure limit, notice of the date and time of such test shall be given in advance to the appropriate Division district office. [11-10-86...2-1-96]



(2) Copies of all injection or disposal well pressure-limit increase applications and supporting documentation shall be submitted to the Division Director and to the appropriate district office. [11-10-86...2-1-96]

## COMMENCEMENT, DISCONTINUANCE, AND ABANDONMENT OF INJECTION OPERATIONS

705.A. The following provisions shall apply to all injection projects, storage projects, salt water disposal wells and special purpose injection wells:

705.B. Notice of Commencement and Discontinuance

(1) Immediately upon the commencement of injection operations in any well, the operator shall notify the Division of the date such operations began. [1-1-50...2-1-96]

(2) Within 30 days after permanent cessation of gas or liquefied petroleum gas storage operations or within 30 days after discontinuance of injection operations into any other well, the operator shall notify the Division of the date of such discontinuance and the reasons therefor. No injection well may be temporarily abandoned for a period exceeding six months unless the injection interval has been isolated by use of cement or a bridge plug. The Director of the Division may delay the cement or bridge plug requirements above upon a demonstration that there is a continuing need for such a well, that the well exhibits mechanical integrity, and that continued temporary abandonment will not endanger underground sources of drinking water. [1-1-50...2-1-96]

(3) Before any injection well is plugged, the operator shall obtain approval for the well's plugging program from the appropriate District Office of the Division in the same manner as when plugging oil and gas wells or dry holes. [1-1-50...2-1-96]

705.C. Abandonment of Injection Operations

(1) Whenever there is a continuous six-month period of non-injection into any injection project, storage project, salt water disposal well, or special purpose injection well, such project or well shall be considered abandoned, and the authority for injection shall automatically terminate ipso facto. [2-1-78...2-1-96]

(2) For good cause shown, the Division Director may grant an administrative extension or extensions of injection authority as an exception to Paragraph (1) above. [2-1-78...2-1-96]

## RECORDS AND REPORTS

706.A. The operator of an injection well or project for secondary or other enhanced recovery, pressure maintenance, natural gas storage, salt water disposal, or injection of any other fluids

shall keep accurate records and shall report monthly to the Division gas or fluid volumes injected, stored, and/or produced as required on the appropriate form listed below:

- (1) Secondary or Other Enhanced Recovery on Form C-115;
- (2) Pressure Maintenance on Form C-115 and as otherwise prescribed by the Division;
- (3) Salt Water Disposal on Form C-120-A;
- (4) Natural Gas Storage on Form C-131-A; and
- (5) Injection of other fluids on a form prescribed by the Division. [1-1-50...2-1-96]

706.B. The operator of a liquefied petroleum gas storage project shall report annually on Form C-131-B, Annual LPG Storage Report. [7-1-81...2-1-96]

#### RECLASSIFICATION OF WELLS

The Division Director shall have authority to reclassify an injection well from any category defined in Rule 701-B to any other category without notice and hearing upon request and proper showing by the operator thereof. [7-1-81...2-1-96]

#### TANSFER OF AUTHORITY TO INJECT

708.A. Authority to inject granted under any order of the Division is not transferable except upon approval of the Division. Approval of transfer of authority to inject may be obtained by filing Form C-104 in accordance with Rule 1104 E. [7-1-81...2-1-96]

708.B. The Division may require a demonstration of mechanical integrity prior to approving transfer of authority to inject. [7-1-81...2-1-96]

1  
2  
3  
4  
5  
6  
7  
8  
9  
10  
11  
12  
13  
14

**Attachment 5**

**Determining Months of Regulated Service  
for Salt Water Disposal and Water Injection Wells**

**Information Only**

**Lea County portion of the Delaware Basin Inside the Nine Townships**

<b>Well Name</b>	<b>API Number (30-025-xxxxx)</b>	<b>Date Converted to Injection</b>	<b>Months of Regulated Service (N ≤ 177, 1982-1996)</b>
Gilmore Federal #1	08109	1992	54
Red Tank Federal #2	08113	1994	29
James Federal #1A	08128	1969	177
Proximity 31 Federal	20423	1995	23
Cuervo Federal	26844	1991	64
Flamenco Federal	31076	1991	64
Union AJS Federal	31412	1993	38
Lost Tank SWD	31443	1992	53
James Federal #1	31515	1992	52
Prohibition Federal #2	31716	1995	20
Kiwi SWD	31889	1993	23
SDE 31 Federal	32868	1996	8
Red Tank 35 Federal #3	33149	1996	12
Red Tank 28	31754	1994	34
Triste Draw 36 State	31929	1995	14

**Total Months of  
Regulated Service: 665  
Total Years: 55.41**

**Eddy County portion of the Delaware Basin Inside the Nine Townships**

Well Name	API Number (30-015-xxxxx)	Date Converted to Injection	Months of Regulated Service (N ≤ 177, 1982-1996)
James A #3	25758	1993	39
James A #12	26761	1992	58
Legg Federal	04734	1994	31
Getty Federal 24	26848	1991	61
Neff Federal #3	28281	1996	12
David Ross "AIT" Federal	26629	1991	69
Todd "26F" Federal #3	20302	1971	177
Todd "26 G" Federal #2	20277	1993	48
Sand Dunes "28" Federal	26194	1993	42
Cal-Mon #5	25640	1993	42
Todd "36D" State #1	20341	1994	30

Total Months of  
Regulated Service: **609**  
Total Years : 50.75

## Lea County portion of the Delaware Basin Outside the Nine Townships

Well Name	API Number (30-025-xxxxx)	Date Converted to Injection	Months of Regulated Service (N ≤ 177, 1982-1996)
Jennings Federal #1	08148	1987	120
U. S. Smetting Federal	08161	1920	177
Cotton Draw Unit 6	08120	1968	177
Cotton Draw Unit 19	08175	1985	144
Cotton Draw Unit 2	08183	1992	41
Cotton Draw Unit 11	08187	1985	144
Cotton Draw Unit 12	08190	1968	177
Cotton Draw Unit 26	08204	1985	144
Cotton Draw Unit 23	08217	1968	177
Cotton Draw Unit 9	08222	1968	177
Thompson 19 Federal #2	08266	1968	177
North El Mar Unit 26	08293	1974	177
North El Mar Unit 50	08305	1974	177
Marshall	08359	1985	144
Antelope Ridge Unit 1	21740	1967	177
Russell Federal #6	22390	1968	177
Ingram O State #2	24432	1974	177
Antelope Ridge Unit #5	24916	1995	9
Conoco Federal #2	08416	1919	177
Exxon A Federal	28202	1985	144
Exxon Federal	28259	1986	132
Bell Lake Unit 2	08484	1972	177
New Mexico EF State	28697	1984	138
Vaca Ridge 30 Federal	28873	1994	28
Federal 30 Unit 2	29069	1993	43

Total Months of  
Regulated Service: 3532  
Total Years: 294.33



## Eddy County portion of the Delaware Basin Outside the Nine Townships

Well Name	API Number (30-015-xxxxx)	Date Converted to Injection	Years of Regulated Service (N ≤ 177, 1977-1996)
Big Eddy Unit 56	22222	1978	177
Golden 8 Federal #3	27283	1994	26
Merlard SWD #1	22980	1988	108
Barbados State #1	27558	1996	3
Salty Bill SWD	10908	1972	177
Rohmer #1	25722	1993	42
New Mexico D4 #1	24531	1994	32
Old Indian Draw 35	22182	1984	146
Old Indian Draw 16	21959	1984	146
Old Indian Draw 21	22101	1984	146
Old Indian Draw 10	21843	1984	145
Old Indian Draw 12	21845	1984	146
Old Indian Draw 5	21618	1984	154
Old Indian Draw 4	21505	1984	146
Old Indian Draw 6	21619	1984	146
Old Indian Draw 2	21391	1984	154
Old Indian Draw 11	21844	1981	190
Big Eddy Unit 117	27261	1994	25
Gourly Federal Unit 4	22661	1991	72
BKE 1	23493	1993	37
Culebra Bluff SWD #1	22754	1993	42
Pardue C 8808	26341	1991	68
East Loving SWD	26764	1991	64
Eddy Gr State #1	22611	1991	65
Pardue Forms 27	26122	1989	102
Nash unit #4	21777	1994	34
Little Field Federal #1	10259	1992	53

**Eddy County portion of the Delaware Basin Outside the Nine Townships  
Continued**

Well Name	API Number (30-015-xxxx)	Date Converted to Injection	Years of Regulated Service (N ≤ 177, 1977-1996)
SDS 11 Federal #1	27627	1993	34
Poker Lake Unit 43	21700	1994	26
Poker Lake Unit 36	10859	1989	86
Sulphate Sister #1	21029	1977	177
State MA Com #1	23709	1994	30
Corral Draw #2	21425	1991	61
Pogo 36 State #1	27398	1993	37
Mobil 22 Federal #5	25321	1990	84
Amoco Federal #1	24466	1989	86
Gulf Pipkin Federal	3751	1971	177
McKenna Federal	20222	1969	177
Zac Federal #1	25745	1989	94
Federal AZ	23324	1989	85
Ross Draw SWD #1	23680	1983	158
Ross Draw Unit 9	23774	1988	99
RT Wilson Federal	5868	1973	177
Hanson Federal #11	5877	1971	177
Russell 35 Federal #2	5891	1992	54

Total Months of  
Regulated Service: 4463  
Total Years: 371.91

**TOTAL YEARS OF SERVICE FOR ALL ACTIVE WELLS: 772.4**

Each of the well files listed in the above table were carefully reviewed to determine the exact number of months each well had operated as an injection or salt water disposal well. Injection dates used began with the first full month of service, through December of 1996, with no credit given for starting dates that began at mid month or earlier. This has resulted in a conservative total for months of service. Once total months of service had been calculated, this number was then converted to total years of service (well years).

**Attachment 2: Technical Review by Swift, et al. of *The HARTMAN Scenario:  
Implications for WIPP*, by John Bredehoeft**

**Information Only**

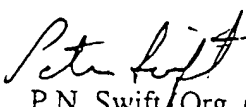
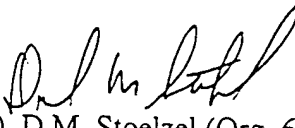

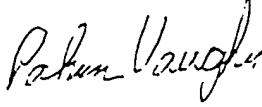
WFO 44158

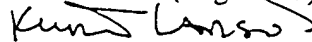
## Sandia National Laboratories

Albuquerque, New Mexico 87185-1341

date: June 13, 1997

to: Margaret S.Y. Chu (Org. 6801), MS 1335  
SWCF WFO # 45839

from:      
P.N. Swift (Org. 6801), D.M. Stoelzel (Org. 6848), R.L. Beauheim (Org. 6115), P. Vaughn  
(Org. 6849), and ~~K.W. Larson (Org. 6821)~~



subject: Technical Review of *The HARTMAN Scenario: Implications for WIPP*, prepared for the New Mexico Attorney General, March 1997, by John Bredehoeft

### Introduction

The Carlsbad Area Office of the Department of Energy has asked us to provide a technical review of *The HARTMAN Scenario: Implications for WIPP* (Bredehoeft, 1997). This report has been prepared by John Bredehoeft of the Hydrodynamics Group of La Honda, California, at the request of the New Mexico State Attorney General, and has been submitted to the EPA as a formal comment on the WIPP Compliance Certification Application.

Our approach in conducting this review has been consistent with standard practice in technical disciplines. Basically, we have examined the report as if we had been asked to comment on it prior to publication, and the questions we raise are those we believe thorough technical peer reviewers should ask of any report. The standards we have applied are essentially the same as those we use in ordinary professional reviews of other reports, both externally and internally within Sandia. The fact that the report has already been published may reduce the usefulness of our observations compared to those made in more typical reviews, but the intent is similar. We have tried to evaluate the merits of the document on its own terms.

Our detailed comments on the report follow in the body of this memorandum, organized in the same format as the major topics in the report. We have attempted to focus our comments on topics addressed in the report, rather than to digress with discussions of external topics. In particular, Bredehoeft states clearly in his report that he makes no attempt to estimate the probability of occurrence of his scenarios. We have tried to honor this condition, although we believe that a complete analysis of the possible effects of fluid

injection on the WIPP must consider both the processes that could lead to high pressure fluid coming into contact with the specific anhydrite marker beds closest to the WIPP, and the probability of their occurrence. Our comments therefore focus almost entirely on the phenomena that Bredehoeft addresses in the report: hydraulic fracturing of marker beds at high pressure and subsequent brine flow through them.

In general, our technical comments are too numerous and too specific to summarize here in introductory paragraphs. Our overall conclusion, however, is straightforward. The report does not present a realistic or reasonable analysis of the phenomena it addresses. From the information available in the document, we conclude that the conceptual models used in the analysis are incompletely explained, sometimes inconsistent with observed data, and sometimes inconsistent from one portion of the report to another. Reasonable alternative models are not considered. Important assumptions made in setting up the computational models, such as the choice of boundary conditions, are, in many cases, neither explained nor justified, and some appear to be physically implausible. Insufficient information is provided to evaluate the adequacy of the computational modeling, and simple checks of the physical reasonableness of the model results are, in general, not presented. Ultimately, the results of the modeling work and the conclusions drawn from them are not credible.

We recognize that these conclusions may be controversial to some readers, and we encourage other interested scientists to conduct their own, independent, technical reviews of *The HARTMAN Scenario: Implications for WIPP*. We also encourage readers preparing to read the remainder of this review to read the subject report first, and to keep a copy of it at hand while considering our comments.

### **Comments on Chapters 1 and 2: *Introduction and Background: Hydraulic Fractures***

The first two chapters provide background information about oil and gas activity at the site and in the region, and general information about hydraulic fracturing. The "Hartman Scenario" is mentioned, but the details of Bredehoeft's interpretation of the blowout in January of 1991 at the Bates # 2 well east of Jal, New Mexico, are presented in Chapter 3.

In general, the material in these chapters would be strengthened by providing references to supporting documentation. For example, the assertions that "leaks are endemic to the high pressure brine injection process" (p. 5) and that "routine hydrofracs are commonly 100 to 200 m in length" should not be assumed to be common knowledge that needs no citation. References should be provided for the source of information about the Hartman case, and care should be taken not to mix observations from the Hartman case with conclusions drawn by the court or by the author. For example, the statement on p. 5 that water injection occurred "where it was not intended" at the Bates # 2 well presupposes that injection was the cause of the blowout. This should be identified as an interpretation, rather than a direct observation.

The relevance of the discussion in Chapter 2 of other examples of hydrofracturing is unclear, and should be explained. The hydrofractures at the Wattenberg Field in Colorado occur at approximately 8000 feet below the ground surface, well below the depth of either the Hartman case or the WIPP, in what is presumably a different stress regime and very different lithologies (for additional information about the Wattenberg fractures, see Smith et al., 1978, cited by Bredehoeft). The fractures were deliberately induced by carefully engineered injection of polymer emulsion fluid and proppant, under circumstances very unlike the inadvertent leakage Bredehoeft proposes for the Hartman case. The Wattenberg fractures are vertically oriented, unlike the horizontal disk-shaped fractures predicted by Bredehoeft at shallower depths (and observed in the WIPP underground), and it is not clear that the total distance they propagated is relevant to the Hartman case. The text of the report should discuss these differences. The relevance of the fractures induced by igneous activity is even less clear (see Zoback and Zoback, 1980, and Hunt, 1954, cited by Bredehoeft). The text should discuss the possible effects of the differences in depth of fracturing and the material properties of the injection fluid (i.e., magma) between these examples and the WIPP.

We note that Bredehoeft omits any mention of the anhydrite hydrofracture experiments that were conducted in Marker Beds 139 and 140 at the WIPP (Beauheim et al., 1993; see also Wawersik et al., 1997, published in May of 1997 and not available at the time of Bredehoeft's report). We believe that this work provides the only direct experimental evidence of the behavior of hydrofractures in the Salado Formation, and is therefore surely relevant to the development of a conceptual model for anhydrite fracturing at the WIPP.

The discussion in Chapter 2 of the mechanisms by which injection wells may fail lacks an adequate description of the construction of a fluid injection well. The text in the section called "Pipe Failure" on page 13 describes the well as a single pipe filled with high-pressure injection fluid and separated from the surrounding rock by an annular space that may be filled with fluid, closed with cement, or closed by rock deformation. As shown in Figure 1, which is a schematic diagram of the construction of the Neff Federal # 3 well discussed in Bredehoeft's report, this is not correct. Wells are not a single column of pipe. All injectors in the WIPP region contain at least two "strings" of steel casing through the near-surface units, and most have two casing strings through the salt section. Furthermore, all injection wells in the WIPP region inject through "tubing," which is an additional column of pipe placed inside the casing. In a properly functioning injection well, the high-pressure brine is confined within the tubing except in the injection interval, which is separated from the overlying (and underlying, if any) formations by a packer which seals the annulus between the tubing and the casing. Above the packer, the annulus between the tubing and the casing is filled with water to maintain a hydrostatic gradient. Thus, as long as the tubing and packer are functioning correctly, the casing will not be exposed to the pressure gradients envisioned by Bredehoeft. Tubing and packer failures are possible, of course, but are readily detected by the operator when pressure in the inner annulus rises at the surface to match the injection pressure. As described by DOE (1997), operators of



injection wells in the New Mexico portion of the Delaware Basin report casing and tubing pressures to the State of New Mexico annually. Once detected, leaks in injection wells are repaired promptly.

The brief comment in Chapter 2 (page 13) in the section titled "Stoelzel and O'Brien Analysis" implies that the Stoelzel and O'Brien (1996) model neglected changes in permeability resulting from hydraulic fracturing. Stoelzel and O'Brien's model explicitly included a permeability increase in the marker beds at the WIPP elevation to account for the effects of fracturing. Bredehoeft's assertion at the end of this paragraph that fracture pressure in injection wells near the WIPP is exceeded at "depths of 2500 to 2000 feet and above, depending upon the injection well-head pressure" should acknowledge that some pressure loss occurs in the flow path between the injection horizon and the interval proposed for fracturing. For the leaky cement sheath discussed by Stoelzel and O'Brien in the quoted text, the pressure drop is likely to be considerable.

### Comments on Chapter 3: *The Hartman Scenario*

This chapter presents a derivation of a value for the permeability of the interval producing the high-volume brine flow at the Bates # 2 well, and then draws the conclusion that flow occurred through fractured anhydrite.

Bredehoeft uses a one-time measurement of the flow rate and a one-time measurement of the shut-in pressure to estimate permeability, based on an assumption that the well was at steady state. In all probability, the flow rate was declining steadily during the entire period the well was producing, so the true steady-state flow rate must be less, possibly orders of magnitude less, than the 840 gpm (1.9 ft<sup>3</sup>/sec) used by Bredehoeft. Likewise, the shut-in pressure may have been continually rising after flow was stopped, and the one-time measurement of 1000 psi may represent an underestimate of the true formation pressure, particularly if the well was producing from a finite reservoir. Therefore, the true formation permeability must be less, and perhaps significantly less, than Bredehoeft estimates. The permeability simply cannot be determined from the available data.

Bredehoeft goes on in Chapter 3 to state that the permeability derived for the Bates # 2 blowout zone "almost surely represents hydrofraced anhydrite in the Salado Formation" (page 16). This is an interpretation, rather than an observation, and should be identified as such. The basis should be explained by which he has excluded reasonable alternative explanations, including the penetration of a local overpressurized reservoir. If it is indeed a consensus interpretation reached by a broad technical community, as implied on page 17, that hydrofracturing at the Bates # 2 well was caused by water injection at the Rhodes-Yates Field, then citations should be provided identifying the origin of the consensus.

Bredehoeft's assumption on page 15 that  $r_1$  in the Theim solution is 0.5 feet, representing the radius of a well bore "slightly larger than the drill bit," has relatively little effect on his

derived permeability, but warrants further explanation because of its relevance to the condition of the borehole and the surrounding formation during the blowout. Examination of Figure 2 (reproduced from Figure 5 of Van Kirk, 1995, cited by Bredehoeft) shows that the cementing of the Bates # 2 borehole required 6900 sacks of cement. The volume of a hole one foot in diameter and 2280 feet deep is 1791 cubic feet. Assuming, in the absence of specific information on the properties of the cement emplaced, that each sack yielded 1 cubic foot of slurry (probably a small underestimation) and neglecting the volume of the hole filled by the stuck drill pipe, it appears that nearly four times more cement was used than would fit in a one-foot hole. Given that the blowout was reported to have been immediately preceded by an 86-foot drilling break (see Figure 2), the most likely explanation is that the extra cement partially filled a cavity in the blowout zone. If Bredehoeft's conceptual model for flow from hydrofractured anhydrite is to be based on the events at the Bates # 2 borehole, the text should include additional discussion of the drilling and plugging of the hole.

Chapter 3 concludes with a brief discussion of a conceptual model for the relationship between permeability and porosity in fractures. The primary purpose of this paragraph appears to be to justify a conceptual model in which porosity increases during fracturing are small enough to be neglected. We have two comments on this paragraph.

First, the text should describe the conceptual model and its basis in more detail. Relevant data, if any, that support a model for fracturing in anhydrites in which porosity changes are negligible should be presented. Data collected from hydrofracturing experiments in anhydrites that do not support this model (e.g., Beauheim et al., 1993) should also be discussed, and alternative conceptual models should be described. As a perhaps minor point, the reference here to "approximately 4%" (0.04) as the value used in the WIPP Compliance Certification Application (CCA) (DOE, 1996) for the porosity of fractured anhydrite is inappropriate. To be consistent with the conceptual model Bredehoeft proposes, the appropriate porosity from the CCA should be the value for unfractured anhydrite: 0.011.

Second, the assertion that an increase in porosity is small does not necessarily mean that it is not important to the simulation results. Bredehoeft provides an example in the final paragraph of Chapter 3 in which pore space is increased by 0.001 m in a 1 m thick anhydrite as a result of fracturing. This means that 0.001 m<sup>3</sup> of fluid would be required to fill the newly created fracture porosity in 1 m<sup>3</sup> of anhydrite. For comparison, we calculate the amount of water that goes into elastic storage in the same rock to be 0.0017 m<sup>3</sup>, assuming, as Bredehoeft does in Chapter 4, that pressure must be increased by 2 MPa to initiate fracturing and that  $1 \times 10^{-5} \text{ m}^{-1}$  is the appropriate specific storage (see Attachment 1). The amount of water required by these two processes differs by less than a factor of 2. As noted by Bredehoeft, model results are quite sensitive to the value of specific storage, and the model may therefore also be sensitive to the assumption that the extra pore space generated by fracturing can be neglected. The text should discuss this point and provide

additional justification for the assumption that porosity increases during fracturing can be neglected.

#### Comments on Chapter 4: *Modeling Hydraulic Fractures*

As Bredehoeft states on page 18, "In this chapter, I describe my numerical model of hydraulic fracturing. Having described the model, I use it to show that hydraulic fractures can extend outward in the anhydrite marker beds to considerable distances."

We do not believe that this chapter contains sufficient information to evaluate either Bredehoeft's conceptual model for fracturing (introduced in Chapter 2 and in the final paragraph of Chapter 3) or its numerical implementation. The chapter should contain a clear discussion of the conceptual model and references to standard documentation of the numerical model and computer code used to implement it. A more complete discussion of this specific application of the model should be provided, including full description of initial and boundary conditions and cell dimensions. The statement on page 19 that "cell dimensions were varied with the virgin permeability so that boundary effects were minimized" should be clarified, given that text on page 18 strongly implies that virgin permeability was spatially invariant. The boundary effects referred to and the performance measure used to quantify their minimization should be described. The assertion made on page 18 that "virgin permeability does not play much of a role in extending the fracture, as long as it is sufficiently low to allow the fracture to extend to two miles" should be justified. The assumption contained in Table 4.1 on page 19 that specific storage does not change as the fracture opens should be discussed in detail and justified. This appears to be a key step in implementing the conceptual model introduced in the last paragraph of Chapter 3.

Bredehoeft's numerical model simulates hydrofracturing by increasing permeability if the pressure reaches a value of 2 MPa above the far field pore pressure. The model apparently does not account for any additional pore volume that would occur as a result of fracturing. This additional pore volume, even if small, would act to decrease fluid pressures and hence slow the rate at which fractures propagate. Therefore, assuming that fractures do not create additional pore volume systematically overestimates the extent of hydrofractures. The impact of this assumption should be discussed in this chapter.

The discussion of model results would benefit from additional detail. For example, the reported time interval is "injection period." This is presumably not the same as the amount of time required to propagate the fracture. How long after the end of the injection period is it before the fracture reaches its maximum radius? Is the reported fracture radius the maximum distance the fracture propagated? What happens to the fracture after injection is turned off? Does the model simulate fracture closing as pressure drops?

Field evidence suggests that 100 days is a long time for a major casing and tubing failure to

persist undetected in an injection well (see DOE, 1997). Given that Bredehoeft's model could perhaps predict that substantially longer injection periods were required to produce long fractures if he considered the effects of additional pore space created by fracturing, it is inappropriate to use these model results as the basis for the assumption made later in the report that the entire regional domain (up to 38 km by 38 km in some cases) is fractured prior to beginning the flow simulations. If this conclusion is to be drawn from the modeling work, results should be presented that show the time required to generate fractures on this scale, accounting for the creation of additional porosity during fracturing.

#### **Comments on Chapter 5: *The Dilemma: Steady Flow***

This chapter presents the results of numerical modeling that show that, for the chosen modeling assumptions and input parameters, steady-state flow between an injection well and the WIPP could occur at a high rate. The chapter goes on to discuss one of the possible conceptual difficulties with the model: that fractures are unlikely to remain open as pressure drops below lithostatic, and that the high permeabilities assumed in the model are therefore unrealistic.

We do not believe that this chapter contains sufficient information to fully evaluate the conceptual model for brine flow in the marker bed or its computational implementation. As is the case for Chapter 4 and other chapters in this report, the text should contain a clear discussion of the conceptual model and its computational implementation. A more complete listing of initial and boundary conditions should be provided.

The assumption stated on page 20 that this is a "steady flow analysis" needs further explanation and justification. As noted previously in comments on Chapter 2, it is not immediately obvious that it is appropriate to model fluid injection processes using steady-state assumptions. As noted in the comments on Chapter 4, the assumption that fracturing occurs over "an extensive area" (shown as 38 x 38 km in Bredehoeft's Figure 5.1, reproduced here as Figure 3) has not been adequately supported by the results of the fracture model given in Chapter 4. More justification is needed. Justification should also be offered for the assumption that the repository pressure remains constant throughout time. No reasonable conceptual model is presented as to how a sealed void can receive large volumes of liquid inflow without changing pressure.

Rates of flow from the injection well predicted by this model should be compared to reported rates injected into real wells in the region, to provide a quick check on the realism of the model. The rate of flow reported into the WIPP for the higher permeability case (88,000 m<sup>3</sup>/yr) is presumably smaller than the total injection rate, and appears unrealistically high compared to field rates. The most prolific injector in the region (the David Ross AIT Federal # 1) injected between 1991 and 1997 at an average rate of approximately 137,000 m<sup>3</sup>/yr (DOE, 1997), with most of this liquid presumably entering the target reservoir in the Bell Canyon Formation. It does not seem credible that more than

one half of the total injection could occur inadvertently into the WIPP through a 1-m thick marker bed.

We agree conceptually with Bredehoeft's conclusion on page 21 that the high-permeability case is unrealistic because "the area where a fracture might remain continuously open is restricted to close into the injection well." Figure 3 (reproduced from Bredehoeft's Figure 5.1), which shows the head surface resulting from the flow model, supports this conclusion. Plots of this sort are difficult to interpret quantitatively because the vertical and horizontal scales are not readily interpreted away from the axes, but it appears that pressures above lithostatic are restricted to a very small portion of the model domain surrounding the injection well, limiting the extent to which fractures might propagate.

As a minor point, it appears that the vertical scale is incorrect on Figure 3. The text indicates that the injection well is maintained at 4 MPa above the far field pressure. Assuming a brine hydrostatic gradient of 0.525 psi/ft (consistent with surface pressure simulated by the well), the injection well should appear in Figure 5.1 with a head approximately 340 m above the far field, rather than the approximately 100 m shown.

The plot also clearly indicates the effect of maintaining WIPP at a constant, relatively low, pressure. It becomes a dimple in the head surface, and functions unrealistically as a permanent sink.

#### **Comments on Chapter 6: *The Stoelzel-O'Brien Cross-Section***

This chapter compares the results of steady-state flow calculations performed using the areal model described in Chapter 5 and a horizontal strip model described briefly here. Results indicate that this horizontal strip model estimates significantly less flow into the WIPP than the areal model. No direct comparison is given with the Stoelzel and O'Brien (1996) vertical cross-section model.

As is the case for other modeling studies summarized in the report, we believe that the text does not provide sufficient information to allow a full evaluation of the horizontal strip model. Based on the information provided, however, we do not believe that the comparison implied between Bredehoeft's model and the Stoelzel and O'Brien model is adequately justified. Specifically, the text should directly address the geometry used by Stoelzel and O'Brien, which included an approximation of radial flaring around the injection wells as well as cross-sectional regions between the repository and the wells. The text should also address the relevance of a comparison between two steady-state flow models as a comment on the adequacy of a transient flow and fracture model, and should evaluate the transient effects of fracturing in each model.

As was noted in comments on Chapter 5, calculated flow rates should be compared to observed field rates as a simple check of the realism of the model. Rates calculated here



seem unreasonably high.

As a perhaps minor point, the vertical scale on Bredehoeft's Figure 6.1 may have the same problem as Figure 5.1 (reproduced here as Figure 3). As is also the case in Figure 3, this figure shows the inappropriateness of assuming that pressure within the repository does not change as flow occurs.

#### **Comments on Chapter 7: *Transport Through WIPP***

The purpose of this chapter is unclear. The title suggests that the chapter addresses transport, but the only model presented is a flow model. As is the case for other chapters, there is insufficient information provided to allow the reviewer to fully understand the model, but based on the available discussion the conceptual basis for the model appears weak.

The basis for the assumption stated on page 25 that there is a region of high pressure and high permeability surrounded by an area of virgin permeability should be stated. Without further explanation, this assumption appears to contradict the conceptual model for fracturing presented in Chapter 2, in which fractures will propagate as long as pressure remains above lithostatic. Some justification other than "purely for convenience" should be offered for the assumption that the flow field is steady state, particularly given the apparent disequilibrium between pressure and fracturing.

The assumption that "WIPP fills with brine until it reaches a pressure that does not impose a perturbation on the flow field" appears consistent with the rest of the assumptions in the model. Why wasn't this same assumption made in Chapters 5 and 6, where pressure in the repository was held constant regardless of brine inflow?

The "Results" section of this chapter provides much less information than is provided in other chapters. For example, what is the rate of flow from the injection well? What is the rate of flow through the WIPP? The text on page 26 notes that "the flow through the region is very small," and is, reasonably enough, "controlled by the surrounding region of virgin permeability." Bredehoeft's Figure 7.1, which shows the head surface resulting from the steady-state flow calculation, suggests that the fractured region is square. The conceptual basis for this assumption should be discussed.

#### **Comments on Chapter 8: *The High Pressure Scenario***

This chapter presents the results of a simulation in which pressure within the entire model domain, including the repository, is at or above lithostatic. This assumption creates conditions which allow regional fractures to occur and remain open, consistent with the conceptual model for fracturing presented in Chapter 2. Steady-state flow calculations show a large rate of brine flow into the WIPP under these conditions.



We do not believe that this chapter contains sufficient information to fully evaluate the conceptual model for brine flow in the marker bed or its computational implementation. As is the case for other chapters in this report, the text should contain a clear discussion of the conceptual model and its implementation. Specific justification of modeling assumptions, including the initial and boundary conditions, should be provided.

Based on the information available, however, we do not believe that this model simulates a physically credible set of conditions. Our specific comments follow.

Bredehoeft's Figure 8.1, showing 10,000-yr histories of pressure in a waste disposal panel for 100 realizations of the Sandia performance assessment for the WIPP CCA, provides the basis for his assertion that pressure in the repository may reach or exceed lithostatic under some circumstances. We agree with this conclusion, but also call attention to the time at which high pressure may occur. As shown in Bredehoeft's Figure 8.1, the earliest time in these 100 realizations at which pressure in the waste panel reached 14.7 MPa is approximately 2,700 years. Thus, one condition, of many, that must occur for Bredehoeft's "High Pressure Scenario" to be possible is that fluid injection in the vicinity of the WIPP must be assumed to persist many thousands of years into the future. The text of Chapter 8 should acknowledge this point, and discuss its conceptual basis.

Text on page 28 states "I model this scenario by 1) creating a hydraulic fracture between the leaking well and WIPP, and 2) examining the flow that might occur should this happen," implying that fracturing is simulated dynamically for this case. Figure 8.2 on page 29, which shows the "area that is hydraulically fractured," appears to show actual model results, reinforcing the implication that Chapter 8 includes results of dynamic fracturing. Examination of the text and model results, however, strongly suggests that fracturing was not actually simulated, but rather was assumed for this model. No discussion is given of the model used to create the fractured domain shown in Figure 8.2, nor is there an interpretation of the figure. The text should discuss the point more clearly.

Several comments common to the flow models presented in Chapters 5 and 6 also apply here. What, for example, is the justification for simulating steady-state flow? What is the justification for assuming that the repository remains at a constant pressure regardless of brine inflow? (Note that this assumption was removed in Chapter 7 and reinstated for Chapter 8.) What is the justification for assuming that the entire model domain is fractured before beginning the steady-state flow calculation? Has the calculated flow rate been compared to actual injection rates? As in previous chapters, the rate reported here (82,000 m<sup>3</sup>/yr entering the WIPP) appears to be unreasonably high when compared to the highest reported injection rates in the region.

Although the text does not mention boundary conditions assumed for the flow model, Bredehoeft's Figure 8.3 (reproduced here as Figure 4) shows that no-flow boundaries were imposed on this model. Despite the assertion in the caption that this figure is "very similar

to Figure 5.1," it is not. The change to a no-flow boundary is a very significant, and unexplained, departure from the approach taken in Chapters 5 and 6, and causes pressure to rise above lithostatic throughout the model domain. The conceptual model underlying this assumption should be described in detail and justified carefully. Without further explanation, the model appears to directly contradict the conceptual model for fracturing described in Chapter 2, in which fractures will propagate as long as pressure remains above lithostatic. Figure 4 also shows clearly the effect of holding the WIPP at a constant pressure throughout the simulation: it functions as the only sink in the steady-state flow model, and all brine that leaves the injection well must enter the repository. This is simply not a plausible assumption: brine cannot enter a sealed void without affecting the pressure.

As a perhaps minor point, the vertical axis of Figure 4 appears to be incorrect. Assuming a brine hydrostatic gradient of 0.525 psi/ft, the injection well should rise approximately 170 m above the lithostatic head.

### **Comments on Chapter 9: *The Pulsing System***

Chapter 9 addresses a phenomenon that Bredehoeft hypothesizes may occur if fractures propagate into a relatively low pressure region such as the repository. Fractures will close as pressure drops below lithostatic, and then reopen as pressure builds back up. The system will "pulse" indefinitely as long as the high pressure source and low pressure sink remain. Bredehoeft concludes that model results of flow into the repository for this condition are not sufficiently reliable to interpret quantitatively, but that the phenomenon remains one of possible concern.

In general, we agree with Bredehoeft's apparent finding that the behavior of fractures breaking through into low pressure sinks is difficult to model numerically. If the phenomenon were plausible at the WIPP, a more sophisticated modeling approach than that presented by Bredehoeft would be needed to develop meaningful results. Based on our review of this chapter and the remainder of the report, however, we disagree with Bredehoeft's conclusion that the phenomenon is likely to occur at the WIPP and that it poses a threat to the facility.

As is the case for other chapters in this report, we do not find sufficient documentation of the conceptual and computational model to allow a complete evaluation of the modeling study. The lack of a clear discussion of the link between the conceptual model for fractured anhydrite and the numerical model may be particularly important in this case, given the strong likelihood, acknowledged by Bredehoeft, that the details of the model results may be artifacts of the numerical implementation.

The lack of detail makes it difficult to determine what was actually done in the simulation. On page 31, text states that "pressure at the well does not change significantly--I hold the injection rate constant." It seems improbable that both portions of this statement are true,

particularly given the statement on page 32 that "pressure in the model suggests that the flow leaking out the injection well is  $2 \times 10^{-3} \text{ m}^3/\text{sec}$ ." If flow at the injection well is specified to be constant, it should not need to be interpreted from the pressure.

Bredehoeft's Figure 9.1 shows a "schematic projection of the area fractured in the pulsing scenario." Given that the modeling performed for Chapter 9 apparently included dynamic calculation of fracturing, why is the figure schematic? Why is the fractured region shown as a square, rather than the disk shape region that would be consistent with the conceptual model for fracturing described in Chapter 2 and illustrated in Chapter 8?

The quantitative time-histories of pressure and flow shown in Bredehoeft's Figures 9.2 and 9.3 raise additional questions. What, for example, is the origin of the second-order pressure peaks in Figure 9.2, and why do they differ in number and duration from one cycle to the next? Why does the first breakthrough to the repository occur at approximately 0.2 days, when the example given in Chapter 4 for the storage coefficient used in Chapter 9 shows that 100 days of injection are required to propagate a 2.8 km fracture? Why does the model appear to develop a stable pattern after 1.5 days?

Bredehoeft concludes that the frequency of the pulsing is "a function of 1) the fluid injection rate, 2) the transmissivity and storage coefficient for the fracture, and 3) the model parameters, especially the cell size, and time step size." The storage coefficient and permeability (but not thickness) of the fractured layer are given, but no discussion is provided of the sensitivity of the model results to changes in these parameters. We suspect that Bredehoeft is correct in his assumptions about the relative importance of the other parameters, particularly the cell dimensions and the time steps, but values are not given.

The final paragraph of Chapter 9 proposes an alternative conceptual model, in which flow into the WIPP might occur through a large enough cross-sectional area of relatively-low permeability material to allow a sufficiently steep pressure gradient to maintain pressures above lithostatic in the marker beds.

The WIPP performance assessment modeled an analogous phenomenon for a different purpose when considering whether or not the disturbed rock zone surrounding the excavation might be of sufficiently low permeability to impede fracturing of the anhydrites while allowing pressure within the repository to rise above lithostatic. Using the two-phase flow model of the repository and surrounding strata developed for performance assessment, Vaughn et al. (1995) concluded that flow through the DRZ was sufficiently rapid at a permeability of  $10^{-15} \text{ m}^2$  that steep pressure gradients would not persist between the repository and the anhydrite layers, and that the anhydrites would fracture in response to elevated repository pressure. Vaughn et al. (1995) did not model the case proposed by Bredehoeft, in which the anhydrite layers are at higher pressure than the repository, but the behavior can be reasonably inferred to be similar. Permeabilities in the near field around the repository that are high enough to allow flow rates comparable to those predicted for the

marker beds will also result in similar pressure conditions within the repository and the adjacent anhydrite layers.

### Comments on Chapter 10: *The Two Well Scenario*

This chapter examines a scenario in which flow occurs from a leaking injection well through fractures in Marker Bed 139 to an unplugged well. The two wells are located on opposite sides of the WIPP, and flow occurs through the repository. Transport of radionuclides is modeled from the repository toward the outflow well. Bredehoeft concludes that transport of radionuclides by this mechanism will be extremely rapid, and that releases will be 50 times the EPA limits within 13 years.

As described in detail in the following comments, we do not believe that the analysis presented in this chapter is credible. Insufficient information is provided to evaluate the model and its results completely, but based on the available documentation, we conclude that the conceptual basis for this model is flawed and that the model results are not meaningful.

Many of our comments are similar to those raised in earlier chapters. For example, the text should provide a more complete discussion of the conceptual model and its implementation in the computational model. Assumptions made in setting up the computational model should be clearly stated and justified. Documentation of the computational model, including a more complete listing of initial and boundary conditions, model parameters, and grid dimensions should be provided. The assumption that flow is steady-state should be justified. The transport model should be described in detail, because this is its first application in the report. Model results, particularly the injection flow rate and the rate at which brine is produced from the marker bed, should be compared to field observations as a simple check of the realism of the model. We do not believe that either the injection rate or the production rate are credible.

Other comments follow that are specific to this chapter and the scenario it addresses.

The chapter begins with the assumption that the scenario could occur. Elsewhere in the report Bredehoeft has stated that he makes no estimates of the probability of occurrence of his scenarios, and the same disclaimer presumably applies here. However, the text should address the conceptual model underlying the scenario in the light of actual drilling practice. Possible leak mechanisms and pathways from injection wells into marker beds should have been discussed earlier in the report (perhaps in Chapter 2). Here, the report should describe the pathway by which leakage occurs from a marker bed into an unplugged borehole. What are the circumstances under which a borehole might be unplugged and open to the marker beds? (Our understanding of current practice in the region indicates that such conditions would be rare: as described in Appendix DEL of the CCA, no oil and gas boreholes in the region are currently abandoned without plugging.)

If the pathway into the unplugged borehole is envisioned to be hydraulic fractures, as stated in the text, then the mechanism by which pressure in the borehole remains high enough to keep the fractures open should be described. Without further explanation, this assumption that fractures will remain open appears to directly contradict the conceptual model for fracturing presented in Chapter 2, in which fractures close if pressure falls below lithostatic.

The fate of the brine that enters the unplugged hole should be discussed at least qualitatively. This is particularly important given the very high rates of flow into the unplugged borehole (73,000 m<sup>3</sup>/yr, reported on page 36 as  $2.3 \times 10^{-3}$  m<sup>3</sup>/sec) calculated by the model and the assumption that the flow system is at steady state. This rate of flow would completely displace the pore volume of a typical borehole within hours or days, and it is highly improbable that it could persist indefinitely.

The scenario calls for two wells symmetrically opposing each other on either side of the WIPP, with one injecting into Marker Bed 139 and one producing from Marker Bed 139. Although Bredehoeft chooses not to address probability, it seems appropriate to discuss the consequences of additional wells or other placements of the wells. Is this scenario the least favorable combination?

The conceptual basis should be provided for the assertions on page 36 that "the repository and the disturbed rock zone (DRZ) provide a high permeability pathway for fluids where it exists" and that brine in the marker bed will have "approximately the same concentration [of radionuclides] as the brine within the WIPP." What is Bredehoeft's estimate of the permeability of the waste and the DRZ? How does it compare to the permeability of his fractured marker bed, and what are reasonable estimates of the flow and transport between the waste panels and the marker bed? If the permeability of the fractured marker bed is much greater than that of the DRZ and waste, most flow may be confined to the marker bed. We believe that Bredehoeft's assumption of instantaneous flow and transport between the repository and the marker bed results in an extreme overestimation of the quantities of radionuclides in marker bed brine.

Pressure in the repository is assumed for the purposes of this simulation to change with brine inflow and outflow, reaching the ambient pressure calculated by the model. This seems to be a reasonable assumption, but it is inconsistent with the unrealistic assumption made in earlier chapters that the repository remains at a constant pressure. The basis for the change in the assumption should be discussed.

Pressure in the outflow well is described on page 36 in Table 10.1, "Model Assumptions" as "0 MPa (atmospheric)" at the surface and 14.7 MPa at depth. The reason for this specification is not stated, but it presumably is to ensure lithostatic pressure in the marker bed so that fractures can be assumed to remain open. Bredehoeft's Figure 10.2 (reproduced here as Figure 5), which shows the head surface resulting from the steady-state flow calculation, suggests that lithostatic pressure is exceeded throughout the model



domain (although no vertical scale or datum are given). The figure also shows that, because no-flow boundaries have been imposed, the outflow well functions as the only sink in the model.

The conceptual basis for the specification of lithostatic pressure in the outflow well is not stated either, and we believe that none can be offered. For an unplugged hole to maintain atmospheric surface pressure and lithostatic downhole pressure it would need to be filled with a liquid with the density of rock (approximately twice the density of brine).

Table 10.1 on page 36 also indicates that the inflow and outflow rates are equal. The conceptual basis for this assumption, and the no-flow model boundaries it requires, should be discussed in detail. What is the justification for the statement on page 37 that "I adjust the flow rate of the outflow well until the head remains above lithostatic throughout the flow domain"? Without further explanation, this model appears to us to simulate physically unreasonable phenomena.

Bredehoeft's Figure 10.6 (reproduced here as Figure 6) shows cumulative radionuclide transport through time at specified distances from the repository. We do not believe these results are credible because of conceptual problems in both the flow and transport models, as discussed above. The report contains insufficient detail about the transport calculations to evaluate the accuracy of the results conditional on the modeling assumptions, but, as Bredehoeft notes in the caption of the figure, "the spread in the curves at later times is some measure of the model error." Based on visual inspection, it appears that approximately 50 EPA units have passed a point 3 km from the repository at 13 years, but that only approximately 43 EPA units were reported in the same time at 2.75 km. The model appears to have created 7 EPA units of radionuclides in 250 m, which is approximately a 16% mass balance error. Transport errors of this magnitude may not be insignificant. The report should discuss this error in more detail, and documentation of the reliability of the code should be provided.

Bredehoeft's Figure 10.4, which shows radionuclide concentrations through time at differing distances from WIPP through time, shows many second-order fluctuations in concentrations, particularly at the outflow well. What do these fluctuations represent, and why do they appear to increase in magnitude through time?

Bredehoeft reports the results of a "Back of the Envelope Check" of his transport calculation on pages 38 and 39. We believe that this check is fundamentally circular, in that it relies on the same steady-state flow field used in the numerical transport calculation, and because it also relies on the same conceptual assumption that all flow in the marker bed beneath the repository passes directly through the waste. As a perhaps minor point, we note that the porosity value used in the check, 0.04, is inconsistent with the conceptual model for fracturing that Bredehoeft presents in Chapters 3 and 4, in which porosity does not increase as fractures open. A more appropriate value to use is the porosity of unfractured anhydrite,



for which we recommend 0.011, as used in the CCA. We presume, but do not know based on the information provided in the report, that the larger value was also used in the numerical transport calculations.

### Comments on Chapter 11: *Summary, Conclusions, & Recommendations*

Based on the work described in the preceding chapters of the report, Bredehoeft identifies three fluid-injection scenarios that he believes are of concern to the WIPP: The "High Pressure Scenario," the "Pulsing Scenario," and the "Two Well Scenario." This chapter summarizes these scenarios briefly, and states that they must be considered by the WIPP performance assessment. Bredehoeft concludes with a recommendation that "a much larger land withdrawal area with indefinite control is needed to protect the WIPP."

Our review has been limited to technical issues, and we offer no comment on his recommendations regarding administrative control and the regulatory process. Our comments on each of the three scenarios are described above in detail in the sections addressing specific chapters. Only major points are repeated here.

*"The High Pressure Scenario."* We do not believe that Bredehoeft has presented either a credible conceptual basis for the scenario or a reasonable simulation of its consequences. The results of his fracture model provide an inadequate basis for the key assumption in this scenario that fractures are fully developed over many hundreds of square kilometers. Furthermore, the conceptual basis for his fracture model itself is unclear. His modeling work showing fractures propagating 2.8 km after 100 days or less of injection is insufficiently documented and appears to be inconsistent with experimental data on hydraulic fracturing in anhydrites. The conceptual basis is not presented for his assumptions that flow in the marker bed following injection can be adequately modeled as steady-state, that no-flow boundary conditions are acceptable, and that WIPP will remain at a constant pressure functioning as the only sink in the model. We believe that these assumptions are unjustified and result in a physically unreasonable flow calculation. Model results showing pressures above lithostatic over the entire model domain and flow rates through the marker bed comparable to injection rates observed into reservoir rocks are unrealistic.

*"The Pulsing Scenario."* Based on the incomplete information provided in the report, we do not believe that Bredehoeft's model is sufficiently realistic to provide a meaningful analysis of the phenomena that may occur as a hydraulic fracture breaks through into a low pressure sink. We agree with Bredehoeft's conclusions that "one should not put too much credence in the actual numbers" and that the frequency of the pulsing he observes is likely to be a function in part of cell size and time steps (page 32). We also agree with the general implication that the breakthrough process is extremely complex and needs more sophisticated modeling treatment if it is to be described quantitatively. However, we do not believe that the modeling work presented here offers a credible argument that the

phenomenon will occur at the WIPP. The same observation applies to the alternative hypothesis proposed by Bredehoeft, in which a permeable zone around the WIPP provides enough flow along a pressure gradient sufficiently steep to keep fractures open in the anhydrites. Modeling work done by the WIPP project for another purpose (Vaughn et al., 1995) suggests that this alternative is unlikely.

*"The Two Well Scenario."* Essentially all of our conclusions about the "High Pressure Scenario" apply here also: we do not believe that Bredehoeft has presented either a credible conceptual basis for the scenario or a reasonable simulation of its consequences. Our concerns remain about the fracture model and the steady-state flow model with no-flow boundaries. For this particular scenario, we believe that the conditions imposed on the outflow well are physically unreasonable and appear to have been contrived to assure sufficiently high pressures to justify fracturing. We do not believe that any plausible conceptual model can be presented that will correspond to the model assumptions applied to the outflow well. As was the case in the "High Pressure Scenario," we do not believe that the flow rates calculated through the marker beds are physically reasonable. In particular, we find the model result indicating that the outflow well produces a steady-state brine flow of 73,000 m<sup>3</sup>/yr (reported on page 36 as  $2.3 \times 10^{-3}$  m<sup>3</sup>/sec) from a one-meter anhydrite layer to be incredible. Regarding the radionuclide transport calculation presented as part of the "Two Well Scenario," we do not believe that sufficient information is provided to evaluate the accuracy of the solution. Graphical displays of the results suggest that the solution may have numerical errors. Regardless of the accuracy of the transport solution, we believe that the flow field calculated for the "Two Well Scenario" is sufficiently unrealistic that no meaning should be attached to Bredehoeft's calculated radionuclide releases from the repository.

## Conclusions

Our technical review of *The HARTMAN Scenario: Implications for WIPP* is complicated by the incompleteness of the information contained in the report, and it is possible that additional documentation could resolve some technical concerns, particularly those related to the mathematical models and their numerical implementation. Other concerns, primarily those relating to the justification of the conceptual models that underlie the analysis, appear to be fundamental and are unlikely to be resolved by further clarification.

Based on the documentation available, we conclude that Bredehoeft's report does not provide a realistic or reasonable analysis of the phenomena it addresses, nor does it support its conclusion that fluid injection scenarios must be included in performance assessment models of the WIPP. Bredehoeft's analysis is sufficiently unrealistic that its results are not meaningful to the assessment of the possible consequences of fluid injection in the vicinity of the WIPP.

## Acknowledgments

The authors assume full responsibility for the interpretations and conclusions presented in this review. However, we would like to thank Peter Davies for thoughtful comments on an earlier draft of the review, Tom Corbet for technical advice and the contribution of the discussion of elastic storage contained in Attachment 1, and Sean McKenna for reviewing Attachment 1.

## References

Beauheim, R.L., W.R. Wawersik, and R.M. Roberts. 1993. "Coupled Permeability and Hydrofracture Tests to Assess the Waste-Containment Properties of Fractured Anhydrite." *Journal of Rock Mechanics*, Vol. 30, No.7, pp. 1159 - 1163.

Bredehoeft, J. 1997. *The HARTMAN Scenario: Implications for WIPP*. Report prepared for the New Mexico Attorney General, March 1997. The Hydrodynamics Group, La Honda, CA. Copy on file at Sandia WIPP Central Files, Albuquerque, NM. WPO # 45839.

DOE, 1996. *Title 40 CFR Part 191 Compliance Certification Application for the Waste Isolation Pilot Plant*. DOE/CAO-1996-2184. United States Department of Energy Carlsbad Area Office, Carlsbad, New Mexico.

DOE, 1997. *Injection Methods: Current Practices and Failure Rates in the Delaware Basin*. DOE/WIPP97-2240, United States Department of Energy, Carlsbad Area Office, Carlsbad, NM.

Hunt, C.B. 1954. *Geology and geography of the Henry Mountains region, Utah*. United States Geological Survey Professional Paper 228.

Smith, M.B., G.B. Homan, C.R. Fast, and R.J. Covlin. 1978, "The azimuth of deep, penetrating fractures in the Wattenberg field," *Journal of Petroleum Technology*, v. 30, p. 185-193.

Stoelzel, D.M., and O'Brien, D.G. 1996. "The Effects of Salt Water Disposal and Waterflooding on WIPP," Summary Memo of Record for NS-7a. Sandia National Laboratories, Albuquerque, NM. WPO 80837.

Van Kirk, C., 1994. "Report Concerning Salt Water Blow-out January 1991 on the "Bates Lease" Sections 10 and 15, Township 26 South, Range 37 East, N.M.D.M., Lea County, New Mexico," unpublished report prepared for Doyle Hartman, dated September 16, 1994. Copy on file at the Sandia WIPP Central Files, Albuquerque, NM. WPO # 45838.

Vaughn, P., M. Lord, and R. MacKinnon. 1995. S-6: "Dynamic Alteration of the

DRZ/Transition Zone: Summary Memo of Record," to D.R. Anderson, September 28, 1995. SWCF-A (WPO #30798). Sandia National Laboratories, Albuquerque, NM.

Wawersik, W.R., L.W. Carlson, J.A. Henfling, D.J. Borns, R.L. Beauheim, C.L. Howard, and R.M. Roberts. 1997. *Hydraulic Fracturing Tests in Anhydrite Interbeds in the WIPP, Marker Beds 139 and 140*. SAND95-0596. Sandia National Laboratories, Albuquerque, NM.

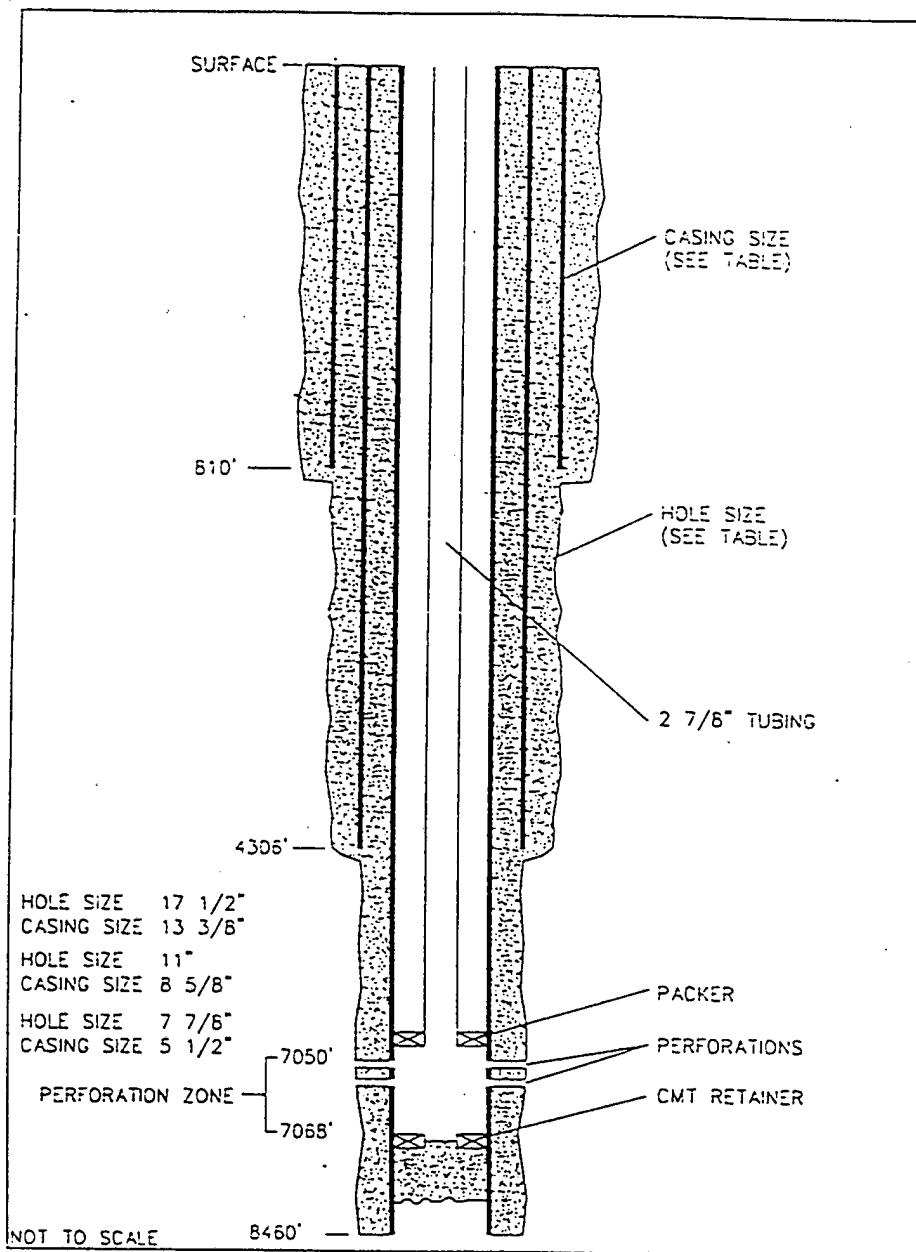
Zoback, M.L., and M. Zoback. 1980. "State of stress in the coterminous United States," *Journal of Geophysical Research*, v. 85, p. 6113-6156.

Distribution:

L.E. Shephard, MS1395  
W.D. Weart, MS 1337  
M.G. Marietta, MS 1395  
P.B. Davies, MS 1324  
D.R. Anderson, MS 1328  
H.-N. Jow, MS 1328  
T.F. Corbet, MS 1324  
S. McKenna, MS 1324  
J.A. Mewhinney, DOE-CAO

# Neff Federal # 3

T22S, R31E, sec.25



CASING AND TUBING FOR WELL # 30015282810000

Figure 1. Schematic Diagram of the Neff Federal # 3 borehole (DOE, 1997)

DOYLE HARTMAN  
C.T. BATES NO. 2

1980' FSL and 760' FWL ILJ  
Section 10, T-26-S, R-37-E  
Lee County, New Mexico

② 1/20/91 - Per NMOCED, cemented annulus with 4400 sx Thixotropic cmt followed by 750 sx of 50-50 blend API Class H cmt and Calseal. Ran temperature survey, found bottom of drill pipe @ 2224', bottom of cmt (BOC) @ 2010', top of cmt (TDC) at the surface.

③ 1/21/91 - Following setup of annulus squeeze cmt job, recorded SIWHP of 1000 psig (gradient = .956 psi/ft). Per NMOCED, pumped 1500 sx Thixotropic cmt followed by 250 sx of 50-50 blend API Class H cmt and Calseal down 4 1/2" drill pipe. Prior to squeezing down drill pipe, flow rate was 12,240 BWPD with a FDPP = 85 psig.

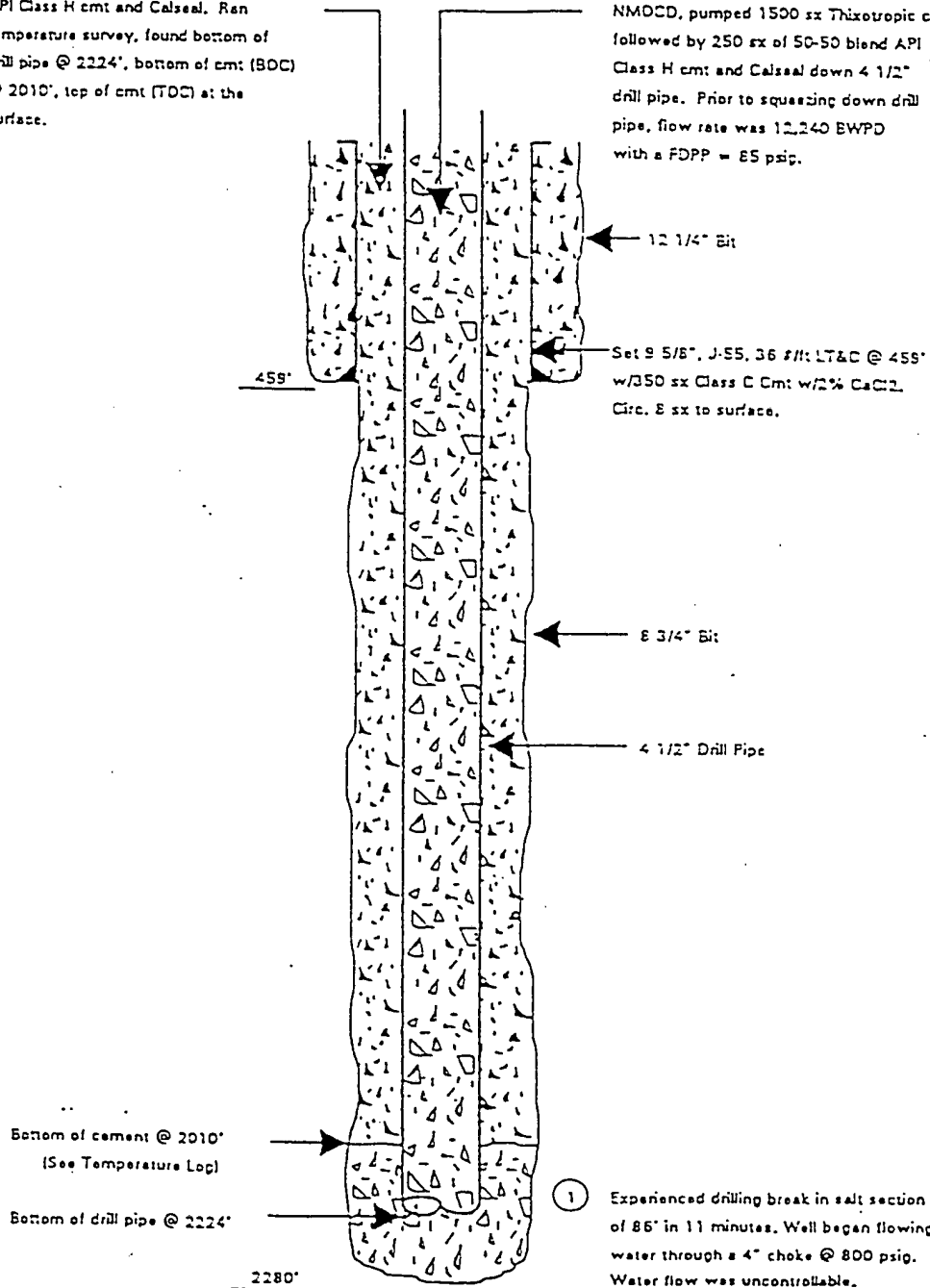


Figure 5

Figure 2. Plugging of the Bates #2 well. (reproduced from Figure 5 of Van Kirk, 1995)



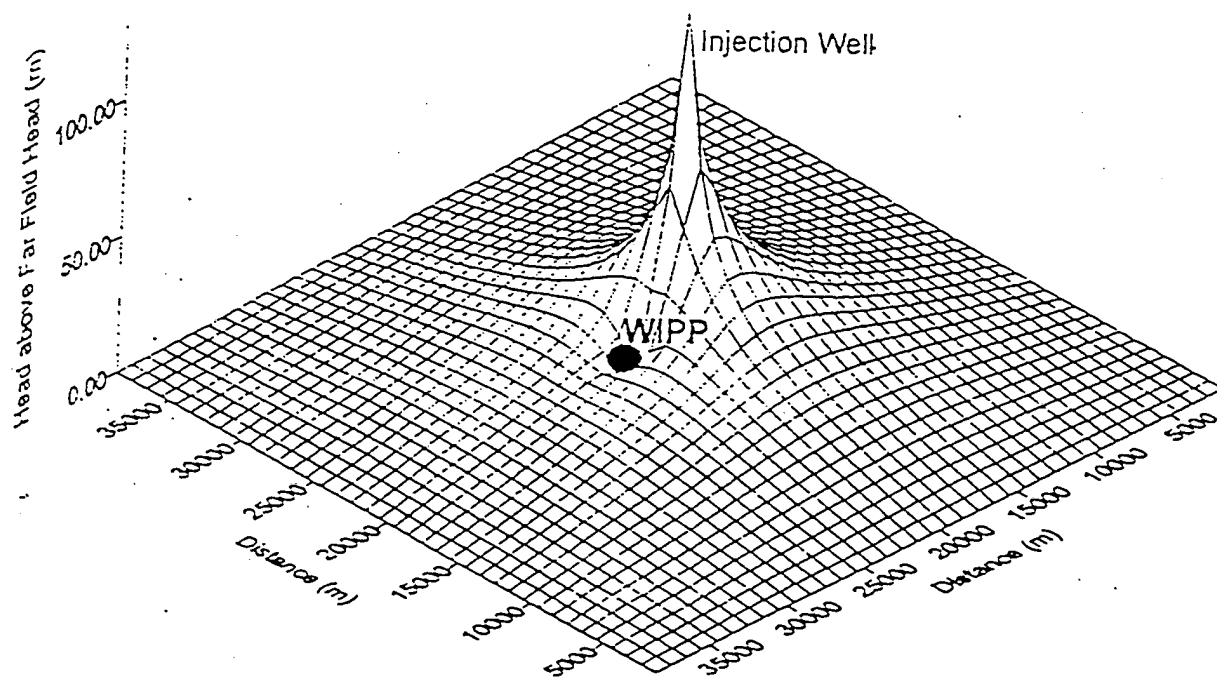


Figure 5.1. Hydraulic head created by flow to WIPP.

Figure 3. Reproduced from Figure 5.1 of Bredehoeft (1997).

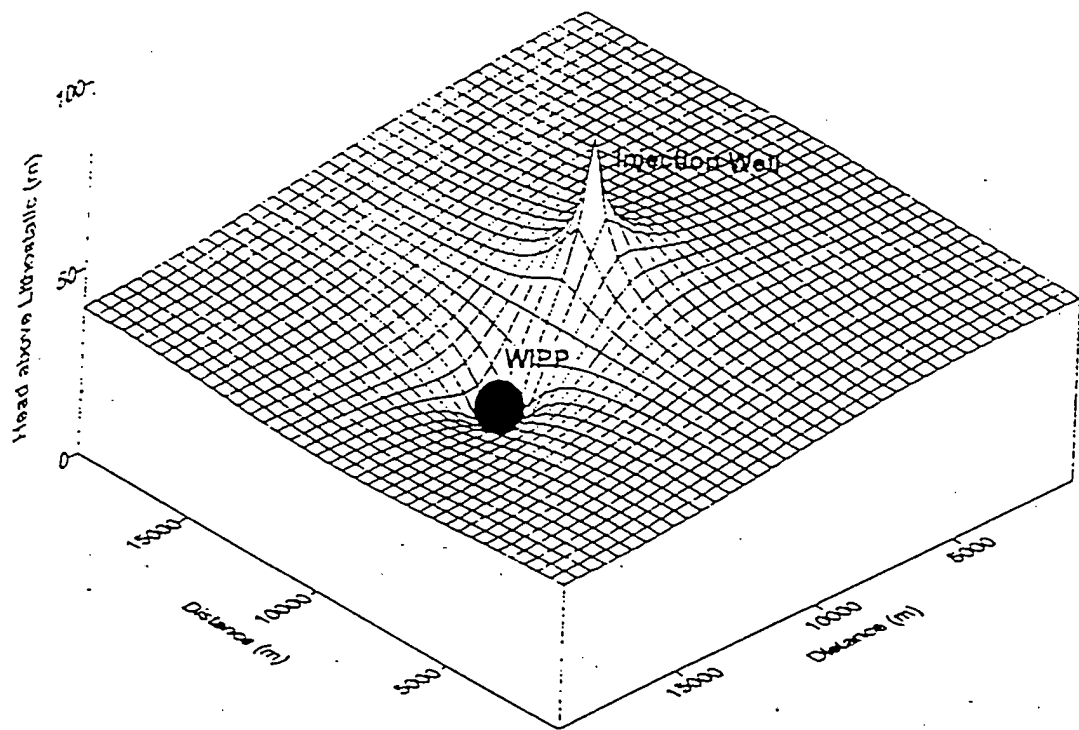


Figure 8.3. Head associated with flow to WIPP; this figure is very similar to Figure 5.1

Figure 4. Reproduced from Figure 8.3 of Bredehoeft (1997)

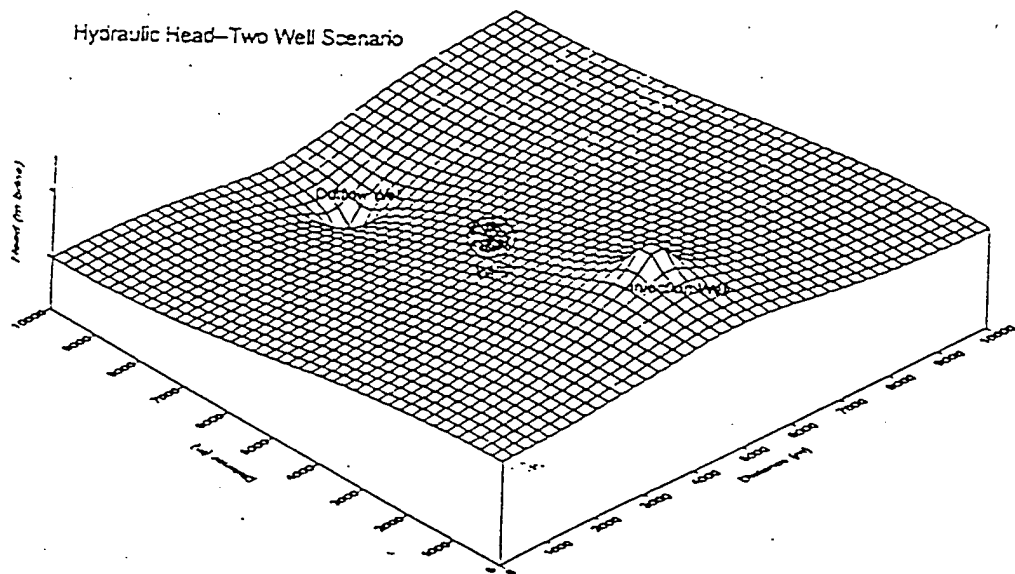


Figure 10.2. head distribution for the two well scenario.

Figure 5. Reproduced from Figure 10.2 of Bredehoeft (1997)

# Integrated WIPP Releases

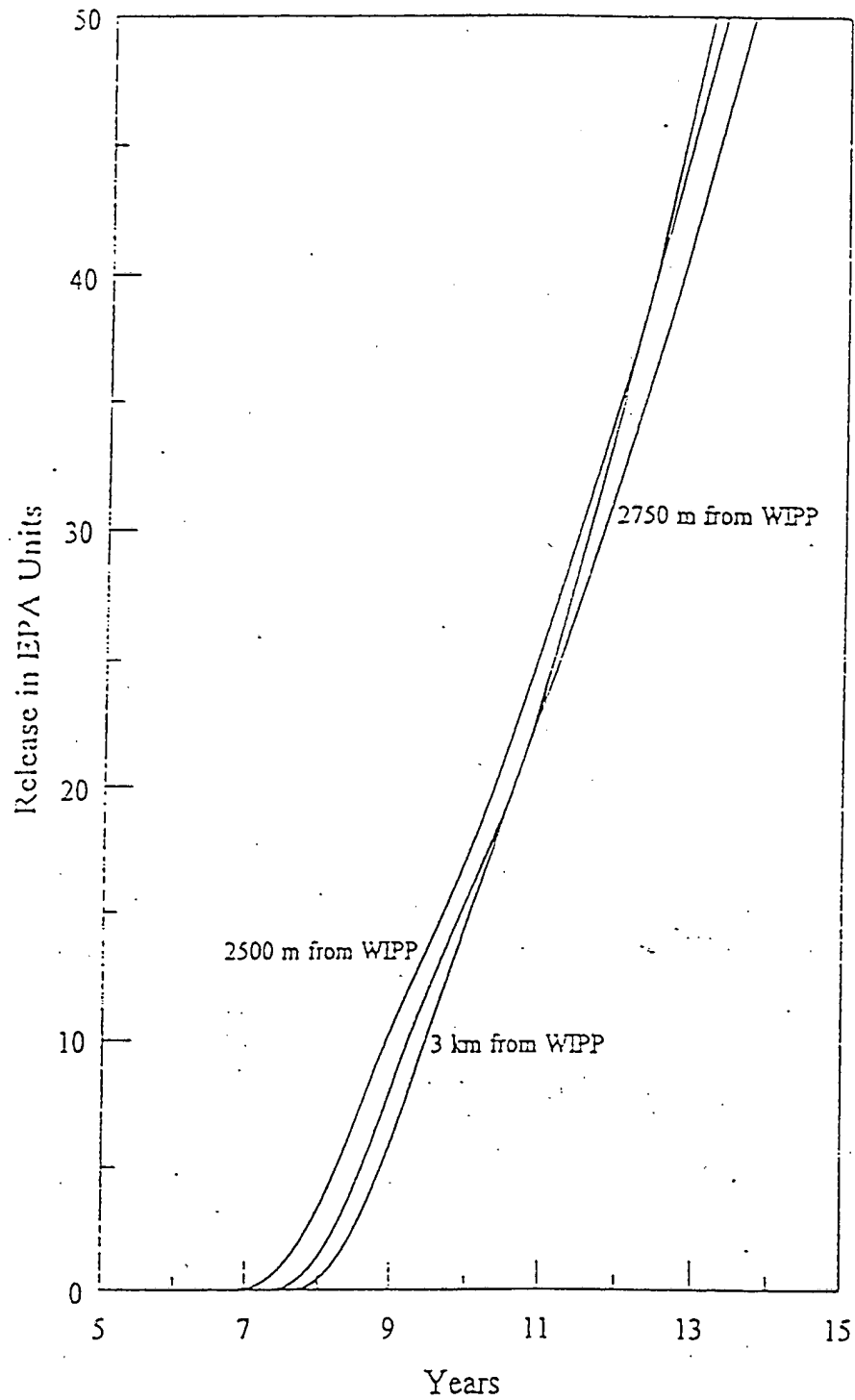


Figure 10.6. Plot of the contaminant mass released from WIPP. The contaminant concentration of WIPP brine is  $10^3$  EPA Units/ $m^3$  for this result. The three curves should converge with time; the spread in the curves at later times is some measure of the model error.

Figure 6. Reproduced from Figure 10.6 of Bredehoeft (1997).

## Attachment 1

### Example Comparison of the Volume of Water Going into Elastic Storage and Fracture Porosity as an Anhydrite is Hydrofractured

#### Elastic storage

In Bredehoeft's calculations the amount of water that goes into elastic storage as the pressure of anhydrite is increased is determined by the specific storage ( $S_s$ ).  $S_s$  is the volume of water that a unit volume of the anhydrite takes into storage per unit increase in hydraulic head. Bredehoeft assumes that fractures initiate if the pore pressure reaches a value 2 MPa above the far-field pressure.

The 2 MPa change in pressure is converted to hydraulic head by dividing by the product of  $\rho_w$  and  $g$ :

$$\Delta h = \Delta P / (\rho_w g) = 2 \times 10^6 \text{ kg/m s}^2 / (\rho_w g) = 167 \text{ m}$$

where

$$\rho_w = 1222 \text{ kg/m}^3 \text{ (CCA Appendix PAR, Table PAR-33)}$$

$$g = 9.792 \text{ m/s}^2 \text{ (CCA Appendix PAR, Table PAR 56)}$$

$$P = 2 \times 10^6 \text{ kg/(m s}^2)$$

On page 19 Bredehoeft notes that he favors the value of  $1 \times 10^{-5} \text{ m}^{-1}$  for  $S_s$  of the anhydrite.

Therefore the volume of water required to raise the pressure of  $1 \text{ m}^3$  of anhydrite by 2MPa is  $\Delta h$  times  $S_s$ , or  $(167\text{m})(1 \times 10^{-5} \text{ m}^{-1}) = 0.0017 \text{ m}^3$ .

#### Storage in fracture porosity

On page 17 Bredehoeft estimates that the additional pore space due to fracturing is a maximum of 0.001 m in an anhydrite that is 1 m thick. This means that  $0.001 \text{ m}^3$  of water would be required to fill the additional fracture porosity in  $1 \text{ m}^3$  of anhydrite.

## **Attachment 3: Derivation of Fracture Parameters Used in Brine Injection Modeling**

**Information Only**



To: Dan Stoelzel (6748) and Peter Swift (6821)  
From: Palmer Vaughn (6849) *Palmer Vaughn*  
Date: June 13, 1997

Subject: Anhydrite Fracture Model parameters for use in simulating water injection near the WIPP site.

The anhydrite interbeds for water injection modeling are conceptualized and modeled in a way that is consistent with their treatment in the CCA Performance Assessment calculations. That is, all anhydrite is assumed to contain pre-existing fractures and that these features will dynamically alter in such a way as to increase the hydrologic properties of permeability and, to a lesser extent, porosity if exposed to elevated pressures. A description of the fracture model can be found in Section 6.4.5.2 of the CCA.

The following parameterization of the anhydrite fracture model is consistent with that used in the CCA Performance Assessment calculations and is based on qualitative in-situ observations made in MB 139 as described in WPO #44704, March 31, 1997 memo from Larson, Beauheim, and Weart to Shephard.

- 1) A 1.0 cm. gap occurs at a pressure of 0.5 MPa over lithostatic pressure.
- 2) An increase in the permeability of 4 orders of magnitude occurs at a pressure of 0.5 MPa over lithostatic.
- 3) Alteration of the hydrologic properties becomes significant at a pressure of 0.2 MPa above the in-situ pore pressure. The sum of these two pressures is the fracture initiation pressure.
- 4) The hydrologic properties are essential fully developed (altered) at a pressure of 3.8 MPa over the fracture initiation pressure. This pressure is called the full fracture pressure and is a numerical modeling end point.

In order to apply this information consistently over all the anhydrite layers considered in the fluid injection model stratigraphy the elevation, thickness, and numbers of distinct layers in each of the 5 composite anhydrite layers in the model stratigraphy must be considered. The 5 composite anhydrite layers considered in the fluid injection model stratigraphy are as follows:

- 1) **Marker Bed 139** - consisting of 1 layer of total thickness 0.85m and located at a depth of 658.145m.
- 2) **Marker Bed 138 and Anhydrite A and B** - consisting of 2 layers of total thickness 1.476m and located at a depth of 654.833m.
- 3) **Upper Anhydrite Composite** - consisting of 5 layers of total thickness 15.85m and located at a depth of 487.13m.
- 4) **Lower Anhydrite Composite** - consisting of 2 layers of total thickness 9.45m and located at a depth of 743.06m.

Information Only

- 5) **Castile Anhydrite**- consisting of 3 layers of total thickness 243.0m and located at a depth of 1051.46m .

The parameters for the fracture model for each of the composite anhydrite layers in the fluid injection model stratigraphy are determined by fitting the equation describing the change in porosity and permeability with pressure , Section 6.4.5.2 of the CCA, to the following three data points conditions :

- 1) **initial data point conditions** - initial pore pressure, initial porosity, and initial permeability
- 2) **fracture initiation data point conditions** - fracture initiation pressure, porosity adjust for formation compressibility at pressure, and initial permeability.
- 3) **Target data point conditions** - Target pressure ( 0.5 MPa over lithostatic ) , Target porosity , Target Permeability ( 4 orders of magnitude increase over initial permeability).

The target porosity is determined for each composite anhydrite by assuming that each layer in the composite dilates by 1.0 cm at a pressure of 0.5Mpa above lithostatic and that the resulting increase in void volume is distributed across the entire thickness of the composite. Because the absolute differences between initial fluid pore pressure, fracture initiation pressure, full fracture pressure, and lithostatic pressure are dependent on depth, corrections are made to the fracture input parameters so that the relative pressure differences for each of the composite layers are the same as those at MB 139. The initial pore pressure of each composite anhydrite is adjusted according to its location relative to MB 139 using a gradient of 0.8376 psi/ft or 18947 pa/m . The fracture initiation pressure for each composite anhydrite is adjusted according to its location relative to MB 139 using a gradient of 0.8510 psi/ft or 19251 pa/m . The full fracture pressure for each composite anhydrite is adjusted relative to its location to MB 139 using a pressure gradient of 1.1062 psi/ft or 25025 pa/m. The lithostatic pressure for each composite anhydrite is adjusted relative to its location to MB 139 using a pressure gradient of 1.0 psi/ft or 22621 pa/m. The above gradients reproduce the the initial pore pressure, fracture initiation pressure, full fracture pressure and lithostatic pressure used consistent with MB 139 and it's depth .

The application of this conceptualization and the various adjustments and assumptions outlined above results in the parameter values indicated on the attached work sheets.

**Information Only**

To: Dan Stoelzel, Dept. 6748

From: Michael Lord, Dept. 6749

Date: April 10, 1997

Subject: Parameters for the markerbeds in the WIPP site water injection/flood BRAGFLO model.

The following data honors the porosity/permeability response as required.

Material	DPHIMAX (fraction)	PI_DELTA (Pa)	PF_DELTA (Pa)	KMAXLOG (m <sup>2</sup> )
Markerbed 139	0.050	0.2000E+06	3.800E+06	1.0E-09
Composite 138 & a+b	0.070	0.1990E+06	3.781E+06	1.0E-10
Upper Anhydrite Composite	0.018	0.1480E+06	2.813E+06	1.0E-11
Lower Anhydrite Composite	0.017	0.2258E+06	4.290E+06	1.0E-10
Castile Anhydrite	0.0125	0.3195E+06	6.071E+06	1.0E-10

Information Only

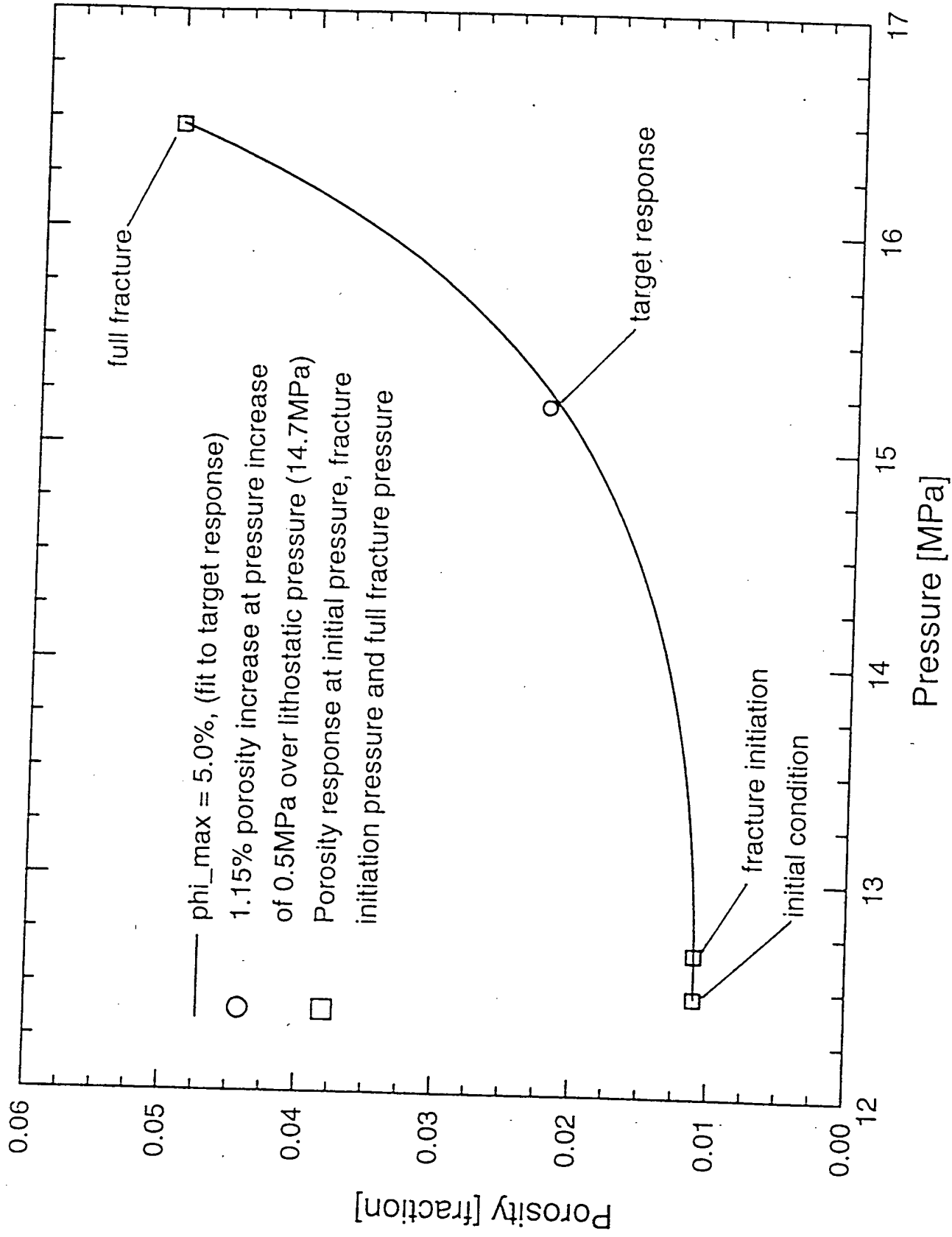


Figure: Fracture Porosity Response in Markerbed 139

Information Only

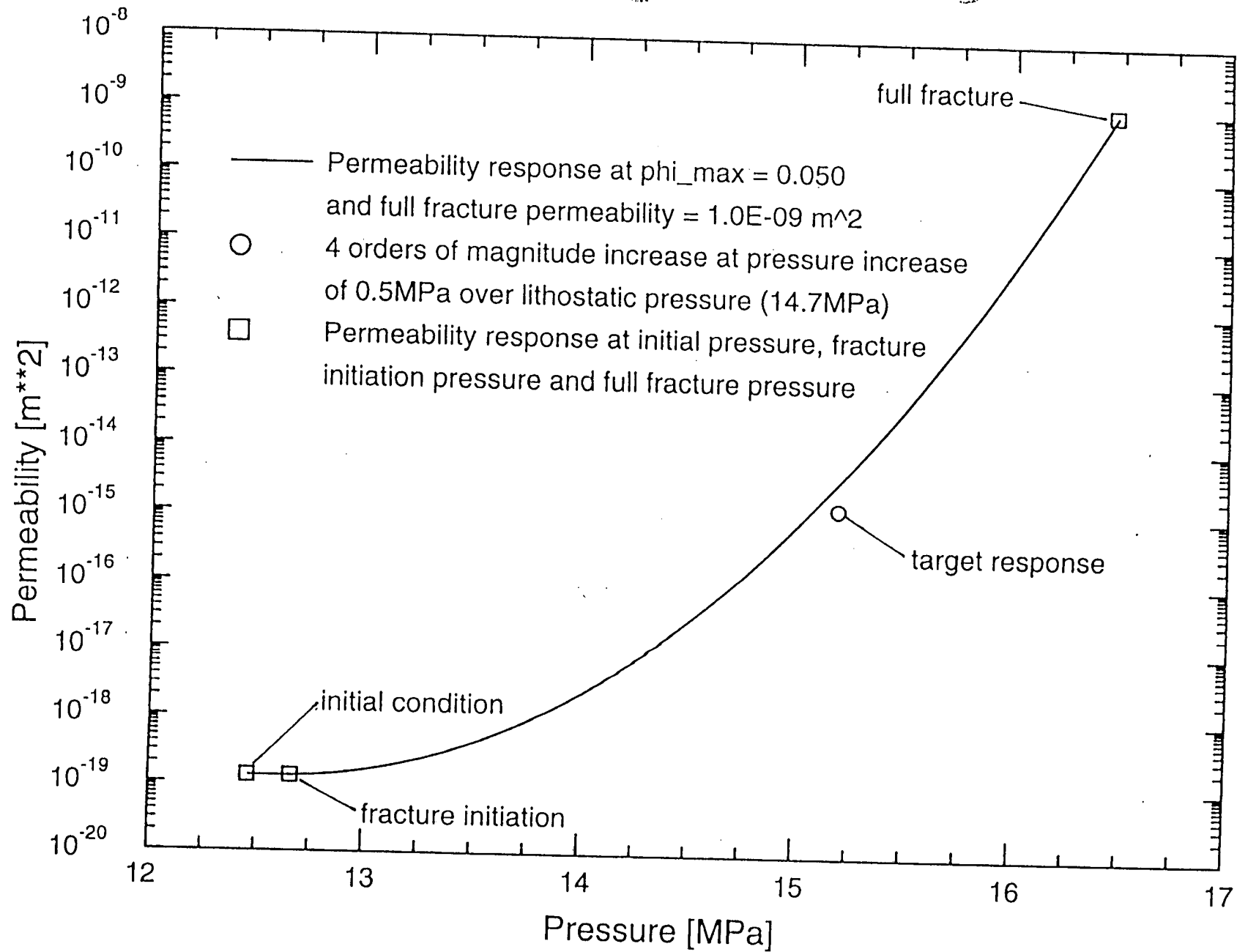


Figure: Fracture Permeability Response in Markerbed 139

Information Only

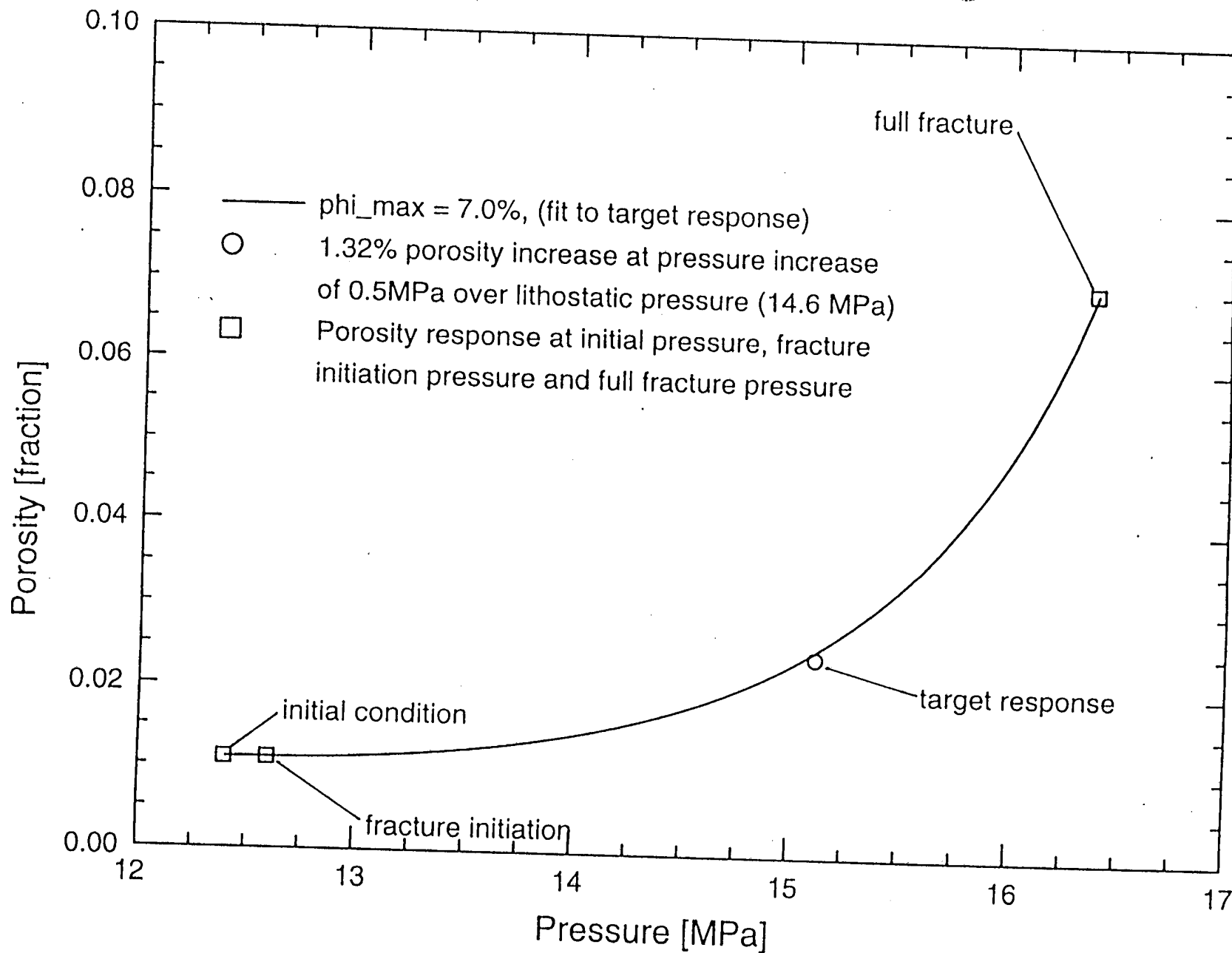


Figure: Fracture Porosity Response in Composite Markerbeds 138 & a+b

Information Only



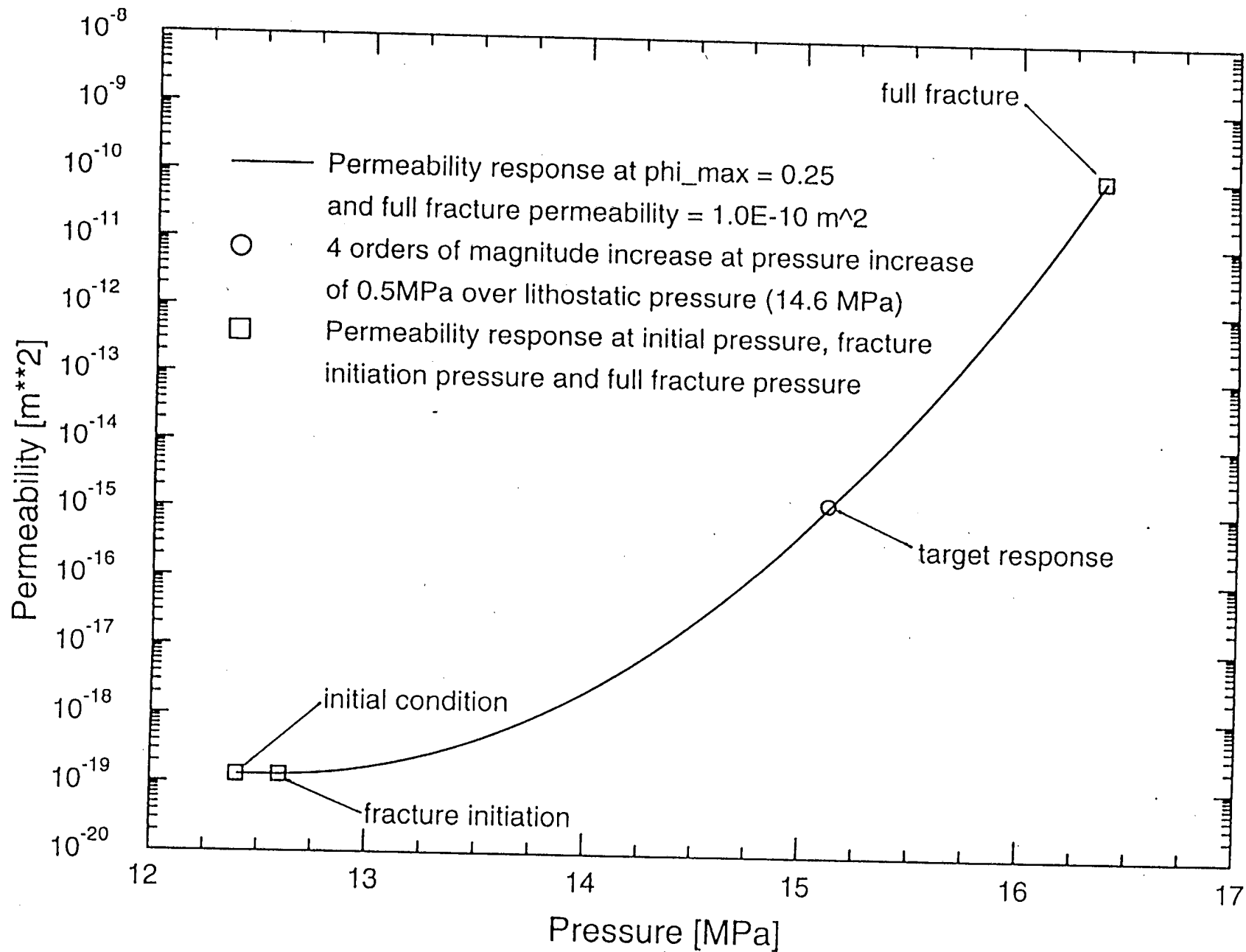


Figure: Fracture Permeability Response in Composite Markerbeds 138 & a+b

Information Only

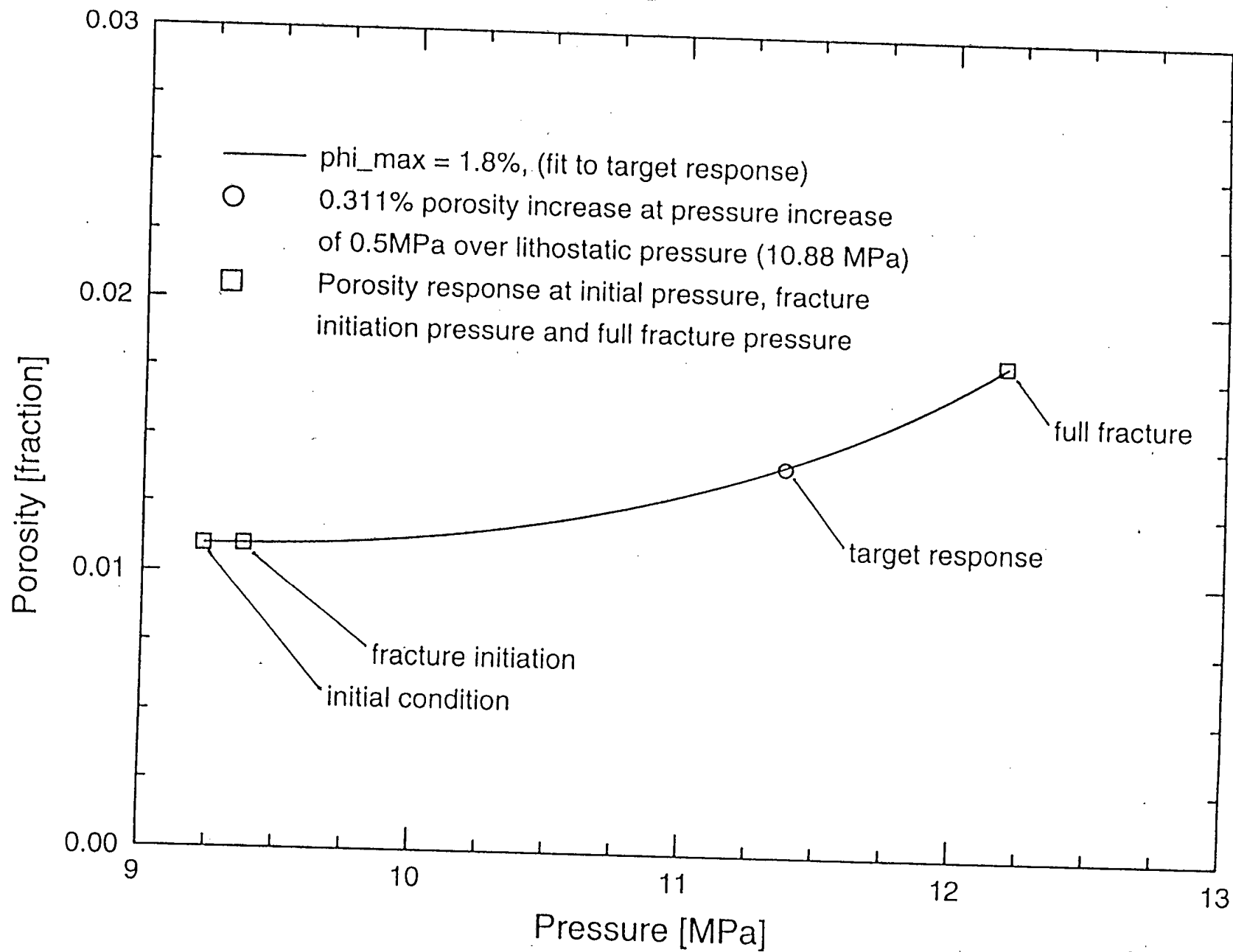


Figure: Fracture Porosity Response in Upper Anhydrite Composite

Information Only

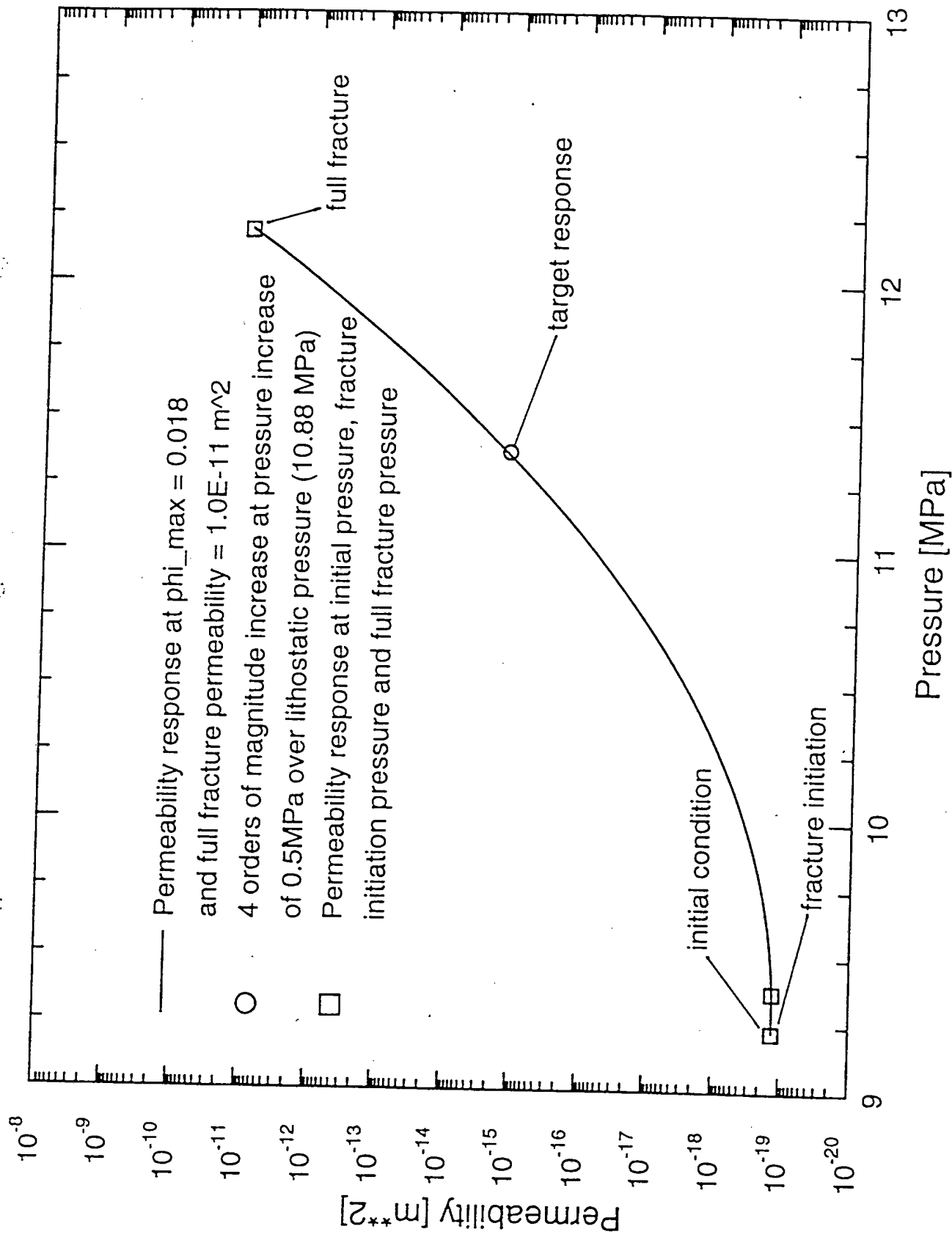


Figure: Fracture Permeability Response in Upper Anhydrite Composite

Information Only

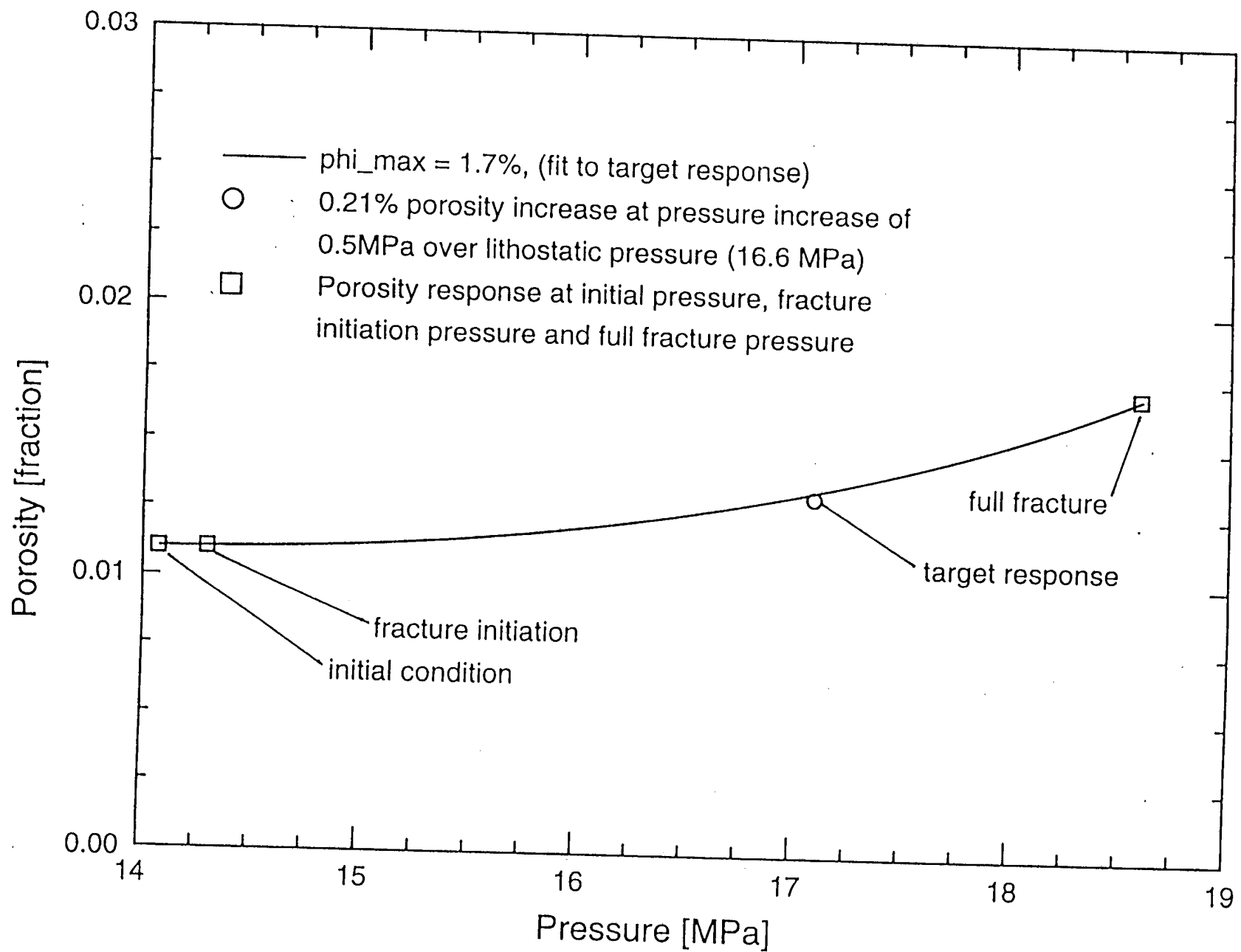


Figure: Fracture Porosity Response in Lower Anhydrite Composite

Information Only

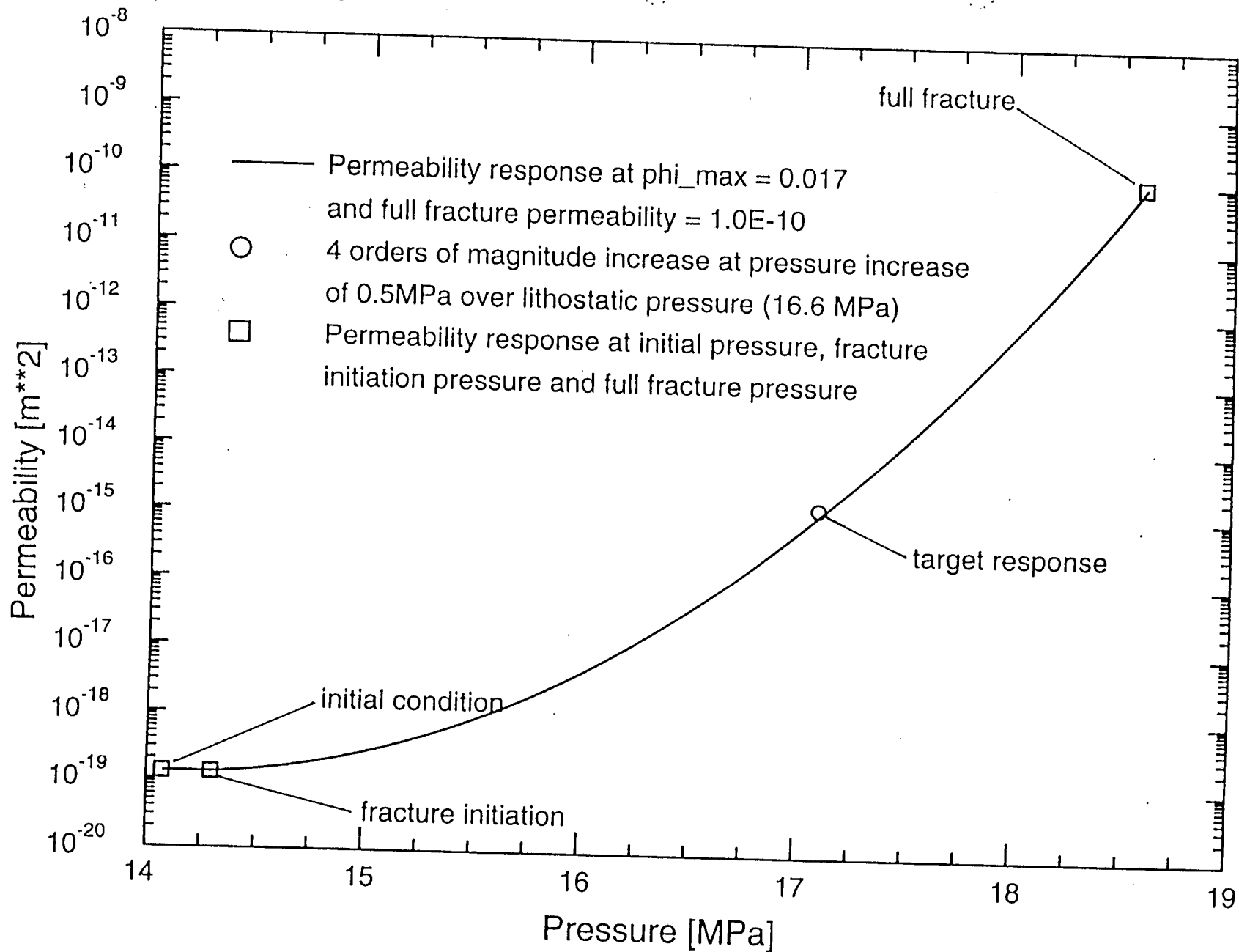


Figure: Fracture Permeability Response in Lower Anhydrite Composite

Information Only

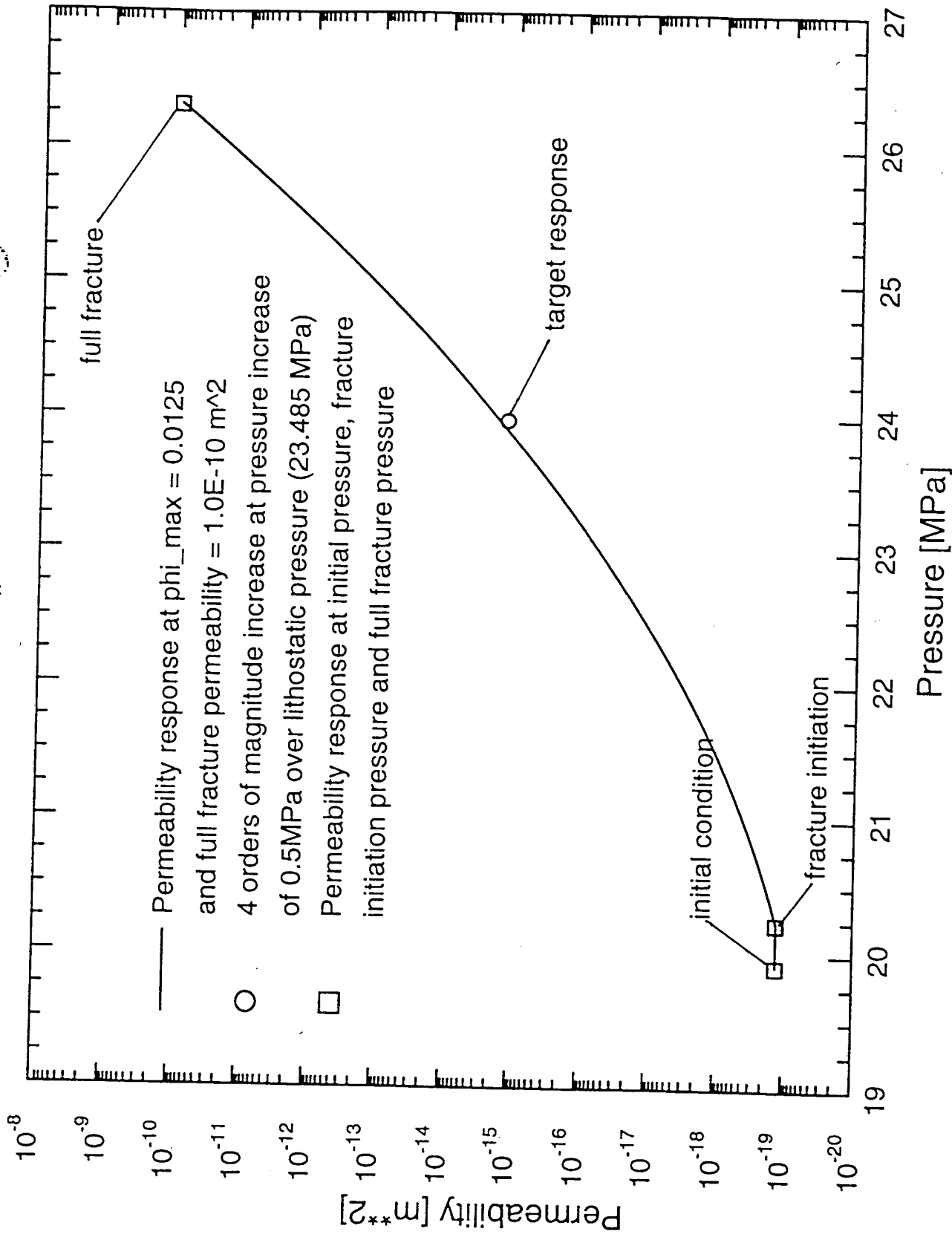


Figure: Fracture Permeability Response in Castile Anhydrite

Information Only



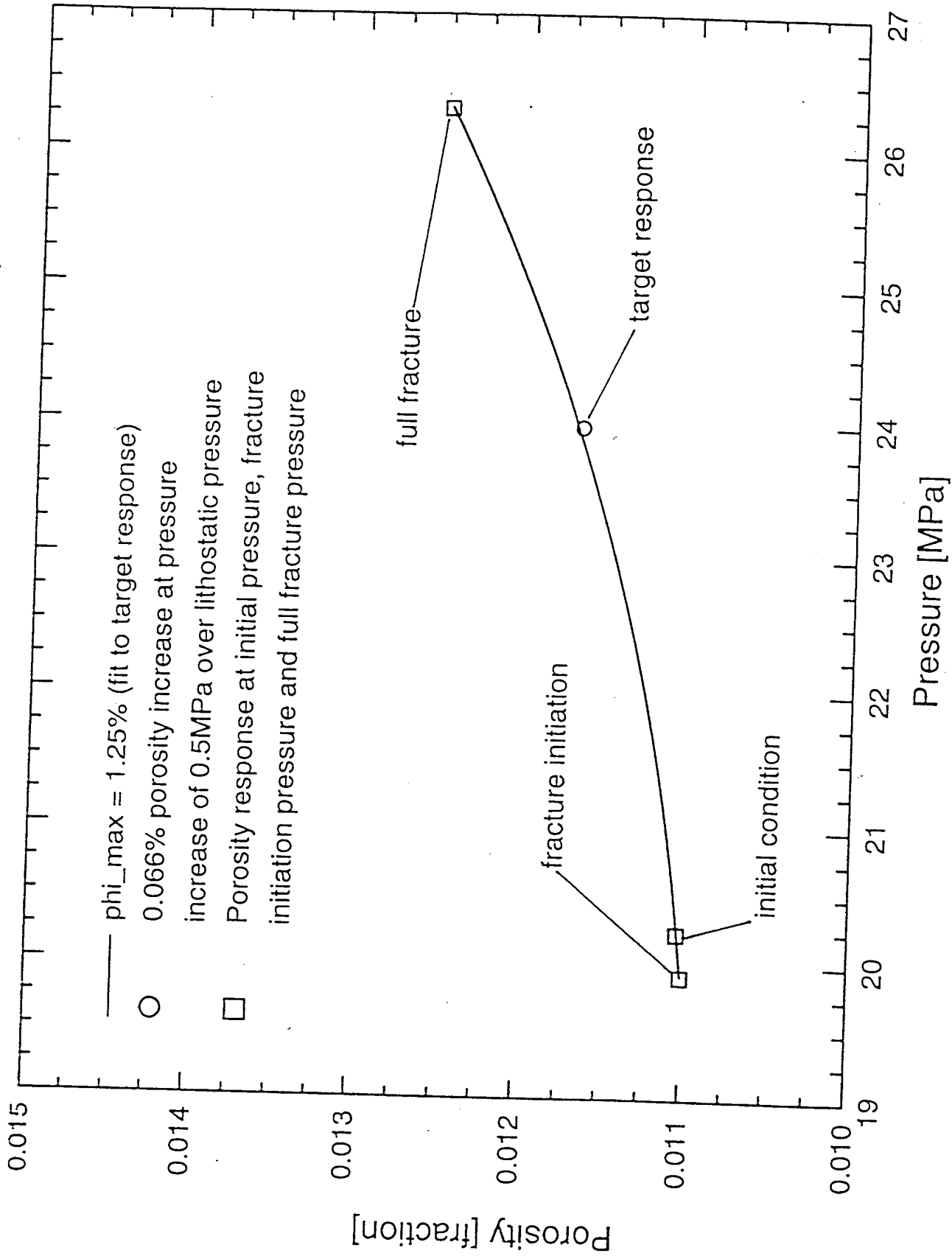


Figure: Fracture Porosity Response in Castile Anhydrite

Information Only